DOCTOR OF PHILOSOPHY

Structural and biochemical characterisation of enzymes involved in mannan biosynthesis

Striebeck, Alexander

Award date:
2013

Awarding institution:
University of Dundee

DOCTOR OF PHILOSOPHY

Structural and biochemical characterisation of enzymes involved in mannan biosynthesis

Alexander Striebeck

2013

University of Dundee

University of Dundee
College of Life Sciences

Structural and biochemical characterisation of enzymes involved in mannan biosynthesis

By
Alexander Striebeck

A thesis submitted for the degree of

Doctor of Philosophy
University of Dundee

March 2013

Meiner Familie

List of Publications

The work described in this thesis has been submitted or is in preparation to be submitted in the following articles:

A. Striebeck, A. W. Schuettelkopf and D. M. F. van Aalten, 'Yeast Mnn9 is both a priming glycosyltransferase and an allosteric activator of mannan biosynthesis', under review with Open Biology.

A. Striebeck, V. S. Borodkin, A. T. Ferenbach and D. M. F. van Aalten, 'The structure of the α-1,6-mannosidase aman6 serves as model for essential yeast proteins', manuscript in preparation

Acknowledgements

I would like to thank my supervisor Prof. Daan van Aalten for giving me the opportunity to work in his laboratory. It was a great experience to learn from him and his expertise. His encouragement helped me knowingly and unknowingly through many unsuccessful times during my PhD and made them successful.

I want to thank many of the current and former members of the group. First and foremost Dr. Alexander Schüttelkopf who was a significant help in the beginning and throughout the first two years. Even after he moved to Glasgow he gave me support whenever I asked for it. My achievements would not be without him. I also want to thank Dr. Vladimir Borodkin for his endless will to synthesise the most different compounds for my research. Half of this thesis could not have been done without his help. Furthermore, I want to thank Dr. Helge Dorfmüller who became a good friend of mine over the past four years, not just because of the endless football sessions and rounds of German spirits. He was a great help for all the little and big problems at work and in my personal life. Thank you. A great inspiration was Dr. Francesco Rao who has a never ending knowledge about everything and I am aiming to become a polymath just as he is. I want to thank all other members of the group who made the past four years a pleasure that I will never forget. In particular these are: Dr. Kaoru Sakabe, Dr. Kelly Sanders, Dr. George Penman, and Susann Krüger. I miss you all. Furthermore I want to mention Nithya Selvan, Dr. Marianne Schimpl, Dr. Andrew Ferenbach and Dr. Shalini Pathak for a lot of input on many different levels and everybody else I did not mention by name. I also want to thank my two and a half Honour's students Satoko Orihashi, Helen Woodroof, and Jason Bolderson who were a pleasure to work with.

A big thank you is for my thesis committee members Prof. Tracy Palmer and Prof. Jason Swedlow who gave me a lot of advice and helped me to put all my efforts and achievements into the big picture. I also want to thank Prof. Neil Gow (University of Aberdeen) for his support during my PhD.

Furthermore I want to thank all the members, present and past, of the MMB

division. You clearly made the four years here in Dundee a blast. I do already and will miss many of you and I hope we can all stay in touch and meet in the future.

I would like to thank the entire College of Life Sciences, in particular Dr. David Robinson for his help with the ligand screen and Prof. Mike Stark for providing me with an essential plasmid for my research. I want to thank all the services that made Dundee such an easy place to work. In particular the media kitchen, the wash-up service and the sequencing service. I really appreciate their work.

I also want to thank my funding bodies SULSA and BBSRC. The financial support that they provided me with made my research much better and helped to focus on my work.

Last but not least I want to thank my entire family. I could have not done it without you. Thank you Mama, Papa, Schwesterchen, Omas, Opas, Tanten und Onkel. I do not know what I would have done without you. I know it was sometimes hard to get a hold of me but I promise this will change.

Declaration

I declare that the following thesis is based on the results of investigations conducted by myself, and that this thesis is of my own composition. Work other than my own is clearly indicated in the text by reference to the relevant researchers or to their publications. This dissertation has not in whole, or in part, been previously submitted for a higher degree.

Alexander Striebeck

I certify that Alexander Striebeck has spent the equivalent of at least nine terms in research work at the College of Life Sciences, University of Dundee, and that he has fulfilled the conditions of the Ordinance General No. 14 of the University of Dundee and is qualified to submit the accompanying thesis in application for the degree of Doctor of Philosophy.

Prof. Daan M.F. van Aalten

Abbreviations and Acronyms

Amino acid	Three letter code	One letter code
Alanine	Ala	A
Arginine	Arg	R
Asparagine	Asn	N
Aspartic acid	Asp	D
Cysteine	Cys	C
Glutamic acid	Glu	E
Glutamine	Gln	Q
Glycine	Gly	G
Histidine	His	H
Isoleucine	Ile	I
Leucine	Leu	L
Lysine	Lys	K
Methionine	Met	M
Phenylalanine	Phe	F
Proline	Pro	P
Serine	Ser	S
Threonine	Thr	T
Tryptophan	Trp	W
Tyrosine	Tyr	Y
Valine	Val	V

Å	Ångström
Amp	Carbenicillin
ANTS	8-Aminonaphthalene-1,3,6-trisulphonic acid
Bc	*Bacillus circulans*
Bs	*Bacillus subtilis*
BSA	Bovine serum albumin
C. albicans	*Candida albicans*
CAZy	Carbohydrate active enzyme
CBM	Carbohydrate-binding motif
CCP4	Collaborative computational project number 4
°C	Degree Celsius
C-terminal	Carboxy-terminal
CWP	Cell wall protein
Da	Dalton
ddH_2O	Double distilled water
DMSO	Dimethyl sulfoxide
DNA	Deoxyribonucleic acid
DSTT	Division of Signal Transduction Therapy
DTT	Dithiothreitol
DvA	Daan van Aalten
EDTA	Ethylenediamine tetraacetic acid
E. coli	*Escherichia coli*
ESRF	European Synchroton Radiation Facility
FACE	Fluorescent-assisted carbohydrate gel electrophoresis
g	gravity
GDP	Guanosine diphosphate
GH	Glycoside hydrolase
GPI	Glycophosphatidylinositol

Continued on next page

GT	Glycosyltransferase
GTP	Guanosine triphosphate
GSH	Glutathione
GST	Glutathione-S-transferase
HEPES	N-(2-Hydroxyethyl)piperazine-N'-(2-ethanesulfonic acid)
HRP	Horseradish peroxidase
IEX	Anion exchange chromatography
IPTG	Isopropyl β-D-thiogalactoside
K	Degree Kelvin
Kan	Kanamycin
K_d	Equilibrium dissociation constant
K_m	Michaelis constant
λ_{em}	Emission wavelength
λ_{ex}	Excitation wavelength
LB	Lysogeny broth
Man	Mannose
Man2	Mannobiose
MBP	Maltose binding protein
Mn	Manganese
NADH	Nicotinamide adenine dinucleotide (reduced)
NAD	Nicotinamide adenine dinucleotide (oxidised)
N-terminal	Amino-terminal
OD	Optical density
OST	Oligosaccharyltransferase
PAGE	Polyacrylamide gel electrophoresis
PCR	Polymerase chain reaction
PBS	Phosphate-buffered saline
PDB	Protein data bank

Continued on next page

PEG	Polyethylene glycol
PEP	Phosphoenolpyruvic acid
PP	PreScission protease
PVDF	Polyvinylidene fluoride
R^2	Coefficient of determination
Rm	*Rhodothermus marinus*
RMSD	Root mean square deviation
rpm	Revolutions per minute
RT	Room temperature/ambient temperature
S. cerevisiae	*Saccharomyces cerevisiae*
Sc	*Saccharomyces cerevisiae*
SDS	Sodium dodecyl sulfate
SEC	Size-exclusion chromatography
SEM	Standard error of the mean
TBS	Tris-buffered saline
TEV	Tobacco etch virus
Tris	Tris(hydroxymethyl)aminomethane
U	Units
UoD	University of Dundee
UTR	Untranslated region
UV	Ultraviolet
w/v	Weight per volume

Summary

Systemic infections caused by fungal pathogens pose a threat to immunocompromised patients worldwide. The structural integrity of fungi is mainly attributed to their rigid cell wall. The three layers of the fungal cell wall – chitin, glucan, and mannan – are mainly formed by carbohydrates. Mannan consists of proteins, mannoproteins, that carry N-linked glycans with a prominent mannose decoration. Mannoproteins have been shown to be involved in the detection of fungal pathogens by the immune system as well as adhesion factors of the pathogen to initiate invasion. The biosynthesis of mannoproteins occurs in the Golgi apparatus. The mannan polymerase complex M-Pol I, containing the glycosyltransferases Mnn9 and Van1, forms an α-1,6-linked mannose backbone that is the base for the extensive decoration of mannoproteins. The mechanisms by which M-Pol I identifies its substrates and its molecular mechanism are not known.

Initially, mannoproteins can be trapped in the fungal cell membrane by a GPI-anchor. The anchor can be cleaved and the mannoproteins will become loosely attached or covalently linked to the glucan in the cell wall. The enzymes involved in these processes are unknown or poorly characterised. The two extracellular fungal proteins Dfg5 and Dcw1 are homologs to the bacterial mannosidase Aman6. The enzymatic function of Dfg5 and Dcw1 is unknown. However, both proteins may be involved in the transglycosylation of GPI-anchored mannoproteins. Dfg5 and Dcw1 are essential in yeasts, making them excellent drug targets against fungal pathogens.

The aim of the work presented here was to structurally and enzymatically characterise the enzymes of the M-Pol I complex, Mnn9 and Van1, as well as the proteins Dfg5 and Dcw1 or their bacterial homolog Aman6. This would serve as a basis for the identification of potent inhibitors and their optimisation to lead compounds as antifungal drugs.

In this work the structure of *Saccharomyces cerevisiae* Mnn9 in complex with GDP and Mn^{2+} is described, the first in its family of glycosyltransferases (GT-62).

Mnn9 consists of a GT-A fold with an unusual extension formed by two β-strands. Mnn9 alone is able to synthesise α-1,6-mannotriose. A novel coupled enzyme assay was used to characterise Mnn9 enzymatically with $K_{m,app}$ = 6.5 mM for the substrate analogue and $K_{m,app}$ = 0.54 mM for the substrate donor GDP-Man. Furthermore, Mnn9 was shown to be manganese-dependent. Structure-guided mutagenesis led to the identification of residues important for the activity of the glycosyltransferase. *In vivo* studies in *S. cerevisiae* Δ*mnn9* knockout cells shows that the catalytic activity of Mnn9 is indispensable. Van1 alone, in contrast to Mnn9, shows no activity. Only in the presence of Mnn9 and its product, Van1 is able to synthesise α-1,6-linked oligomannose. The N- and C-terminus of Van1 are important for activity and/or dimerisation with Mnn9.

In addition, the bacterial mannosidase Aman6 was used as an essential part of the development of the novel enzymatic assay for Mnn9. Aman6 has further been used as a model for the essential fungal proteins Dfg5 and Dcw1. The structure of Aman6 is the first in its glycoside hydrolase familiy (GH-76) with a known enzymatic function. The mannosidase consists of 12 α-helices forming an α_6/α_6 barrel with six inner and six outer helices. The active site is surface exposed and the residues D124 and D125 are likely involved in the hydrolysis of the Aman6 substrate analogue α-1,6-mannobiose-4MU. Furthermore side chains close to both residues are important for binding and hydrolysis of the substrate. Aman6 was used to identify fragments that could act as potential inhibitors of the fungal homologues. However, none of these fragments inhibited the activity of Aman6 in an *in vitro* assay.

The results presented in this thesis can be the basis for further structural studies of the mannoprotein biosynthetic pathway as well as for the identification of potent inhibitors of the enzymes involved.

Contents

List of Figures

List of Tables

1 Introduction

1.1 Fungi

The fungal kingdom is believed to encompass 1.5–5.0 million species of which only 5 % have been classified today. Fungi can be found in many environments, such as soil, air, water and on decomposing material. Some fungi have adapted to even harsh conditions (Mehrotra and Aneja, 1990). The presence of fungi can have beneficial but also adverse effects on humans, animals, plants and bacteria. Humans use the yeast *Saccharomyces cerevisiae* for the fermentation of sugars to produce ethanol and carbon dioxide (*e. g.* to make bread). Mushrooms are part of the human diet. Other fungi live in a symbiotic relationship with algae or cyanobacteria to form lichen (Dobson, 2005). Secondary metabolites can be used as antibiotics (*e. g.* penicillin) or food additives (*e. g.* riboflavin). Fungi are also important saprophytes, decaying and liberating organic and inorganic material. However, to date more than 300 pathogenic fungi have been described to cause infections in humans, many others are animal and plant pathogens (Baron, 1996). Even though humans are constantly exposed to fungi, healthy individuals tend not to be affected by them. However, humans that have a weakened immune system or an altered bacterial flora have an increased risk to develop a fungal infection, such as candidiasis or aspergillosis.

1.1.1 Morphology of Fungi

Fungi are one of the kingdoms of life in the domain Eukarya (Moore, 1980). Most of the higher fungi are grouped into the phyla Ascomycota and Basidiomycota. Fungi are distinct from plants and animals in that they have a cell wall that contains both glucans and chitins. However, fungi also share features with these two kingdoms. In addition to a cell wall, fungi share the presence of vacuoles (Shoji *et al.*, 2006), the sexual and asexual reproduction and the formation of spores with plants (Mehrotra and Aneja, 1990). However, fungi lack chloroplasts, hence they are heterotrophic organisms like animals. Few fungi grow as unicellular yeast, but the majority form a thallus of tubular filaments, the hyphae.

1.1.2 Yeasts

Many Ascomycota and Basidiomycota are unicellular yeasts with a cell size of 2–50 µm in length and 1–10 µm in width. Two of the best studied fungi are yeasts, *S. cerevisiae* and *Candida albicans*.

Saccharomyces cerevisiae

S. cerevisiae is an unicellular, ellipsoid yeast with a diameter of 1–10 µm. Although it is not regarded as a pathogen, it is still a fungus of importance due to its wide use as a eukaryotic model organism in fundamental research. Its culture conditions are simple and it doubles every 90–120 min at 30 °C. Molecular techniques, such as transformations and gene knockouts can be easily carried out. Recently *S. cerevisiae* has been used as a model to study the effects of ageing (Wei *et al.*, 2011, Zadrag *et al.*, 2008), anti-cancer drugs (Matuo *et al.*, 2012) and to understand the formation of yeast biofilms, an important route of infection for *C. albicans* (see next section) (Bojsen *et al.*, 2012). Furthermore the principles of the secretory pathway, through which many of the fungal cell wall components are synthesised and secreted, has been extensively studied in *S. cerevisiae* (Barnes *et al.*, 1984,

Li *et al.*, 2005, Orlean, 1990, Ruiz-Herrera and Sentandreu, 1975, Tillmann *et al.*, 1987, Welten-Verstegen *et al.*, 1980).

Candida albicans

C. albicans is a commensal, polymorphic yeast found in over 60 % of the population (Odds, 1988). Healthy individuals can develop mild forms of candidiasis, commonly known as thrush, on the mucus membrane of the mouth, throat and vagina (Calderone and Clancy, 2002). However, immunocompromised patients and patients with an impaired bacterial flora, *e. g.* after antibiotic treatment (Seelig, 1966, Woods *et al.*, 1951), can suffer from the pathogenic effects of *C. albicans*. Systemic infections in immunocompromised patients have mortality rates of 30–40 % (Wisplinghoff *et al.*, 2004). *C. albicans* is also able to form biofilms on and in medical devices, resulting in systemic infections in patients that came in contact with the infected devices (Holmes *et al.*, 2006, Salamon *et al.*, 2007).

Various virulence factors, such as adhesins and hydrolytic enzymes, enable *C. albicans* to infect its host (Banno *et al.*, 1985, Barrett-Bee *et al.*, 1985, Fu *et al.*, 1998, Gaur and Klotz, 1997, Gaur *et al.*, 1999, Hube *et al.*, 1991, Staab *et al.*, 1996, Wright *et al.*, 1992). Many of the adhesins are in fact glycosylated proteins, highlighting the importance of this post-translational modification for the virulence of *C. albicans*. For example, a double knockout of the mannosylated *Candida* spp. adhesin Hwp1 led to reduced virulence in a mouse model (Staab *et al.*, 1999). Deletion of the gene encoding the α-1,2-mannosyltransferase Mnt1 leads to an avirulent strain (Buurman *et al.*, 1998). This shows that the glycosyltransferases (GT) involved in the glycosylation of proteins are potential drug targets against *C. albicans*.

1.1.3 Filamentous fungi

Aspergillus fumigatus

A. fumigatus is a saprophytic fungus that survives and grows on organic material (Haines, 1995, Pitt, 1994). Its airborne conidia can easily reach the lung alveoli due to their small size of 2 µm (Raper and Fennell, 1965). Inhaling these conidia is usually no problem for immunocompetent individuals, because they can be easily cleared by the innate immune system (Hospenthal *et al.*, 1998). However, in immunocompromised patients *A. fumigatus* can cause severe and often lethal invasive aspergillosis (IA), making it the most prevalent airborne fungal pathogen (Bodey and Vartivarian, 1989, Denning, 1998, Dixon *et al.*, 1996). To increase chances of survival for patients with IA, quick and reliable diagnosis of an *A. fumigatus* infection is crucial. The most common antigens for a serological diagnosis are an RNase (Lamy and Davies, 1991, Lamy *et al.*, 1991, Latgé *et al.*, 1991), a catalase (Calera *et al.*, 1997, Hearn *et al.*, 1992, Lopezmedrano *et al.*, 1995) and a dipeptidylpeptidase (Beauvais *et al.*, 1997, Harvey and Longbottom, 1987, Kobayashi *et al.*, 1993). In addition, the presence of galactomannan (GM), a cell wall component, is used clinically as a diagnostic marker. GM is the only polysaccharide antigen that has been characterised in *A. fumigatus*. GM has been identified to contain a linear mannan backbone of α-1,2- and α-1,6-linked mannose (Man) residues with the antigenic part made of β-1,5 galactofuranosyl residues linked to two α-1,2-Man (Azuma *et al.*, 1971, Bardalaye and Nordin, 1977, Barretobergter and Travassos, 1980, Bennett *et al.*, 1985, Latgé *et al.*, 1994, Mischnick and Deruiter, 1994, Van Bruggen-Van Der Lugt *et al.*, 1992). Interestingly, this epitope is also present on intra- and extracellular glycoproteins (Latgé *et al.*, 1994).

Other components of the *A. fumigatus* conidial cell wall are putative virulence factors. Amongst these are adhesins that bind to host proteins, such as fibrinogen (Annaix *et al.*, 1992, Bouchara *et al.*, 1988, Coulot *et al.*, 1994), Igs (Sturtevant and Latgé, 1992) and collagen (Thau *et al.*, 1994). Hydrophobic, low molecular weight and highly stable proteins (hydrophobins) confer hydrophobic properties on

A. fumigatus conidia (Thau *et al.*, 1994). One of the genes encoding for such a protein, RodA, has been deleted (Parta *et al.*, 1994, Thau *et al.*, 1994). Mortality rates remained comparable in an animal IA model, but the inflammatory response was retarded (Thau *et al.*, 1994). Carbohydrates present in the conidial cell wall can bind specifically to host proteins, such as pulmonary surfactant proteins A and D (Madan *et al.*, 1997), or in the form of fucose and sialic acid-specific lectins (Bouchara *et al.*, 1997). A conidial cell wall glycoprotein confers laminin binding (Tronchin *et al.*, 1997). These early results highlight the importance of a functional carbohydrate system in *A. fumigatus* for pathogen-host interaction. Any impact on this biosynthesis pathway may have a negative effect on virulence.

1.1.4 Treatment of Fungal Infections

Because fungi have many common features, *i. e.* cell wall and similar biosynthetic pathways, infections by *C. albicans* and *A. fumigatus* can often be treated with the same drugs. The major drugs or drug classes used today to treat systemic fungal infections are amphotericin B (AmB), the azoles itraconazole and voriconazole, and caspofungin (Gallis *et al.*, 1990, Johnson and Kauffman, 2003). Even though they are efficient at killing *A. fumigatus* under *in vitro* conditions, their efficacy *in vivo* remains low resulting in the high mortality rates of IA patients of 80–90 %. The mechanism of how AmB works is still not completely understood (Brajtburg and Bolard, 1996). It is known that it binds to membrane sterols (Bolard, 1986), and thus creates channels that lead to the increased permeability of cations. In addition, it inhibits proton ATP pumps, leading to a decrease in cellular energy (Brajtburg *et al.*, 1985, Ramos *et al.*, 1989, Surarit and Shepherd, 1987). However, AmB can cause severe side effects in the patient (Clements and Peacock, 1990, Surarit and Shepherd, 1987). In contrast, the mode of action of the azoles is well understood (van den Bossche *et al.*, 1987). The free azole nitrogen competes with the heme iron of cytochrome P450 14α-demethylase. This prevents the synthesis of ergosterol in the membrane. As a result, this eventually leads to the accumulation

of phospholipids and unsaturated fatty acids within the fungal cell due to a lack of deposition in the membrane. A major drawback of the azoles is the recent development of resistance against this class of drugs in *Candida* spp. and *A. fumigatus* (Chryssanthou, 1997, Denning *et al.*, 1997a,b, Perfect *et al.*, 2003). One explanation for this resistance is the possibility of an altered affinity of 14α-demethylase for the drug (Tobin *et al.*, 1997). The most recently approved drug against fungal infections by *C. albicans* and *A. fumigatus* is caspofungin, a member of the echinocandins (Deresinski and Stevens, 2003). It is a semi-synthetic lipopeptide connected to a fatty acid chain. Caspofungin's target is the β-1,3-glucan synthase. β-1,3-glucan is a major component of the fungal cell wall (see p. 11). The inhibition of β-1,3-glucan synthase results in an osmotically unstable cell wall, affecting viability. Caspofungin has fewer side effects than AmB or the azoles because β-1,3-glucan is not present in the human body. In contrast to *C. albicans* where caspofungin is fungicidal (Ernst *et al.*, 1999), it is only a fungistatic for *A. fumigatus* (Kurtz *et al.*, 1994). A possible explanation for the fungistatic effect is the concentration of β-1,3-glucan in the apical tips during growth of *A. fumigatus*. However, recent reports demonstrate the development of resistance against caspofungin in both fungal pathogens (Krogh-Madsen *et al.*, 2006, Pang *et al.*, 2012, Thompson *et al.*, 2008).

1.2 Fungal cell wall

The cell wall is the outer layer of a fungal cell and defines its shape by providing resistance against the turgor. The wall is composed of carbohydrates and proteins that are linked at the intra- and intermolecular level (Fig 1.1). These connections provide many benefits for the cell, such as the controlled passage of macromolecules to and from the cell, protection from the environment and to shield the cell from the host immune system - particularly important for pathogenic fungi. However, the wall also provides socialising features for the cell, such as the presentation of agglutinins and flocculins.

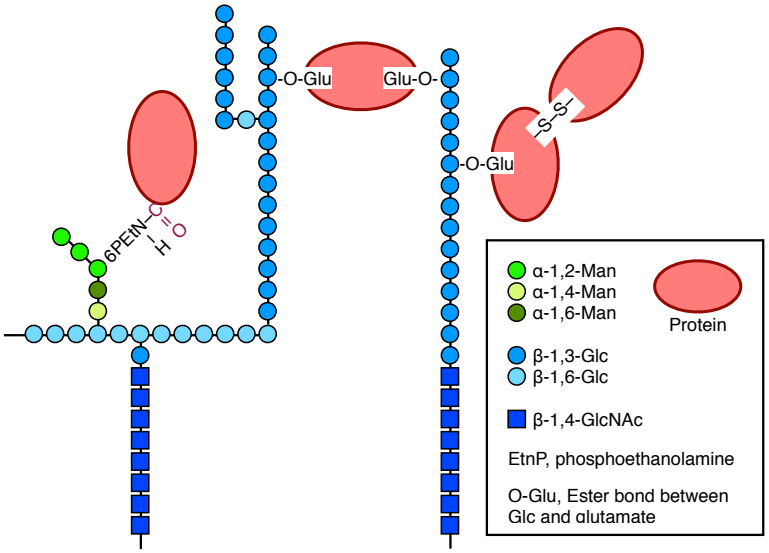

Figure 1.1: Components of and cross-links in the fungal cell wall. Chitin, made of β-1,4-linked GlcNAc, is located on top of the extracellular face of the plasma membrane. β-Glucan is covalently linked to chitin and is acting as a matrix for the integration of mannoproteins and O-linked glycosylated proteins. Figure adapted from Orlean 2013

The cell wall can account for 15–30 % of the cell dry weight (Aguilar-Uscanga and François, 2003, Yin *et al.*, 2007). In *S. cerevisiae* the wall can reach a thickness of 100–200 nm (Dupres *et al.*, 2010, Yamaguchi *et al.*, 2011). To date, about 180 proteins have been identified that are directly involved in the biosynthesis and remodelling of the wall (Orlean, 2013). Over 90 % of the fungal cell wall consists of carbohydrates. In *S. cerevisiae* and *C. albicans* these carbohydrates are β-1,3- and β-1,6-glucan, chitin and mannose on mannoproteins. These mannoproteins form the outermost layer of the wall, mannan. In contrast, the cell wall of *A. fumigatus* additionally contains α-1,3-glucan and galactomannan. β-1,6-glucan plays an important role, as it provides a network to which all of the other cell wall components can be linked (Kollár *et al.*, 1997). The function of mannoproteins is not well understood. The function of mannosylated proteins can span from hydrolase and transglycosidase activity to provide structural features or act as agglutinins and flocculins (Beauvais *et al.*, 2009, Bojsen *et al.*, 2012, Reynolds and Fink, 2001).

The composition of the cell wall has been identified by chemical and enzymatic release of the individual components (Fleet, 1991). Cells were first treated with

alkali and acid to release the polysaccharides. The alkali wash releases the glucans depending on the intermolecular links between glucan and chitin (Magnelli *et al.*, 2002). Mannoproteins linked to the glucan are released by an acid treatment (Dallies *et al.*, 1998, Ram *et al.*, 1994). Further enzymatic digests with specific hydrolases release carbohydrates for further analysis of their composition and linkages (Aimanianda *et al.*, 2009, Boone *et al.*, 1990, Magnelli *et al.*, 2002).

Despite its rigid nature, the cell wall and its components undergo many changes depending on the stage of the cell cycle, growth phase, availability of nutrients, or environmental stress (de Nobel and Barnett, 1991). Interestingly, the cell walls of cells in logarithmic growth are more porous compared to cells in the stationary phase. It has been shown that glycoproteins with a molecular mass of 400 kDa can pass from the cell into the medium while at logarithmic growth (de Nobel *et al.*, 1990, Kuranda and Robbins, 1991). However, it is unclear if this is due to fewer cross-links while the cells are growing or if the proteins are released whilst the mother cell wall is degraded during budding.

1.2.1 Chitin

Characteristics of Chitin

Chitin is a carbohydrate polymer made of β-1,4-*N*-acetylglucosamine (GlcNAc) (Fig. 1.2). It is only a minor component of the cell wall (1–2 % in *S. cerevisiae* or 7–15 % in *A. fumigatus*) (Fontaine *et al.*, 2000). Chitin is usually found in the budding neck between a mother cell and bud, in the division septum, and in the lateral wall of daughter cells. The polymer can be visualised by staining cells with Calcofluor White (CFW). Furthermore, the amount of chitin can be determined by an alkali/acid wash followed by the specific enzymatic hydrolysis of the polymer, *e. g.* by a chitinase of *Serratia* spp., and the measurement of the released GlcNAc by ion-exchange chromatorgraphy (Dallies *et al.*, 1998, Kang and Cabib, 1986, Magnelli *et al.*, 2002, Orlean *et al.*, 1985). Interestingly, chitin exists in three different forms in the cell wall. It can exist as free chitin, bound to β-1,3-glucan, or linked

to β-1,6-glucan which itself is linked to β-1,3-glucan and mannan (Cabib, 2009, Cabib and Durán, 2005). It has been shown that the rigidity of the *S. cerevisiae* cell wall is the result of the covalent cross-link between chitin and glucan.

Synthesis and remodelling of Chitin

In *S. cerevisiae* three enzyme complexes are known to be involved in the synthesis of chitin: Chitin synthase (CS) I–III. The complexes need the activity of the three enzymes Chs1, Chs2, and Chs3. All three enzymes are located in the plasma membrane, use UDP-GlcNAc as their donor and belong to the GT-2 family of processive inverting GTs (Jimenez *et al.*, 2010, Merzendorfer, 2011). The sequence QXRRW has been identified as a signature motif for chitin synthases (Cos *et al.*, 1998, Merzendorfer, 2011, Nagahashi *et al.*, 1995, Ruiz-Herrera *et al.*, 2002, Saxena *et al.*, 1995, Yabe *et al.*, 1998). The exact mechanism of chitin synthesis remains unknown. However, studies performed with bacterial homologs (NodC) or non-fungal chitin synthases support a mechanism where chain extension occurs at the non-reducing end of the chitin polymer (Imai *et al.*, 2003, Kamst *et al.*, 1999). The length and amount of the chitin present in the *S. cerevisiae* cell wall is highly variable. Increased amounts of chitin can be found if the synthesis of other cell wall components, such as β-glucan, mannan or GPI anchors, is negatively affected (Grabinska *et al.*, 2007). The majority of chitin synthesis in *S. cerevisiae* is carried out by Chs3 (Orlean, 1987). Chs3 is highly dependent on four auxiliary proteins

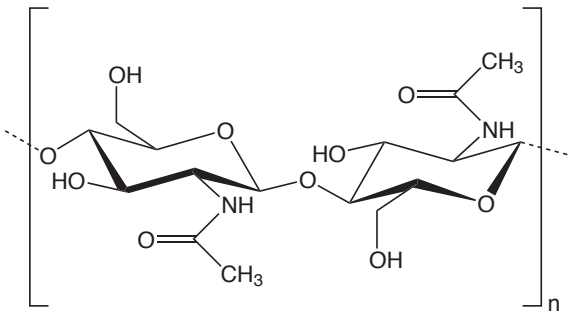

Figure 1.2: Chemical structure of chitin. Chitin is a polymer made of N-acetylglucosamine linked vi an β-1,4-O-glycosidic bond

(Chs4–7) that activate and regulate the synthase along the secretory pathway until it reaches the plasma membrane (Gonzalez Montoro *et al.*, 2011, Lam *et al.*, 2006, Santos and Snyder, 1997, Santos *et al.*, 1997, Ziman *et al.*, 1998). Cells lacking Chs7, for example, show very similar effects on chitin levels as *chs3*Δ cells (Trilla *et al.*, 1999).

Chitin synthesis in *A. fumigatus* is carried out by at least eight chitin synthases (*Af*ChsA-G and *Af*ChsE') (Mellado *et al.*, 1996a,b, 2003, Munro and Gow, 2001), and five of them are unique to filamentous fungi (*Af*ChsC, *Af*ChsD, *Af*ChsG, *Af*ChsE, and *Af*ChsE') (Mellado *et al.*, 2003). They are grouped into two groups, based on the location of sequence motifs within the synthase (Latgé and Calderone, 2006). Cells lacking *Af*ChsA, *Af*ChsB, *Af*ChsC, *Af*ChsD, or *Af*ChsF show no growth phenotype compared to wild type cells (Mellado *et al.*, 1996a,b). In contrast, *chsE*Δ and *chsG*Δ cells show altered growth, reduced mycelial chitin, reduced chitin synthase activity and swollen hyphae (Aufauvre-Brown *et al.*, 1997, Mellado *et al.*, 1996a). The regulation of chitin synthesis in *A. fumigatus* has not been characterised yet.

Chitinases cleave the glycosidic bond between β-1,4-GlcNAc residues. *S. cerevisiae* has two chitinases, Cts1 and Cts2. Cts1 is a plant-type chitinase with a potential endo-hydrolytic activity (Hurtado-Guerrero and van Aalten, 2007) whereas Cts2 is a bacterial-like chitinase presumably showing exo-hydrolytic activity (Brurberg *et al.*, 1996) (see explanation in 1.4, p. 38). Both chitinases are found to be heavily O-mannosylated (Kuranda and Robbins, 1991). The function of Cts2 is only poorly understood. *cts1*Δ cells form cell aggregates joined at their chitin-containing septa, highlighting the importance of Cts1 for cell separation (Kuranda and Robbins, 1991).

A. fumigatus has 18 predicted chitinases (Gastebois *et al.*, 2009). Five belong to the fungal/plant-like chitinases, twelve to the fungal/bacterial-like chitinases and one is a class C chitinase. However, their function remains largely unknown. Upon deletion of one of the fungal/bacterial-like chitinases (ChiB1) the fungus developed no apparent phenotype (Jaques *et al.*, 2003).

1.2.2 Glucan

Characteristics of Glucan

Glucan represents the majority of carbohydrates found in the fungal cell wall, making up to 30–60 % of the cell wall dry weight. It is formed by α- or β-linked glucose polysaccharides. *S. cerevisiae* and *C. albicans* possess only β-1,3- and β-1,6-glucan, whereas the cell wall of *A. fumigatus* also contains α-1,3-glucan. Not only is glucan the major part of the cell wall, it is also important for the integrity of the cell as it serves as a platform to which all the other cell wall components can be covalently linked (Fig 1.1). This link occurs via glycosidic bonds between the carbohydrates of the cell wall components.

β-1,3-glucan

The synthesis of β-1,3-glucan is dependent on the proteins of the Fks family and the regulatory subunit Rho1 GTPase. Fks1, Fks2, and Fks3 are UDP-glucose (UDP-Glc) dependent, belong to GT-48 and are located in the plasma membrane (Drgonová *et al.*, 1996, Kang and Cabib, 1986, Mazur and Baginsky, 1996, Qadota *et al.*, 1996, Shematek *et al.*, 1980). Fks1 and Fks2 are essential proteins, and Fks1 is responsible for the majority of the β-1,3-glucan biosynthesis (Inoue *et al.*, 1995, Mazur *et al.*, 1995). However, the mechanism of glucan biosynthesis is unknown. The growing β-1,3-glucan chain is exported through the membrane and can be linked to chitin by Crh1 and Crh2, two translycosylaes (Cabib, 2009), further extended by Gas1 (Mouyna *et al.*, 2000a), or decorated with β-1,6-Glc (Ecker *et al.*, 2006).

β-1,3-glucan undergoes constant remodelling once it has been deposited to the cell wall. In *S. cerevisiae* the Gas1 family members Gas1–5, GH-72 β-1,3-glucanosyltransferases, are responsible for these changes (de Groot *et al.*, 2003, Popolo and Vai, 1999). They cleave β-1,3-glucan and transfer the new reducing end to an existing non-reducing end of another β-1,3-glucan chain (Carotti *et al.*, 2004, Mazáň *et al.*, 2011, Mouyna *et al.*, 2000a, Ragni *et al.*, 2007b). All pro-

teins contain a GPI-ω-attachment site (Caro *et al.*, 1997, de Groot *et al.*, 2003, Fankhauser *et al.*, 1993) and Gas1, Gas3, and Gas5 have been found to be covalently linked to the cell wall (De Sampaïo *et al.*, 1999, Yin *et al.*, 2005). Cells of a *S. cerevisiae gas1*Δ knockout have increased chitin and mannan content (Popolo *et al.*, 1997, Ram *et al.*, 1995, Valdivieso *et al.*, 2000) and release β-1,3-glucan into the medium (Ram *et al.*, 1998), indicating that Gas1 is important for the incorporation of β-1,3-glucan chains into the cell wall. Whilst Gas1, Gas3, and Gas5 can be found in vegetative cells, Gas2 and Gas4 are only found in sporulating cells. A double knockout of *gas2* and *gas4* leads to sporulation defects (Ragni *et al.*, 2007a). Similar remodelling of β-1,3-glucan occurs also in *A. fumigatus*. The GPI-anchored β-1,3-glucanosyltransferases Gel1 and Gel2, both GH-72 members as well, perform these reactions in the filamentous fungus (Hartland *et al.*, 1996, Mouyna *et al.*, 2000b). Both enzymes have the same activity as Gas1 in *S. cerevisiae* (Mouyna *et al.*, 2000a, 2005).

Further reorganisation of the β-1,3-glucan is achieved by many exo- and endo-β-1,3-glucanases present in the*S. cerevisiae* cell wall (Baladrón *et al.*, 2002, Cappellaro *et al.*, 1998, Larriba *et al.*, 1995, Mrsa *et al.*, 1993, Sestak *et al.*, 2004). None of the glucanases known so far are essential. Most of them are for cell wall maintenance. Bgl2, an endo-β-1,3-glucanase, is believed to be involved in branching of the β-1,3-glucan as it is not only able to hydrolyse β-1,3-links but also able to create β-1,6-links (Goldman *et al.*, 1995). Deletion Bgl2 and other glucanases has only minor effects on the cells, usually manifested in an increased chitin content (Cappellaro *et al.*, 1998, Klebl and Tanner, 1989, Sestak *et al.*, 2004). In *A. fumigatus* β-1,3-glucanases are important during conidial germination and mycelial branching. The only characterised enzyme of this class is the endo-β-1,3-glucanase Eng1 (Mouyna *et al.*, 2002). However, the deletion does not lead to a phenotype.

Synthesis of β-1,6-glucan

To date, the *in vivo* biosynthesis of β-1,6-glucan has not been characterised. Two major drawbacks make it difficult to identify the protein(s) involved in the synthesis. Firstly, if there is only a single essential β-1,6-glucan synthase it is impossible to screen for knockouts of this synthase (Lesage and Bussey, 2006). Secondly, in the case of multiple synthases, all of them could have redundant activity and mutations in individual synthases would not give any phenotype. Additionally, β-1,6-glucan is widely present in fungi, whereas most other organisms lack glucan, making it difficult to study homologous enzymes. *Actinobacillus suis* synthesises a β-1,6-glucan attached to a lipopolysaccharide, but its biosynthesis has not been characterised (Monteiro *et al.*, 2000). Other bacteria synthesise a β-1,6-GlcNAc polymer with GT-2 synthases that resemble the *S. cerevisiae* Chs transferases (Gerke *et al.*, 1998, Itoh *et al.*, 2008). Taking all of this into account, a potential β-1,6-glucan synthase could define a new GT family or a otherwise known GT is able to form β-1,6-glycosidic bonds using UDP-Glc as the donor.

Synthesis of α-1,3-glucan

In addtion to the two types of β-glucan discussed above, the *A. fumigatus* cell wall also contains α-1,3-glucan (Latgé and Calderone, 2006). However, much like with β-1,6-glucan, the exact mechanism or substrate for α-1,3-glucan synthesis *in vivo* is unknown. Two genes, AGS1 and AGS2, have been identified in *A. fumigatus* based on homology with the AGS genes in *S. pombe* (Beauvais *et al.*, 2005), that may act as α-1,3-glucan synthases. Neither of the two *A. fumigatus* proteins is essential. Both proteins contain two amylase-like domains and a glycogen-like domain carrying a UDP-Glc-binding motif (Beauvais *et al.*, 2005). The amount of α-1,3-glucan can be reduced to approximately 50 % by deletion of AGS1 and the expression level of AGS2 is upregulated upon deletion of AGS1, indicating that they can compensate for each other (Beauvais *et al.*, 2005).

1.2.3 Mannan

Characteristics of Mannan

Mannan forms the outer layer of the fungal cell wall. It is formed by mannoproteins that bear N- and O-linked glycans. Some of the mannoproteins carry a GPI anchor which traps them in the plasma membrane (Fig. 1.3), others are covalently linked to the β-glucan via glycosidc bonds between the glycan of a GPI anchor remnant and the β-glucan (Fig. 1.1). Mannan consists of three types of proteins. The first group consists of hydrolases and transglycosidases that are involved in the formation and remodelling of the cell wall. The second group encompasses agglutinins and flocculins, important factors for cell-cell adhesion (Dranginis *et al.*, 2007, Goossens and Willaert, 2010, Klis *et al.*, 2006, 2010). The third group is formed by proteins that carry long extracellular Ser/Thr-rich N-termini and are trapped in the plasma membrane by a single-pass domain and a short C-terminal cytosolic tail (Levin, 2011). Members of this group are thought to act as mechanosensors that detect cell wall stress and can induce rescue pathways (Rodicio and Heinisch, 2010).

Members of the first two groups can be covalently linked to the β-glucan present in the fungal cell wall and are referred to as cell wall proteins (CWP) (Yin *et al.*, 2005). CWPs can be subdivided into three groups: 1) GPI proteins have a GPI-anchor that fixes them in the plasma membrane (Gonzalez *et al.*, 2009) (Fig. 1.1 and 1.3). However, the GPI can be cleaved and eventually the protein will be covalently linked to β-1,6-glucan via a GPI remnant (Gonzalez *et al.*, 2009). Some of these proteins are enzymatically active, others may have purely structural roles in the cell wall. 2) Proteins that can be released by alkali treatment or β-1,3-glucanases (Mrsa *et al.*, 1997, Tohe *et al.*, 1993), which are referred to as proteins with internal repeats (PIR), since they carry multiple copies of the DGQ(hydrophobic residue)Q motif (Klis *et al.*, 2010). These proteins are linked to the β-1,3-glucan via ester bonds that are formed between an glutamine of the repeat sequence and a glucose (Ecker *et al.*, 2006). 3) Proteins linked via disulfide-bonds, which can be released by reducing agents (Cappellaro *et al.*, 1998, Moukadiri *et al.*, 1999,

Moukadiri and Zueco, 2001, Orlean *et al.*, 1986, Rosa Insenser *et al.*, 2010). These proteins create a shield to prevent glycoside hydrolases (GHs) from degrading the cell wall polysaccharides (Zlotnik *et al.*, 1984).

Synthesis of Mannoproteins

Membrane and cell wall proteins are synthesised along the secretory pathway. Proteins will receive N- and O-linked glycosylation as well as a GPI-anchor on the lumenal side of the endoplasmic reticulum (ER). Further modifications of the glycans occur in the Golgi apparatus. The modified proteins are deposited in the plasma membrane or secreted to become covalently attached to the cell wall carbohydrates. The processes involved in the secretory pathway have been extensively studied in *S. cerevisiae*. Hence, the processes will be described as they occur in baker's yeast. Differences, if known, to other fungi will be pointed out.

N-linked Glycosylation The glycosylation of asparagine residues in a discrete sequon (N-X-S/T, where X can be any amino acid except P) is called N-linked glycosylation. Proteins are glycosylated in a one-step reaction with a glycan that is synthesised on the cytoplasmic and lumenal face of the ER (Burda *et al.*, 1999, Helenius and Aebi, 2004, Larkin and Imperiali, 2011, Lehle *et al.*, 2006) (Fig 1.4). The initial steps of glycan formation occur on the cytosolic face of the ER. GlcNAc-1-P is transferred from UDP-GlcNAc to dolichol phosphate by the GT Alg7 (Barnes *et al.*, 1984). The heterodimeric Alg13/Alg14 adds a β-1,4-GlcNAc (Bickel *et al.*, 2005, Chantret *et al.*, 2005, Gao *et al.*, 2005) which is further extended with β-1,4-Man by Alg1 (Couto *et al.*, 1984). Subsequently, Alg2 transfers α-1,3-Man and α-1,6-Man (Kaempf *et al.*, 2009, O'Reilly *et al.*, 2006). The cytoplasmic part of the glycan synthesis is finished with the addition of an α-1,2-Man by Alg11 resulting in a Dol-PP-$GlcNAc_2Man_5$ glycan (Absmanner *et al.*, 2010, Cipollo *et al.*, 2001, O'Reilly *et al.*, 2006).

To date, it is unknown how the Dol-PP precursor translocates through the ER membrane, but a potential flippase is Rft1 (Helenius *et al.*, 2002). After transloca-

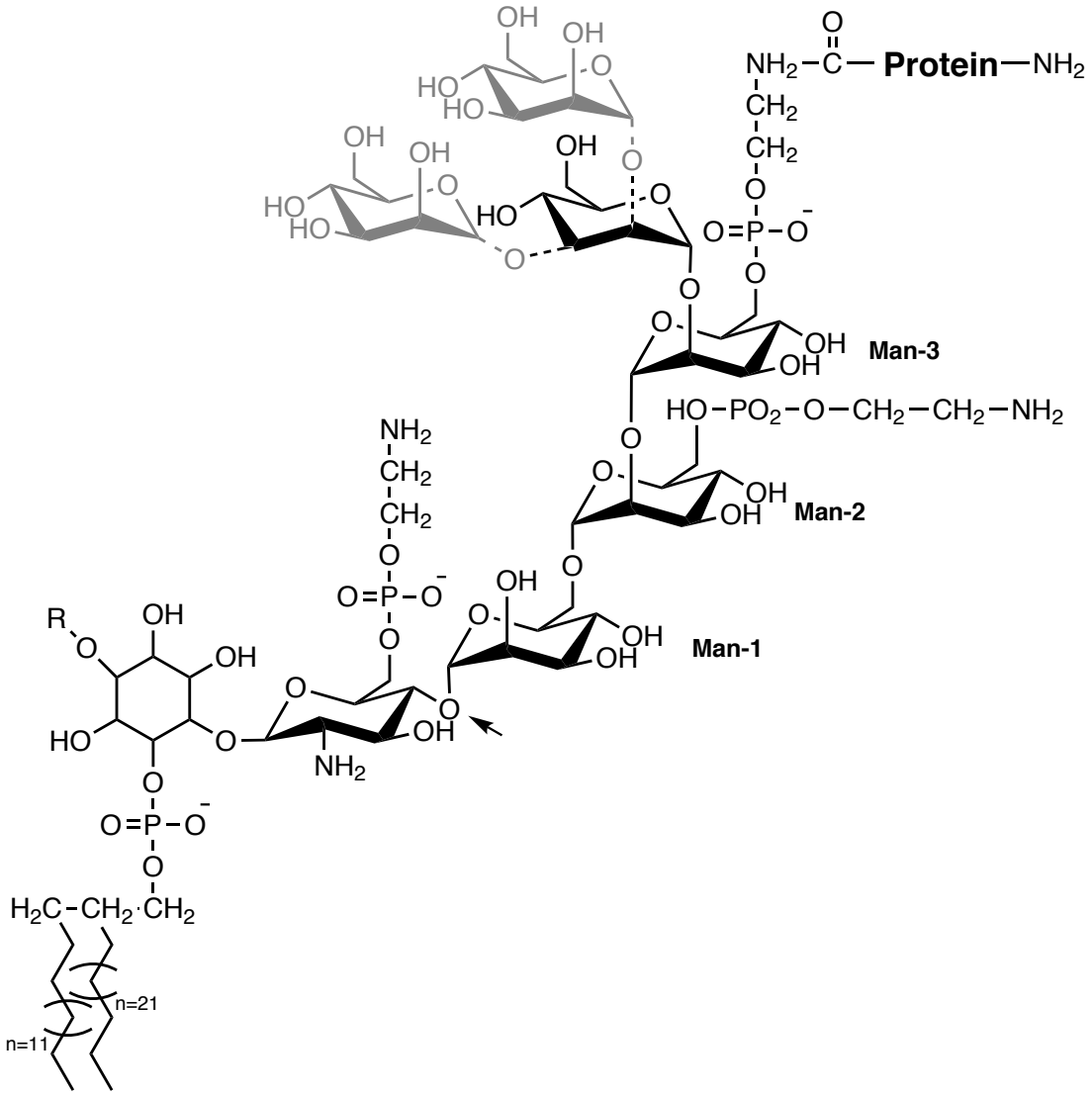

Figure 1.3: Structure of the *S. cerevisiae* GPI-anchor. The protein is linked to phosphoethanolamine and connected via a glycan core to the phosphatidylinositol (PI) residue and the fatty acids that keep the GPI-anchored protein membrane-bound. The grey α-1,2- and α-1,3-linked mannose residues represent alternative products of the last Golgi-located transferase reaction. The arrow indicates the site of hydrolysis creating the GPI-remnant protein structure that will be transferred onto α-1,6-glucan in the cell wall.

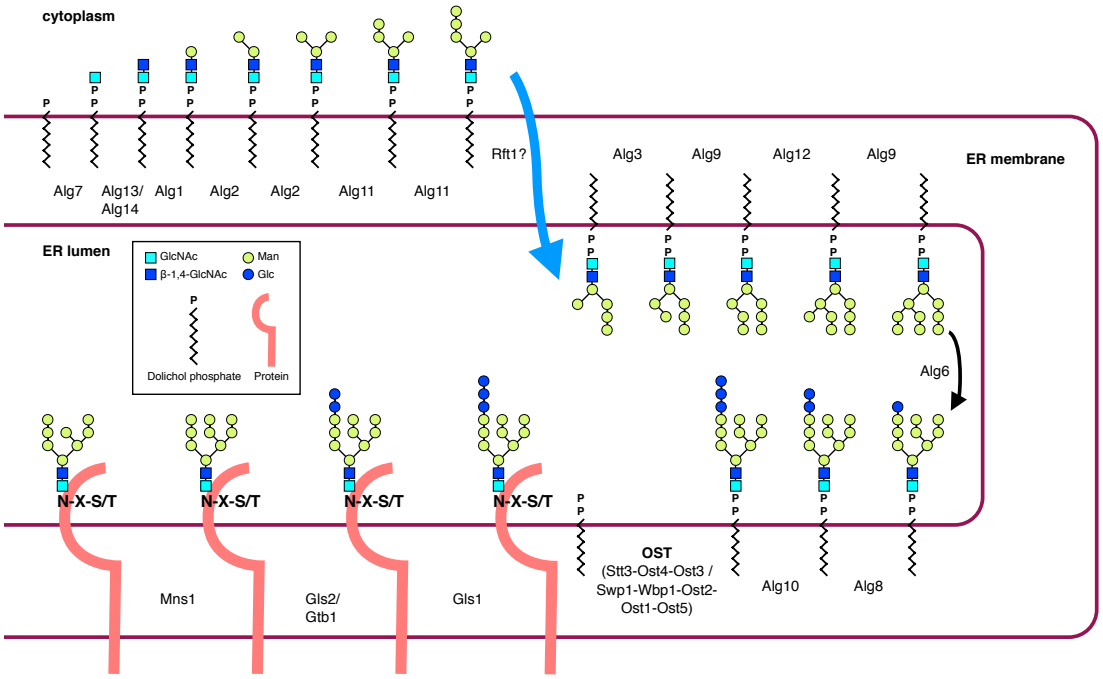

Figure 1.4: N-linked glycosylation in the ER. A precursor glycan is formed by the orchestrated interaction of multiple GTs and GT complexes on the cytoplasmic and lumenal side of the ER. The precursor is transferred in a single-step reaction onto an asparagine residue in a growing, nascent peptide chain. Figure adapted from Orlean 2013

tion, Dol-PP-$GlcNAc_2Man_5$ is further extended on the lumenal side of the ER by a plethora of membrane-bound GTs. In contrast to the cytosolic transferases, the lumenal GTs use sugars activated by Dol-P instead of UDP (UDP-GlcNAc) or GDP (GDP-Man). The α-1,6-Man of the precursor is extended with α-1,3-Man by Alg3 (Aebi *et al.*, 1996, Sharma *et al.*, 2001), α-1,2-Man by Alg9 (Burda *et al.*, 1999, Cipollo and Trimble, 2002), α-1,6-Man by Alg12 (Burda *et al.*, 1999), and another α-1,2-Man by Alg9 (Frank and Aebi, 2005) to produce Dol-PP-$GlcNAc_2Man_9$. The α-1,2-Man that was added by Alg11 on the cytosolic side is extended with two α-1,3-Glc by the transferases Alg6 and Alg8 (Reiss *et al.*, 1996, Stagljar *et al.*, 1994). The formation of the glycan is finished with the addition of an α-1,2-Glc by Alg10 (Burda and Aebi, 1998) to form the Dol-PP-$GlcNAc_2Man_9Glc_3$ precursor.

The glycan precursor is transferred from Dol-PP in a single step by the oligosaccharyltransferase complex (OST) to the asparagine in the sequon N-X-S/T of nascent growing polypeptide chains that are synthesised by ribosomes of the rough ER

(Kelleher and Gilmore, 2006, Knauer and Lehle, 1999, Larkin and Imperiali, 2011, Lehle *et al.*, 2006, Lennarz, 2007, Yan and Lennarz, 2005). The recent structure of a bacterial OST gave first insights into the mechanism of this transfer (Lizak *et al.*, 2011). OST contains two binding sites, one for the glycan donor and one for the protein that will receive the N-linked glycosylation. The sites are connected through a tunnel in which the acceptor asparagine can bind. In yeast, OST is formed by Stt3, Ost1, Ost2, Wbp1, Swp1, Ost4, Ost5, and Ost3 or Ost6 (Schwarz *et al.*, 2005, Spirig *et al.*, 2005, Yan and Lennarz, 2005). The proteins form three different subunits (1, Swp1+Wbp1+Ost2; 2, Stt3+Ost4+Ost3/Ost6; 3, Ost1+Ost5) (Karaoglu *et al.*, 1997, Kelleher and Gilmore, 2006, Kim *et al.*, 2003, Knauer and Lehle, 1999, Li *et al.*, 2003, Reiss *et al.*, 1997, Spirig *et al.*, 1997). Stt3 has been identified as the catalytically active enzyme of the complex (Hese *et al.*, 2009, Kelleher *et al.*, 2007, Lizak *et al.*, 2011, Wacker *et al.*, 2002, Yan and Lennarz, 2002). The other subunits are important to delay protein folding (Ost3 or Ost6) (Kelleher and Gilmore, 2006, Schulz and Aebi, 2009), for donor substrate specificity (Swp1, Wbp1, Ost2) (Kelleher and Gilmore, 2006, Pathak *et al.*, 1995), for recruitment of other subunits (Ost4) (Karaoglu *et al.*, 1997, Knauer and Lehle, 1999, Spirig *et al.*, 2005) and for the translocation of the growing peptide chain (Ost1) (Lennarz, 2007).

The steps after the transfer by OST are important for protein quality control (Aebi *et al.*, 2010, Herscovics, 1999). Only properly folded proteins will be exported from the ER. In contrast, misfolded proteins will be sent for degradation. The processes involved in quality control begin by the removal of the α-1,2-Glc by Gls1/Cwh41 (glucosidase I) (Romero *et al.*, 1997) followed by the trimming of the two α-1,3-Glc by Gls/Ro2 and Gtb1 (glucosidase II) (Quinn *et al.*, 2009, Trombetta *et al.*, 1996). Eventually, Mns1 (mannosidase I) removes α-1,2-Man to produce $GlcNAc_2Man_8$ (Herscovics, 1999, Jakob *et al.*, 1998). Only correctly folded proteins carrying this trimmed glycan will be exported from the ER. If a protein is misfolded it will be bound by Pdi1 which removes another Man to form $GlcNAc_2Man_7$ (Clerc *et al.*, 2009). The misfolded protein will then be degraded by the ER-associated protein degradation system (Helenius and Aebi, 2004).

Glycosylation in the Yeast Golgi Apparatus N-linked glycosylated proteins that arrive from the ER can be further extended in the *cis*-Golgi apparatus by mannose to form a core-type glycan or can be decorated with 150–200 Man to form mannoproteins (Ballou *et al.*, 1990, Jigami, 2008) (Fig. 1.5). The Man is transferred from GDP-Man by a large number of redundant GTs.

Och1 initiates the formation of core-type glycosylation and mannoproteins by the transfer of a α-1,6-Man to the α-1,3-Man added by Alg2 in the ER (Nakayama *et al.*, 1997). Deletion of OCH1 results in severe growth defects (Nakayama *et al.*, 1997).

The formation of the poly-α-1,6-Man backbone of mannoproteins occurs in the *cis*-Golgi apparatus by the two heteromeric GT complexes M-Pol I and M-Pol II (Hashimoto *et al.*, 1997, Jungmann and Munro, 1998, Jungmann *et al.*, 1999). M-Pol I is formed by the two homologous GT-62 GTs Mnn9 and Van1. M-Pol I adds the first 10–15 α-1,6-Man to the Man that has been attached by Och1 (Rodionov *et al.*, 2009, Stolz and Munro, 2002). To date, results suggest that Mnn9 adds the first α-1,6-Man whilst Van1 adds the remaining Man residues (Stolz and Munro, 2002). Further elongation of up to 80 α-1,6-Man is carried out by the heteroheptameric complex M-Pol II containing Mnn9, Anp1, Hoc1, Mnn10, and Mnn11 (Jungmann *et al.*, 1999).

In contrast, core-type mannoproteins receive an α-1,2-Man by an unknown GT, which is added to the α-1,6-Man added by Och1. This addition blocks it from further elongation to a α-1,6-Man backbone. Mnn1 further elongates the N-linked glycan with three more α-1,3-Man residues (Lewis and Ballou, 1991).

To date, it is unclear how the transferases in the yeast Golgi can discriminate between proteins that will receive the poly-α-1,6-Man-backbone or the core-type structure. The GT that adds the α-1,2-Man to the Och1-derived α-1,6-Man has not been identified yet. However, it has been proposed that either the unidentified GT(s) or M-Pol I are able to determine if a protein receives the core-type mannosylation or becomes hypermannosylated. A proposed mechanism assumes that Mnn9 is able to perform the GT reactions that lead to α-1,6-linked or α-1,2-

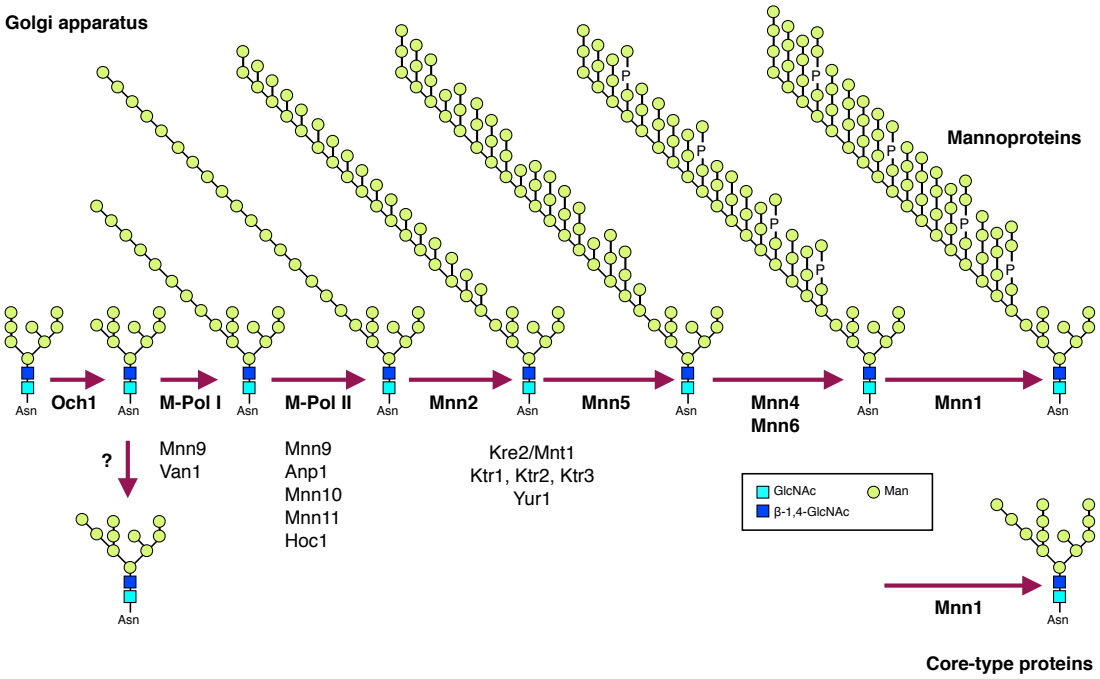

Figure 1.5: Mannosylation in the yeast Golgi apparatus. N-linked glycosylated proteins arrive in the *cis*-Golgi apparatus. Och1 attaches an α-1,6-Man which can be further extended by M-Pol I and other complexes and single GTs to form mannoproteins (top). In contrast, core-type mannosylation is initiated by an/multiple unidentified GT(s) that attach an α-1,2-Man to the Och1 product. Minor mannosylation by Mnn1 finishes the core-type glycan. Figure adapted from Orlean 2013

linked Man (Stolz and Munro, 2002). If this is the case, the discrimination between mannoproteins and core-type mannosylated proteins would work as follows. An N-linked glycosylated protein arrives from the ER and receives the first α-1,6-Man from Och1. Then, the protein arrives at M-Pol I. Mnn9 is able to change its GT activity depending on the protein substrate, presumably through recognition of an as yet unidentified sequon or a different fold of protein that will receive either the Man backbone or the core-type structure. If a protein is supposed to receive the Man backbone, Mnn9 will add an α-1,6-Man that will be extended by Van1 (Stolz and Munro, 2002). Core-type proteins will receive an α-1,2-Man by Mnn9 and are subsequently extended by Mnn1 (Stolz and Munro, 2002). However, this mechanism is controversial because these results were obtained from samples that were immunoprecipitated from *S. cerevisiae* and may have been contaminated with other GTs that can perform the α-1,2-Man reaction (Rodionov *et al.*, 2009, Stolz and Munro, 2002). After expression of Mnn9 and Van1 in *Pichia pastoris* the only reaction product that could be found was poly-α-1,6-Man, indicating that M-Pol I can only carry out this type of glycosyltransfer (Rodionov *et al.*, 2009).

The poly-α-1,6-Man backbone formed by the two M-Pol complexes can be further decorated with α-1,2-Man and phosphomannose. The first α-1,2-Man is added by Mnn2 to each of the α-1,6-backbone Man (Rayner and Munro, 1998). Mnn5 adds a second α-1,2-Man (Rayner and Munro, 1998). Subsequently, the transferases Ktr1, Ktr2, Ktr3, Kre2/Mnt1, and Yur1 add further α-1,2-Man thereby extending the N-linked outer chain (Lussier *et al.*, 1996, 1997, 1999). In addition, mannoproteins as well as core-type mannosylation can be further extended by phosphomannose. This is mainly carried out by Mnn6/Ktr6 which transfers Man-1-P (Jigami and Odani, 1999, Wang *et al.*, 1997). Many glycosylated proteins receive a final α-1,3-Man cap on their terminal α-1,2-Man or Man-1-P which is added by Mnn1 (Ballou *et al.*, 1990, Yip *et al.*, 1994).

O-Mannosylation O-mannosylation is the formation of linear oligomannose on serine or threonine residues on many yeast proteins. This process is essential,

because mutants lacking combinations of the GTs involved are not viable.

The first step is carried out on the lumenal side of the ER. Six substrate specific GTs are responsible for the addition of the initial Man from Dol-P-Man (Lehle *et al.*, 2006, Lommel and Strahl, 2009, Strahl-Bolsinger *et al.*, 1999). All belong to the family of dolichyl phosphate mannose-dependent protein O-mannosyltransferases (Pmt1-6) (Girrbach *et al.*, 2000, Lommel *et al.*, 2011, Strahl-Bolsinger and Scheinost, 1999). PMTs can form homo- and heterodimers to achieve their substrate specificity (Girrbach and Strahl, 2003), *e. g.* the Pmt1/Pmt2 heterodimer can mannosylate soluble or membrane-bound proteins whereas the homodimer of Pmt4 can only mannosylate proteins with a GPI anchor or with a transmembrane domain (Hutzler *et al.*, 2007). Generally, O-mannosylation precedes N-linked glycosylation. However, because O-mannosylation occurs on Ser or Thr, the N-linked glycosylation sequon N-X-S/T is a potential target. In fact, in *pmt4*Δ *S. cerevisiae* cells the protein Cwp5 gets N-linked glycosylated because O-mannosylation cannot occur (Ecker *et al.*, 2003). This implies that O-mannosylation can regulate the N-linked glycosylation of a protein.

The initial Man is extended with up to four α-Man by GDP-Man dependent GTs in the Golgi apparatus (Lussier *et al.*, 1999). The first two α-1,2-Man are transferred by Ktr1, Ktr3 and Kre2 – the same GTs that carry out the outer chain synthesis of N-linked glycosylated mannoproteins (Lussier *et al.*, 1997). The remaining two α-1,3-Man are added by Mnn1, Mnt2, and Mnt3 (Romero *et al.*, 1999).

GPI-Anchored Proteins GPI-anchored proteins initially remain attached to the plasma membrane. However, the glycan present in GPI can be cleaved and the protein can be covalently linked to the β-glucan in the cell wall via glycosidic bonds (Kollár *et al.*, 1997). A protein is highly likely to receive a GPI anchor if it contains a hydrophobic N-terminal secretion signal and a C-terminal GPI-anchor signal sequence that contains a specific amino acid, ω, The GPI anchor is attached to ωvia an amide-bond (Nuoffer *et al.*, 1991, 1993).

The structure of the GPI anchor is organism-specific. In *S. cerevisiae* the car-

boxyl end of ω is covalently linked to NH_2-CH_2-CH_2-PO_4-6-Man-α-1,2-Man-α-1,6-Man-α-1,4-GlcN-α-1,6-myoinositol phospholipid (Fankhauser *et al.*, 1993) (Fig. 1.3). The α-1,2-Man is extended with another α-1,2-Man which in turn can be further decorated with α-1,2-Man or α-1,3-Man. Additionally, α-1,4-Man and α-1,6-Man are modified with ethanolamine phosphate (Etn-P) (Orlean and Menon, 2007, Pittet and Conzelmann, 2007).

The synthesis of the GPI precursor is carried out by at least 21 proteins of which 18 are essential (Fig. 1.6). The synthesis is initiated at the cytoplasmic side of the ER (Tiede *et al.*, 2000, Vidugiriene and Menon, 1993, Watanabe *et al.*, 1996). GlcNAc is transferred to PI by a heterohexameric complex (Gpi1, Gpi2, Gpi3, Gpi15, Gpi19, Eri1) (Leidich and Orlean, 1996, Leidich *et al.*, 1995, Newman *et al.*, 2005, Sobering *et al.*, 2004, Yan *et al.*, 2001). GlcNAc-PI is de-acetylated by Gpi12 (Vidugiriene and Menon, 1993, Watanabe *et al.*, 1999). Subsequently, GlcN-PI is translocated through the ER membrane and the subsequent steps occur on the lumenal side of the ER. The flippase for this translocation has not been identified (Vishwakarma and Menon, 2005).

On the lumenal side of the ER the inositol of GlcN-PI is acetylated on the 2-OH by Gwt1 using acyl-CoA as donor (Costello and Orlean, 1992). Then, GlcN-(acyl)PI is extended with α-1,4-Man by the heterotrimeric complex of Gpi14, Arv1, and Pbn1 (Ashida *et al.*, 2005, Kajiwara *et al.*, 2008, Maeda *et al.*, 2001), α-1,6-Man by the heterodimeric complex of Gpi18 and Pga1 (Fabre *et al.*, 2005, Kang *et al.*, 2005, Sato *et al.*, 2007), and two α-1,2-Man added by Gpi10 and Smp3 (Canivenc-Gansel *et al.*, 1998, Grimme *et al.*, 2001, Sutterlin *et al.*, 1998), respectively. The mannose residues are modified by the addition of Etn-P (Orlean, 2009). α-1,4-Man is modified at 2-OH by Mcd4, whereas Man-2 and Man-3 (Fig. 1.3) are modified at 6-OH by Gpi13 and Gpi7, respectively (Benachour *et al.*, 1999, Galperin and Jedrzejas, 2001, Gaynor *et al.*, 1999). This forms the GlcN-(acyl)PI-Man_4-Etn-P_3 anchor which will be transferred to the ω site of a GPI acceptor protein. This transfer is done by the transamidation of the amino group of Etn-P on Man3 and the carboxyl group of the ω residue and carried out by the essential heteropen-

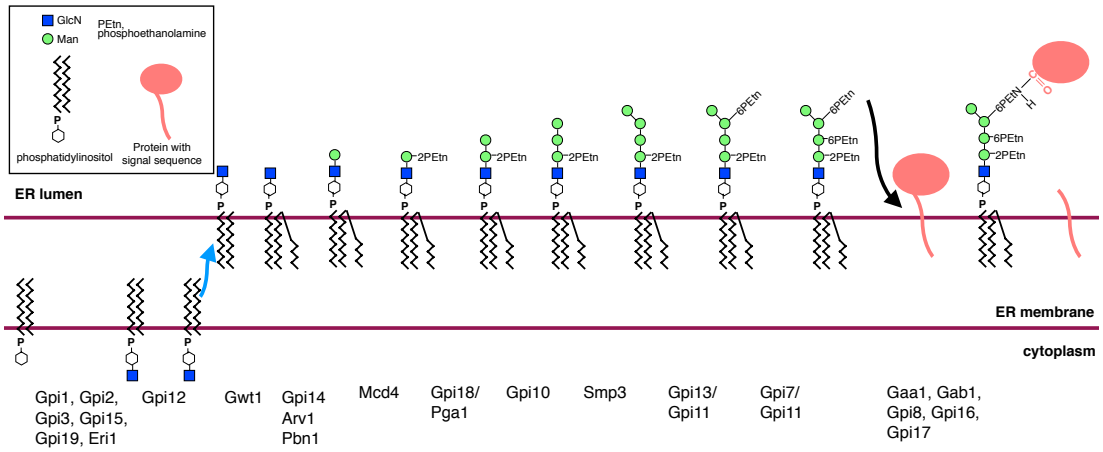

Figure 1.6: Synthesis of the GPI-anchor at the ER membrane. GPI-anchor synthesis is carried out by at least 21 proteins. A glycan structure is built on PI and the anchor is transferred in a one-step reaction onto the ω-site of an acceptor protein. Figure adapted from Orlean 2013

tameric complex formed by Gaa1, Gab1, Gpi8, Gpi16, Gpi17 (Benghezal *et al.*, 1996, Fraering *et al.*, 2001, Grimme *et al.*, 2004, Hamburger *et al.*, 1995, Hong *et al.*, 2003, Ohishi *et al.*, 2000, 2001).

Remodelling of the GPI anchor occurs immediately after the transfer to a protein acceptor (Fujita and Kinoshita, 2010). First, the inositol acyl residue is removed by Bst1 (Fujita *et al.*, 2006, Tanaka *et al.*, 2004). Then the acyl chain of diacylglycerol is replaced with a C_{26} acyl group (a completely saturated fatty acid) to improve the transition from the ER to the Golgi apparatus (Bosson *et al.*, 2006). In the Golgi apparatus further Man can be added to the glycan core of the GPI anchor (Fankhauser *et al.*, 1993). Once the protein reaches the plasma membrane it can be directly cross-linked to the β-1,6-glucan. However, the GPI glycan can also be cleaved, by yet unidentified hydrolases, and the protein with the GPI remnant cross-linked to the β-1,6-glucan in a transglycosidation reaction. These GPI-CWP confer structural integrity and enzymatic activity in the cell wall.

Galactomannan Galactomannan describes proteins that carry a linear α-poly-mannose backbone that has side-branches of chains of β-1,5-galactofuranose. Galactomannan is not present in the cell wall of *S. cerevisiae* and *C. albicans* but can make up to 25 % of the *A. fumigatus* cell wall (Fontaine *et al.*, 2000). In

fact, diagnostic tools to identify invasive aspergillosis are based on the detection of galactomannan (Pfeiffer *et al.*, 2006).

The biosynthetic pathway of galactomannan formation is unknown. The formation of mannoproteins in *A. fumigatus* has not been described and comparative studies with homologs of the yeast proteins have identified four orthologs of Och1 as well as orthologs for Mnn9, Van1 and Anp1 (Gastebois *et al.*, 2009). However, it is unknown whether these *A. fumigatus* orthologs perform the same reactions as described in baker's yeast.

1.2.4 Remodelling and Crosslinking of Cell Wall Components

The components of the cell wall – carbohydrates, proteins and GPI – can undergo further remodelling or they can be crosslinked once they reach the extracellular face of the plasma membrane. The order of cell wall assembly has been extensively studied in *S. cerevisiae* spheroplasts and on mutants lacking individual cell wall components. Cell wall assembly is initiated by the synthesis of β-1,3-glucan, as it serves as a scaffold for the incorporation of β-1,6-glucan and mannoproteins. GPI-CWPs are incorporated after the formation of the β-1,6-glucan layer. Chitin is only visible after cytokinesis, hence it is believed to be the last component added to the cell wall.

Crosslinking of GPI-anchor proteins

GPI-anchored proteins can be retained in the plasma membrane or are incorporated into the cell wall as GPI-CWPs (Gonzalez *et al.*, 2009). This depends on the N-terminal region of the ω residue (ω(–)) in those proteins (Caro *et al.*, 1997, De Sampaïo *et al.*, 1999, Frieman and Cormack, 2004, Hamada *et al.*, 1998b, 1999). The signal for membrane retention are two basic amino acid residues in this region (Caro *et al.*, 1997, Frieman and Cormack, 2003), whilst GPI-CWPs either lack these residues or carry hydrophobic residues instead (Frieman and Cormack, 2003, Hamada *et al.*, 1998a, 1999). However, this is not a strict rule and proteins of

either group have been found to be located in their "non-natural" location (Frieman and Cormack, 2004). The location of a GPI-anchored protein can be important as it has been shown for Ecm33, a protein that is necessary for growth at elevated temperatures, which is only active when it remains attached to the plasma membrane, and replacement of the (ω(–)) region with a sequence for association of Ecm33 with the cell wall results in the loss of function of this protein (Terashima *et al.*, 2003).

So far it is unclear how GPI-CWPs are released from the plasma membrane and covalently linked to the β-1,6-glucan. Two mechanisms are possible: 1) in a single-step reaction the GPI-anchored protein is hydrolysed and the reducing end of the GPI remnant is transferred and covalently linked to β-1,6-glucan, or 2) the reaction is carried out in multiple steps, performed by separate enzymes. The two essential and homologous *S. cerevisiae* enzymes Dfg5 and Dcw1 are potential candidates for the cross-linking (Kitagaki *et al.*, 2002, 2004). Both have been identified based on sequence alignment with the α-1,6-mannosidase Aman6 from *Bacillus circulans* TN-31, a member of the GH-76 family (Maruyama and Nakajima, 2000, Nakajima *et al.*, 1976). Interestingly, the *dfg5*Δ *dcw1*Δ double knockout is lethal and *dcw1*Δ cells are more sensitive to the cell wall digesting enzyme Zymolyase (Kitagaki *et al.*, 2002). A first insight into the function of both proteins was achieved by controlled depletion of either of the proteins in a double knockout background (Kitagaki *et al.*, 2002, 2004). These cells showed increased cell volume, delocalised chitin and the release of a GPI-CWP into the medium. Due to these results and the possible mannosidase activity by homology to a bacterial enzyme, it is believed that Dfg5 and/or Dcw1 are able to hydrolyse one of the α-linked Man in the GPI-anchored proteins. If the enzymes are also involved in the transglycosylation is unclear.

Crosslinking of PIRs

PIRs are covalently linked to the β-1,3-glucan in the cell wall (Ecker *et al.*, 2006). The internal repeats are necessary for this link as deletion of them results in the release of the proteins into the medium (Castillo *et al.*, 2003, Sumita *et al.*, 2005). The proteins are linked via an alkali-labile ester bond between the γ-carboxyl group of glutamate in the repeating sequence DGQ(hydrophobic residue)Q and a hydroxyl group in the β-1,3-glucan (Ecker *et al.*, 2006). It is unclear if an unknown transglutaminase creates that link or if the PIRs are able to perform this reaction as the amide hydrolysis itself could provide enough energy to form the ester bond (Ecker *et al.*, 2006).

Crosslinking of Chitin to Glucan

The homologous *S. cerevisiae* GPI-proteins Crh1 and Crh2, as well as Crr1, are able to crosslink the reducing end of chitin to the non-reducing end of β-1,3-glucan linked to β-1,6-glucan or β-1,3-glucan alone (Cabib, 2009, Cabib *et al.*, 2007). All three proteins are GH-16 members and Crh2, as well as Crr1, contain a chitin-binding module (Cabib *et al.*, 2008, Rodriguez-Pena *et al.*, 2000).

Similar crosslinks have been identified in the cell wall of *A. fumigatus* (Gastebois *et al.*, 2009). Many of the enzymes that are involved in the remodelling of the cell wall in *S. cerevisiae* have homologs in *A. fumigatus*, *e. g.* the Gas family, Dfg5/Dcw1 and Crh1/Crh2 (Latgé, 1999). However, specific activities of any of these enzymes have not been described in the filamentous fungus.

1.3 Glycosyltransferases

The plethora of oligosaccharides found in nature are the product of the directed action of GTs, GHs, glycan phosphorylases and lyases (Lairson *et al.*, 2008). GTs form glycosidic bonds by the transfer of a sugar from an activated donor to an acceptor. Such activated sugars contain a phosphate leaving group as found in

UDP, GDP or Dol-P, for example. The acceptor is usually another sugar but can also be a protein (*e. g.* N-linked glycosylation, O-GlcNAcylation), lipid (*e. g.* GPI-anchor synthesis), nucleic acid or many other small molecules. The reaction of GTs is regio- and stereospecific and GTs can be classified into inverting or retaining GTs based on the anomeric configuration relative to the substrate donor.

1.3.1 Classification of GTs by Their Fold

Like many other enzymes, GTs can be grouped into different families by their amino acid sequence similarity (Campbell *et al.*, 1997, Coutinho *et al.*, 2003). The Carbohydrate-Active enZymes database (CAZy) (`http://www.cazy.org`) is a curated online resource to access the different families of GTs (Cantarel *et al.*, 2009). To date, the database contains over 100 000 entries which are classified ino 94 families.

Based on the known structures of GTs, they can be classified into three groups based on their overall fold: GT-A, GT-B, or GT-C (Bourne and Henrissat, 2001) (Fig. 1.7). All structures of nucleotide-sugar-dependent GTs solved so far either adopt the GT-A or GT-B fold (Coutinho *et al.*, 2003, Hu and Walker, 2002, Unligil and Rini, 2000). Lipid-phosphate-dependent GTs (*e. g.* OST), however, can adopt the more recently discovered GT-C fold (Henrissat *et al.*, 2008, Lizak *et al.*, 2011).

Because of the high similarity of their overall structure it is believed members of the GT-A and GT-B families have evolved from only a few ancestors. The members of GT-2 (~33 000) adopt the GT-A fold and members of the GT-4 (~25 000) family adopt the GT-B fold. GT-As and GT-Bs are very similar, *i. e.* both contain two Rossmann-like folds ($\beta/\alpha/\beta$), a typical structural motif found in nucleotide-binding proteins. However, in GT-As the two Rossmann-like folds are in close proximity giving the impression of a single β-sheet. This was first observed in SpsA from *B. subtilis* which defined the GT-As (Charnock and Davies, 1999) (Fig. 1.7A). Many eukaryotic GT-As are membrane-bound with a short cytoplasmic N-terminus, followed by the transmembrane domain, a linker region and the catalytically active

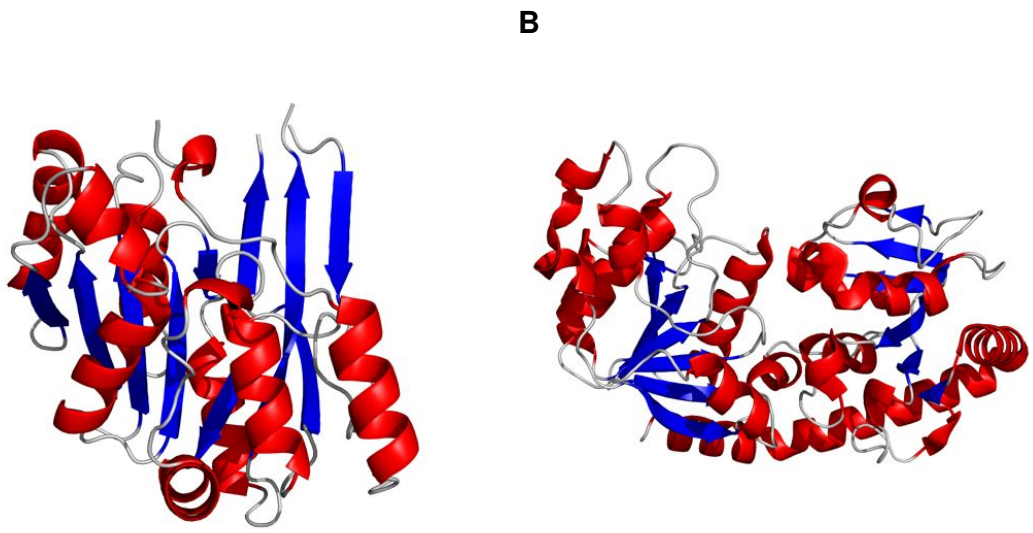

Figure 1.7: Overall fold of glycosyltransferases. **A**, Structure of SpsA from *Bacillus subtilis* representing the GT-A fold (Charnock and Davies 1999, PDB ID: 1QGQ). **B**, Structure of β-glucosyltransferase from bacteriophage T4 representing the GT-B fold (Vrielink *et al.* 1994, PDB ID: 1JG7).

globular domain (Breton and Imberty, 1999). The majority of GT-As possess the amino acid motif aspartate–any amino acid–aspartate (DXD). The carboxylates are necessary for the coordination of a divalent cation and/or the ribose of the sugar-nucleotide (Breton *et al.*, 1998, Wiggins and Munro, 1998). The DXD motif used to be considered the signature of GT-A members. However, a recently discovered enzyme adopts the GT-A fold but does not contain the DXD motif (Pak *et al.*, 2006).

The first ever structure of a GT was that of the β-glucosyltransferase from bacteriophage T4 (Vrielink *et al.*, 1994) (Fig. 1.7B). In recent years with the establishment of GT-A and GT-B fold families this GT has been classified as a GT-B and is now considered as the model structure for this fold. Both Rossmann-like domains are less tightly associated than in GT-A GTs. The active site of GT-Bs is in a groove located between the two domains.

Because structures of GT-C GTs have only recently been solved, the definition of the GT-C fold is not as detailed as for the other two folds. GT-Cs are predicted to be large integral proteins with 8–13 transmembrane domains with the active site

being located in a loop (Lizak *et al.*, 2011, Maeda *et al.*, 2001, Strahlbolsinger *et al.*, 1993, Takahashi *et al.*, 1996). This is consistent with the observation that GTs that are known or suggested to adopt the GT-C fold use lipid phosphate-activated donor substrates (*e. g.* Dol-P-sugars). These reactions can only occur at membranes.

Besides the classification of GTs by their fold, these enzymes can also be grouped based on stereochemistry of the glycosidic bond that is formed during the reaction realtive to the donor substrate. To date, there are many examples of inverting and retaining GTs adopting either the GT-A or the GT-B fold (Coutinho *et al.*, 2003). In contrast, all GTs adopting the GT-C fold characterised to date are inverting GTs. The majority of inverting GTs perform the glycosyltransfer reaction via a single S_N2-like displacement reaction (Fig 1.8). In contrast, there is still much speculation about the mechanism(s) of retaining GTs.

1.3.2 Inverting Glycosyltransferases

During the reaction of inverting GTs the stereochemistry at the anomeric centre of the sugar in the product will be inverted with respect to the donor substrate. Such a reaction is carried out by the chitin synthases, for example. Results from the studies described below indicate that inverting GTs work via an S_N2-like displacement reaction mechanism. In such a reaction, an active-site residue acts as a base deprotonating the nucleophile of the acceptor thereby promoting the S_N-like displacement of the phosphate leaving group. The side chains that are possibly involved in the reaction have been identified in many enzymes.

Inverting GT-A GTs

SpsA from *B. subtilis* was the first structure to be solved for an inverting GT-A GT (Charnock and Davies, 1999) (Fig. 1.9). The structure could not be solved with the native acceptor in complex with SpsA. However, due to the presence of a glycerol molecule that acted as cryoprotectant, it was speculated that D191 acts as the base during the glycosyltransfer reaction (Charnock and Davies, 1999). The increased

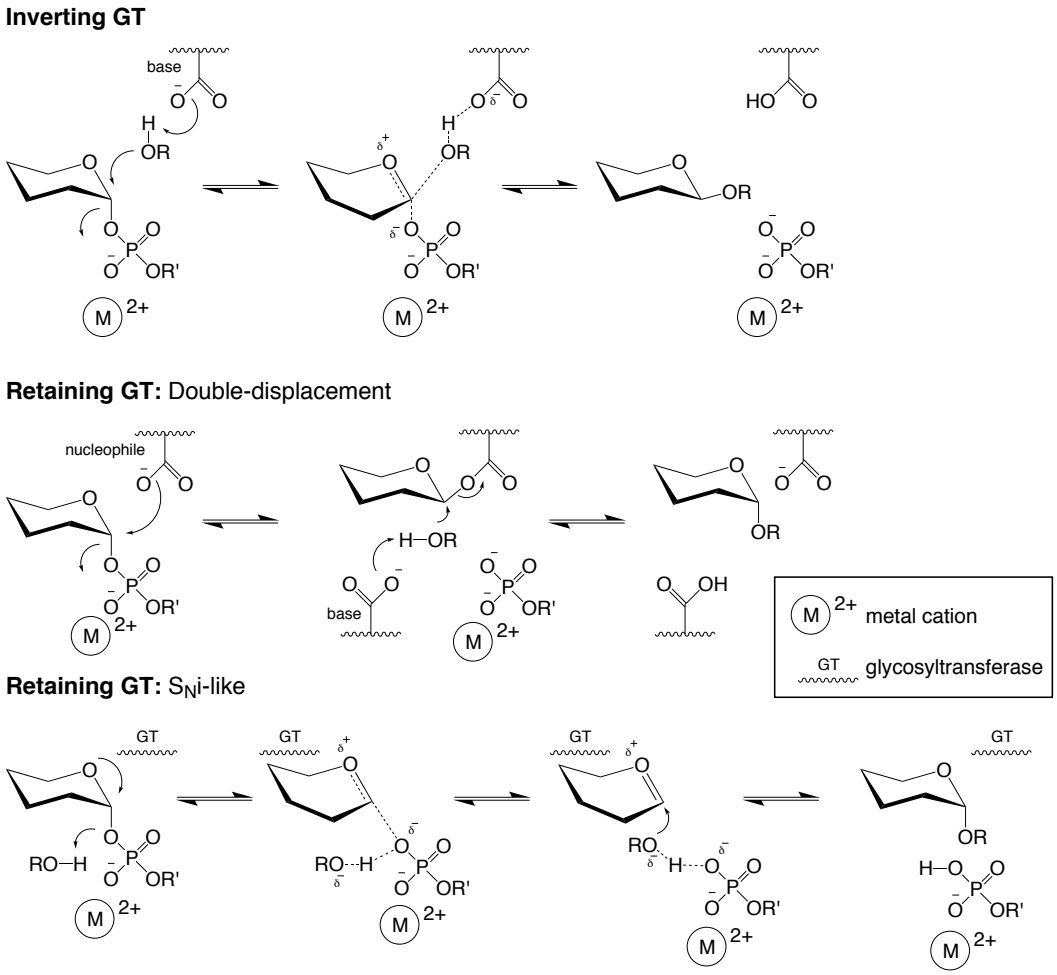

Figure 1.8: Mechanisms of inverting and retaining GTs. Inverting GTs use an S_N2-like displacement reaction. In contrast, the mechanism of retaining GTs is controversial. The reaction may occur by double-displacement with an enzyme-glycosyl intermediate or via an S_Ni-like mechanism in which the hydroxyl group of the acceptor attacks the anomeric carbon of the donor from the same side as where the leaving group departs.

availability of other GT-A structures later supported the idea of D191 being the base catalyst in SpsA. By superpositioning these GT-As in complex with their substrate on SpsA, it became evident that the other GTs have an aspartic acid similarly positioned and within hydrogen-bonding distance to the nucleophilic acceptor hydroxyl group (Kakuda *et al.*, 2004, Ohtsubo *et al.*, 2000, Pedersen *et al.*, 2000, 2002, Ramakrishnan and Qasba, 2001, Ramakrishnan *et al.*, 2002, Ramasamy *et al.*, 2005). One example is the β-1,4-galactosyltransferase-7 from *Drosophila melanogaster*. In this GT D211 may act as the base which deprotonates a hydroxyl group of the xylose acceptor.

Most inverting GT-As that have been characterised to date are dependent on a divalent cation, such as Mn^{2+} or Mg^{2+}. The metal is, at least partially, coordinated by the DXD motif. The metal is believed to be necessary to stabilise the negative charge of the diphosphate after the reaction and to facilitate its departure. Notable exceptions are metal-ion independent GTs such as GT-14 β-1,6-GlcNAc transferases (Pak *et al.*, 2006) and the GT-42 sialyltransferases (Chiu *et al.*, 2004). These enzymes use basic amino acids (Arg and Lys) or the ability to form hydrogen bonds with the hydroxyl groups of tyrosine side chains to support the departure of the leaving group, respectively.

The GT-2 family contains the transferases that synthesise cellulose, chitin, and hyaluronan. There is still much controversy about the mechanism that is used to extend the polysaccharides formed by these GTs. It is unclear if a UDP-monosaccharide is the donor that extends the oligosaccharide or if an UDP-activated oligosaccharide is transferred onto a UDP-monosaccharide. Recent developments suggest that both reactions are possible. *In vitro* experiments with hyaluronan synthase from *Streptococcus equisimilis* indicate that the growing chain is transferred onto the UDP-monosaccharide (Hubbard *et al.*, 2012). In contrast, the crystal structure of *Rhodobacter sphaeroides* cellulose synthase shows a growing oligoglucose chain without UDP attached to it, suggesting that UDP-Glc acts as the donor (Morgan *et al.*, 2013). This is one of the many examples that shows how little knowledge we currently have about the exact mechanisms of GTs.

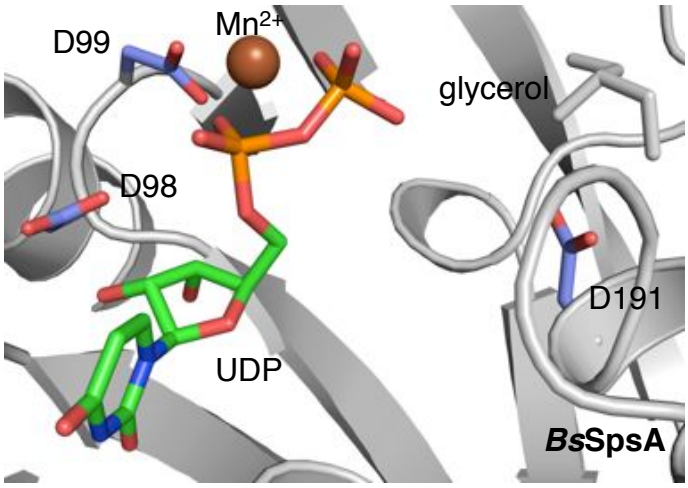

Figure 1.9: Active site of *Bacillus subtilis* SpsA. The pyrophosphate of UDP is coordinated by the metal cation Mn^{2+} which in turn is coordinated by the carboxyl group of D99. Glycerol occupies the site that is predicted to be the acceptor binding site.

Inverting GT-B GTs

The modes of glycosyl transfer in GT-Bs are much more diverse than in inverting GT-As. This might be a result of the larger distance between the two Rossman-like domains and the resulting flexibility of both domains.

The first GT-B structure, and nucleotide sugar GT structure in general, to be solved was of the β-glucosyltransferase (BGT) from T4 bacteriophage (Vrielink *et al.*, 1994). The enzyme transfers glucose onto cytosine bases to prevent DNA degradation by host nucleases (Kornberg *et al.*, 1961). In contrast to SpsA, BGT could be solved in complex with UDP and a DNA acceptor (Lariviere and Morera, 2002). The structure revealed that BGT is able to specifically flip out the DNA stretch that will become glycosylated. The candidate for the base is residue D100. This has been supported by mutagenesis of D100 to alanine which abolished activity and the fact that a UDP-Glc complex was only observed in the mutant but not in the wild type enzyme (Lariviere *et al.*, 2003). Another observation was the fact that short soaks of BGT crystals with UDP-Glc and an excess of metal did not reveal any density for the metal in the active site (Lariviere *et al.*, 2003). Positively charged side chains neutralised the negative charge of the diphosphate instead.

However, when BGT crystals were soaked with UDP and a metal, the metal was found to coordinate the diphosphate. The authors concluded that the cation facilitates product release rather than cleavage of the donor substrate.

The GT-1 family has been extensively studied because its members glycosylate organic molecules, such as terpenes, steroids, and antibiotics. Three GT-1s that have been well structurally and biochemically characterised are GtfA, GtfB, and GtfD (Mulichak *et al.*, 2001, 2003, 2004). All three GTs are involved in the biosynthesis of the antibiotic vancomycin. These enzymes use an aspartic acid residue as the base and the departure of the leaving group is metal-independent. This is achieved by stabilising the negative charge with hydroxyl and imidazole groups.

In contrast to the examples above, no catalytic base could be identified in the *Caenorhabditis elegans* POFUT1 GT-65 (Lira-Navarrete *et al.*, 2011). The enzyme O-fucosylates proteins on serine or threonine side chains (Klinger *et al.*, 1981). Only two aspartic acid residues could be found close to the sugar donor site. However, upon mutation they showed only a moderate decrease in activity. Activity was completely abolished by the mutation of R240. This led the authors to propose an S_N1-like mechanism for POFUT1 (Lira-Navarrete *et al.*, 2011). In this scenario, the β-phosphate of the sugar donor acts as the catalytic base via hydrogen bonds with an incoming water or Ser/Thr side chains of the EGF repeat. R240 forms a hydrogen bond with the glycosidic bond oxygen, thereby hydrolysing the glycosidic bond first. This creates an oxocarbenium ion transition state and the incoming acceptor transfers a proton to the leaving phosphate resulting in the attack of the acceptor substrate. However, the structure and mutagenesis of POFUT2 indicated that a glutamic acid (E54) can act as the catalytic base (Chen *et al.*, 2012).

Recently, there has been two controversial proposals for the mechanism of O-GlcNAc transferase (OGT) (Lazarus *et al.*, 2012, Schimpl *et al.*, 2012). OGT is an inverting GT-B in GT family 41. OGT transfers GlcNAc onto serine or threonine in an acceptor protein substrate (Kreppel *et al.*, 1997). Schimpl *et al.* (2012) propose that the catalytic base is not a side chain of OGT, but instead the α-phosphate of the nucleotide-sugar. Lazarus *et al.* (2012) claim that neither a carboxylate side

chain nor the β-phosphate are at the right distance to perform the glycosyl transfer. They also suggest that the α-phosphate is not involved in the reaction because the basicity of one of the oxygens is attenuated by a peptide backbone hydrogen bond. Instead, they propose an electrophilic migration mechanism in which the anomeric carbon moves from bonding to the pyrophosphate to the nucleophilic hydroxyl group of the acceptor serine – a mechanism that has so far only been described for GHs.

1.3.3 Retaining Glycosyltransferases

Retaining GTs differ from inverting GTs in that the anomeric configuration of the transferred sugar is retained. To date, two mechanisms have been proposed to perform such a reaction (Lairson *et al.*, 2008). One possibility is a double-displacement mechanism in which the donor sugar and the transferase form an enzyme-glycosyl intermediate (Koshland, 1953) (Fig. 1.8). For this mechanism to work, a side chain has to be in the correct position to act as a nucleophile to create the glycosyl-enzyme bond. The leaving group would work as a base and activate the hydroxyl group of the acceptor for nucleophilic attack.

Alternatively, retaining GTs could use an S_Ni-like mechanism in which the nucleophilic hydroxyl group of the acceptor attacks the anomeric carbon of the donor from the same side as where the leaving group departs (Fig. 1.8). S_Ni-like reactions are a form of S_N1 reaction. In this special reaction a discrete ion pair intermediate is formed that can either collapse or yield a product that retains the stereochemistry of the reaction centre (Hughes *et al.*, 1941, Lewis and Boozer, 1952). Retention of the stereochemistry is achieved by decomposition of the leaving group that in turn leads to the formation of a nucleophile which is positioned on the same face.

Retaining GT-A GTs

Many members of the family of retaining GT-As share structural and mechanistic features. Only few ternary complexes of retaining GT-As have been solved so

far. However, these are necessary to elucidate the mechanism of a given GT. One example is the ternary complex of GT-8 galactosyltransferase LgtC from *Neisseria meningitidis*, the substrate analogue 5'-diphospho-(2-deoxy-2-fluoro)-α-D-galactopyranose (UDP-2F-Gal), and the acceptor analogue 4'-deoxy lactose (Persson *et al.*, 2001). The structure showed a Mn^{2+} that is coordinated by the carboxylate groups in the DXD motif as well as the diphosphate of the leaving group. The only functional group to activate the 4'-hydroxyl group that would be present in the natural acceptor was an oxygen of the β-phosphate of the leaving group, an indicator that the diphosphate acts as the base. The best positioned catalytic nucleophile is Q189. However, the Q189A mutant retained 3 % activity, indicating that Q189 is not essential for the reaction. The enzyme was also tested in experiments with possible intermediates of a double-displacement mechanism (Persson *et al.*, 2001). However, these intermediates were not turned over and the possibility of this mechanism for LgtC was discounted. Q189 was mutated into a glutamic acid which was proposed would make it an even better nucleophile (Lairson *et al.*, 2004). Surprisingly, this substitution lead to a glycosyl-enzyme complex. However, instead of residue E189, D190 was found to be glycosylated. Mutation of D190 to asparagine showed 3000-fold slower catalytic activity. Interestingly, D190 is almost 9 Å away from the anomeric centre. Based on the results, LgtC must undergo considerable structural changes during the reaction to facilitate the proposed mechanism. Furthermore the authors concluded that D190 is the catalytic nucleophile and that the LgtC GT uses a double displacement mechanism during the transfer reaction.

The GT-6 bovine α-1,3-galactosyltransferase (α3GalT) has been extensively studied (Gastinel *et al.*, 2001, Monegal and Planas, 2006). The most likely residue to act as a nucleophile is E317, which is in a structurally similar position to Q189 of LgtC (Gastinel *et al.*, 2001). Firstly, it was believed that a glactosyl residue and E317 formed a covalent bond. However, this idea was quickly discarded based on the weak electron density around the possible covalent bond (Gastinel *et al.*, 2001). In contrast to LgtC, E317 was initially found to be predominantly required for correct acceptor substrate orientation. However, mutation of E317 led to a 2400-fold

decrease in activity (Zhang *et al.*, 2003). Eventually, the structure in complex with UDP-2F-Gal was solved and showed that E317 was indeed in a good position to act as a nucleophile during the reaction (Jamaluddin *et al.*, 2007). Further studies with α3GalT by chemically rescuing the E317A mutant supported the double-displacement mechanism.

Another pair of GT-6 family members are the human blood group GTs α-1,3-N-acetylgalactosaminyltransferase (GTA) and α-1,3-galactosyltransferase (GTB) (Yamamoto *et al.*, 1990). Both GTs differ only in four out of 354 amino acids. The distinction between the two substrates is achieved only by L266 and G268 in GTA with M266 and A268 in GTB (Patenaude *et al.*, 2002). Both enzymes have been trapped in complex with donor as analysed by mass spectrometry, suggesting that GTA and GTB work by the double-displacement mechanism (Soya *et al.*, 2011).

Retaining GT-B GTs

As has been shown for inverting GT-Bs, retaining GT-Bs use a metal-independent mechanism for leaving group departure.

The current knowledge of the mechanisms and residues involved in the reaction of retaining GT-Bs has been learned from the extensive structural studies of the GT-35 glycogen and starch phosphorylases. These enzymes phosphorylate glycogen or starch to Glc1P which in turn is isomerised to Glc6P and immediately used in glycolysis (Fletterick and Sprang, 1982, Green and Cori, 1943, Raibaud and Schwartz, 1984). The best studied GT-35 member is the rabbit muscle glycogen phosphorylase (rmGP) (Mitchell *et al.*, 1996, Watson *et al.*, 1994). Glycogen phosphorylases are unique as they have a phosphate bound via a Schiff base on a lysine residue. This phosphate is able can protonate a inorganic phosphate, which in turn will be deprotonated by the glycosidic bond oxygen of α-1,4-linked glycogen. The deprotonated inorganic phosphate acts as a nucleophile resulting in the release of Glc-1-P and a glycogen chain shortened by one glucose (reviewd in Livanova *et al.* 2002). The binary complex of rmGP and the transition state analogue

nojirimycin-tetrazole revealed that the main chain amide of H377 could act as the catalytic nucleophile (Mitchell *et al.*, 1996).

The *E. coli* trehalose β-phosphate synthase OtsA is member of the GT-20 family of retaining GT-B GTs. OtsA synthesises the stress response molecule α-α-trehalose-β-phosphate. Extensive studies have been performed on this GT to elucidate its mechanism (Gibson *et al.*, 2004). There is chemical and structural evidence that OtsA works by a front-side S_Ni mechanism in which the nucleophile, Glc-6-P, approaches the reaction from the same side as the leaving group (Ardèvol and Rovira, 2011, Errey *et al.*, 2010, Lee *et al.*, 2011).

1.4 Glycoside Hydrolases

The hydrolysis of oligosaccharides is an important biological process to gain energy, degrade the fungal cell wall and to turn over signalling molecules. It has been shown that a hexasaccharide can form more than 10^{12} different isoforms (Laine, 1994). This explains the vast amount of glycoside hydrolases (GHs) (more than 137 000 entries in 131 families according to CAZy) that hydrolyse the glycosidic bond between two carbohydrates or between a carbohydrate and a non-sugar molecule, such as a protein.

Historically, GHs were classified by their substrate specificity. Nowadays, GHs are grouped into families based on their amino acid sequence similarities (Cantarel *et al.*, 2009, Henrissat, 1991, Henrissat and Bairoch, 1993). In contrast to GTs, where only three major folds have been described to date (GT-A, B, and C), GHs can be grouped into 14 clans (GH-A–N) that represent different folds (Henrissat and Bairoch, 1996).

Because of the nature of oligosaccharides, GHs can be further classified as endo- or exo-hydrolysing enzymes. Endo-GHs can cleave in the middle of an oligosaccharide, whereas exo-GHs cleave, mostly, at the reducing end of a disaccharide or carbohydrate chain.

Furthermore, GHs can be classified according to their active site conformation

(Davies and Henrissat, 1995):

- A **pocket** is usually found in exo-hydrolases in which the active site is buried at the centre of the enzyme. One end of the carbohydrate substrate enters the active site, hydrolysis occurs and the product(s) is/are released. Members of this group are, for example, β-galactosidase and β-amylase.
- **Clefts** are common amongst endo-acting GHs, such as lysozymes, chitinases and α-amylases. Due to the open conformation a cleft allows random binding of the oligosaccharide.
- **Tunnels** have evolved from GHs with clefts that have long loops that cover the cleft partially. The oligosaccharide will be moved through the tunnel during the reaction. This conformation has been observed in cellobiohydrolases (Rouvinen *et al.*, 1990). The advantage is that the substrate remains bound to the enzyme at all times.

The reaction of most GHs is carried out by two amino acid side chains, usually aspartate or glutamate, that act as acid and base in inverting GHs and as acid/base and nucleophile in retaining GHs (Koshland, 1953, Sinnott, 1990) (Fig. 1.10). The result of the reaction is either an inversion or retention of stereochemistry of the product relative to the substrate (Koshland, 1953). In both reactions, the proton donor is within hydrogen bonding distance of the oxygen of the glycosidic bond. Interestingly, the base in inverting hydrolases is further away from the acid compared to the distance between the acid/base and the nucleophile in retaining GHs. This is because the active site of inverting GHs has to accomodate a water molecule while the substrate is present. The distance between the two catalytic residues in inverting GHs is about 10 Å, whereas in retaining GHs the distance is only about half of this (McCarter and Withers, 1994). However, some GHs use mechanisms that differ from this general acid/base reaction. Notable exceptions will be described in the sections below.

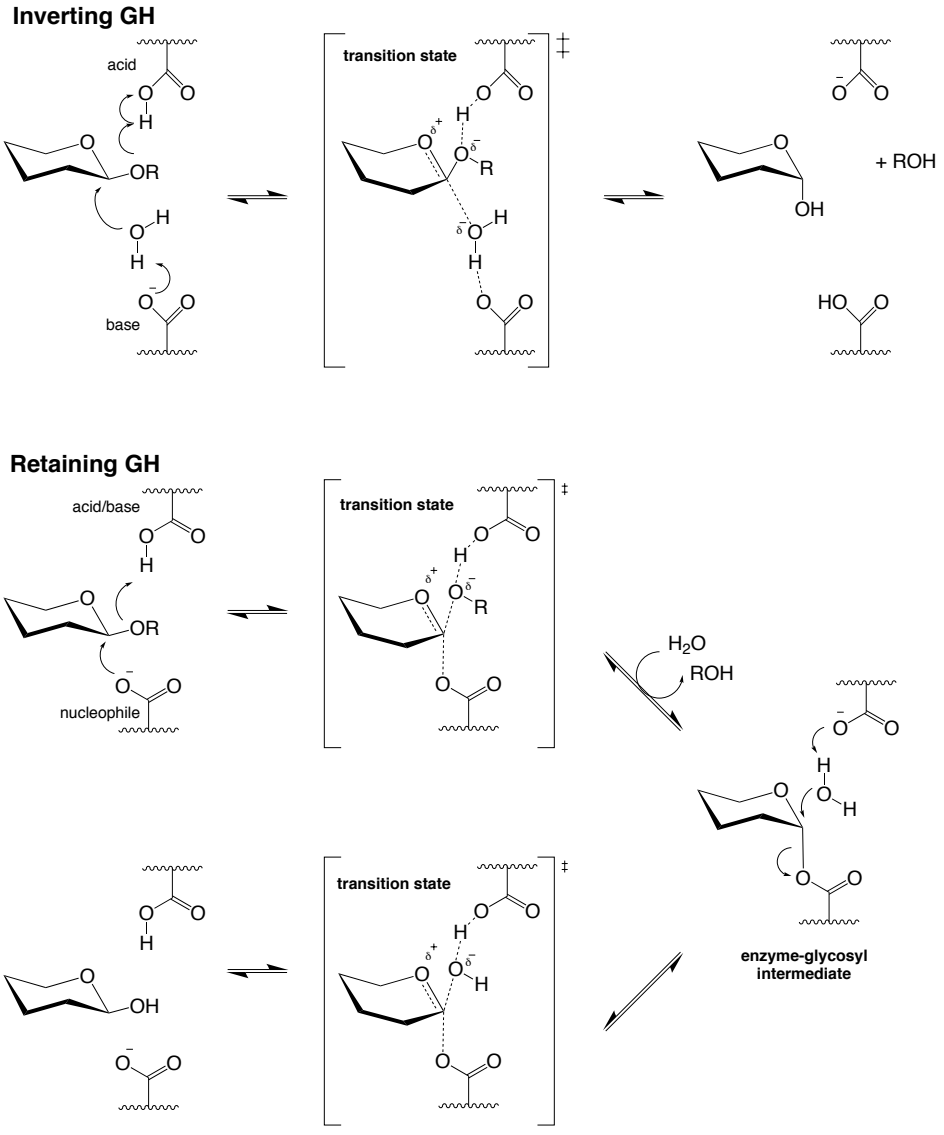

Figure 1.10: Mechanisms of inverting and retaining GHs. Inverting GHs use a one-step, single-displacement mechanism. Retaining GHs use a double-displacement reaction with a covalently bound enzyme-glycosyl intermediate.

1.4.1 Inverting Glycoside Hydrolases

The hydrolysis of a glycosidic bond with the inversion of stereochemistry at the anomeric centre of product relative to substrate is usually carried out via a one-step, single-displacement mechanism with an oxocarbenium ion-like transition state (Fig. 1.10).

Inverting GHs without a general acid. The Man-6-P-Man mannosidase from *Cellulosimicrobium cellulans* is an exception of the GH-92 family of exo-acting α-mannosidases because it lacks the necessary base that has been identified as crucial for the reaction in other enzymes of this family. Instead, it carries a glutamine in a structurally equivalent position (Tiels *et al.*, 2012), which is not a good proton donor. However, the phosphate of the substrate is a much better leaving group than a sugar. This indicates that the reaction does not require a proton donor.

1.4.2 Retaining Glycoside Hydrolases

Retaining GHs use a double-displacement reaction with a covalently bound enzyme-glycosyl intermediate (McCarter and Withers, 1994, Sinnott, 1990, Vocadlo *et al.*, 2001) (Fig. 1.10). In the first step, one of the carboxyl groups (called acid/base) acts as a general acid to protonate the glycosidic oxygen to aid leaving group depature. The other carboxyl residue functions as a nucleophile to form the enzyme-glycosyl intermediate. During the second step, the acid/base deprotonates an incoming water, which in turn attacks the anomeric centre to release the sugar.

Most GHs cleave their substrates based on this mechanism. However, several retaining GHs have developed variations of this reaction to accomodate their substrates. Some examples are listed below.

Neighbouring group participation. The substrates of GH families 18, 20, 25, 56, 84, and 85 contain an N-acetyl or N-glycolyl group at the 2'-position instead

of a hydroxyl group (Fig. 1.11). These hydrolases have no catalytic nucleophile. Instead, the 2'-acetamido group acts as an intramolecular nucleophile, leading to the formation of an oxazolinium intermediate via substrate-assisted catalysis (Mark and James, 2002, Terwisscha van Scheltinga *et al.*, 1995, Vocadlo and Withers, 2005).

Use of exogenous base Some of the hydrolases of GH-1 cleave thioglycosides found in plants. In these enzymes the acid/base is replaced by a glutamine (Fig. 1.12). This might be beneficial in order to reduce the charge repulsion created by an acid residue and the sulfate leaving group (Burmeister *et al.*, 2000). Such a mechanism has been proposed based on structural studies of the myrosinase from *Sinapis alba*. The sulfate aglycon itself is a good leaving group that facilitates hydrolysis and the formation of an enzyme-sugar intermediate. For the hydrolysis of this intermediate, the enzyme uses the co-factor L-ascorbate as an alternative base (Burmeister *et al.*, 2000).

Other nucleophiles The sialidases and trans-sialidases of GH families 33 and 34 use a conserved tyrosine as a catalytic nucleophile instead of an acid (Fig. 1.13). The tyrosine is activated by a neighbouring base (Amaya *et al.*, 2003, Watts *et al.*, 2003). The structure of a covalent intermediate of a substrate analogue bound to the tyrosine of *Trypanosoma cruzi* trans-sialidase has been solved, which supported the predicted mechanism (Amaya *et al.*, 2004).

NAD-dependent hydrolysis The members of GH families 4 and 104 are remarkably different compared to any other GHs in two respects. Firstly, both families contain GHs that are able to bind and/or cleave both α- and β-oligosaccharides. Secondly, these hydrolases use a novel hydrolytic mechanism in which a tightly bound NAD^+ acts as a co-factor for the reaction (Fig. 1.14). The mechanism has been proposed and described by Yip *et al.* (2004) for a β-glycosidase from *Thermotoga maritima* and by Rajan *et al.* (2004) for a phospho-α-glucosidase from *B. sub-*

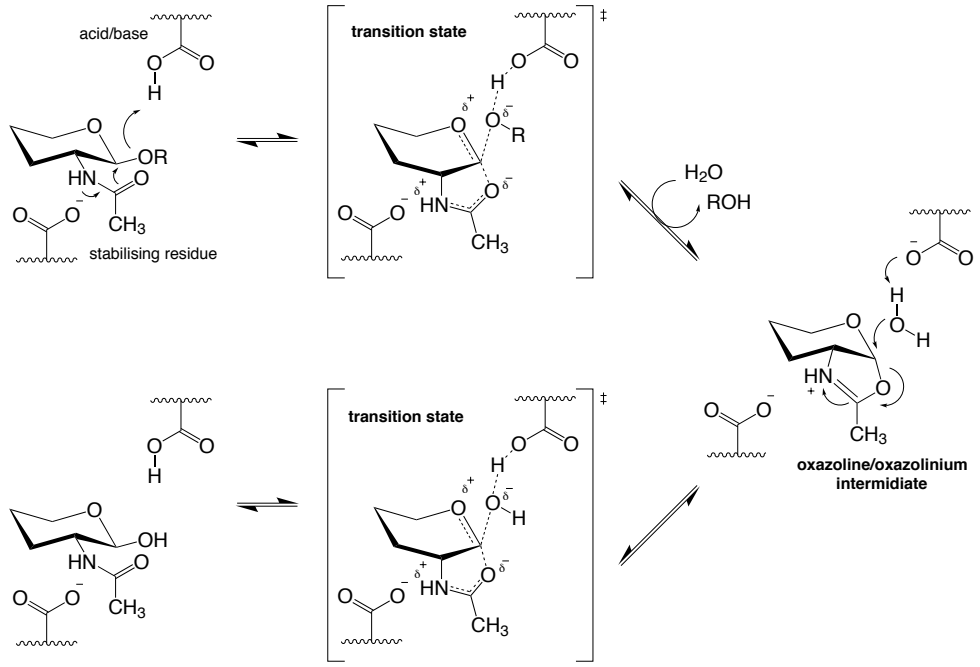

Figure 1.11: Mechanism of neighbouring group participation used by some GHs. Hydrolysis occurs in the absence of a catalytic nucleophile. The 2'-acetamido group acts as an intramolecular nucleophile leading to substrate-assisted catalysis via an oxazolinium intermediate.

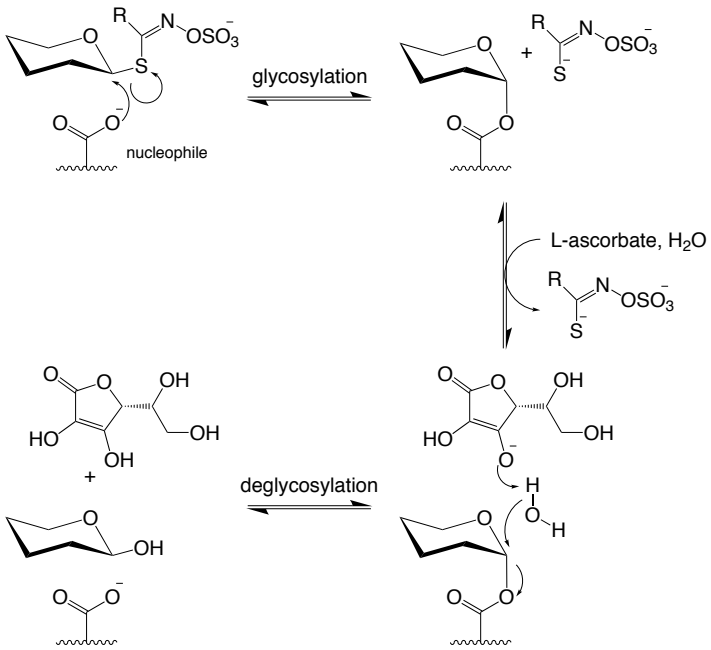

Figure 1.12: Hydrolytic mechanism of myrosinases. Myrosinases use an exogenous base for hydrolysis, here L-ascorbate, due to the lack of an acid/base residue.

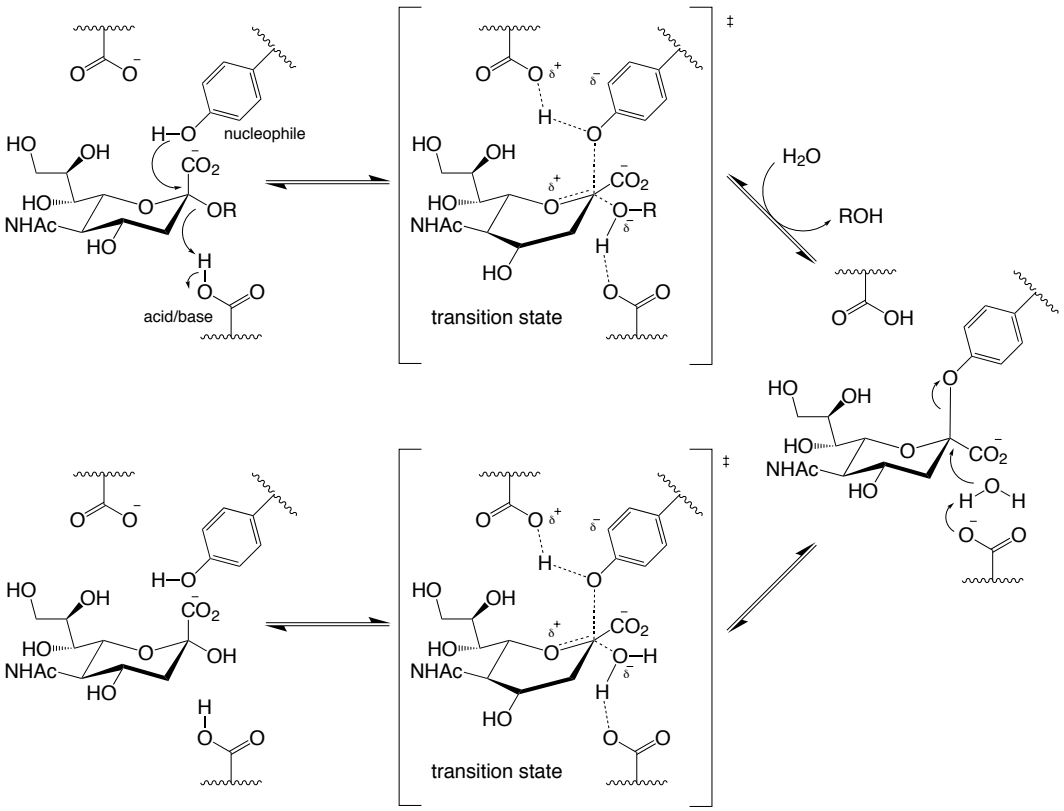

Figure 1.13: Mechanism of GHs bearing a different nucleophile. Some GHs use a different nucleophile, here tyrosine, that is activated by a near base.

tilis. During the reaction, NAD abstracts a hydride from the 3'-OH of the substrate in a redox reaction. An enzymatic base deprotonates C2 to form an unsaturated intermediate while an acid protonates the glycosidic oxygen to aid leaving group depature. The intermediate undergoes base-catalysed attack by a water to form 3'-keto glucose derivative which in turn is reduced by NADH to form the product (Rajan *et al.*, 2004).

A clinically important member of this group is GH-104, a α-N-acetylgalactosaminidase from *Elizabethkingia meningosepticum* that is capable of hydrolysing the A and B antigens on red blood cells (Liu *et al.*, 2007). After purification of this enzyme from *E. coli* it was shown that NAD was so tightly bound that addition of the co-factor in enzyme assays was not necessary.

1.5 Inhibitors of Carbohydrate-Processing Enzymes

Inhibitors of GTs and GHs are essential tools in glycobiology to study the cellular roles of the glycans that these enzymes form or degrade. A major drawback in the development of inhibitors for carbohydrate-processing enzymes is the vast amount of possible combinations of different sugars attached to each other (Laine, 1994), making it difficult to identify specific and efficient inhibitors. Inhibitors acting on glycan-processing enzymes can be classified into carbohydrate-based or non-carbohydrate-based (Gloster and Vocadlo, 2012).

A large group of carbohydrate-based inhibitors are based on naturally occuring compounds. Others are derivatives based on the structure of the catalytic transition states or the substrate. Much effort has gone into the design of such inhibitors in the past (Leeson and Springthorpe, 2007) to produce potent inhibitors. In contrast, the high polarity and the often time-consuming synthesis of such inhibitors is challenging.

In contrast, the list of non-carbohydrate-based inhibitors to date is comparably small. Derivatisation of these molecules is usually simpler compared to carbohydrate-based inhibitors. However, most of the non-carbohydrate-based inhibitors are very

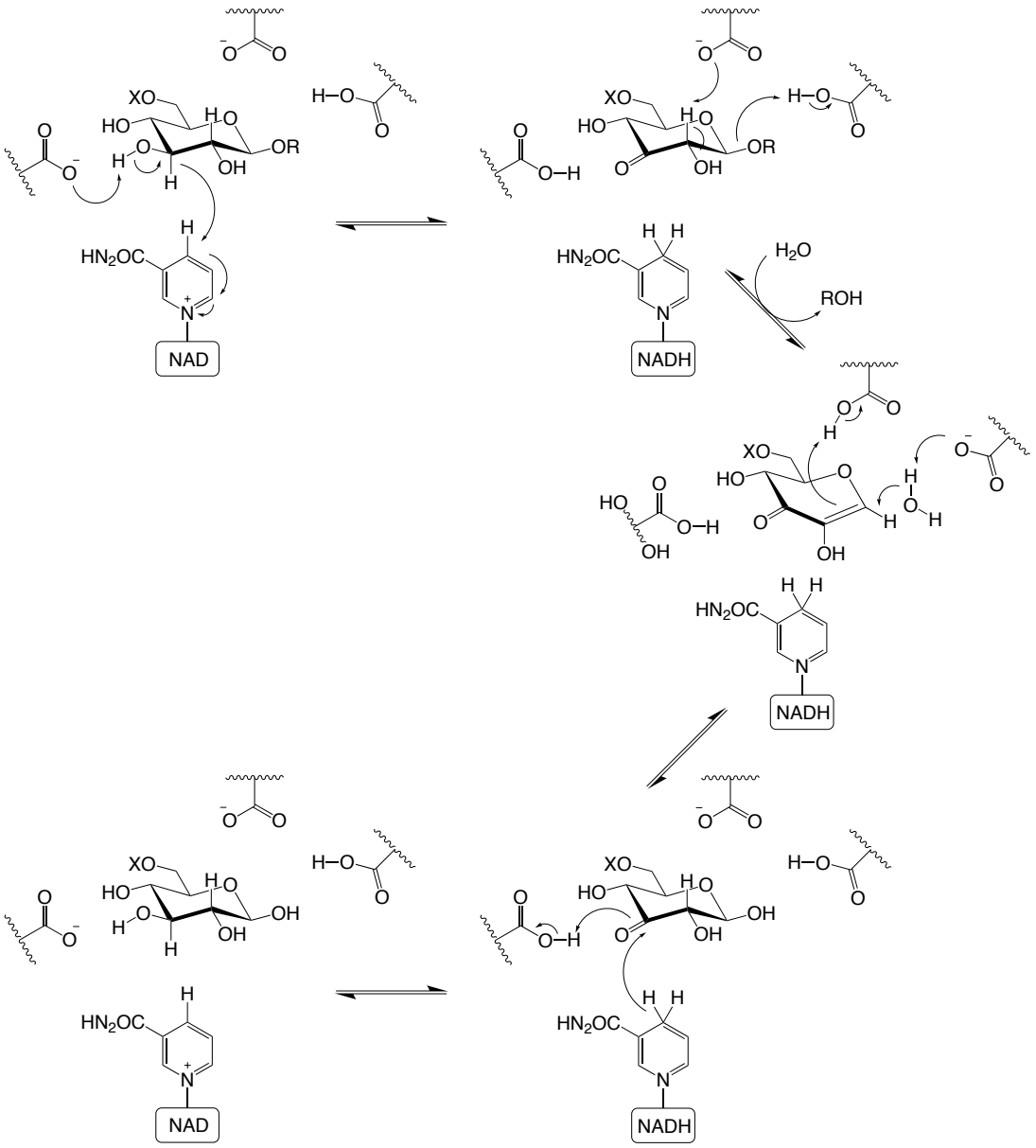

Figure 1.14: Mechanism of GHs using NAD as a co-factor. NAD is reduced during the hydrolysis by abstracting an hydride from the substrate. The intermediate is attacked by water to form a 3'-keto derivative that is reduced by NADH to reconstitute the original environment.

lipophilic, hence have a low solubility, making them less useful for *in vivo* studies.

With the advancements made in high-throughput screening, mass spectrometry, structural biology and chemical techniques, the identification of potent, specific and cell-permeable inhibitors may improve over the next decades.

1.5.1 Glycosyltransferase Inhibitors

The lack of a proper understanding of GT reaction mechanisms and their ability to undergo dramatic structural changes during glycosyl transfer are only two of the reasons for the lack of potent GT inhibitors (Breton *et al.*, 2012, Qasba *et al.*, 2005). GT-A GTs in particular undergo many rearrangements of flexible loops during donor binding. Furthermore, most GT inhibitors are donor or substrate analogues that have only limited "drugability" for *in vivo* applications (Qian *et al.*, 2008).

A novel class of galactosyltransferase (GalT) inhibitors has been described recently (Descroix *et al.*, 2012). GalT is important for the synthesis of human blood group antigen B (Patenaude *et al.*, 2002) and the lipopolysaccharide of some Gram-negative bacteria (Zhu *et al.*, 2006). Instead of modifying the sugar or pyrophosphate moiety, the novel GalT inhibitor carries a modification of the uracil of UDP-Gal (Descroix *et al.*, 2012). It is believed that this addition interferes with the reorganisation of an internal loop during catalysis (Pesnot *et al.*, 2010). The inhibitor had a K_i one order of magnitude lower than the K_m for the UDP-Gal substrate (Descroix *et al.*, 2012). Additionally, *in vivo* experiments suggested that this inhibitor is taken up by cells and localises to the ER and Golgi, despite its polar nature (Descroix *et al.*, 2012). However, the molecular mechanism of inhibition could not be elucidated because the binary complex of GalT and the inhibitor shows no electron density for the loop that is supposed to be affected by the compound (Descroix *et al.*, 2012).

Another approach is the *in silico* design of a GalT inhibitor based on pentitol-linked uric acid derivatives that are non-ionic analogues of the nucleotide donor (Schaefer *et al.*, 2012). The authors showed that the compound bound with similar

affinity to GalT compared to the substrate UDP-galactose. The replacement of the pyrophosphate could lead to the development of novel inhibitors that can penetrate the cell membrane and are able to enter the Golgi (Schaefer *et al.*, 2012).

Recently a MALDI-TOF high-throughput approach for the search of potent GT inhibitors has been described (Hosoguchi *et al.*, 2010). In this approach a library containing desired azidosugar nucleotides derivatised with different alkynes was used to identify novel inhibitors for a range of GTs. Using this technique the authors were able to identify a highly specific inhibitor for rat recombinant α-2,3-(N)-sialyltransferase with good binding affinity. Additionally, two more selective inhibitors for human recombinant α-1,3-fucosyltransferase V and α-1,6-fucosyltransferase VIII were identified.

1.5.2 Glycoside Hydrolase Inhibitors

In contrast to GTs, the field of GH inhibitors has made better progress over recent years. This is due to the extensive knowledge about transition states and substrate specificity of many GHs. Hence, many potent GH inhibitors are carbohydrate-based transition state analogues (Mader and Bartlett, 1997). However, similar to GT inhibitors, the synthesis and class promiscuity of most GH inhibitors results in limited biological applications.

O-GlcNAcase Inhibitors O-GlcNAcase (OGA) is the GH that removes O-linked GlcNAc from proteins that had been attached by the O-GlcNAc transferase (OGT) (Dong and Hart, 1994, Gao *et al.*, 2001, Kreppel *et al.*, 1997). This dynamic post-translational modification has implications in cancer (Caldwell *et al.*, 2010, Shi *et al.*, 2010) and neurodegenerative diseases (Lefebvre *et al.*, 2003, Liu *et al.*, 2004, Yuzwa *et al.*, 2008). To study the effects of O-GlcNAcylation, a lot of research has been done to identify potent OGA inhibitors in order to increase cellular levels of the post-translational modification. The first potent inhibitor described for OGA was PUGNAc (Dong and Hart, 1994, Horsch *et al.*, 1991), a nanomolar in-

hibitor with poor selectivity. Selectivity was improved with NButGT (Macauley *et al.*, 2005) which was derivatised to thiamet-G, a low-nanomolar inhibitor with 37 000-fold selectivity for OGA over other hexosaminidases (Yuzwa *et al.*, 2008). Recently, thiamet-G has been shown to slow the neurodegeneration in an Alzheimer's mouse model, showing the clinical relevance of potent and selective inhibitors (Yuzwa *et al.*, 2012). Coinciding with the development of thiamet-G, others identified another potent OGA inhibitor, GlcNAcstatin (Dorfmueller *et al.*, 2006), a low nanomolar inhibitor with a 900 000-fold selectivity over other hexosaminidases (Dorfmueller *et al.*, 2010). The development of these potent inhibitors was facilitated by the use of structure-based design and synthesis of derivatives of weak inhibitors (Dorfmueller *et al.*, 2010, Rao *et al.*, 2006). Further studies have been done to identify new micromolar OGA inhibitors that could act as scaffolds for non-carbohydate-based drugs (Dorfmueller and van Aalten, 2010).

GH-18 Chitinase Inhibitors Chitin is the second most abundant carbohydrate on earth. Chitinases can cleave the glycosidic bond between two β-1,4-GlcNAc. Chitinases of GH-18 are interesting drug targets, since they are present in pathogenic fungi as well as in humans. In fungi, chitinases are needed for the breakdown of the cell wall chitin during replication. The reason for the presence of chitinases in humans is not understood, but they could be used to act as a defence mechanism against pathogenic fungi. The human acidic mammalian chitinase (AMCase) is upregulated in lungs of asthma patients (Zhu *et al.*, 2004). Therefore, GH-18 members are potential drug targets against pathogenic fungi as well as against asthma. The natural product argifin, a cyclic peptide, is a nanomolar inhibitor of GH-18 chitinases. However, argifin is a large molecule that can not serve as a platform for drug design. Interestingly, by linearisation of the peptide and gradually removing amino acids, it could be shown that even a tripeptide is still a low micromolar inhibitor of ChiB, a chitinase present in *A. fumigatus*, and of chitinase activity in a mouse lung homogenate (Andersen *et al.*, 2008). Rational design lead to the synthesis of Bisdionin C (Schüttelkopf *et al.*, 2011). Bisdionin C shows good inhibition of

the *A. fumigatus* chitinase ChiB1 and moderate inhibition of AMCase. Hence, Bisdionin C can act as a starting point for the development of potent ChiB1 or AMCase inhibitors. Recently the use of a fragment-based high-throughput screen identified a high nanomolar inhibitor for AMCase (Cole *et al.*, 2010). This compound can be taken orally and shows reduced AMCase activity in an asthma mouse model.

2 Aims of the study

The fungal cell wall is an entity with unique features. Not only does it define the size of the fungal cell but protects it from bursting due to turgor pressure and from environmental stress factors, and masks the cell from detection by the host immune system. Many components of and processes occuring in the cell wall are present only in fungal cells and have no equivalent in human cells. This makes the biosynthetic pathways involved in the formation and remodelling of the fungal cell wall interesting drug targets. Recently approved antifungal drugs, such as the echinocandins, specifically block the biosynthesis of cell wall components (Bal, 2010).

The outer layer of the fungal cell wall is formed by mannan. Mannan is composed of O- and N-linked glycosylated proteins that are decorated with an extensive number of differently linked mannose residues (Kollár *et al.*, 1997). The biochemical processes involved in the formation of mannoproteins are well understood (Ballou *et al.*, 1980, 1991, Hernández *et al.*, 1989, Jungmann and Munro, 1998, Raschke *et al.*, 1973, Stolz and Munro, 2002, Tsai *et al.*, 1984) (see section 1.2.3, p. 19). However, the processes that determine which type of mannosylation a protein will receive are still unclear and may only be understood with structural information of the enzymes involved (*Sc*Mnn9 and *Sc*Van1). The structural information about the proteins involved in these processes, however, is limited. The fungal commensal *C. albicans* is the most common cause of mycotic infections in immunocompromised patients (McNeil *et al.*, 2001). The mannan layer of *C. albicans* has been shown to be an important antigen to activate the host immune response (Cambi *et al.*, 2008, Gingras *et al.*, 2011, Shibata *et al.*, 2012). Additionally, several ad-

herence factors of *C. albicans*, necessary to bind to epithelial cells, have been shown to contain mannan structures (Kanbe and Cutler, 1998, Kanbe *et al.*, 1993, Miyakawa *et al.*, 1992). This makes mannoproteins themselves and the enzymes involved in their synthesis potential drug targets. It is interesting to study not only the effects on host recognition upon altering the biosynthesis but also the possibility of blocking adhesion factors of fungal pathogens, such as *C. albicans*.

Furthermore, the extracellular GPI-anchored proteins *Sc*Dfg5 and *Sc*Dcw1 are homologs of the *Bacillus circulans* mannosidase (*Bc*Aman6) and seem to be involved in the transglycosylation of mannoproteins in yeasts and filamentous fungi (Kitagaki *et al.*, 2002, 2004, Maddi *et al.*, 2012, Spreghini *et al.*, 2003, Trow and Cormack, 2009) (see section 1.2.4, p. 25). Both proteins are essential in *S. cerevisiae* and *C. albicans*, making them excellent drug targets. However, their catalytic function and structure are unknown.

The aims of this study are to obtain structural and enzymatic insights into the formation and remodelling of mannoproteins by solving the structure of *Sc*Mnn9 and *Sc*Van1, as well as *Sc*Dfg5, *Sc*Dcw1 or their bacterial homolog *Bc*Aman6. In particular, the structure of the GTs *Sc*Mnn9 and *Sc*Van1 could serve as a foundation for the characterisation of processes involved in the identification of mannoprotein substrates and the formation of the mannose backbone formed by both enzymes. Additionally, the structure of all proteins could aid the identification of potent inhibitors. In combination with fragment library screens of chemical compounds, the development of such inhibitors could be significantly improved with structural inforamtion.

3 Materials and Methods

3.1 Reagents

3.1.1 Cloning

Oligonucleotides were obtained from in-house synthesis services (University of Dundee, UoD) or Integrated DNA Technologies (Leuven, Belgium). Deoxyribonucleotides (dNTPs) were purchased from Bioline (London, UK). All restriction endonucleases and T4 DNA ligase were purchased from Fermentas (Vilnius, Lithuania). Agarose was purchased from Invitrogen (Paisley, UK). KOD hot start DNA polymerase was purchased from Novagen (Merck, Darmstadt, Germany). SafeView DNA stain was bought from NBS Biologicals (Huntingdon, UK). DNA 1 kb ladder was obtained from Promega (Southampton, UK). QIAGEN Mini-Prep plasmid kit and gel-extraction kit were obtained from Qiagen (Crawley, UK).

3.1.2 Protein expression and purification

Tris base and sodium chloride were obtained from VWR (Lutterworth, UK). DNase I was purchased from Sigma-Aldrich (Dorset, UK). Hydrochloric acid (HCl) was purchased from BDH Chemicals Ltd. PreScission protease was expressed in the Daan van Aalten (DvA) laboratory (UoD). Glutathione sepharose 4B (GSH sepharose), HiTRAP IMAC FF, Q FF and Superdex 75 were all from Amersham Pharmacia Biosciences (Bucks, UK).

3.1.3 Sodium dodecyl sulphate polyacrylamide gel electrophoresis

Reagents necessary for SDS-PAGE were 40 % (w/v) 29:1 acrylamide was purchased from Flowgen Bioscience (Nottingham, UK). N,N,N',N'-tetramethylethylenediamine (TEMED) was purchased from Sigma-Aldrich (Dorset, UK). β-mercaptoethanol (BME) was obtained from Fluka (Sigma-Aldrich, Dorset, UK). Sodium dodecyl sulphate (SDS) was bought from Melford (Ipswich, UK). Glycine was purchased from VWR (Lutterworth, UK). Page-Ruler unstained and pre-strained protein ladder was obtained from Fermentas (Paisley, UK).

3.1.4 Fluorophore-assisted carbohydrate gel electrophoresis

Samples for fluorophore-assisted carbohydrate gel electrophoresis (FACE) were labelled using 8-aminonaphthalene-1,3,6-trisulphonic acid (ANTS) obtained from Apollo Scientific and sodium cyanoborohydride ($NaBH_3CN$) purchased from Sigma-Aldrich.

3.1.5 Protein crystallisation

Ammonium sulphate, sodium malonate (Na-malonate), calcium chloride ($CaCl_2$), manganese chloride ($MnCl_2$), guanosine diphosphate (GDP) and GDP-mannose (GDP-Man) were all purchased from Sigma-Aldrich (Dorset, UK). 2-[4-(2-hydroxyethyl)piperazin-1-yl]ethanesulfonic acid (HEPES) was obtained from VWR (Lutterworth, UK). PEG 6000 was bought from Duchefa Biochemie (Haarlem, Netherlands). α-1,6-mannobiose (Man2) was purchased from Carbosynth (Compton, UK). 4-methylumbelliferyl-α-1,6-mannobiose (4MU-Man2) was synthesised in the DvA laboratory by Dr. Vladimir Borodkin (UoD).

3.1.6 Enzyme kinetics

Bovine serum albumin was purchased from Thermo Scientific (Northumberland,UK). 4MU, pyruvate kinase/lactate dehydrogenase, potassium acetate (KAc), and dithiothreitol (DTT) were all obtained from Sigma-Aldrich (Dorset, UK). 4-methylumbelliferyl-mannopyranoside (4MU-Man) was bought from Carbosynth. Reduced nicotinamide adenine dinucleotide (NADH) and phosphoenolpyruvate (PEP) were purchased from Apollo Scientific (Stockport, UK).

3.1.7 Bio-layer interferometry fragment screen

5-amino-2-methylindole and 1-(4-chlorophenyl)-3-oxoisoindoline were purchased from Sigma-Aldrich. 2-(4-methylpiperazin-1-yl)aniline, 2-(1H-imidazol-1-yl)aniline, and (1-methyl-1H-pyrrol-2-yl)methylamine were bought from Maybridge (Tintagel, UK).

3.2 Equipment

3.2.1 Cloning

Polymerase chain reactions (PCRs) were carried out in a Bio-Rad MyCycler Thermocycler. Agarose DNA gel electrophoresis was performed in a Scie-plas HU10 mini-plus horizontal electrophoresis unit (Cambridge, UK). Concentration of DNA was determined on a Thermo Scientific Nanodrop ND-1000.

3.2.2 Protein purification

The FPLC systems AKTA purifier and AKTA prime were from Amersham Pharmacia Biosciences (Bucks, UK). Centrifuges, centrifuge rotors, and centrifuge tubes were all obtained from Beckmann Coulter (High Wycombe, UK). 15 ml Amicon Ultra-15 centrifugal filter units with a molecular weight (MW) cut-off (MWCO) of

10 000 units were purchased from Merck Millipore (Billerica, VA, USA). Vivaspin 20 and 500 centrifugal concentrators with a MWCO of 10 000 units, filters for syringes and filter devices (GF-prefilter, 0.2 µm and 0.45 µm pore size) were bought from Satorius (Surrey, UK). Disposable 25 ml EconoPac chromatography columns for batch binding were obtained from BioRad (Herts, UK). Snake Skin dialysis tubing with a MWCO of 10 000 units was purchased from Thermo-Pierce (Northumberland, UK). Protein concentration was determined on a Thermo Scientific Nanodrop 1000.

3.2.3 SDS-PAGE

SDS-PAGE was carried out in an ATTO AE-6450 dual mini slab kit electrophoresis system (Tokyo, Japan) using an Invitrogen Zoom Dual Power power supply.

3.2.4 FACE

FACE was carried out in an ATTO AE-6450 dual mini slab kit electrophoresis system using a Bio-Rad Powerpac Basic power supply.

3.2.5 Protein crystallisation

24-well hanging drop, pre-greased VDX plates, 18 mm circle cover slips, goniometer heads and additional X-ray equipment and tools were from Hampton Research (California, USA). 96-well sitting drop MRC plates were from Greiner Sciences (Stonehouse, UK) and crystal clear sealing tape was from Douglas Research (Berkshire, UK). Two in-house diffractometers were used to test crystals prior to data collection at a synchrotron. One diffractometer was a Rigaku (Sevenoaks, UK) Micromax-007 rotating anode generator equipped with a R-AXIS IV++ image plate detector and an Rigaku XStream nitrogen cryostream. The other diffractometer was a Rigaku Micromax-007 HF equipped with a Saturn 944 HG CCD detector and an ACTOR robot system.

3.2.6 Enzyme kinetics

A Bio-Tek FLX 800 microtiterplate fluorescence reader (Vermont, USA) was used to measure the release of 4MU. The oxidation of NADH and the growth of *S. cerevisiae* were measured on a Bio-Tek Synergy 2 multi-mode microplate reader.

3.2.7 Bio-layer interferometry fragment screen

A Fortebio Octet RED384 (Menlo Park, CA, USA) machine was used to carry out the bio-layer interferometry fragment screen.

3.3 Solutions and buffers

3.3.1 Tris-buffered saline

Tris-buffered saline (TBS) was prepared and kindly provided by the media kitchen (UoD). TBS was prepared as a 10× stock solution containing 500 mM Tris and 1.5 M NaCl. The pH was adjusted to 7.6 and the solution was autoclaved at 121 °C for 20 min.

3.3.2 Bacterial media

Lysogeny broth (LB) (Bertani, 2004) medium was prepared and kindly provided by the media kitchen (UoD) as follows: 1 % (w/v) tryptone, 0.5 % (w/v) yeast extract, and 0.5 % (w/v) NaCl were dissolved in ddH_2O, the pH was adjusted to 7.0 and the solution was autoclaved at 121 °C for 20 min. LB-agar plates were prepared by the addition of 1.5 % agar to the liquid medium before autoclaving. The liquid medium containing agar was poured into petri dishes and left to settle.

Autoinduction medium was prepared and kindly provided by the media kitchen (UoD) according to Studier (2005): 42 mM Na_2HPO_4, 22 mM KH_2PO_4, 85 mM NaCl, 1 % (w/v) tryptone, and 0.5 % (w/v) yeast extract were dissolved in ddH_2O,

the pH was adjusted to 7.2 and the solution was autoclaved at 121 °C for 20 min. After autoclaving, sterile filtered stock solutions were added to achieve the following final concentrations: 0.5 % glycerol, 0.05 % glucose, and 0.2 % lactose.

Antibiotics were added to the medium after autoclaving to achieve the following final concentrations: 100 µg/ml carbenicillin (from here on referred to as LB+Amp or Autoinduction+Amp) and 20 µg/ml chloramphenicol (from hereon referred to as LB+Amp+CML).

Super optimal broth with catabolite repression (SOC) medium was prepared by the media kitchen (UoD) and contained 2 % (w/v) tryptone, 0.5 % (w/v) yeast extract, 10 mM NaCl, 2.5 mM KCl, and 10 mM $MgCl_2$ dissolved in ddH_2O and autoclaved at 121 °C for 20 min. A sterile stock solution of glucose was added to achieve a final concentration of 20 mM.

3.3.3 Yeast medium

YPD medium was prepared and kindly provided by the media kitchen (UoD) as follow: 1 % (w/v) yeast extract, 2 % peptone (w/v). The solution was autoclaved and sterile glucose (dextrose) was added to a final concentration of 1 % (w/v). YPD-agar plates were prepared by the addition of 2 % agar.

DOA–Leu medium was a selection medium lacking the essential amino acid leucine. It was prepared and kindly provided by the media kitchen (UoD) and contained the following components: 0.7 % (w/v) yeast nitrogen base without amino acids, 20 mg arginine, 30 mg isoleucine, 30 mg lysine, 20 mg methionine, 50 mg phenylalanine, 200 mg threonine, 30 mg tyrosine, 200 mg uracil, 150 mg valine, 10 mg adenine, 10 mg histidine, 10 mg tryptophan. For plates, agar was added to a final concentration of 2 % (w/v). The solution was autoclaved and sterile glucose solution was added to a final concentration of 2 %.

3.3.4 DNA agarose gel electrophoresis

The 50× TAE stock solution was kindly provided by the media kitchen (UoD) and contained 2 M Tris base, 950 mM acetic acid, and 50 mM EDTA (pH 8.0). A 50-fold dilution was prepared in order to obtain a 1× working solution. 6× DNA loading buffer (Promega, Southampton, UK) was mixed with sample containing DNA to achieve a 1× final concentration.

3.3.5 SDS-PAGE buffer

A 10× stock solution of SDS-PAGE running buffer contained 250 mM Tris base, 192 mM glycine, and 0.1 % (w/v) SDS. The stock was diluted 10-fold to obtain a 1× working solution prior to electrophoresis.

3.3.6 SDS-PAGE staining and destaining solution

Proteins on an SDS-PAGE gel were visualised using a solution containing 50 % methanol, 20 % acetic acid, and 0.05 g/l Coomassie brilliant blue R250. The solution was filtered to remove colloidal Coomassie brilliant blue. After staining, the gel was washed several times with the same solution lacking Coomassie brilliant blue.

3.3.7 Tris-borate EDTA buffer for FACE

FACE gels were prepared with an acrylamide concentration of 30 % using 10× TBE (890 mM Tris base, 890 mM boric acid, and 20 mM EDTA, pH 8.0). A 10× stock solution of TBE was diluted 10-fold to obtain a 1× working solution for electrophoresis.

3.4 Bacterial strains

For cloning the *Escherichia coli* (*E. coli*) cell line DH5α (Promega, Southampton, UK) was used, whilst *E. coli* BL21(DE3) pLysS cells (Promega, Southampton, UK)

were used for recombinant protein expression.

3.5 Cell culture

3.5.1 Preparation of competent *E. coli* cells

E. coli DH5α or BL21(DE3) pLysS cells were streaked from a glycerol stock on a fresh LB-agar plate and incubated for 16 h at 37 °C. A single colony was used to inoculate 5 ml of SOC medium which was incubated for 8 h at 37 °C and 200 rpm. The pre-culture was used to inoculate 1 L of SOC medium which was incubated at 18 °C until the OD_{600} reached approximately 0.75. The cells were placed on ice for 10 min and then harvested in a sterile centrifuge bottle by centrifugation for 20 min at 3300 × g and 4 °C. The pellet was re-suspended in 50 ml sterile, ice-cold TB buffer (10 mM Pipes, 15 mM $CaCl_2$, 250 mM KCl, 55 mM $MnCl_2$, pH 6.7) per OD_{600}=0.1, incubated on ice for 10 min, and centrifuged again as before. The pellet was re-suspended in 13 ml ice-cold TB buffer per OD_{600}=0.1 and 7 % sterile DMSO. The re-suspended cells were incubated for 5 min on ice and then aliquoted into sterile tubes (100 µl per tube). The aliquots were flash frozen in liquid nitrogen and stored at −80 °C.

3.5.2 Transformation of competent *E. coli* cells

To prepare large quantities of plasmid DNA or to recombinantly overexpress genes, chemically competent *E. coli* DH5α or BL21(DE3) pLysS cells were, respectively, transformed with plasmid DNA. Cells had been stored at −80 °C and thawed on ice. An aliquot of 100 µl of cells was mixed with 200 ■ plasmid DNA and left on ice for 20 min. Cells were heat-shocked for 30 s at 42 °C and then left on ice for another 2 min. Cells transformed with a plasmid containing a gene to confer ampicillin resistance were spread onto LB+Amp plates and incubated at 37 °C for 16 h. BL21(DE3) pLysS carrying an additional chloramphenicol resistance cassette on

the pLysS plasmid were mixed with 500 µl SOC medium after transformation and incubated for 60 min at 200 rpm and 37 °C. Cells were collected by centrifugation at 4300 × g for 3 min. Five-hundred microlitre of supernatant was discarded, and the cell pellet was resuspended in the remaining volume, spread on LB-agar plates with the corresponding antibiotics and incubated at 37 °C for 16 h.

3.5.3 Transformation of *S. cerevisiae*

Transformation of *S. cerevisiae* cells was carried out according to a protocol developed by Gietz and Woods (2002). A single colony of *S. cerevisiae* was used to inoculate 20 ml YPDA medium and the cells were grown for 16 h at 30 °C at 220 rpm. The culture was spun down for 5 min at 1000 × g, and the pellet was washed twice in 5 ml sterile ddH_2O. For a single transformation, 100 µl of resuspended cells was mixed with 2 µg of the yeast expression plasmid pRS315 containing the gene of interest and 300 µl of transformation buffer (40 % PEG 3350, 120 mM lithium acetate, 0.8 mg/ml single-stranded salmon sperm DNA). The transformation mixture was incubated at 42 °C for 45 min. Cells were spun down for 5 min at 6000 × g, the supernatant was aspirated and the pellet was resuspended in 100 µl sterile ddH_2O. The transformed cells were spread on DOA-agar plates lacking leucine and incubated for 48 h at 30 °C.

3.6 Molecular biology

3.6.1 DNA concentration determination

DNA concentration was determined by measuring the absorbance of a DNA sample at λ=260 nm and with an extinction coefficient for double-stranded DNA of 0.020 $(\mu g/ml)^{-1}\,cm^{-1}$.

3.6.2 PCR

PCR was used to amplify DNA from genomic or plasmid templates in order to clone the product into expression plasmids or to confirm a successful transformation. Furthermore it was used to introduce mutations into genes leading to mutations in the protein of interest. A DNA polymerase with 3'->5' exonuclease activity, KOD DNA polymerase (Novagen), was used to amplify the DNA. A typical 25 µl reaction is shown in Table 3.1.

Table 3.1: Typical PCR reaction with KOD DNA polymerase

Component	[stock]	volume (µl)	[final]
ddH_2O	—	16	—
Reaction buffer	10x	2.5	1x
MgSO4	25 µM	1.5	1.5 µM
dNTPs	25 mM	1.5	1.5 mM
sense/anti-sense primer	10 µM	1.0	0.4 µM
Template DNA	50 ng/µl	1.0	2 ng/µl
KOD DNA polymerase	1 U/µl	0.5	0.02 U/µl

Table 3.2 lists the oligonucleotides used to synthesise the DNA amplicons used in this thesis.

Table 3.2: Oligonucleotides used for PCR to synthesise gene products of interest. Italic nucleotides indicate the restriction site. F, forward. R, reverse.

		*Sc*Mnn9	
Δ92	F	*Kas*I	AT*GGCGCC*GAAGGTCATATTGCACATTATGATT TGAACAAATTGC
Δ92	R	*Bam*HI	AT*GGATCC*ATCAATGGTTCTCTTCCTCTATGTG ATAAACC
		*Sc*Van1	
Δ86	F	*Kas*I	GC*GGCGCC*ATGGGCATTGGTGTATCCACGC
Δ136	F	*Kas*I	GC*GGCGCC*GATGGTGTGCAACATTATC
Δ146	F	*Kas*I	GC*GGCGCC*TTTGGTTCAGAAGTGTTG
Δ156	F	*Kas*I	GC*GGCGCC*GATGAAAAATACCAAAGGG

Construct	Direction	Restriction enzyme	DNA sequence (5'→3')
Δ166	F	*Kas*I	GC*GGCGCC*CTTTTTGATTCCACTGTTGAGGAGT ACGAC
x—513	R	*Bam*HI	AT*GGATCC*ATAAATATGCCAAATAGTATAATGCG
x—535	R	*Bam*HI	AT*GGATCC*ATTACTCTGATTGTCTTCTCTTCTC TCTTTCCC
		*Bc*Aman6	
35–375	F	*Bgl*II	AT*AGATCT*TATACCGCATCAGATGGGGATAC
35–375	R	*Not*I	AT*GCGGCCGC*ACTAGATACCGTTTAAAGCTTG

The reaction was mixed, briefly centrifuged and transferred to a PCR thermocycler which ran the program shown in Table 3.3.

Table 3.3: Thermocycler settings for a PCR with KOD DNA polymerase

Reaction	temperature (°C)	time (s)
1 Polymerase activation	94	240
2 Denaturation	94	30
3 Annealing	56	30
4 Elongation	70	20 per 1kb
5 Final elongation	70	600
6 Hold step	20	infinite

Steps 2–4 were repeated 25–30 times.

To confirm successful transformation by colony PCR, GoTAQ (Promega) was used typically in a 15 µl reaction as shown in Table 3.4.

Table 3.4: PCR reaction with GoTAQ DNA polymerase

Component	[stock]	volume (µl)	[final]
ddH2O		4.5	
Reaction buffer	2x	7.5	1x
sense/anti-sense primer	10 µM	1	0.4 µM
Template DNA	50 ng/µl	1.0	2 ng/µl

The reaction buffer contained the dNTPs and the GoTAQ DNA polymerase. After a brief mix and collection of the sample at the bottom of the tube, a program, as shown in Table 3.5, was run on a PCR thermocycler.

Table 3.5: Thermocycler settings for a PCR with GoTAQ DNA polymerase

Reaction	temperature (°C)	time (s)
1 Polymerase activation	94	240
2 Denaturation	94	30
3 Annealing	56	30
4 Elongation	72	60 per 1kb
5 Final elongation	70	600
6 Hold step	20	infinite

Steps 2–4 were repeated 18 times.

3.6.3 Mutagenesis PCR

In order to obtain point mutants of the proteins of interest, mutagenesis PCR was carried out to introduce mutations in the corresponding genes. KOD hot start DNA polymerase was used. A typical 25 µl PCR reaction is shown in Table 3.1, except that only 5 ng/µl template PCR were used to obtain a final concentration of 0.2 ng/µl.

A list of the mutagenesis oligonucleotides used in this thesis is shown in Table 3.6.

Table 3.6: Oligonucleotides used for mutagenesis PCR. F, forward. R, reverse

*Sc*Mnn9Δ92

Q124A	F	GCATATTTTGATATTGACTCCAATGGCAACATTTCATC AACAATACTGGGAC
Q124A	R	GTCCCAGTATTGTTGATGAAATGTTGCCATTGGAGTCA ATATCAAAATATGC
Q187A	F	CTCAAAGATTTAGTAAAATTACTATTTTGCGAGCTAAT TCCCAGAGTTTTGATAAGTTGATGGAG

Continued on next page

Mutagenesis	Direction	DNA sequence (5'→3')
Q187A	R	CTCCATCAACTTATCAAAACTCTGGGAATTAGCTCGCA AAATAGTAATTTTACTAAATCTTTGAG
R209A	F	GCTTTAGATGTTCAAAAGGAAGCTCGTGCAGCAATGGC TTTGGCG
R209A	R	CGCCAAAGCCATTGCTGCACGAGCTTCCTTTTGAACAT CTAAAGC
M213A	F	GGAAAGACGTGCAGCAGCGGCTTTGGCGCGCAATG
M213A	R	CATTGCGCGCCAAAGCCGCTGCTGCACGTCTTTCC
R217A	F	GTGCAGCAATGGCTTTGGCGGCCAATGAATTACTATTC TCC
R217A	R	GGAGAATAGTAATTCATTGGCCGCCAAAGCCATTGCTG CAC
D236N	F	GGTGCTGTGGCTAAATGCCGATATTATAGAGACACC
D236N	R	GGTGTCTCTATAATATCGGCATTTAGCCACAGCACC
Y267-P274_GGGG (primer to remove hairpin loop)	F	CATTTATCAAAGATTTGGTGGCGGAGGGTCAATCAGAC
Y267-P274_GGGG (primer to remove hairpin loop)	R	GTCTGATTGACCCTCCGCCACCAAATCTTTGATAAATG
Y279F	F	CAATCAGACCATTCGATTTCAAC
Y279F	R	GTTGAAATCGAATGGTCTGATTG
D280N	F	ATCAGACCATACAATTTCAACAACTGG
D280N	R	CCAGTTGTTGAAATTGTATGGTCTGAT
E305A	F	GAGATTATTGTCCAGGGTTATGCAGAA
E305A	R	TTCTGCATAACCCTGGACAATAATCTC
T365A	F	CCATTTTATCACTTGATTGAAGCAGAAGGTTTTGCTAA GATGGC
T365A	R	GCCATCTTAGCAAAACCTTCTGCTTCAATCAAGTGATA AAATGG
H389A	F	GGCTTACCAAACTATTTGGTTTATGCTATAGAGGAAGA GAACCATTGATGGATCC
H389A	R	GGATCCATCAATGGTTCTCTTCCTCTATAGCATAAACC AAATAGTTTGGTAAGCC

Continued on next page

Mutagenesis	Direction	DNA sequence (5'→3')
		*Sc*Van1
D361N	F	GGTTTATTGGAGAAATGCTGATGTAGAGCTGTGCCCTGG
D361N	R	CCAGGGCACAGCTCTACATCAGCATTTCTCCAATAAACC
		*Bc*Aman6
F72A	F	CATCAAGACGCCTGGGTGGAG
F72A	R	CTCCACCCAGGCGTCTTGATG
W73A	F	CAAGACTTCGCGGTGGAGGCTG
W73A	R	CAGCCTCCACCGCGAAGTCTTG
N120A	F	TGGACGAATGCCCCGTTCAATG
N120A	R	CATTGAACGGGGCATTCGTCCA
F122A	F	AATAACCCGGCCAATGACGATATTATG
F122A	R	CATAATATCGTCATTGGCCGGGTTATT
D124N	F	CCGTTCAATAACGATATTATG
D124N	R	CATAATATCGTTATTGAACGG
D125N	F	GTTCAATGACAATATTATGTGG
D125N	R	CCACATAATATTGTCATTGAAC
D124/D125N	F	CCGTTCAATAACAATATTATGTGG
D124/D125N	R	CCACATAATATTGTTATTGAACGG
W128A	F	GATATTATGGCGTGGGCGATG
W128A	R	CATCGCCCACGCCATAATATC
W172A	F	GGCATTTGGGCGCTGAACAGC
W172A	R	GCTGTTCAGCGCCCAAATGCC
R229A	F	GTGTTCGACGCCATCGAAATTG
R229A	R	CAATTTCGATGGCGTCGAACAC
Y243A	F	GCCACTCACGCCAACCAGGGTAC
Y243A	R	GTACCCTGGTTGGCGTGAGTGGC
N292A	F	GAAGGTCCCGCCGGGGATCTG
N292A	R	CAGATCCCCGGCGGGACCTTC
D294N	F	CCCAACGGGAATCTGAAAGGC
D294N	R	GCCTTTCAGATTCCCGTTGGG

The reaction was mixed, briefly centrifuged and transferred to a PCR thermocy-

cler which ran the program shown in Table 3.4, except that the time of the elongation step (step 4) was increased to 30 s per 1kb.

Steps 2–4 were repeated 16 times. The reaction was mixed with 10 U *Dpn*I, to degrade the parental strand used as template, and incubated at 37 °C for 60 min. Five microlitre of the product was used to transform *E. coli* DH5α cells.

3.6.4 Cloning

PCR amplicons were inserted into expression vectors (Table 3.7). The help of Dr. Andrew Ferenbach for many cloning experiments was very welcome and appreciated. An aliquot of the gene amplification reaction containing PCR was separated on a DNA agarose gel in order to confirm the correct length of the product. The amplicon and the target vector were incubated with the appropriate restriction endonucleases according to manufacturer's guidelines. In order to remove the endonucleases and the excised fragment of the vector after digest, the PCR product and the vector were run on a DNA agarose gel. Gel pieces of both, the vector and the insert, were excised from the gel and the gel piece containing the amplicon and vector were combined and purified as described in section 3.6.7. Both DNA products were eluted into 20 µl ddH_2O. Thirteen microlitres of the eluate were combined with 1.5 µl 10× ligation buffer and 0.5 µl T4 ligase. Ligation occurred at room temperature (RT) for 60 min. *E. coli* DH5α cells were transformed with 5 µl of the ligation mixture according to the protocol described in section 3.5.2.

3.6.5 DNA preparation

In order to obtain pure plasmid DNA, the QIAGEN plasmid mini-prep kit was used. Briefly, a single colony of *E. coli* DH5 α containing the plasmid of interest was used to inoculate 5 ml LB-medium containing the appropriate antibiotic. The cells were grown for 16 h at 37 °C and 200 rpm. The cells were harvested for 5 min at 3500 × g. The plasmid DNA was extracted according to the manufacturer's handbook. DNA was eluted into 40 µl ddH_2O.

Table 3.7: Expression vectors used in this thesis. R, selection by resistance against the antibiotic indicated.

Vector name	Backbone	Selection	Features
		E. coli expression vectors	
pNIFTY/MBP	pST35 (Tan, 2001)	Amp^R	Introduces a maltose binding protein (MBP), 6xHis tag and a tobacco etch virus (TEV) protease cleavage site at the N-terminus of the protein of interest
pGEX-6P-1	pBR322	Amp^R	Introcuces a gluthathione-S-transferase (GST) and a PreScission protease cleavage site at the N-terminus of the protein of interest
		Pichia pastoris expression vectors	
pPIC9	pBR322	His(–)	Introduces a cleavable secretion signal at the N-terminus of the gene of interest.
pPICZα	pUC	$Zeocin^R$	Introduces a cleavable secretion signal at the N-terminus of the gene of interest.
		S. cerevisiae expression vectors	
pRS315	pBLUESCRIPT	Leu(–)	Contains a centromere sequence and an autonomously replicating sequence (Sikorski and Hieter, 1989)

3.6.6 Agarose DNA gel electrophoresis

Agarose DNA gel electrophoresis was used to separate DNA fragments by size. Agarose (Invitrogen) was dissolved in 1$\times$ TAE to a final concentration of 1 % by bringing the suspension to a boil. The solution was left until it cooled down to approximately 70 °C when it was mixed with 5 µl SafeView (NBS Biologicals) DNA stain. The solution was poured into a gel cradle and a comb was inserted to form sample pockets. A gel formed after 30 min at ambient temperature. The comb was removed and the gel was transferred to an electrophoresis chamber and submerged in 1$\times$ TAE. Samples were mixed with 6$\times$ DNA loading buffer prior to loading them in the sample pockets. The samples were run from the anode to the cathode alongside a DNA standard ladder (Promega) for 25 min at 120 V. DNA was visualised on a UV transilluminator (Bio-Rad) and images were taken digitally for further processing.

3.6.7 DNA extraction from agarose gels

A QIAGEN gel extraction kit was used to extract DNA according to the manufacturer's handbook. Briefly, a gel piece containing the DNA of interest was solubilised and DNA was bound to a binding resin. The DNA was washed and eluted with ddH_2O.

3.7 Protein expression, analysis and purification

3.7.1 Preparation of gels for SDS-PAGE

In order to prepare SDS-PAGE gels, two glass plates were assembled with rubber gaskets and clamps according to the manufacturer's protocol. First, the separation gel was prepared by mixing the individual chemicals shown in Table 3.8. Six millilitre of the solution was poured between the two glass plates per gel. In order to avoid air bubbles and to create a smooth surface, the solution was covered with iso-propanol. The mixture was left to polymerise for at least 20 min at RT. The iso-propanol was thoroughly washed away with water and any remaining water was removed using Whatman filter paper. The stacking gel solution was prepared as shown in Table 3.8, mixed and poured on top of the polymerised separation gel. A comb was inserted to create sample pockets. The stacking gel was left to polymerise for at least 20 min. Gels were used immediately or stored in a humid bag at 4 °C.

Table 3.8: Recipe for the stacking and separating solutions for a 10 % SDS-PAGE gel, volumes per gel is shown.

		Stacking gel	Separation gel
Component	[stock]	volume	volume
ddH_2O	—	2.4 ml	3.4 ml
bis-acrylamide (29:1)	40 %	284 µl	1.8 ml
Tris-HCl, pH 6.8	2.0 M	186 ml	—
Tris-HCl, pH 8.6	1.5 M	—	1.8 ml
SDS	10 % (w/v)	30 µl	70 µl
TEMED	—	3 µl	6 µl
APS	10 % (w/v)	26 µl	24 µl

3.7.2 SDS-PAGE

SDS-PAGE was performed in order to judge the level of protein expression or to follow protein enrichment. The sample of interest was mixed with 4× Laemmli buffer (Laemmli, 1970). The samples were heated to 95 °C for 5 min and then centrifuged for 1 min at 12 000 × g to remove any precipitation. The sample was loaded into a pocket formed by the comb during gel polymerisation on a gel that was submerged in Tris-glycine running buffer in the electrophoresis system. A protein molecular weight standard ladder was run alongside. The gel was run at 200 V until the bromophenol blue running front reached the bottom end of the gel. The gel was removed from the electrophoresis system and the glass plates were separated to gain access to the gel. The proteins were visualised with staining solution for 30 min under constant agitation. To remove excess stain, the gel was rinsed three times with water and subsequently washed several times for at least 10 min each time in destaining solution until a good contrast between the background and the proteins on the gel was achieved.

3.7.3 Protein concentration determination

Protein concentration was determined by measuring the absorbance of a protein sample at λ=280 nm and its calculated extinction coefficient (ProtParam, Wilkins *et al.* 1999) using formula 3.1:

$$c = \frac{A}{Eb} \tag{3.1}$$

where c is the concentration of the protein, A is the absorbance at λ=280 nm, E is the extinction coefficient, and b is the path length.

3.7.4 Glycerol stocks of bacterial expression cells

A single colony of *E. coli* BL21(DE3) pLysS cells containing the plasmid of interest was used to inoculate 2 ml of LB medium containing the appropriate antibiotic. The culture was incubated for 16 h at 37 °C and 200 rpm. Cells were mixed with the equivalent volume of sterile 80 % glycerol and flash frozen in liquid nitrogen. The frozen cells were transferred to −80 °C for long-term storage.

3.7.5 Expression conditions of *Sc*Mnn9Δ92

E. coli BL21(DE3) pLysS cells were transformed with pNIFTY/MBP containing the gene encoding *Sc*Mnn9Δ92. A fresh overnight culture of *E. coli* BL21 transformants was diluted 1:50 in autoinduction medium (Studier, 2005) containing 100 µg/ml carbenicillin and grown at 18 °C for 24 h. Cells were harvested by centrifugation at 3300 × g for 30 min at 4 °C and the pellet was resuspended in lysis buffer (25 mM Tris-HCl, pH 7.5, 250 mM NaCl, 30 mM imidazole) and kept frozen at −80 °C until lysis.

3.7.6 Cell lysis and purification of *Sc*Mnn9Δ92

Resuspended cells were supplemented and DNase I (Sigma-Aldrich, 1 mg/l of expression culture) and lysed on a constant cell disruptor system at 15 kpsi (Avestin). The lysate was spun down for 30 min at 31 000 × g and 4 °C. The soluble fraction was passed through a 0.2 µm filter and bound to Ni^{2+} charged immobilised metal-affinity chromatography (IMAC) resin (GE Healthcare) by batch binding for 45 min at 4 °C. Unspecific proteins were washed off by applying ten column volumes (CV) of lysis buffer. The protein of interest was eluted with three CV lysis of buffer supplemented with 200 mM imidazole. The eluate was dialysed against buffer A (25 mM Tris-HCl, pH 7.5) for 2 h at RT. The MBP-6xHis-tag was cleaved off by adding 500 µg TEV protease and incubating for 16 h at 4 °C. Cleaved protein was injected onto a 5 ml HiTRAP Q FF column (GE Healthcare) equilibrated in buffer A. The MBP-6xHis tag was removed by washing with two CV buffer A containing 150 mM NaCl. *Sc*Mnn9Δ92 was eluted using three CV buffer A containing 400 mM NaCl. Fractions containing the protein of interest were pooled and dialysed against buffer B (25 mM Tris-HCl, pH 7.5, 150 mM NaCl and 2 mM $MnCl_2$) for 2 h at RT. The sample was concentrated to 1 ml and injected onto a Superdex 75 size exclusion column equilibrated in buffer B. Fractions containing *Sc*Mnn9Δ92 were pooled, concentrated to 5 mg/ml, flash frozen in liquid nitrogen and stored at −80 °C.

3.7.7 Expression conditions, cell lysis and purification of *Sc*Van1Δ86

Expression of *Sc*Van1Δ86 in *E. coli* BL21(DE3) pLysS cells, cell lysis and purification was essentially carried out as described for *Sc*Mnn9Δ92 in sections 3.7.5 and 3.7.6.

3.7.8 Expression conditions of *Bc*Aman6

E. coli BL21(DE3) pLysS cells were transformed with pGEX-6P-1 (GE Healthcare), introducing an N-termainl GST-tag and a PreScission protease cleavage site, and containing the gene encoding *Bc*Aman6. A fresh overnight culture of *E. coli* BL21 transformants was diluted 1:50 in autoinduction medium (Studier, 2005) containing 100 µg/ml carbenicillin and grown for 24 h at 20 °C and 130 rpm. Cells were harvested by centrifugation at 3300 × g for 30 min at 4 °C and the pellet was resuspended in lysis buffer (25 mM Tris-HCl, pH 7.5, 300 mM NaCl) and kept frozen at −80 °C until lysis.

3.7.9 Cell lysis and purification of *Bc*Aman6

Resuspended cells were supplemented with DNase I (Sigma-Aldrich, 1 mg/l of expression culture) and lysed on a constant cell disruptor system (Avestin) at 15 kpsi. The lysate was spun down for 30 min at 31 000 × g and 4 °C. The soluble fraction was passed through a 0.2 µm filter and bound to glutathione sepharose 4B resin (GE Healthcare) for 45 min at 4 °C. Unspecific proteins were washed off by applying ten CV of lysis buffer. The protein of interest was eluted with three CV lysis buffer supplemented with 50 mM glutathione. The eluate was dialysed against lysis buffer for 2 h at RT. The GST tag was cleaved off by adding 20 µg PreScission protease and incubated for 16 h at 4 °C. Cleaved protein was mixed with glutathione sepharose 4B resin and incubated for 30 min at 4 °C. The unbound material, containing cleaved *Bc*Aman6, was collected, concentrated and injected onto a Superdex 75 size exclusion column equilibrated in lysis buffer. Fractions containing BcAman6 were pooled, concentrated to 40 mg/ml, flash frozen in liquid nitrogen and stored at −80 °C.

3.8 Enzymology

3.8.1 Steady state kinetics of *Sc*Mnn9Δ92

A description of the assay used to determine steady-state kinetics of *Sc*Mnn9Δ92 can be found in section 4.3 and Fig. 4.9A. Briefly, *Sc*Mnn9Δ92 transfers mannose from GDP-Man to the acceptor analogue 4-methylumbelliferyl-α-D-mannopyranoside (4MU-Man) to form 4MU-Man2. This product is the substrate for the mannosidase *Bc*Aman6 which releases 4MU. To determine steady state kinetics of *Sc*Mnn9Δ92 and the two substrates GDP-Man and 4MU-Man, 500 nM *Sc*Mnn9Δ92 was incubated in 20 mM HEPES, pH 7.5, 10 mM $MnCl_2$, 0.2 mg/ml BSA, 10 µM *Bc*Aman6 with GDP-Man and 4MU-Man in a total volume of 50 µl. Initial rates of mannotriose formation were measured with substrate concentrations ranging from 0–1.2 mM GDP-Man with 10 mM 4MU-Man, and from 0–10 mM 4MU-Man with 1.2 mM GDP-Man. Product formation was determined fluorimetrically by detection of 4MU at λ_{ex}=360 nM and λ_{em}=460 nM over a time course that was within the linear range of the reaction and during which less than 10 % of the substrate was converted. The data were corrected for background emission from the buffer and the substrate alone and Michaelis-Menten parameters were obtained using GraphPad Prism 5.

3.8.2 *In vitro* mannosyltransferase assay

Mannosyltransferase assays containing 500 nM *Sc*Mnn9Δ92 and/or 500 nM *Sc*Van1, 20 mM HEPES, pH 7.5, 10 mM $MnCl_2$, 10 mM α-1,6-D-mannobiose (Man2), and 1.2 mM GDP-Man were incubated for 16 h at 30 °C, and stopped by adding 3 volumes of ice-cold ethanol. The reaction products were labeled with 750 nmol 8-Aminonaphthalene-1,3,6-trisulphonic acid (ANTS) and used in FACE based on a published protocol (Jackson, 1990) and described in section 3.8.3.

3.8.3 FACE

FACE was used to visualise the reaction products after *in vitro* mannosyltransfer. In order to separate the reaction products according to their molecular weight, an 8 % stacking gel and a 30 % separation gel were used. The preparation was similar to an SDS-PAGE gel (section 3.7.1). However, the components and volumes used for the gel were different and a are shown in Table 3.9. The polymerised gel was transferred to a electrophoresis system filled with 1× TBE buffer and pre-run for 20 min at 4 °C and 300 V.

Table 3.9: Recipe for the stacking and 30 % separating solutions for a FACE gel, volumes per gel is shown.

		Stacking gel	Separation gel
Component	[stock]	volume	volume
ddH_2O	—	2.3 ml	1.0 ml
bis-acrylamide (29:1)	40 %	375 µl	5.3 ml
TBE	10×	300 µl	700 µl
TEMED	—	3 µl	3 µl
APS	10 % (w/v)	30 µl	70 µl

Meanwhile, the excess of DMSO and $NaBH_3CN$ of the ANTS-labelled samples was removed in a vacuum centrifuge at 45 °C for 60 min. The samples were re-suspended in 30 µl FACE loading buffer (1:4 glycerol:water), and loaded onto the pre-run gel. Electrophoresis occurred for 90 min at 300 V and 4 °C. After electorphoresis, the glass plates were separated, the gel was transferred between two plastic sheets and the ANTS-labelled carbohydrates were visualised on a UV-transilluminator. A digital copy of the gel was saved for further processing.

3.8.4 Steady state kinetics of *Bc*Aman6

To determine enzyme kinetics of *Bc*Aman6 with the substrate analogue 4MU-Man2, 500 nM *Bc*Aman6 was incubated in 100 mM HEPES, pH 7.0, 10 mM $CaCl_2$, 0.2 mg/ml BSA and 4MU-Man2 in a total volume of 50 µl. Initial rates of α-1,6-

mannobiose-4MU hydrolysis were measured with substrate concentrations in the range of 0–5 mM in 3.8 % DMSO. This concentration of DMSO was necessary to achieve substrate solubility and did not effect enzyme activity. The liberation of 4MU was measured fluorimetrically at λ_{ex}=360 nm and λ_{em}=460 nm over a time course that was within the linear range of the reaction and during which less than 10 % of the substrate was converted. The data were corrected for background emission from the buffer and the substrate alone and Michaelis-Menten parameters were obtained using GraphPad Prism 5.

3.8.5 Bio-layer interferometry fragment screen

To identify chemical compounds that bind to *Bc*Aman6 a novel bio-layer interferometry fragment screen was used. *Bc*Aman6 was biotinylated with Thermo Scientific EZ-Link NHS-PEG4-Biotin according to manufacturer's instructions in an equimolar ratio in 100 mM HEPES, pH 7.0, 10 mM $CaCl_2$ (buffer A). The help obtained from Dr. David Robinson (DDU) in order to carry out the fragment screen is appreciated. Biotinylated *Bc*Aman6 at a final concentration of 12.5 µg/ml was bound to superstreptavidin-coated biosensors and free streptavidin sites were blocked with 10 µg/ml biocytin. All fragments were used at a final concentration of 200 µM. Streptavidin-bound *Bc*Aman6 was first equilibrated in buffer A for 60 s, followed by a 60 s association step in the fragment solution and a 60 s dissociation step in buffer A. Good binders were selected by using fragments that showed a higher than 3σ response compared to the median. The compounds that fulfilled this criterium were further analysed by testing five concentrations each at a 3-fold serial dilution starting at 500 µM to confirm hits, determine stoichiometry and characterise initial kinetic parameters.

3.9 Protein crystallography

3.9.1 Crystallisation methods

Crystals of proteins described in this thesis were grown by two different techniques: sitting-drop vapour diffusion (*Sc*Mnn9Δ92) and hanging-drop vapour diffusion (*Bc*Aman6). For sitting-drop vapour diffusion a 96-well MRC plate was used and the reservoir well was filled with 60 µl of mother liquor from a crystal screen kit or of the known crystallisation condition. Half a microlitre of the protein was manually pipetted onto the sitting-drop platform and mixed with the same volume of mother liquor from the reservoir and/or another additive. Finally, the plate was sealed air-tight with Crystal Clear tape.

For the hanging-drop vapour diffusion method a 24-well pre-greased, VDX plate was used. Each well was filled with 500 µl mother liquor. One microlitre of protein solution was pipetted onto a circular glass cover slip and mixed with the same volume of mother liquor from the well and/or another additive. The glass cover slip was inverted and used to seal the well air-tight. Crystals were grown at 20 °C.

3.9.2 Crystal handling

Crystals were handled with nylon loops matching the crystal's size. In order to obtain structures in complex with substrate(s), product(s) and/or a heavy metal derivative, protein crystals were soaked in a solution containing the mother liquor and the substrate(s), product(s), and/or heavy metal derivative of interest for a given time. Prior to freezing, the crystal was transferred into a solution containing the mother liquor, the substrate(s) and/or the product(s), and an appropriate cryoprotectant. The cryoprotectant was identified by mixing the mother liquor with various concentrations of known protectants such as glycerol, low-molecular weight PEG, isopropanol, ethylene-glycol, or 2-methyl-2,4-pentanediol (MPD). The suitability of the protectant was tested by putting a loop containing mother liquor and cryoprotectant into a cryostream at a temperature of 100 K. If the solution remained clear

the cryoprotectant was deemed suitable to avoid the formation of ice. However, further testing was done to identify if the cryoprotectant affected the diffraction of the protein crystal. Diffraction data were solely collected from crystals frozen in liquid nitrogen and kept in a cryostream at 100 K during data collection.

3.9.3 Determination of the *Sc*Mnn9Δ92-GDP complex structure

Octahedral *Sc*Mnn9Δ92 crystals were grown by vapour diffusion in 1 µl sitting drops containing 0.5 µl protein and 0.5 µl mother liquor (0.1 M HEPES, pH 7.5 and 2 M ammonium sulphate). Crystals were transferred to 50 % Na-malonate, pH 7.5 containing 100 mM mersalyl acid and soaked for 16 h at 20 °C. Soaked crystals were frozen directly in liquid nitrogen since the Na-malonate acted as a cryoprotectant (Holyoak *et al.*, 2003). A 38-fold redundant 2.2 Å data set, collected at beamline ID14-4 at the European Synchrotron Radiation Facility (ESRF, Grenoble, France), which was used for single-wavelength anomalous dispersion (SAD) phasing. Initial phases were calculated from a single Hg-site using the SHELX program suite (Sheldrick, 2010). Solvent flattening was also performed with SHELX, which gave a good quality map showing protein/solvent boundaries and some secondary structure elements. The map was used as input for warpNtrace (Perrakis *et al.*, 1999) which built 200 out of 305 residues. There is one molecule in the asymmetric unit. Model building and refinement was continued in COOT (Emsley and Cowtan, 2004) and REFMAC (Murshudov *et al.*, 1997), yielding the final model with statistics shown in Table 4.1.

Crystals of *Sc*Mnn9Δ92 D236N were transferred to 50 % Na-malonate, pH 7.5 and soaked with 3 mM GDP and 10 mM $MnCl_2$ for 10 min at 20 °C and then flash frozen in liquid nitrogen. Diffraction data were collected at beamline ID14-4 at the ESRF to 2.0 Å. Refinement was initiated from the native structure using rigid body refinement. This revealed well defined $|F_O|-|F_C|$ electron density for GDP and Mn^{2+}. Model building and refinement was performed as described above. Statistics of the final model are shown in Table 4.1.

3.9.4 Determination of the *Bc*Aman6 structure

Rod shaped crystals of *Bc*Aman6 were grown by vapour diffusion in 2 µl hanging drops containing 1 µl protein and 1 µl mother liquor (0.1 M HEPES, pH 7.0, 0.2 M $CaCl_2$ and 20 % (w/v) PEG 6000). Crystals were transferred to a drop containing the original condition supplemented with 20 % glycerol prior to freezing in liquid nitrogen. A 12-fold redundant data set was collected at beamline I-24 at the Diamond Light Source (Didcot, UK). The structure was solved by molecular replacement with the coordinates of a model of *Bc*Aman6 produced by RaptorX (Källberg *et al.*, 2012) and Phaser (McCoy *et al.*, 2007). The resulting model was refined using REFMAC (Murshudov *et al.*, 1997). The refined model was used as input for Phenix AutoBuild (Adams *et al.*, 2010). Stretches of amino acids without clear density from the resulting model were removed in COOT (Emsley and Cowtan, 2004). The trimmed model was used as input for warpNtrace (Perrakis *et al.*, 1999). The output gave a better model of *Bc*Aman6 in agreement with the electron density. Model building and refinement was continued in COOT and REFMAC, yielding the final refinement statistics shown in Table 6.1.

3.10 Figures

3.10.1 Structure representation

All figures representing protein structures were created with the molecular visualisation program PyMOL. Alignments were carried out with the programme ALINE (Bond and Schüttelkopf, 2009). Structures of chemical compounds were drawn with CS ChemDraw Ultra 12 (CambridgeSoft, Cambridge, MA, USA).

3.10.2 Structure superimposition

Structure superpositions were made with the SSM Superpose command in COOT (Emsley and Cowtan, 2004).

3.10.3 Data analysis and enzymological figures

All non-linear regression analysis was carried out using the programme Prism 5 (GraphPad, La Jolla, CA, USA).

3.10.4 Image annotation

Images shown in this thesis were annotated using Apple Pages (Apple, Cupertino, CA, USA).

4 Mannosyltransferase *Sc*Mnn9 – Results and Discussion

4.1 Cloning, heterologous expression and purification of *Sc*Mnn9Δ92

Mnn9 from yeasts and filamentous fungi possess high levels of sequence conservation, in particular in the C-terminal globular domain that forms the active site (Fig. 4.1). The *S. cerevisiae* Mnn9 was used for the experiments described here because of the extensive knowledge about its *in vivo* and *in vitro* activity. This information was useful for the determination of a construct that was both active and likely to crystallise due to the lack of membrane domains or disordered regions.

In order to membrane domains and disordered regions at the protein level, the amino acid sequence of *Sc*Mnn9 was used as input to several prediction tools available on the world wide web. The TMHMM server (Krogh *et al.*, 2001) was used to predict the transmembrane domain, which isnecessary to anchor *Sc*Mnn9 in the Golgi membrane (Fig. 4.1) To identify the disordered linker region, the secondary structure of *Sc*Mnn9 was predicted by PORTER (Pollastri and McLysaght, 2005) (Fig 4.1). Using this information and the alignment across several fungal species, the *mnn9* gene encoding for amino acid residues 93–395 (*Sc*Mnn9Δ92) was amplified from the genomic DNA of *S. cerevisiae* (Fig. 4.1). The gene was cloned into an *E. coli* expression vector (pNIFTY/MBP), which introduced an N-terminal maltose-binding protein (MBP)-tag, followed by a hexahistidine tag and a tobacco

Figure 4.1: Alignment of Mnn9 from different fungal species. The amino acid sequences were aligned and conservation and similarity is shown in grey scale with black being identical between all species. The secondary structure prediction of *Sc*Mnn9 is shown above the amino acid sequence, where red cylinders represent α-helices and blue arrows represent β-strands. The predicted N-terminal transmembrane domain is indicated by a box with a green line, whereas the canonical DXD motif is indicated by a filled green box. The star indicates the start of the construct of *Sc*Mnn9 used for this thesis (*Sc*Mnn9Δ92).

etch virus (TEV) protease cleavage site. *E. coli* BL21(DE3) pLysS cells were transformed with the expression plasmid containing the *mnn9* gene and the protein was expressed in autoinduction medium (Studier, 2005). After lysis, the protein was bound to immobilised metal affinity chromatography (IMAC) resin charged with Ni^{2+} and eluted with imidazole (Fig. 4.2). After dialysis, the MBP-6×His-TEV tag was cleaved off by TEV protease and the tag was completely removed from cleaved *Sc*Mnn9Δ92 by anion exchange chromatography. Uncleaved and cleaved *Sc*Mnn9Δ92 were separated by size-exclusion chromatography and the enriched cleaved protein was concentrated to 5 mg/ml. Overall a yield of 2 mg of protein per litre of bacterial culture was obtained (Fig. 4.2).

Crystals grew from the protein at a concentration of 5 mg/ml within 24 h in a condition containing ammonium sulphate as precipitant (Fig. 4.3A). A 2.2 Å diffraction data set of a mersalyl acid soaked crystal was collected and used for single-wavelength anomalous dispersion (SAD) phasing in order to determine the structure of *Sc*Mnn9Δ92 (Fig. 4.3B, Table 4.1). The structure of *Sc*Mnn9Δ92 D236N, a mutation similar to D236A that has been shown to be inactive (Stolz and Munro, 2002), in complex with GDP and Mn^{2+} was solved using the initial model from the SAD experiment and a 2.0 Å data set of the mutant (Fig. 4.4A). Refinement of this complex yielded a final R/R_{free} of 0.19/0.24 (Table 4.1).

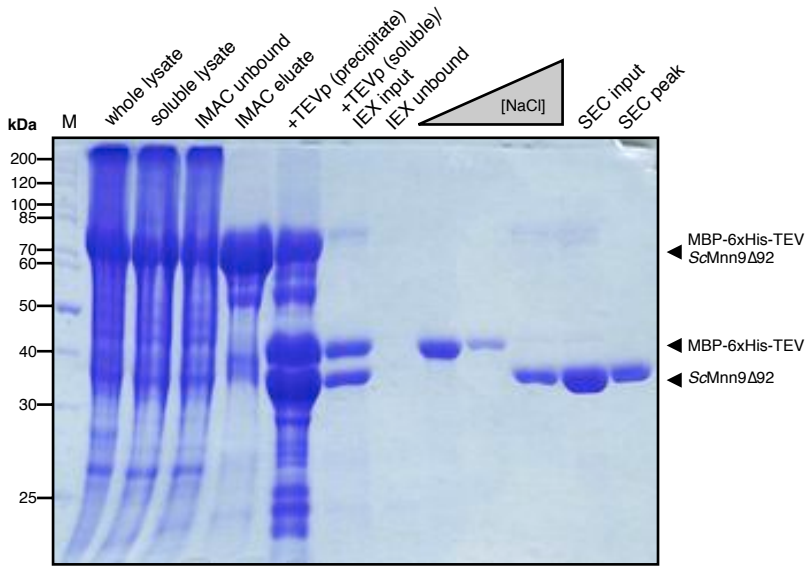

Figure 4.2: Enrichment of *Sc*Mnn9Δ92. Coomassie-blue stained SDS-PAGE gel of different steps during the enrichment of *Sc*Mnn9Δ92. M, molecular weight ladder; TEVp, TEV protease; SEC, size-exclusion chromatography. The grey triangle indicates an increase in concentration of NaCl during anion exchange chromatography.

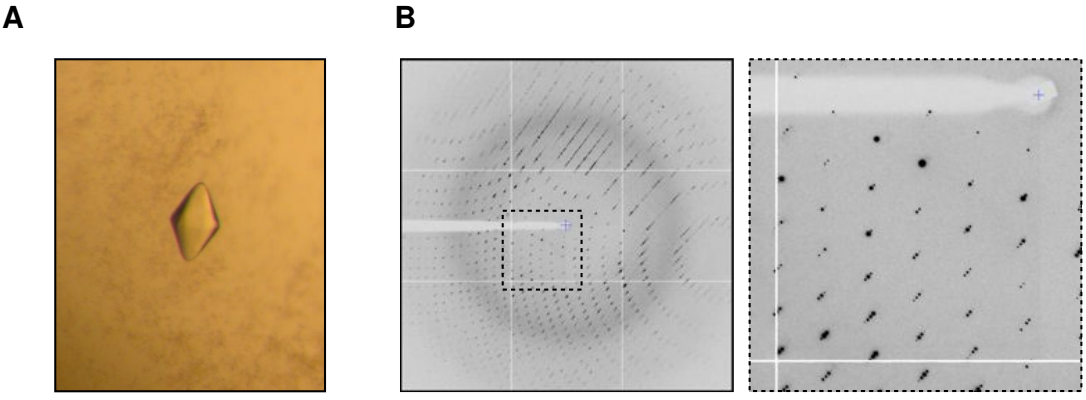

Figure 4.3: Crystallisation and diffraction of *Sc*Mnn9Δ92. A, Crystal of *Sc*Mnn9Δ92 grown in a solution containing ammonium sulphate as precipitant. **B,** Diffraction of a crystal of *Sc*Mnn9Δ92 collected at the ESRF (Grenoble, France). The right frame is a 100 % crop of the area indicated in the left frame.

Table 4.1: Details of data collection and structure refinement. Values in parenthesis are for the highest resolution shell

	*Sc*Mnn9Δ92 + Hg-SAD	*Sc*Mnn9Δ92 apo	*Sc*Mnn9Δ92 D236N + Mn^{2+} + GDP
Space group	$P6_522$	$P6_522$	$P6_522$
Cell dimensions			
a, b, c (Å)	57.05, 57.05, 330.17	57.04 57.04 331.01	57.09, 57.09, 330.91
α, β, γ (°)	90, 90, 120	90, 90, 120	90, 90, 120
Resolution range (Å)	25.0–2.1 (2.2–2.1)	39.6–2.0 (2.1–2.0)	55.0–2.0 (2.1–2.0)
Number of observed reflections	1 342 417	175 192	366 234
Number of unique reflections	19 947	22 986	23 775
Redundancy	37.8 (33.4)	7.6 (8.3)	9.7 (10.1)
$I/\sigma(I)$	37.0 (13.6)	18.7 (11.2)	11.8 (5.0)
Completeness (%)	99.9 (100.0)	99.8 (100.0)	100.0 (100.0)
R_{merge}	0.148 (0.579)	0.070 (0.175)	0.149 (0.482)
Number of protein residues	288	287	288
Number of water molecules	–	37	148
R_{work}, R_{free}	–	0.21, 0.25	0.19, 0.24
RMSD from ideal geometry			
bond lengths (Å^2)	–	0.024	0.012
bond angles (°)	–	1.93	1.43
B-factors (Å^2)			
protein	–	11.3	17.9
ligand	–	–	GDP: 34.7 Mn^{2+}: 45.2
water	–	9.2	19.7

4.2 *Sc*Mnn9Δ92 is structurally similar to GT-15 and GT-78 mannosyltransferases

The structure reveals that *Sc*Mnn9Δ92, and by extension the entire GT-62 glycosyltransferase family, is a GT-A fold GT as it was previously proposed by sequence analysis (Liu and Mushegian, 2003) (Fig. 4.4A). Ten β-strands form a sheet that is covered on both sides by seven α-helices. This arrangement is the result of two Rossmann-like domains that are in close proximity. As most GT-A GTs have a high structural similarity around the active site, the identification of structural homologs was crucial to spot novel features of *Sc*Mnn9Δ92. Using the DALI server (Holm and Rosenström, 2010) the *Rhodothermus marinus* mannosylglycerate synthase from GT-76 (*Rm*MGS, PDB: 2Y4M, Fig. 4.4B) (Nielsen *et al.*, 2011) as well as the *S. cerevisiae* α-1,2-mannosyltransferase Kre2p/Mnt1p from GT-15 (PDB: 1S4O, Fig. 4.4C) (Lobsanov *et al.*, 2004) were identified as structural homologs (Z-score=13.7, RMSD=3.4 Å on 188 equivalent Cα atoms for *Rm*MGS and Z-score=9.8, RMSD=3.8 Å on 185 equivalent Cα atoms for Kre2p/Mnt1p). Despite the fact that neither of the structures were among the top ten hits, they were used because both GTs use GDP-Man as the donor substrate which may be important for the architecture of the active site. *Rm*MGS uses GDP-Man to transfer mannose onto D-glycerate, D-lactate or glycolate (Borges *et al.*, 2004, Martins *et al.*, 1999). *Sc*Kre2p/Mnt1p synthesises O-linked oligomannose and the terminal oligomannose decorations on mannoproteins (Lussier *et al.*, 1999). Superposition of *Sc*Mnn9Δ92, *Rm*MGS and *Sc*Kre2p/Mnt1p reveals the structural similarity derived from the GT-A fold around the catalytic site (Fig. 4.4). However, *Sc*Mnn9Δ92 has a unique hairpin loop formed by the two elongated β-strands 6 and 7 (residues 262–283, Fig. 4.4A). The loop clearly stands out from the globular active site domain opposite the N-terminus (Fig. 4.4A). This loop is positioned in line with the active site and could serve a number of purposes. It could act as a molecular ruler for the formation of a mannose backbone of defined length or act as a guide to recognise and correctly position protein N-linked glycans for to which mannose

is added. Alternatively, it could serve as a dimerisation domain for *Sc*Mnn9 and *Sc*Van1. In contrast, *Rm*MGS has a more extended C-terminus formed by six helices and a short β-strand whilst *Sc*Kre2p/Mnt1p does not contain any protruding features. Interestingly, the interactions between GDP and the enzymes are very similar (Fig. 4.5). The guanine forms hydrogen bonds between the N1 amine and the amide oxygen of a glutamine (*Sc*Mnn9Δ92 and *Rm*MGS) or an aspartic acid (*Sc*Kre2p/Mnt1p). In all three enzymes the guanine is buried by residues with relatively long side chains, *e. g.* Q124 in *Sc*Mnn9Δ92, K9 in *Rm*MGS and R130 in *Sc*Kre2p/Mnt1p (Fig. 4.5). The ribofuranose forms extensive hydrogen bonds with the side chains of residues in the active site. Manganese is coordinated by a histidine side chain, a carboxylate and the pyrophosphate moiety of GDP. The histidine, common to many retaining GT-A GTs, occupies a similar position within the active site of all three transferases (Fig. 4.5) and is one of the very few (five) conserved residues in the sequences of the GT-15, GT-62 and GT-76 glycosyltransferases compared here (Fig. 4.5). The carboxylate metal ligand is part of the canonical GT-A fold DXD motif (Figs. 4.1, 4.5). Both the α and β-phosphates of the GDP interact with the metal in *Sc*Mnn9, which is similar to the *Rm*MGS enzyme (Fig. 4.5).

Despite the fact that *Sc*Mnn9Δ92 D236N was soaked or co-crystallized with GDP-Man, electron density for mannose was not observed. The mannose of GDP-Man in the *Rm*MGS complex forms hydrogen bonds with K76 and D192 and several backbone amides (Fig. 4.5B). In order to identify potential residues involved in the co-ordination and the glycosyl transfer of mannose in *Sc*Mnn9Δ92, the structures of *Sc*Mnn9Δ92 and *Rm*MGS were superimposed using GDP as the reference (Fig. 4.6). Based on this superpositioning it appears that mannose is in hydrogen bonding distance to residues N(D)236, R210 and D280. D280 is the acid potentially involved in the glycosyl transfer. In fact, expression and purification of a D280N mutant usually led to considerably lower yields compared to WT and other mutants. This may indicate that the residue also has important effects on the folding of the protein during expression. Misfolded protein could be subject to degradation in *E. coli* after expression. In *Rm*MGS, D192 is located at the opposite side of man-

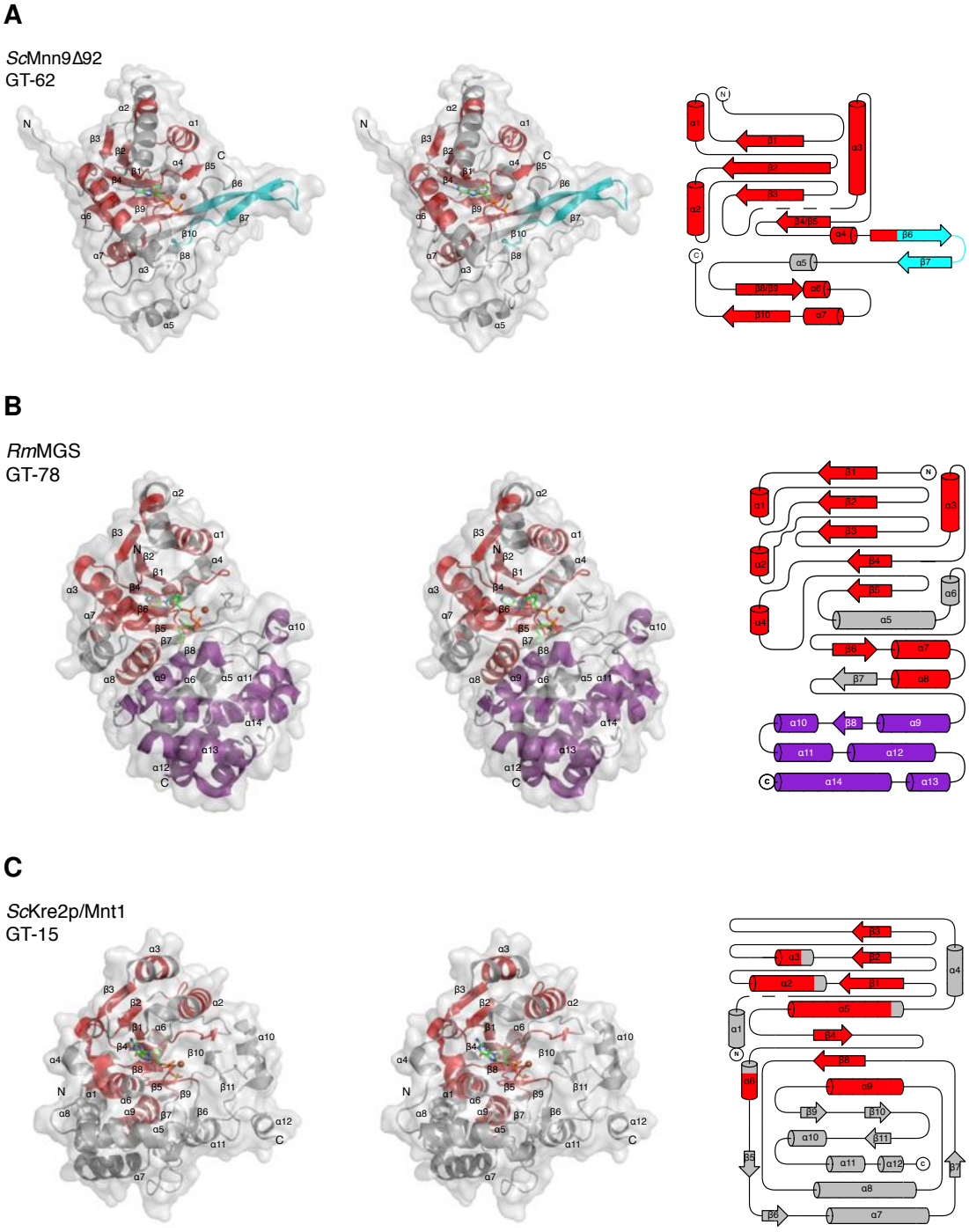

Figure 4.4: Stereoscopic images and topology of *Sc*Mnn9Δ92, GT-78 *Rm*MGS, and GT-15 *Sc*Kre2p/Mnt1p. All structures are shown with the same viewing matrix applied. **A,** *Sc*Mnn9Δ92 in complex with GDP and Mn^{2+}. **B,** *Rm*MGS in complex with GDP-Man and Mg^{2+} (PDB: 2Y4M). **C,** *Sc*Kre2p/Mnt1p in complex with GDP and Mn^{2+} (PDB: 1S4O). Red indicates secondary structure elements that are struturally similiar between all three GTs. Cyan indicates the protruding loop found in *Sc*Mnn9δ92. Purple shows the C-terminal dimerisation domain of *Rm*MGS. Grey represents secondary structure elements that are not structurally similar between the GTs.

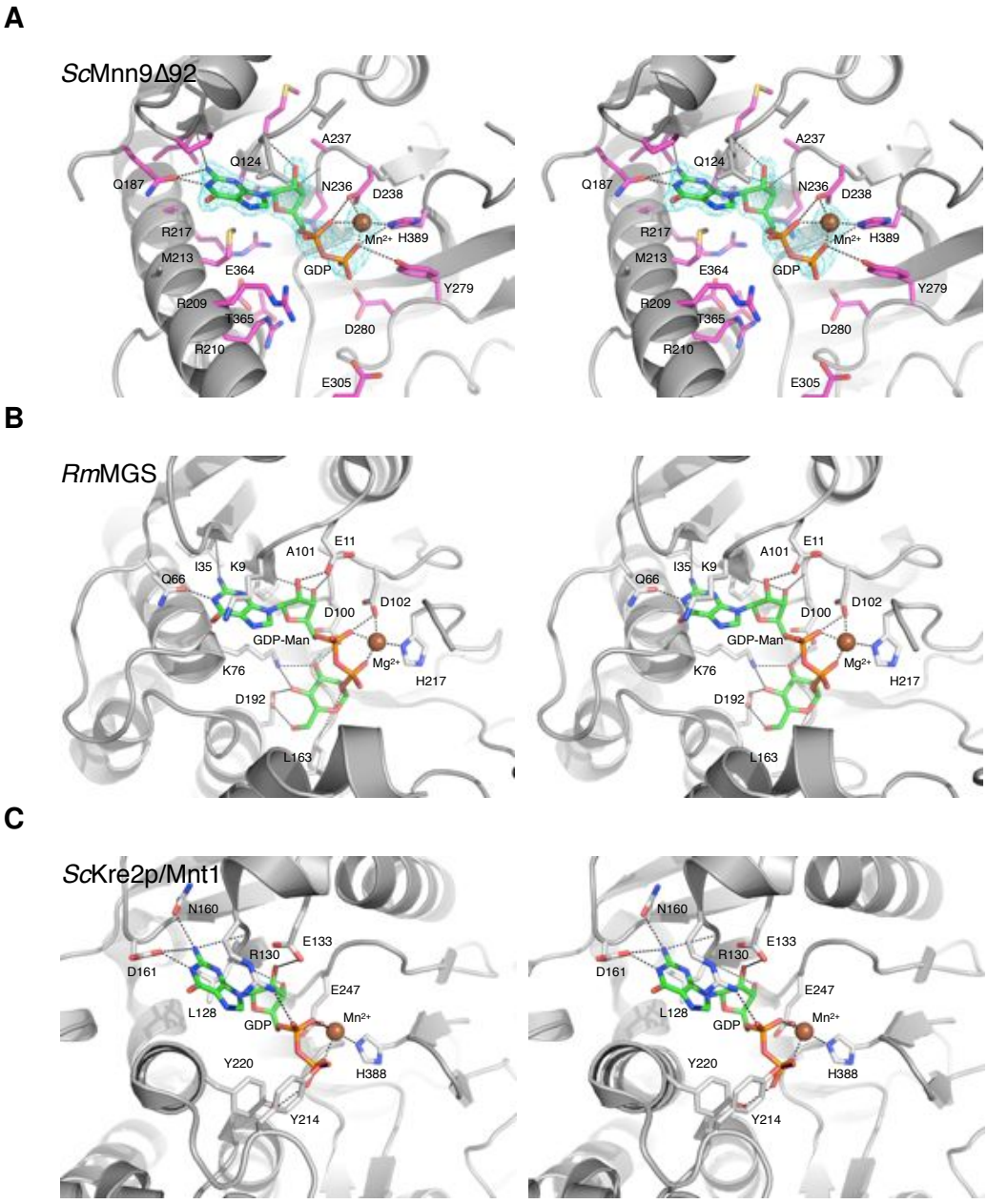

Figure 4.5: Stereoscopic images of the active sites of *Sc*Mnn9Δ92, GT-78 *Rm*MGS, and GT-15 *Sc*Kre2p/Mnt1p. A, *Sc*Mnn9Δ92 in complex with GDP and Mn^{2+}. Residues within 6 Å distance of GDP as sticks with purple carbon atoms. The unbiased $|F_O|-|F_C|$ map (1.75σ) is shown as cyan mesh around GDP and Mn^{2+}. **B,** *Rm*MGS in complex with GDP-Man and Mg^{2+} (PDB: 2Y4M). Residues that have been described to interact with the substrate and the metal are shown as sticks with grey carbon atoms (Nielsen *et al.*, 2011). **C,** *Sc*Kre2p/Mnt1p in complex with GDP and Mn^{2+} (PDB: 1S4O). Residues that have been described to interact with the nucleotide-diphosphate and the metal are shown as sticks with grey carbon atoms (Lobsanov *et al.*, 2004). All panels: Mn^{2+} and Mg^{2+} are shown as brown spheres. Hydrogen bonds are shown as dashed black lines.

nose, forming hydrogen bonds with OH3 and OH4, instead of OH2 as is the case for D280 in *Sc*Mnn9Δ92 (Fig. 4.5A, B). D192 is essential for activity in *Rm*MGS (Nielsen *et al.*, 2011). D280 in *Sc*Mnn9Δ92 could have similar importance for the activity of the yeast GT.

4.3 Recombinant *Sc*Mnn9Δ92 possesses mannosyltransferase activity *in vitro*

To date, enzyme activity of *Sc*Mnn9 has only been demonstrated in the presence of *Sc*Van1p (Rodionov *et al.*, 2009, Stolz and Munro, 2002). Hence, it was necessary to test the activity of bacterially expressed *Sc*Mnn9Δ92 in the presence of manganese, GDP-Man and a model acceptor substrate, α-1,6-linked mannobiose. This model acceptor has been used before (Rodionov *et al.*, 2009, Stolz and Munro, 2002) and was chosen because of its nature to mimic the reaction product of the Och1 GT. Och1 transfers a mannose to the α-1,3-Man in the N-linked glycan core forming an α-1,6-mannobiose (Nakayama *et al.*, 1997) (Fig. 1.5. Reaction products were separated and visualised by fluorophore-assisted carbohydrate gel electrophoresis (FACE) (Fig. 4.7A), which showed that *Sc*Mnn9Δ92 alone is able to transfer mannose from the sugar donor onto a disaccharide acceptor substrate, forming mannotriose.

Furthermore, manganese is required for activity, and cannot be substituted by other divalent cations, such as magnesium or calcium (Fig. 4.7B).

Structure guided point mutations of *Sc*Mnn9Δ92 were designed, cloned, expressed, and tested in an activity assay (Figs. 4.5A and 4.7C). R209 lines the putative mannose binding site and mutation to alanine results in loss of *Sc*Mnn9Δ92 activity (Fig. 4.7C). Similar effects were reported for the equivalent K76A mutation in *Rm*MGS (Nielsen *et al.*, 2011). *Sc*Mnn9Δ92 D236 is the first aspartic acid in the canonical GT-A DXD catalytic motif and mutation to an isosteric asparagine results in loss of activity (Fig. 4.7C), similar to the previously reported less conser-

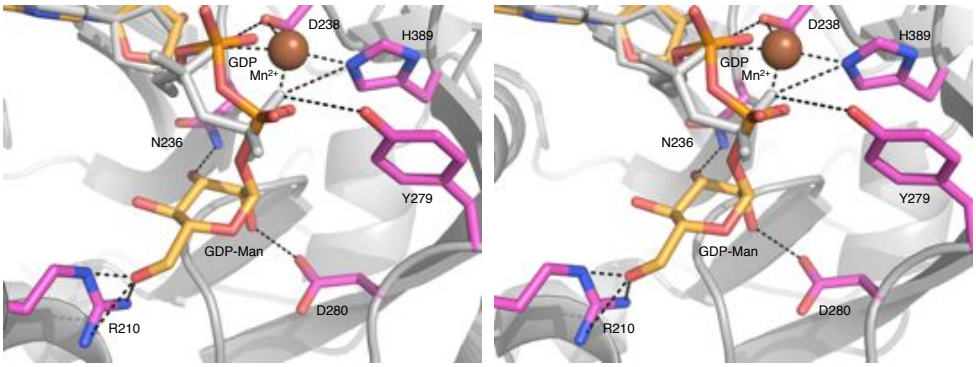

Figure 4.6: Stereo images of *Sc*Mnn9Δ92 and GDP-Man modelled based on the superposition with *Rm*MGS GDP-Man. The structures of *Sc*Mnn9Δ92 D236N in complex with GDP (grey sticks) and *Rm*MGS in complex with GDP-Man (orange sticks) were superimposed using GDP as the reference. Potential hydrogen bonds formed between GDP-Man and *Sc*Mnn9Δ92 D236N are shown as dashed lines.

vative D236A mutation (Stolz and Munro, 2002). Interestingly, the D236N mutant is still able to form a hydrogen bond with mannose as suggested by the superposition of GDP-Man on to the *Sc*Mnn9ΔD236N structure (Fig. 4.6). It is possible that the carboxyl group of the native aspartic acid is involved in the reaction. The equivalent residue in *Rm*MGS, D100, forms a hydrogen bond with the mannose O3 hydroxyl (Fig. 4.5B). Extensive attempts to obtain a binary complex of *Sc*Mnn9Δ92 and GDP-Man were not successful. However, inspection of the superimposed *Rm*MGS complex suggests that *Sc*Mnn9Δ92 D280 would also line the putative mannose binding site, positioned close to the O2 hydroxyl group. Mutation of this aspartic acid to asparagine (D280N) results in an inactive enzyme (Fig. 4.7C). *Sc*Mnn9Δ92 H389 coordinates the manganese and is indispensable for catalytic activity (Fig. 4.7C).

*Sc*Mnn9Δ92 is able to hydrolyse GDP-Man in the absence of an acceptor (Fig. 4.7D). Several point mutants were also tested in an assay in which the acceptor α-1,6-mannobiose was missing. The mutants Q187A and E305Q showed a comparable ability to hydrolyse GDP-Man compared to WT, as determined by semi-quantitative analysis. The D280N mutant was able to hydrolyse 50 % GDP-Man compared to WT. This can be taken as an indicator that D280 is at least partially

involved in the transfer. The mutant is still able to hydrolyse GDP-Man, but is not able to transfer it onto an acceptor (Figs. 4.7C and 4.7D). In contrast, mutants R209A and H389A lose 86 % and 90 % of the hydrolytic activity compared to WT, respectively. From the GDP complex and the superpositioned GDP-Man (Figs. 4.5A and 4.6) it does not appear as if R209 is involved in the co-ordination or binding of the substrate which would explain this loss in activity. However, it has to be mentioned, that the superposition of GDP-Man onto *Sc*Mnn9Δ92 could be wrong and that if mannose is positioned differently in the active site there may be an important interaction of R209 and mannose. The loss in activity of the H389A mutant can be explained by the loss of the co-ordination of the manganese ion. The metal is potentially needed to neutralise the pyrophosphate leaving group. In the absence of H389 this can not be achieved, rendering *Sc*Mnn9Δ92 inactive.

In order to obtain information about the importance of the extension formed by β-strands 6 and 7, a construct was designed in which residues 267–274 were replaced with four glycine residues (*Sc*Mnn9Δ267–274_GGGG, Fig. 4.1). The protein expressed in a similar yield and could be purified equally well as *Sc*Mnn9Δ92 WT. This indicated that the protein was still in a folded state. However, crystals of this protein did not grow in the condition used for the WT protein and could not be obtained in any other crystallisation condition tested, suggesting that folding and/or packing of the protein was influenced by the removal of the extension. The mutant protein was used in an activity assay and the products were labelled with ANTS and separated on a FACE gel (Fig. 4.7E). *Sc*Mnn9Δ267–274_GGGG showed no formation of mannotriose, indicating that the extension is important for activity.

Previously, it has been shown that *Sc*Mnn9 is able to add an α-1,2-mannose to the α-1,6-mannobiose substrate analogue (Stolz and Munro, 2002). Hence, the product of the glycosyl transfer reaction of *Sc*Mnn9Δ92 and α-1,6-mannobiose was incubated with an α-1,2-specific mannosidase and the reaction products were labelled with ANTS and speparated on a FACE gel (Fig. 4.8). The product formed by *Sc*Mnn9Δ92 was resistant to the mannosidase suggesting that the product does not have an α-1,2-linked mannose.

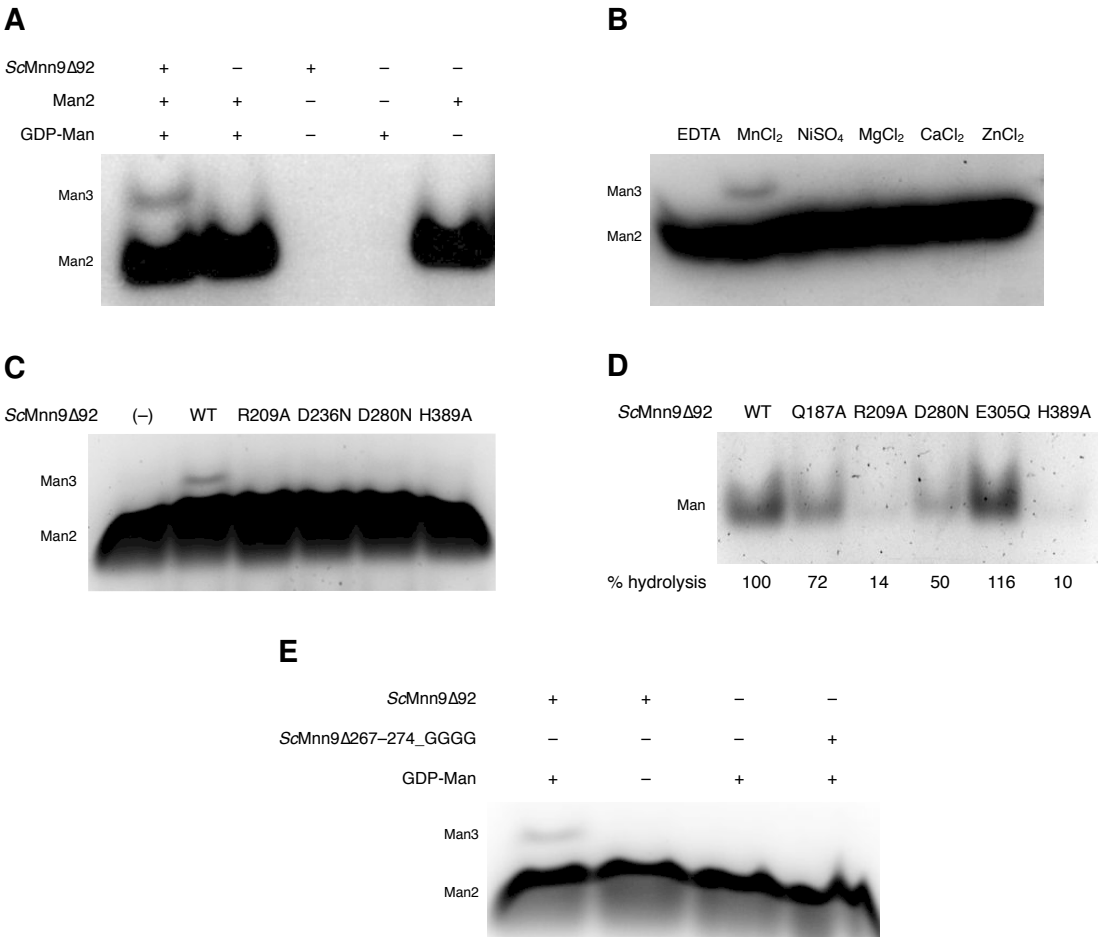

Figure 4.7: FACE gels showing activity of *Sc*Mnn9Δ92 WT and mutants. A, FACE gel of ANTS-labelled products after the transferase reaction in the presence and/or absence of *Sc*Mnn9Δ92, α-1,6-mannobiose (Man2), and GDP-Man. $MnCl_2$ was present in all reactions. **B,** Metal-dependency of *Sc*Mnn9Δ92. Reactions as in A, lane 1, however here in the presence of 10 mM of EDTA or metal indicated above the gel at 10 mM. **C,** Activity of *Sc*Mnn9Δ92 WT and point mutants. Reactions as in A, either in absence of *Sc*Mnn9Δ92 WT or in presence of *Sc*Mnn9Δ92 WT and mutants. **D,** Hydrolysis of GDP-Man by *Sc*Mnn9Δ92 WT and point mutants. Reactions were carried out in the absence of the acceptor α-1,6-Man2. The relative hydrolysis of GDP-Man was determined by semi-quantitative measurements. **E,** FACE gel of ANTS-labelled products after the transferase reaction in the presence and/or absence of *Sc*Mnn9Δ92, *Sc*Mnn9Δ267–274_GGGG, and GDP-Man. α-1,6-Man2 and $MnCl_2$ were present in all reactions.

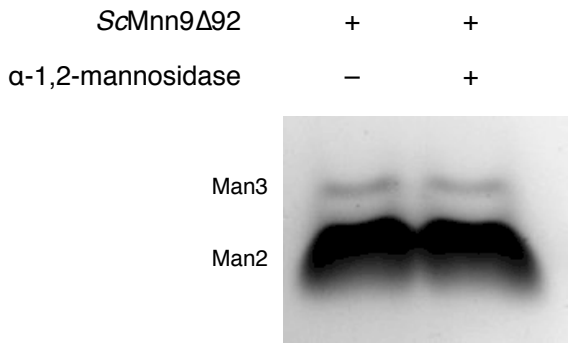

Figure 4.8: α-1,2-mannosidase treatment of the *Sc*Mnn9Δ92, GDP-Man and Man2 reaction product. FACE gel of ANTS-labelled *Sc*Mnn9Δ92 reaction products after incubation in the absence or presence of α-1,2-specific mannosidase from *A. saitoi*.

To study *Sc*Mnn9Δ92 steady state kinetics, a novel coupled enzyme assay was developed that involves only one additional enzyme, in contrast to the established glycosyltransferase assays where the release of GDP is measured by NADH oxidation through pyruvate kinase and lactate dehydrogenase (Gosselin *et al.*, 1994). Here, the gene product of *Bacillus subtilis* TN-31 aman6 (*Bc*Aman6), an α-1,6-mannosidase (Maruyama and Nakajima, 2000, Nakajima *et al.*, 1976), was used as a coupling enzyme (Fig. 4.9A). This mannosidase has been reported to act on mannotriose as a minimal substrate (Nakajima *et al.*, 1976). This enzyme is also able to liberate 4-methylumbelliferone (4-MU) from 4MU-α-1,6-mannobiose (4MU-Man2), but crucially not from 4MU-Man. Thus, only in the presence of active *Sc*Mnn9Δ92, which transfers a mannose onto 4MU-Man, would the *Bc*Aman6 mannosidase be able to liberate fluorescent 4MU from the resultant 4MU-Man2 product (Fig. 4.9B). This assay was used to establish steady state kinetics for wild type *Sc*Mnn9Δ92 (Figs. 4.9C and D). The $K_{m,app}$ determined for the 4MU-Man acceptor is 6.5 ($\pm$0.3) mM with an V_{max} of 77.7 ($\pm$2) nM/min resulting in a k_{cat} of 0.2 s^{-1}. The $K_{m,app}$ for GDP-Man is 0.54 ($\pm$0.2) mM, V_{max} of 1.9 ($\pm$0.3) µM/min resulting in a k_{cat} of 3.8 min^{-1}. Compared to the K_m and V_{max} of *Rm*MGS using glycerate as acceptor (Flint *et al.*, 2005, Nielsen *et al.*, 2011), *Sc*Mnn9Δ92 seems to have low affinity for both of its substrate. Interestingly, the k_{cat} for *Sc*Mnn9Δ92 and GDP-Man is comparable to *Rm*MGS and GDP-Man (1.9 min^{-1}). In contrast, Kre2p/Mnt1p is

considerably faster than *Sc*Mnn9Δ92 with k_{cat} of 12.8 s^{-1} for GDP-Man and 10.8 s^{-1} for methyl-α-mannoside, whilst the $K_{m,app}$ of 26 mM for the Kre2p/Mnt1p acceptor substrate analogue methyl-α-mannoside can be interpreted as a sign of poor substrate binding. The low substrate affinity of *Sc*Mnn9Δ92 and *Sc*Kre2p/Mnt1p *in vitro* might be a result of the artificial acceptor substrates used. Whilst for *Sc*Kre2p/Mnt1p the physiological substrate is an α-1,2-mannobiose attached to a serine or threonine (Häusler and Robbins, 1992, Häusler *et al.*, 1992), the substrate of *Sc*Mnn9 is an N-linked core glycan extended with a mannose attached by Och1p (Jungmann and Munro, 1998) – structurally rather dissimilar from the 4MU-Man pseudo-acceptor used here. Furthermore, *Sc*Mnn9 is found in the multimeric glycosyltransferase complexes M-Pol I and II (Jungmann and Munro, 1998, Jungmann *et al.*, 1999) and intermolecular interactions in these complexes may well increase affinity of *Sc*Mnn9 for its substrates. It is also possible that *Sc*Mnn9 has a comparatively low affinity for its substrates in order to limit its consumption of cellular GDP-Man, which may be particularly important as M-Pol I activity is the starting point of extensive additional mannosylation (Jungmann *et al.*, 1999), requiring large amounts of additional GDP-Man. Another explanation is the absence of the predicted disordered linker in this construct of *Sc*Mnn9. This linker may have an impact on activity of the GT.

4.4 *Sc*Mnn9Δ92 catalytic activity is indispensable for mannoprotein synthesis in yeast

Strains of *S. cerevisiae* and *C. albicans* with defects in mannan synthesis show hypersensitivity to hygromycin B and reduced sensitivity to sodium orthovanadate (Ballou *et al.*, 1991, Dean, 1995). Guided by the crystal structure, catalytically inactive mutants of *Sc*Mnn9Δ92 were identified (Fig. 4.5A and 4.7C) that could be used to dissect the function of the protein with the help of a Δ*mnn9* strain of *S. cerevisiae*. Wild type and point mutants Q124A, R209A, D236N, D280N, and

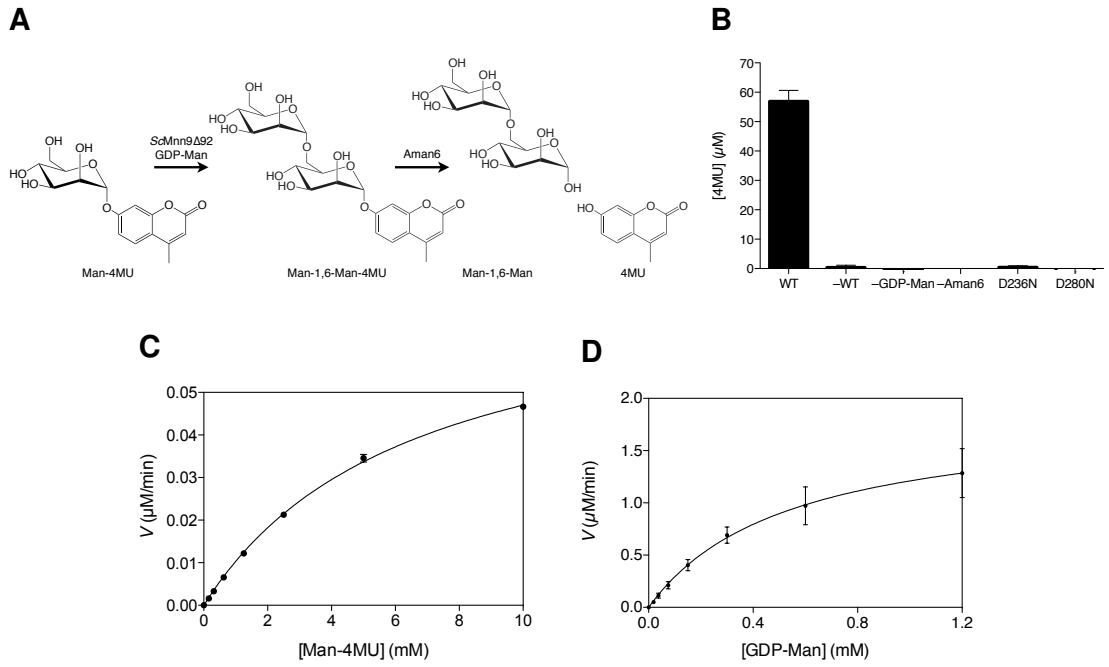

Figure 4.9: Fluorescent assay to determine steady state kinetics of *Sc*Mnn9Δ92. A, Man-4MU is a substrate analogue for *Sc*Mnn9Δ92. It is extended to Manα-1,6-Man-4MU in the presence of the transferase, GDP-Man and $MnCl_2$. The bacterial α-1,6-specific mannosidase *Bc*Aman6 liberates 4MU. The release can be measured at λ_{ex}=360 nm and λ_{em}=460 nm. **B,** The release of 4MU was measured in the presence or absence of components of the reaction or point mutants of *Sc*Mnn9Δ92. **C,** Steady state kinetics of ScMnn9Δ92 in the presence of 1.2 mM GDP-Man and variable concentrations of Man-4MU. **D,** Steady state kinetics of ScMnn9Δ92 in the presence of 10 mM Man-4MU and variable concentrations of GDP-Man. All error bars represent the standard error of the mean, n=3.

H389A of the gene encoding *Sc*Mnn9, including the 5'- and 3'-untranslated region (UTR), were cloned into the yeast expression vector pRS315 (a kind gift from Prof. Mike Stark, Division of Gene Regulation and Expression, UoD) (Sikorski and Hieter, 1989). *S. cerevisiae* BY4741 wild type and Δ*mnn9* cells were transformed with these plasmids. Successfully transformed cells were selected on DOA-Leu(–) plates. Δ*mnn9* cells transformed with wild type MNN9 grew at a similar rate, but to slightly lower density, in yeast peptone dextrose medium (YPD) compared to wild type cells carrying the empty pRS315 vector control (Fig. 4.10A). Similar observations were made in complementation experiments of the *C. albicans* Δ*mnn9* mutant (Southard *et al.*, 1999). Indistinguishable growth to the reconstituted WT *Sc*Mnn9 was observed for cells carrying the plasmid encoding for the Q124A mutant, a mutant used as a control. Based on the structure Q124 did not seem to be involved in substrate binding or glycosyl transfer (Fig. 4.5A). In contrast, cells lacking *Sc*Mnn9 grew noticeably slower and to lower densities than wild type cells. Interestingly, *S. cerevisiae* cells expressing *Sc*Mnn9 with the inactivating mutations showed a delay in growth, but ultimately reached similar densities to the cells complemented with wild type *Sc*Mnn9 (Fig. 4.10A). Thus, catalytically inactive *Sc*Mnn9 can partially rescue the Δ*mnn9* growth phenotype. On YPDA plates, the Δ*mnn9* phenotype is presented as an increased sensitivity to hygromycin B and reduced susceptibility to Na_3VO_4 (Fig. 4.10B). Cells complemented with the catalytically impairing *Sc*Mnn9 point mutations were able to grow on plates with concentrations of Na_3VO_4 at which wild type cells or cells reconstituted with wild type *Sc*Mnn9 and *Sc*Mnn9 Q124A did not grow, or grew to lower density (Fig. 4.10B). However, cells lacking *Sc*Mnn9 or carrying the point mutations, except Q124A, were susceptible to lower concentrations of hygromycin B than wild type or reconstituted cells (Fig. 4.10B). Notably, cells expressing *Sc*Mnn9 with a point mutation did not grow at the lowest concentration of hygromycin B tested while *Sc*Mnn9 knockout cells were still able to grow, suggesting that the complete loss of *Sc*Mnn9 may activate rescue pathways for cell survival whilst these pathways are not being activated in the presence of inactive *Sc*Mnn9. This result indicates that the presence of an in-

active form of *Sc*Mnn9 has a more severe impact on cell wall architecture than the complete absence of the transferase. This is similar to previous reports, although these only covered tested knockouts or a single point mutant (Southard *et al.*, 1999, Stolz and Munro, 2002).

4.5 Concluding Remarks

The structural basis of mannoprotein synthesis is poorly understood. The results presented in this work show for the first time the structure of a GT-62, *Sc*Mnn9. The overall fold of Mnn9 resembles a GT-A fold. However, in comparison with close structural homologs, it becomes evident that Mnn9 carries an extension of two β-strands as a unique feature (Fig. 4.4A). In absence of a structure of *Sc*Mnn9 with a substrate, or heterodimeric complex with Van1, or a heterodimeric complex with an acceptor protein, the purpose of this extension remains unclear. However, a dimerisation domain is one of the most likely options as the extension is in close proximity to the active site and is in fact partly involved in the formation of the active site. In the presence of Van1 it could be helpful to have both active sites in close proximity in order to facilitate the rapid extension of mannotriose to oligomannose.

The absence of a substrate complex is not unusual for GTs. These enzymes can undergo tremendous structural rearrangements upon substrate binding. Soaks with the substrate analogue GDP-S-Man in the presence of $MnCl_2$ resulted in the apo structure only, indicating that substrate binding is not favourable in the crystallisation condition obtained. Another objective of future experiments could be the co-crystallisation of Mnn9 with an acceptor analogue, such as mannobiose or even parts of the N-glycan, as well as with a putative acceptor protein. The extension observed in Mnn9 could also act as a dimerisation domain for the acceptor protein rather than Van1.

Structure-guided mutagenesis lead to the identification of residues important for the activity of Mnn9. The discrimination between residues involved in the hydrolysis and in the transfer gave novel insights into the molecular mechanism of this GT.

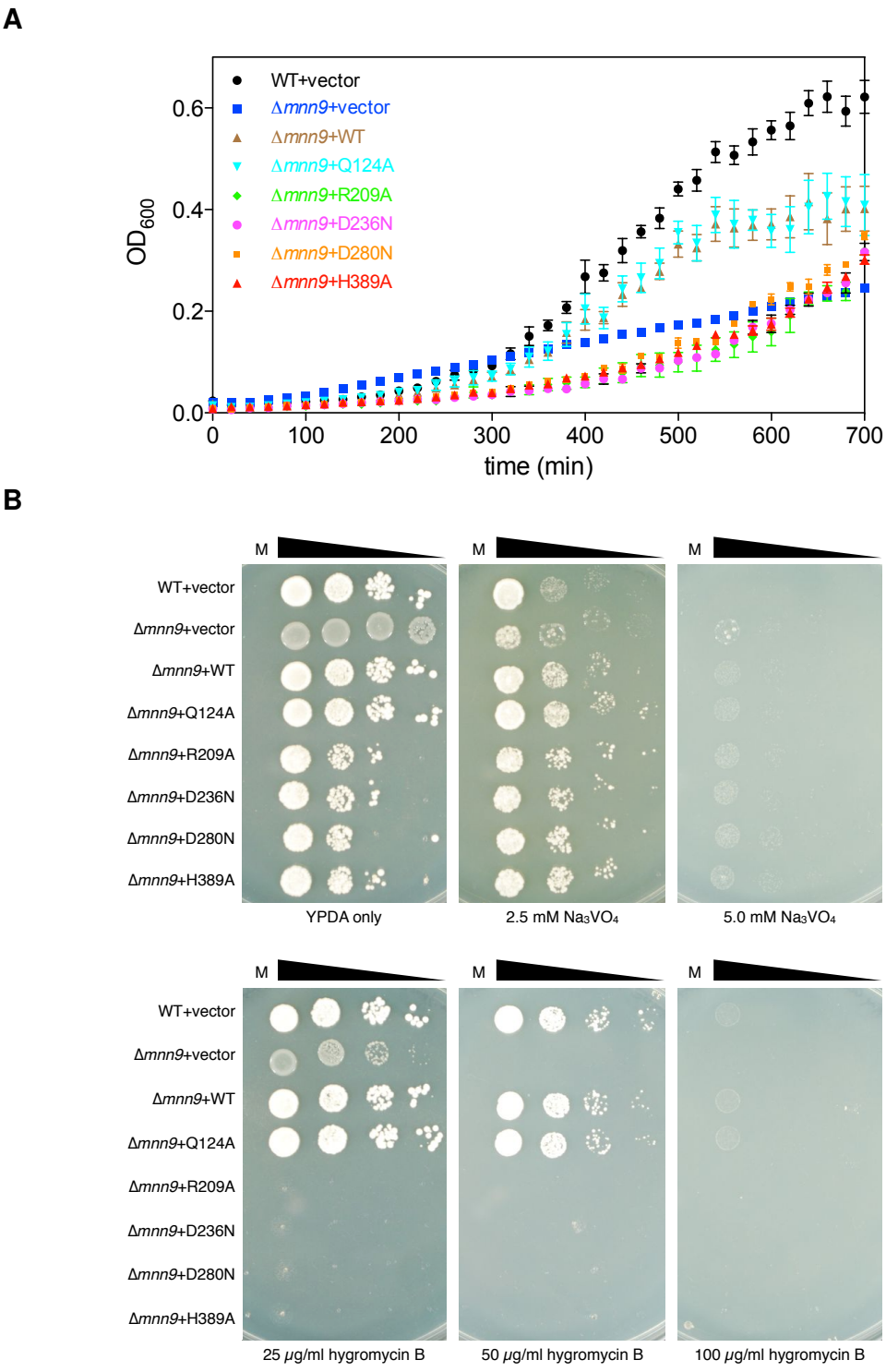

Figure 4.10: Growth of *S. cerevisiae* WT and Δ*mnn9*. **A,** *S. cerevisiae* WT or Δ*mnn9* cells were transformed with the yeast expression plasmid pRS315 containing different *Sc*Mnn9 point mutations. Cells were grown for 12 h at 30 °C and the growth was followed by measuring the OD_{600}. Error bars represent the standard error of mean. **B,** The same cells as in A were spotted in a serial dilution on YPDA-agar plates containing either no additive, Na_3VO_4, or hygromycin B. Plates were incubated at 30 °C for 48 h. M, medium only control.

Furthermore with the development of a novel coupled enzyme assay (Fig. 4.9A) it could be possible to screen for fragments that may inhibit the activity of Mnn9. Since mannoproteins can act as adherence factors of fungal pathogens to epithelial cells (Kanbe and Cutler, 1998, Kanbe *et al.*, 1993, Miyakawa *et al.*, 1992), the inhibition of their synthesis can be exploited as a drug target. Additionally, the addition of mannose in the Golgi has not been shown in human cells, making Mnn9 and other GTs in the mannoprotein biosynthetic pathway fungal-specific targets.

5 Mannosyltransferase *Sc*Van1 – Results and Discussion

5.1 Cloning, heterologous expression and purification of *Sc*Van1

Van1, like Mnn9, is highly conserved amongst yeasts and filamentous fungi (Fig. 5.1). Several prediction programmes were used in order to identify features that may interfere with expression and crystallisation of *Sc*Van1 (Fig. 5.1). The transmembrane prediction server TMHMM (Krogh *et al.*, 2001) identified residues 65–91 form a transmembrane helix, to integrate *Sc*Van1 in the Golgi membrane. Secondary structure prediction by PORTER (Pollastri and McLysaght, 2005) helped to identify a potentially disordered region between residues 86–128 (Fig. 5.1), which may act as a linker between the membrane and the globular domain of *Sc*Van1. Residues 129–166 potentially form three α-helices that, however, are part of an unconserved region before the well conserved globular domain.

Based on these results a multitude of constructs of *Sc*Van1 were designed that encoded for the corresponding *Sc*Van1 expression products (Table 5.1). The majority of these expression products differed in the length of their N-terminus compared to full length *Sc*Van1 .

The primary target was to express *Sc*Van1 and *Sc*Mnn9 in *P. pastoris*. The reasons for that were two-fold: 1) *Sc*Van1 has been shown to be N-linked glycosylated (Rodionov *et al.*, 2009). The post-translational modification is often related

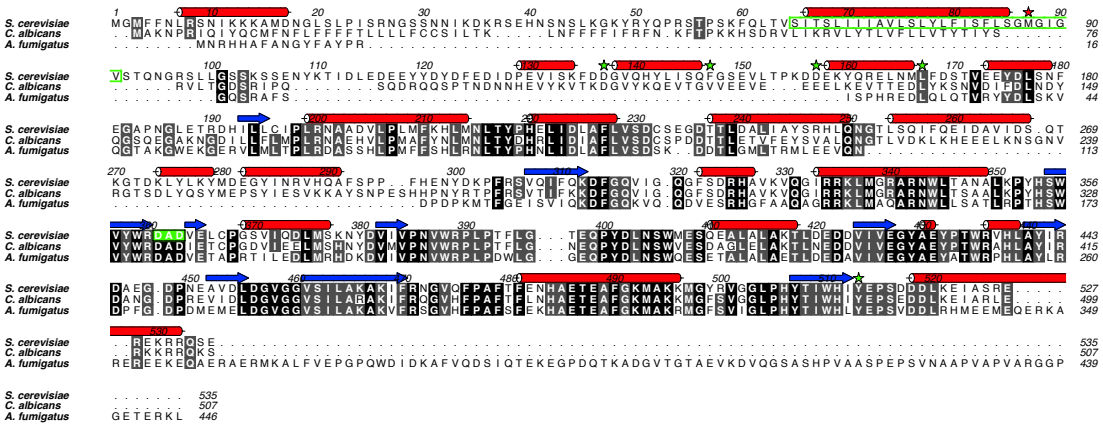

Figure 5.1: Alignment of Van1 of different fungal species. The amino acid sequences were aligned and conservation and similarity is shown in grey scale with black being identical between all species. The secondary structure prediction of *Sc*Van1 is shown above the amino acid sequence, where red cylinders represent α-helices and blue arrows represent β-strands. The predicted N-terminal transmembrane domain is indicated by a box with a green line, whereas the canonical DXD motif is indicated by a filled green box. The red star indicates the start of the construct of *Sc*Van1 mainly used for this thesis (*Sc*Van1Δ86). The green stars indicate the starts and ends of different truncations of *Sc*Van1 used in the thesis as well.

Table 5.1: Constructs of *Sc*Van1 used throughout the thesis

Construct name	Residues	Features
*Sc*Van1Δ86	87–535	*Lacks:* Cytosolic tail, transmembrane domain. *Includes:* Linker region, globular domain.
*Sc*Van1Δ136 *Sc*Van1Δ146 *Sc*Van1Δ156	137–535 147–535 157–535	*Lack:* Cytosolic tail, transmembrane domain, parts of the linker region. *Include:* Globular domain.
*Sc*Van1Δ166	167–535	*Lacks:* Cytosolic tail, transmembrane domain, linker region. *Includes:* Globular domain.
*Sc*Van1_87–513 *Sc*Van1_137–513 *Sc*Van1_147–513 *Sc*Van1_157–513 *Sc*Van1_167–513	87–513 137–513 147–513 157–513 167–513	As the constructs shown above. However, these constructs additionally lack residues 514–535.

to correct protein folding and could therefore be crucial for solubility and activity. 2) *Sc*Van1 and *Sc*Mnn9 have been shown to co-express recombinantly in *P. pastoris* (Rodionov *et al.*, 2009). This was achieved by co-transforming two different expression vectors (pPIC9 and pPICZαA). The authors were not able to express either of the proteins separately, suggesting that instability of either of the transferases is high in the absence of the other GT. Hence, the use of a prokaryotic expression system was not considered with a high priority. The genes encoding *Sc*Van1Δ86 and *Sc*Mnn9Δ36 were cloned into the *P. pastoris* expression vectors pPICZαA and pPIC9, respectively. The vectors introduce an N-terminal secretion signal, which leads to the export of the expression product into the medium, protecting it from cellular proteases. *P. pastoris* cells were transformed first with the Mnn9/pPIC9 plasmid, selected and the successful transformation was confirmed by colony PCR. Positive clones were transformed with the Van1/pPICZαA plasmid. After selection on YPDA plates containing 100 µg/ml zeocin and confirmation of the insertion of the DNA into genome by colony PCR (Fig. 5.2A), positive double-transformants were used for expression upon methanol induction. The medium, containing the expression products, was concentrated 40-fold. However, no expression products were visible after 48 h of induction (Fig. 5.2B). Several other constructs as well as expression of the single proteins, were tried without success. *P. pastoris* was not a suitable expression system under these conditions.

The gene encoding *Sc*Van1 was amplified from the genomic DNA of *S. cerevisiae* by PCR and various truncations of the gene were cloned into the *E. coli* expression vector pNIFTY/MBP, which introduces an N-terminal MBP, a hexahistidine tag and a TEV protease cleavage sequence. After transformation, *E. coli* BL21(DE3) pLysS cells were used for recombinant expression at 20 °C for 24 h in autoinduction medium (Studier, 2005). After expression, cells were lysed and *Sc*Van1 was enriched using Ni^{2+}-IMAC (Fig. 5.3). The MBP-6×His-TEV tag was removed in the presence of TEV protease which was incubated overnight. Further enrichment was carried out using IEX chromatography and SEC to remove the MBP-6×His-TEV tag and residual unwanted proteins. Fractions containing

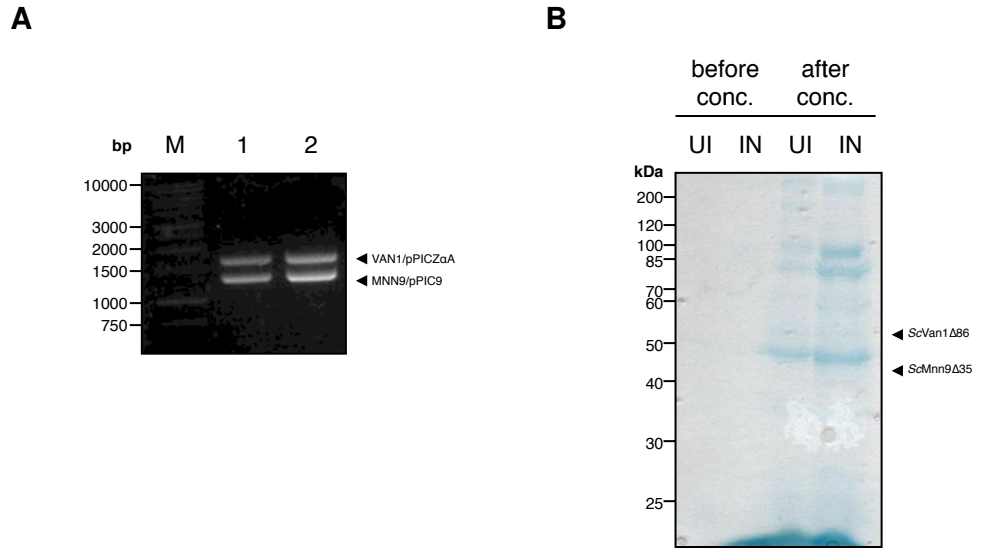

Figure 5.2: Transformation and expression of *Sc*Van1Δ86 and *Sc*Mnn9Δ36 in *P. pastoris*. A, *P. pastoris* cells were first transformed with *mnn9*/pPIC9, screened and successful transformants were transformed with *van1*/pPICZαA. The products of the colony PCR of two selected clones was run on a DNA agarose gel. M, molecular weight standard ladder; 1 and 2, clone 1 and 2. **B,** Clone 1 from panel A was used for expression. A sample of the expression medium was taken before (UI) and after (IN) induction with 2 % methanol. The medium was concentrated 40-fold. All samples were run on an SDS-PAGE gel gel.

*Sc*Van1 were pooled and concentrated to 5.5 mg/ml (Fig. 5.3).

It must be noted that early attempts to purify *Sc*Van1Δ166 failed due to the loss of the protein during the concentration step prior to SEC. This led to the design of another expression construct (*Sc*Van1Δ86) of *Sc*Van1 as it was assumed that the protein precipitated after exceeding a certain critical concentration. However, this protein was lost during the concentration step as well. This led to a change of the filter concentrator used from Sartorius Vivaspin20, containing a filter membrane made of polyethersulfone, to Millipore Amicon Ultra-15, containing a filter membrane made of regenerated cellulose. Only after this change was it possible to purify *Sc*Van1Δ86 further by SEC. It is unclear what caused the possible interaction of *Sc*Van1Δ86 with the polyethersulfone since the highly similar *Sc*Mnn9 did not show this effect. However, the yield of *Sc*Mnn9 was improved using the cellulose-based filter concentrators.

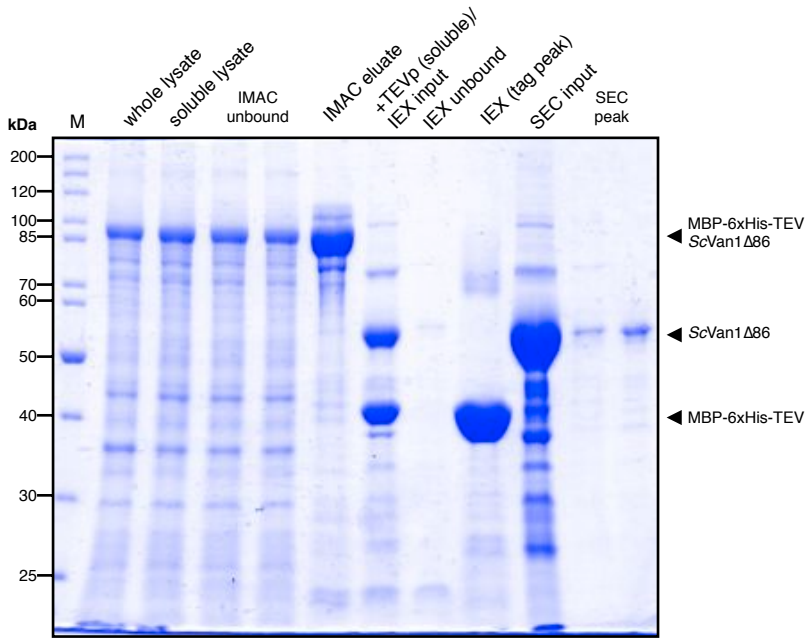

Figure 5.3: Enrichment of *Sc*Van1Δ86. Coomassie-blue stained SDS-PAGE of different steps during the enrichment of *Sc*Van1Δ86. This protein serves as an example for the purification of all *Sc*Van1 constructs used throughout this thesis. The eluate from the IEX containing *Sc*Van1Δ86 was concentrated and used as SEC input. M, molecular weight ladder; IMAC, immobilised metal affinity chromatography; TEVp, tobacco etch virus protease; IEX, anion exchange chromatography; SEC, size exclusion chromatography.

5.2 Formation of α-1,6-oligomannose by *Sc*Van1 is *Sc*Mnn9-dependent

Enzymatic activity of a protein is an indicator for correct folding after recombinant expression. *Sc*Van1 has high similarity to *Sc*Mnn9 (Fig. 5.4) and forms the mannosyltransferase complex M-Pol I with *Sc*Mnn9 (Jungmann and Munro, 1998). Purified *Sc*Van1Δ86 was incubated with GDP-Man, α-1,6-mannobiose and $MnCl_2$ at 30 °C for 16 h. The reaction products were labelled with ANTS and separated on a FACE gel (Fig. 5.5A). Surprisingly, *Sc*Van1Δ86 alone showed no product formation. However, in the presence of *Sc*Mnn9Δ92 the formation of a ladder, representing different oligomers of mannose was observed. The amount of the oligomannose products could be controlled by changing the concentration of *Sc*Van1Δ86 present in the reaction. It appeared that once *Sc*Mnn9Δ92 had formed mannotriose, only *Sc*Van1Δ86 was necessary for the extension of this product to longer mannose chains (Fig. 5.5A). This dependency was further underlined by incubating *Sc*Mnn9Δ92 with the *Sc*Van1Δ86 D361N point mutant. The mutated aspartic acid is the first residue in the canonical DXD motif and most likely involved in the substrate binding and/or the transfer reaction (Fig. 5.1). This mutation abolished the formation of the mannose products completely but did not affect the formation of mannotriose by *Sc*Mnn9Δ92 (Fig. 5.5B).

Strikingly, attempts to co-express the genes for *Sc*Van1Δ86 and *Sc*Mnn9Δ92 from a co-expression plasmid in *E. coli* BL21(DE3) pLysS cells in autoinduction medium failed (Fig. 5.6). This was tried multiple times, and in parallel with cells expressing the genes individually. The lack of growth may suggest that both proteins are active in the *E. coli* cytosol. It is possible that both proteins consume GDP-Man that may be necessary for *E. coli* metabolism or that the formation of the oligomannose products within the cells interferes with the integrity of the bacterial cells. Using IPTG induction in LB medium resulted in a lower yield of cell mass compared to IPTG induction in LB medium of the single genes, and poor expression levels of both genes.

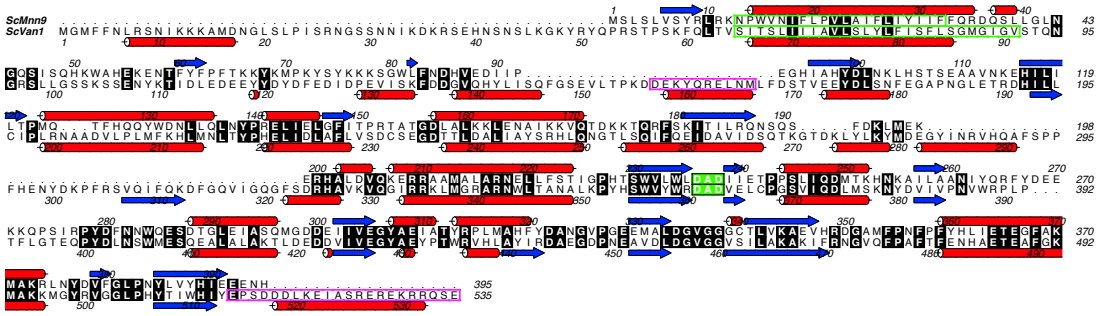

Figure 5.4: Alignment of *Sc*Van1 and *Sc*Mnn9. The amino acid sequences were aligned and conservation and similarity is shown in grey scale with black being identical between both proteins. The secondary structure prediction is shown above (*Sc*Mnn9) and below (*Sc*Van1) the corresponding sequence with the same colour code as in Fig. 5.1. The purple boxes in the *Sc*Van1 sequence indicate regions important for activity.

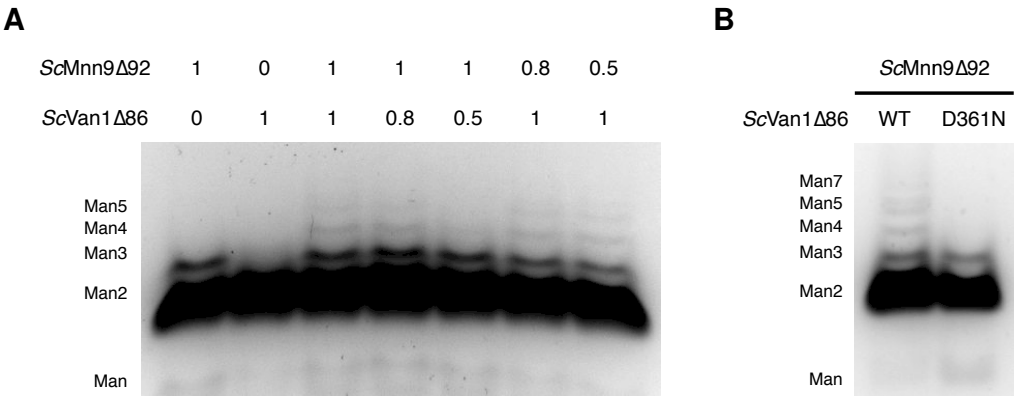

Figure 5.5: FACE gels of *Sc*Van1Δ86 and *Sc*Mnn9Δ92. A, FACE gel of ANTS-labelled products of reactions containing *Sc*Van1Δ86, *Sc*Mnn9Δ92, GDP-Man, α-1,6-mannobiose, and $MnCl_2$. The numbers above the gel indicate relative molarity of both GTs in the reaction. **B,** FACE gel of ANTS-labelled products of the reaction as described in panel A, lane 3, but additionally in the presence of the *Sc*Van1Δ86 D361N point mutant.

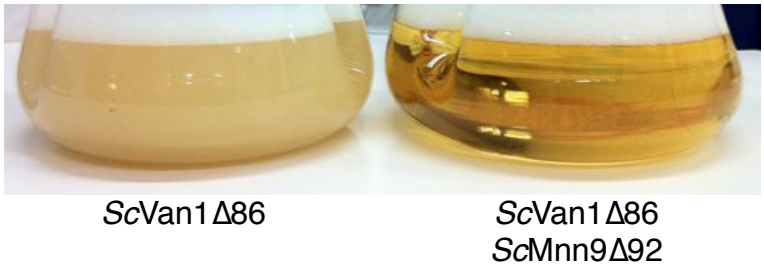

Figure 5.6: Expression of *Sc*Van1Δ86 alone or with *Sc*Mnn9Δ92. *E. coli* BL21(DE3) pLysS cells were transformed either with pNIFTY/MBP containing the gene for *Sc*Van1Δ86 or with pOPC containing the genes for *Sc*Van1Δ86 and *Sc*Mnn9Δ92. Transformed cells were used to inoculate autoinduction medium and incubated for at 20 °C for 24 h.

The product of the reaction containing *Sc*Van1Δ86 and *Sc*Mnn9Δ92 was treated with two specific glycoside hydrolases: the α-1,6-linked mannose specific mannosidase Aman6 from *B. circulans* and the α-1,2-linked mannose specific mannosidase from *Aspergillus saitoi*. The reaction products were labelled with ANTS and separated on a FACE gel (Fig. 5.7). The oligomannose products formed by *Sc*Van1Δ86 and *Sc*Mnn9Δ92 (corresponding to M-Pol I) could only be degraded in the presence of the α-1,6-mannose specific *Bc*Aman6, indicating that the products are made of α-1,6-linked oligomannose. This is in agreement with previous results (Stolz and Munro, 2002) and shows that the truncated expression products of both transferases are still capable of performing their native reaction.

5.3 *Sc*Mnn9 has an allosteric effect on *Sc*Van1 activity

To date, it has been assumed that an N-linked glycosylated substrate protein arrives at the M-Pol I complex and based on unknown features in the acceptor protein, M-Pol I can catalyse either an α-1,2 or an α-1,6 transfer on the mannose attached by Och1 (Stolz and Munro, 2002). However, so far it is unknown if *Sc*Van1 alone can extend the single α-1,6-linked mannose to form the oligomannose backbone because all studies have looked only at the complex of both transferases (Rodionov *et al.*, 2009, Stolz and Munro, 2002). Furthermore, the *Sc*Van1 and *Sc*Mnn9 used in those studies were either immunoprecipitated from *S. cerevisiae* or expressed in *P. pastoris* with the possibility of other yeast glycosyltransferases contaminating the activity assays. Being able to express both transferases individually provided the opportunity to identify if the product of *Sc*Mnn9, mannotriose, and/or the presence of *Sc*Mnn9 is necessary for *Sc*Van1 to be active.

To do so, the reaction of *Sc*Mnn9Δ92 and *Sc*VanΔ86 was split into two steps. This provided the ability to be able to separate mannotriose, the *Sc*Mnn9Δ92 reaction product, from *Sc*Mnn9 and use it to incubate it with *Sc*VanΔ86 and GDP-Man

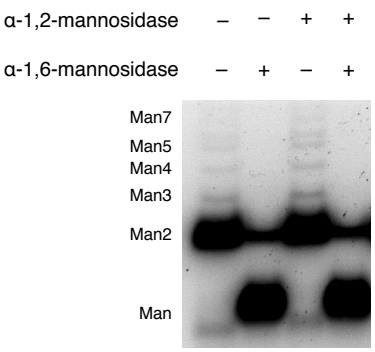

Figure 5.7: FACE gel of mannosidase treated products of the reaction of *Sc*Van1Δ86 and *Sc*Mnn9Δ92. The product of the reaction of *Sc*Van1Δ86, *Sc*Mnn9Δ92, GDP-Man, α-1,6-mannobiose, and $MnCl_2$ was treated with an α-1,2 or α-1,6-specific mannosidase and the reaction products were labelled with ANTS and separated on a FACE gel.

either in the presence or absence of the inactive *Sc*Mnn9Δ92 D236N mutation. (Fig. 5.8). In the presence of inactive *Sc*Mnn9Δ92 neither mannotriose nor oligomannose was formed, indicating that the activity of *Sc*Van1Δ86 is dependent on the product of the *Sc*Mnn9Δ92 reaction. After removing *Sc*Mnn9Δ92 and incubating mannotriose with *Sc*Van1Δ86 in the presence of GDP-Man, no formation of oligomannose could be detected, indicating that mannotriose alone is not enough for *Sc*Van1Δ86 to form its product. Oligomannose could only be detected when mannotriose, *Sc*Van1Δ86, inactive *Sc*Mnn9Δ92, and GDP-Man were incubated together (Fig. 5.8). This indicates that the enzymatic activity of *Sc*Van1Δ86 is not only depends on the product of the *Sc*Mnn9Δ92 reaction but also on the dimerisation of *Sc*Van1Δ86 with *Sc*Mnn9Δ92, even if inactive, making *Sc*Mnn9Δ92 an allosteric affector of *Sc*Van1Δ86.

The enzymatic assay that was developed to determine steady-state kinetics of *Sc*Mnn9Δ92 (Section 4.3, page 95) was initially used to measure the activity of *Sc*Van1Δ86 alone or in the presence of *Sc*Mnn9Δ92 (Fig. 5.9). No 4MU was liberated in the presence of *Sc*Van1Δ86 alone, indicating that *Sc*Van1Δ86is not able to transfer mannose onto 4MU-Man. This supports the data obtained by FACE gel analysis where no formation of mannotriose or even longer chains was observed. In presence of both transferases, the 4MU released was equal to the amount re-

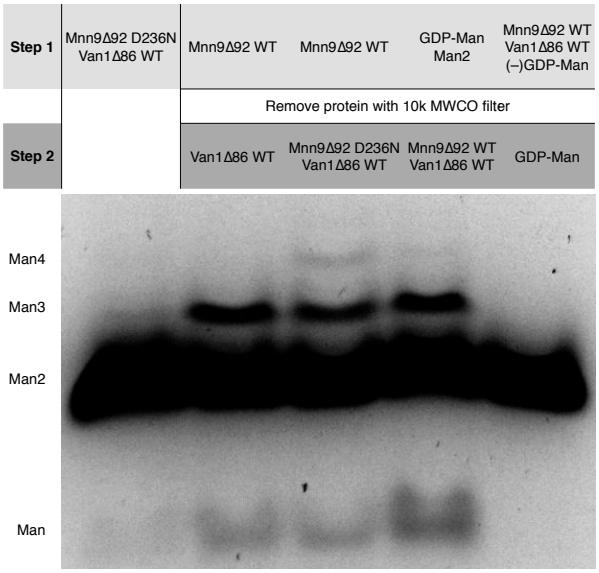

Figure 5.8: FACE gel of two step reaction of *Sc*Mnn9Δ92 and *Sc*Van1Δ86, GDP-Man, α-1,6-mannobiose (Man2) and $MnCl_2$. First lane: *Sc*Mnn9Δ92 D236N and *Sc*Van1Δ86 wild type were incubated together, the reaction was stopped and the products were labeled before the separation on a FACE gel. Second and third lane: *Sc*Mnn9Δ92 D236N was in absence of *Sc*Van1Δ86, *Sc*Mnn9Δ92 was removed using a 10,000 MWCO filter and *Sc*Van1Δ86 wild type alone (second lane) or *Sc*Mnn9Δ92 D236N and *Sc*Van1Δ86 wild type (third lane) were added to the reaction. Fourth lane: The first step contained only GDP-Man and Man2. The GTs were added in the second step. This acted as postive control for the passage of the substrates through the filter. Fifth lane: *Sc*Mnn9Δ92 and *Sc*Van1Δ86 were incubated in absence of GDP-Man but presence of Man2. GDP-Man was only added after the filter step, acting as control for the reliable removal of the GTs by the filter. The second step of the reaction was stopped and the products were labeled before being separated on a FACE gel.

leased by *Bc*Aman6 in the presence of *Sc*Mnn9Δ92 alone (Fig. 5.9). The most likely explanation for this result is the fact that only one 4MU will be released per oligomannose chain. Hence, the amount of 4MU is not stoichiometrically equal to the amount of mannose incorporated into oligomannose synthesised by M-Pol I. This is in contrast to the reaction that occurs in the presence of *Sc*Mnn9Δ92 alone, because mannotriose only product of the reaction in which a single mannose is added to the mannobiose substrate. As a consequence, the 4MU-based assay was unsuitable to determine enzyme kinetics for the complex of *Sc*Van1Δ86 and *Sc*Mnn9Δ92.

Another coupled enzyme assay to determine enzyme kinetics of glycosyltransferases has been described by Gosselin *et al.* (1994) (Fig. 5.10A). Briefly, the assay relies on the liberation of a nucleotide-diphosphate after the transfer of the sugar from the activated substrate. The diphosphate-nucleotide is phosphorylated by pyruvate kinase by converting phosphoenolpyruvate to pyruvate. In a redox reaction, pyruvate is reduced to lactate by lactate dehydrogenase whilst NADH is oxidised to NAD^+. The oxidation of NADH can be followed by the loss in absorbance at λ=340 nm. The loss in signal can be converted to a concentration, and represents the amount of mannose that has been incorporated into the oligomannose chain formed by M-Pol I.

This assay was used to compare the activity of the two transferases of M-Pol I separately or in complex (Fig. 5.10B). Similar to the 4MU-based assay, *Sc*Van1Δ86 alone did not lead to any signal above background. In contrast, in the presence of *Sc*Mnn9Δ92 and *Sc*Van1Δ86 the change in absorbance over time was 28-fold higher than compared to *Sc*Mnn9Δ92 alone. This showed that the NADH-dependent assay is suitable to characterise the activity of M-Pol I. However, it is unclear if the increase in activity of both GTs compared to *Sc*Mnn9Δ92 alone is the result of a faster enzymatic reaction of the complex or the result of the release of more molecules of GDP due to the formation of the oligomannose products.

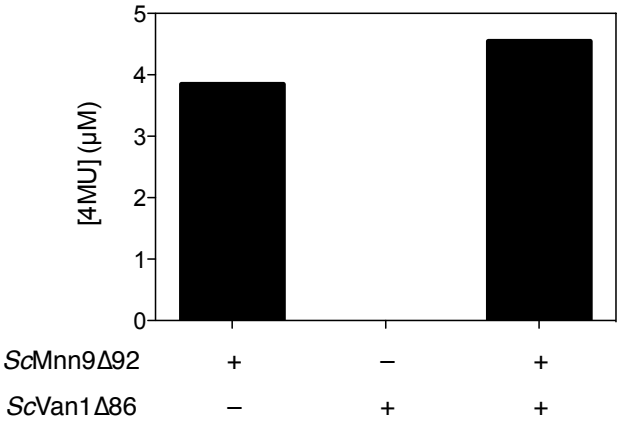

Figure 5.9: Coupled enzyme assay using Man-4MU as substrate analogue. *Sc*Van1Δ86 was incubated with GDP-Man, $MnCl_2$, Man-4MU and *Bc*Aman6 in the presence or absence of *Sc*Mnn9Δ92. The release of 4MU by Aman6 was measured at λ_{ex}=360 nm and λ_{em}=460 nm.

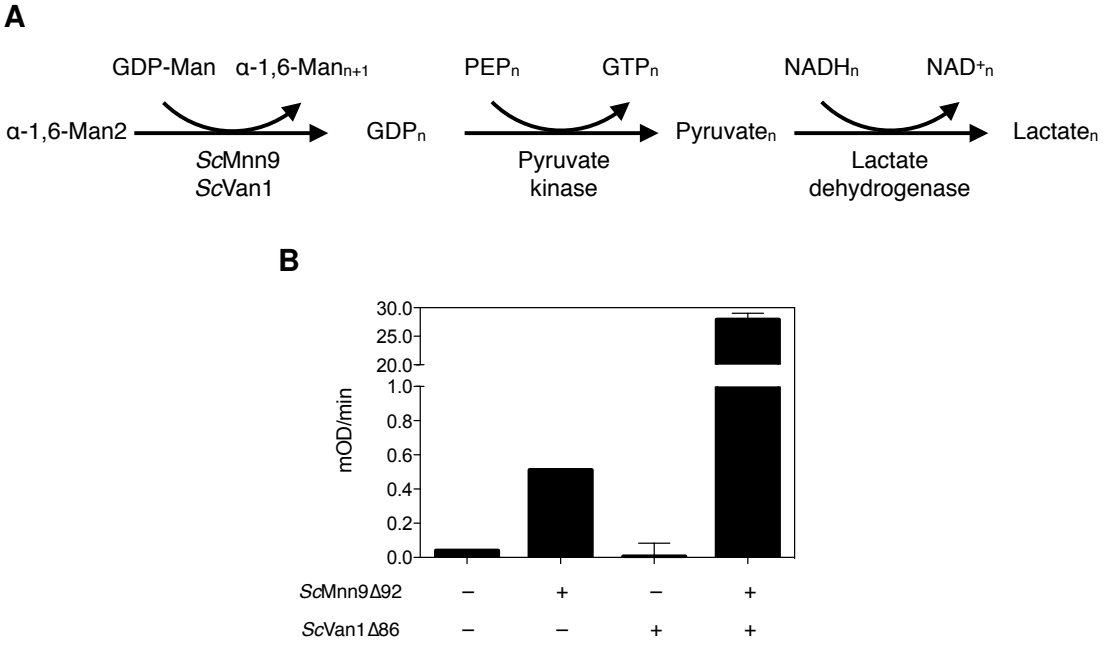

Figure 5.10: Coupled enzyme assay to determine enzyme kinetics of M-Pol I. A, Diagram of the coupled enzyme assay used for determination of enzyme kinetics of M-Pol I. **B,** Oxidation of NADH over time in the absence and presence of M-Pol I or its individual transferases. Error bars represent standard error of the mean, n=3.

5.4 The N-terminus and C-terminus of *Sc*Van1 are important for activity

Extensive trials to crystallise *Sc*Van1Δ86, *Sc*Van1Δ166 and to co-crystallise these proteins with *Sc*Mnn9Δ92 were carried out, but no protein crystals formed over the course of the available experimental time.

In order to obtain information about the interaction between *Sc*Van1 and *Sc*Mnn9, several different constructs of *Sc*Van1 were designed and expressed (Table 5.1). First, the N-terminus was systematically truncated to remove the linker region without any predicted secondary structure elements, followed by the removal of predicted α-helices that are part of an unconserved region (Fig. 5.1). Each of these truncated proteins was tested in activity assays in the presence of *Sc*Mnn9Δ92, GDP-Man, α-1,6-mannobiose and $MnCl_2$ (Fig. 5.11A).

The truncation of the N-terminus between residues 87 and 157 did not affect the formation of the α-1,6-oligomannose (Fig. 5.11A). However, after removal of the first 166 N-terminal residues, activity of *Sc*Van1Δ166 could not be detected any more, indicating that the predicted α-helix formed between residues 158–166 is important for the transfer activity of *Sc*Van1 (Fig. 5.1).

After attempts to crystallise any of the N-terminal truncations of *Sc*Van1 failed, another prediction server (RONN, Yang *et al.* 2005) was used in order to identify possible disordered and flexible regions that may interfere with crystal formation. The prediction program identified the last 22 C-terminal residues (514–535) to be disordered (Fig. 5.11B and 5.1). The prediction also identified several regions up to residue 165 as being disordered, supporting the design of the N-terminal truncations described (Table 5.1). Based on the RONN server result, C-terminal truncations of *Sc*Van1 lacking residues 514–535 were designed, expressed and tested in activity assays. Each of the C-terminal truncations of *Sc*Van1 lost the ability to synthesise α-1,6-oligomannose, indicating that the C-terminus is involved in activity of the *Sc*Van1. It is unlikely the inactivity is caused by misfolded protein, because all truncations gave similar elution profiles during SEC compared to the proteins that

included the C-terminal residues.

The loss in activity of *Sc*Van1 in the truncations described could be due to two reasons: 1) Residues 158–166 and 514–535 have both been predicted to form α-helices, contradicting the disordered region prediction. These helices could be necessary to form the active site of *Sc*Van1, *e.g.* for the formation of the Rossmann-like fold. Many GT-As undergo considerable conformational changes upon substrate binding and during the transfer reaction. Lacking either of these helices may disrupt the substrate binding site formation. 2) Both regions could be involved in the formation of the heterodimeric complex of *Sc*Van1 and *Sc*Mnn9. The complex is necessary for *Sc*Van1 activity as shown in section 5.3. Strikingly, the *Sc*Van1 amino acid sequences 158–166 and 514–535 have no sequences homology in *Sc*Mnn9 (Fig. 5.4, purple boxes), *i.e.* they are absent in a sequence alignment. This can be taken as an indicator that these sequences may be necessary for dimerisation of *Sc*Van1 with *Sc*Mnn9. However, these extra regions in *Sc*Van1 could also be necessary for the recognition of mannotriose and the accomodation of the oligomannose products formed by *Sc*Van1.

5.5 Concluding Remarks

One of the main aims for the experiments conducted on *Sc*Van1 was the crystallisation and structural characterisation of the GT alone and in complex with *Sc*Mnn9. This aim was not achieved. The results from the experiments presented in this chapter, however, may give rise to possible explanations. In my hands, *Sc*Van1 only shows activity in the presence of *Sc*Mnn9 and the *Sc*Mnn9 product, mannotriose (Fig. 5.8). Glycosyltransferases can undergo considerable conformational changes upon binding of their substrate. It is possible that *Sc*Van1 is not in a properly folded conformation in the absence of *Sc*Mnn9 and mannotriose. This could be one explanation why even co-crystallisation attempts of both GTs, but in absence of mannotriose, did not lead to the formation of crystals. This is further supported by the experiments carried out with the N- and C-terminal truncations.

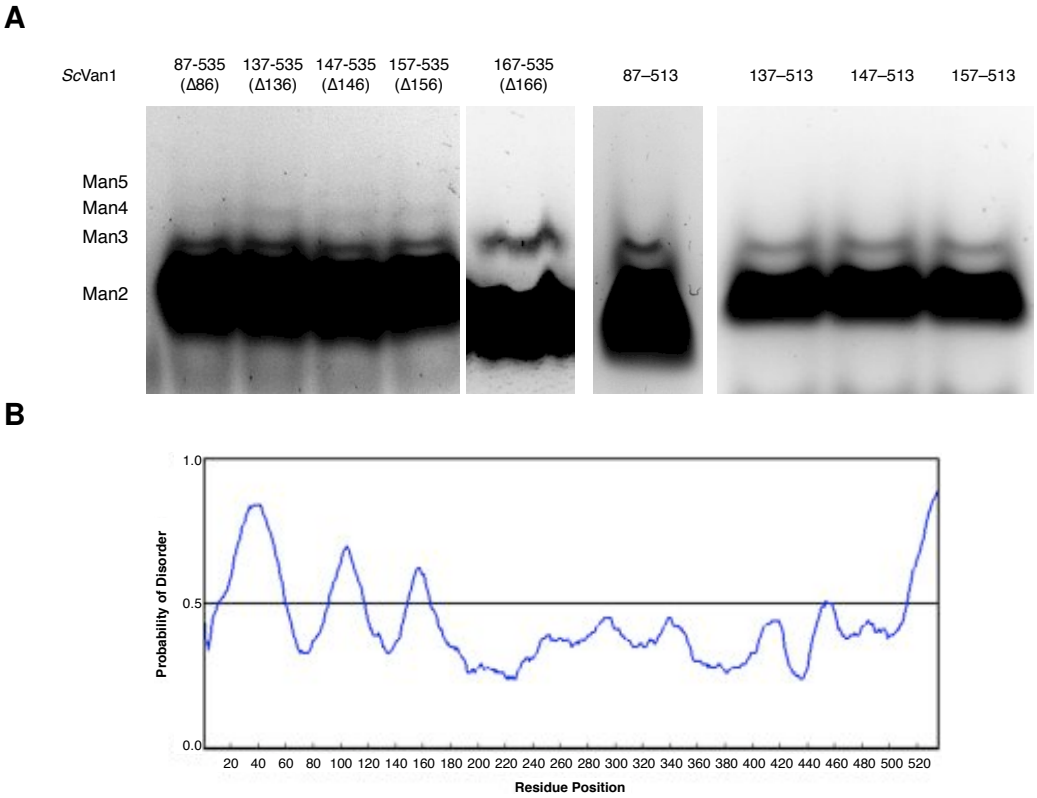

Figure 5.11: FACE gels of N- and C-terminal truncations of *Sc*Van1 and prediction of a C-terminal disordered region. *A,* N- and C-terminal truncations of *Sc*Van1, as indicated above the gels, were incubated with *Sc*Mnn9Δ92, GDP-Man, α-1,6-mannobiose and $MnCl_2$. The reaction products were labelled with ANTS and separated on a FACE gel. *B,* Output of the disordered region prediction programme RONN (Yang *et al.*, 2005) using the full length amino acid sequence of *Sc*Van1.

Two predicted α-helices are either directly involved in the glycosyl transfer activity of *Sc*Van1 or important for the formation of the dimer between *Sc*Van1 and *Sc*Mnn9 (Fig. 5.11A).

The cooperative effect of *Sc*Mnn9 on *Sc*Van1 could be the result of a general allosteric effect of *Sc*Mnn9 in the biosynthesis of mannoproteins. *Sc*Mnn9 is not only present in the heterodimeric complex M-Pol I but also in the heteropentameric complex M-Pol II (Jungmann and Munro, 1998, Jungmann *et al.*, 1999, Kojima *et al.*, 1999). This is surprising as *Sc*Mnn9 alone only produces mannotriose, the substrate for *Sc*Van1. The presence of *Sc*Mnn9 in M-Pol II could be due to two reasons: 1) *Sc*Mnn9 in M-Pol II could serve a similar purpose as it does in M-Pol I, that is, to have an allosteric effect on other GTs present in the complex. 2) *Sc*Mnn9 could participate in the elongation of the oligomannose backbone. The results shown in Fig. 5.8 (lane 3) are not clear in regards to the number of mannose residues attached, *i. e.* if the mannose backbone is elongated greater than Man4. Due to the absence of active *Sc*Mnn9 in the second reaction one interpretation of the results could be that *Sc*Van1 and *Sc*Mnn9 act in an alternating mechanism. That means that *Sc*Mnn9 forms Man3, *Sc*Van1 forms Man4, *Sc*Mnn9 forms Van5, and so on. A similar mechanism could be true for the presence of *Sc*Mnn9 in M-Pol II.

The results gained from the experimental work on *Sc*Van1 can be used to develop new approaches to obtain a crystal structure of M-Pol I. If large amounts of α-1,6-linked mannotriose are available, co-crystallisation trials with *Sc*Van1Δ156 and *Sc*Mnn9Δ92 may lead to a stable complex between the components and ultimately to crystals of the complex. Further experiments will have to be carried out to identify whether the formation of the α-1,6-oligomannose backbone (Man4, Man5, and so on) is carried out by *Sc*Van1 alone or if *Sc*Mnn9 and *Sc*Van1 work in concert, alternatingly adding α-1,6-mannose.

6 Mannosidase *Bc*Aman6 – Results and Discussion

6.1 *Bc*Aman6 is a bacterial homologue of the yeast enzymes *Sc*Dfg5 and *Sc*Dcw1

*Sc*Dfg5 and *Sc*Dcw1 show moderate amino acid conservation to two GH-76 family members, the endo-α-1,6-mannosidase Aman6 from *Bacillus circulans* TN-31 (Kitagaki *et al.*, 2002, Nakajima *et al.*, 1976) and the structurally characterised *Listeria innocua* Lin0763 (*Li*Lin0763 protein of unknown function (PDB code: 3K7X) (Fig. 6.1). The conservation between *Sc*Dfg5 and *Bc*Aman6 is 26 % and between *Sc*Dcw1 and *Bc*Aman6 it is 21 % (Kitagaki *et al.*, 2002). The mannosidase *Bc*Aman6 has been found to be active on the α-1,6-mannose backbone present in yeast mannoproteins (Maruyama and Nakajima, 2000, Nakajima *et al.*, 1976). So far, *Bc*Aman6 is the only protein with a known function in the GH-76 hydrolase family. Hence, *Bc*Aman6 could serve as a model for this class of mannosidases. Structural insights into the binding and hydrolysis of its substrate could be projected onto its yeast homologues and could serve as a model for the identification of potent inhibitors of this class of GH. Importantly, the aspartic acid residues 124 and 125, that could potentially serve as the general acid/base and nucleophile in the hydrolytic activity of *Bc*Aman6, are conserved as well as many other hydrophobic residues that could aid binding of the mannose polymer (Fig. 6.1). *Bc*Aman6 was used as a model for GH-76 enzymes because of its known activity and be-

cause extensive attempts to express DFG5 and/or DCW1 in heterologous expression systems (*Escherichia coli* BL21(DE3) pLysS cells and *Pichia pastoris*) did not result in considerable yields. Both *Sc*Dfg5 and *Sc*Dcw1 have been shown to be N-linked glycosylated (Kitagaki *et al.*, 2002, Spreghini *et al.*, 2003) and the lack of the post-translational modification may have led to misfolding of the proteins during translation in a prokaryotic expression system.

6.2 Cloning, heterologous expression and purification of *Bc*Aman6

Several programs were used to predict the secondary structure, a possible signal sequence and the location of a carbohydrate-binding motif (CBM) of Aman6 (Finn *et al.*, 2010, Petersen *et al.*, 2011, Pollastri and McLysaght, 2005) (Fig. 6.1). Based on these results a construct lacking the N-terminal residues 1–34 containing the the predicted signal peptide and the C-terminal residues 376–589 containing a predicted CBM (CBM)-6 was designed. The gene encoding for this truncated protein was amplified from genomic DNA obtained from *B. circulans* TN-31 cells (ATCC© 29101™) and cloned into the pGEX-6P-1 *E. coli* expression plasmid, which introduces an N-terminal glutathione-S-transferase (GST) tag followed by a PreScission protease cleavage site. The gene encoding *Bc*Aman6 was expressed in *E. coli* BL21(DE3) pLysS cells at 20 °C for 24 h in autoinduction medium. After lysis the protein was enriched using glutathione (GSH) resin and the GST tag was removed by PreScission protease cleavage (Fig. 6.2). Most of the cleaved GST tag was removed by rebinding to GSH resin and the unbound material, containing cleaved *Bc*Aman6 was collected. Size exclusion chromatography was used to remove minor contaminations. Purified *Bc*Aman6 was concentrated to 40 mg/ml and used for activity assays and crystallography.

textitV_{max} of 77.7 ($\pm$2) nM/min resulting in a k_{cat} of 0.2 s^{-1}

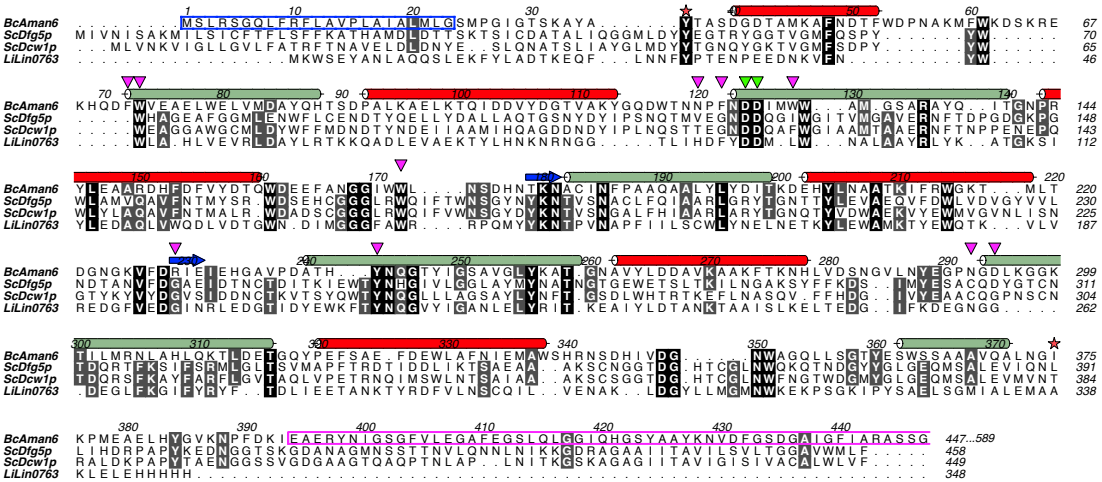

Figure 6.1: Alignment of selected GH-76 GH family members. The amino acid sequences of fungal and bacterial GH-76 GHs were aligned and conservation and similarity is shown in grey scale with black being identical between all species. The secondary structure prediction of *Bc*Aman6 is shown above the amino acid sequence, where red and seagreen cylinders represent α-helices (outer and inner helices, respectively) and blue arrows represent β-strands. The predicted signal sequence is indicated by a box with a blue line. The purple open rectangle indicates the start of the predicted CBM-6 and the remaining residues 448–589 of *Bc*Aman6 have been removed from the figure for simplification. The red stars indicate start and end of the construct of *Bc*Aman6 used for this thesis. Green arrowheads indicate the aspartic acid residues most likely involved in hydrolysis. Green and purple arrowheads indicate residues that form part of the active site and have been mutated.

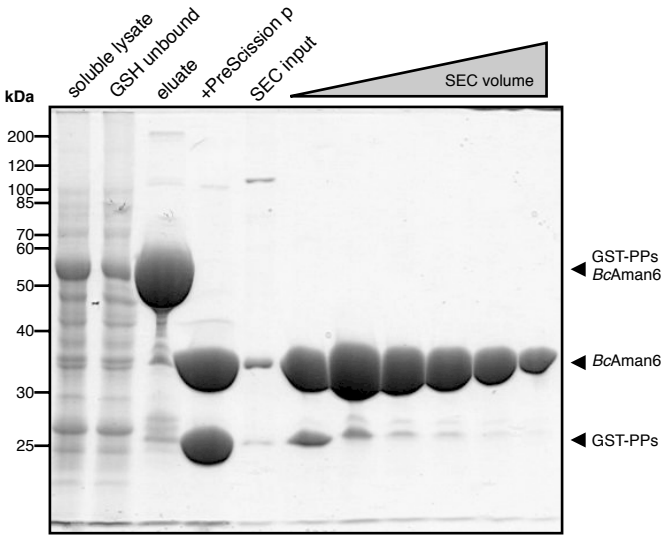

Figure 6.2: Enrichment of *Bc*Aman6. Coomassie-blue stained SDS-PAGE gel of different steps during the enrichment of *Bc*Aman6. GSH, glutathione resin; PreScission p, PreScission protease; PPs, PreScission protease cleavage site; SEC, size exclusion chromatography.

6.3 The carbohydrate-binding domain is dispensable for *Bc*Aman6 activity

To determine if the truncations have an impact on the activity of *Bc*Aman6 compared to the full-length protein (Nakajima *et al.*, 1976), a fluorescent based enzyme assay was used to determine steady state kinetics (Fig. 6.3A). The minimum length of substrate of *Bc*Aman6 is α-1,6-linked mannotriose (Maruyama and Nakajima, 2000, Nakajima *et al.*, 1976). This led to the design of the substrate analogue α-1,6-mannobiose-4MU (Man2-4MU) that was synthesised and kindly provided by Dr. Vladimir Borodkin in our group. The release of 4MU was used to measure the enzyme activity of *Bc*Aman6, which when fitted could be used to determine the K_m which was 1.0 ($\pm$0.1) mM Man2-4MU, the V_{max} of 0.5 ($\pm$0.02) µM/min and the k_{cat} of 1.1 ($\pm$0.04) min^{-1} (Fig. 6.3B and Table 6.2). This is in agreement with previous results obtained using α-1,6-mannotriose (K_m = 1.0 mM, Nakajima *et al.* 1976) and the full length *Bc*Aman6 including the CBM-6. This result indicates that Man2-4MU binds similarly well to *Bc*Aman6 as the natural substrate. Hence, Man2-4MU is a good substrate analogue that can be used in this activity assay. Furthermore, the lack of the CBM of *Bc*Aman6 does not affect the ability to bind Man2-4MU.

6.4 *Bc*Aman6 possesses an α_6/α_6 helix barrel fold

In order to characterise potential inhibitors of *Bc*Aman6, to determine the mode of binding of a *Bc*Aman6 substrate and to understand the hydrolytic mechanism, the X-ray crystal structure of the *Bc*Aman6 was solved. Crystallisation trials were set up with *Bc*Aman6 at a concentration of 40 mg/ml in 480 different conditions. Crystals of *Bc*Aman6 grew in a solution containing 0.1 M HEPES, pH 7.0, 0.2 M $CaCl_2$ and 20 % (w/v) PEG 6000 (Fig. 6.4A). The crystal structure of *Bc*Aman6 was determined from a 2.0 Å dataset by molecular replacement using the co-ordinates of a predicted structure of *Bc*Aman6 obtained by the structure prediction server

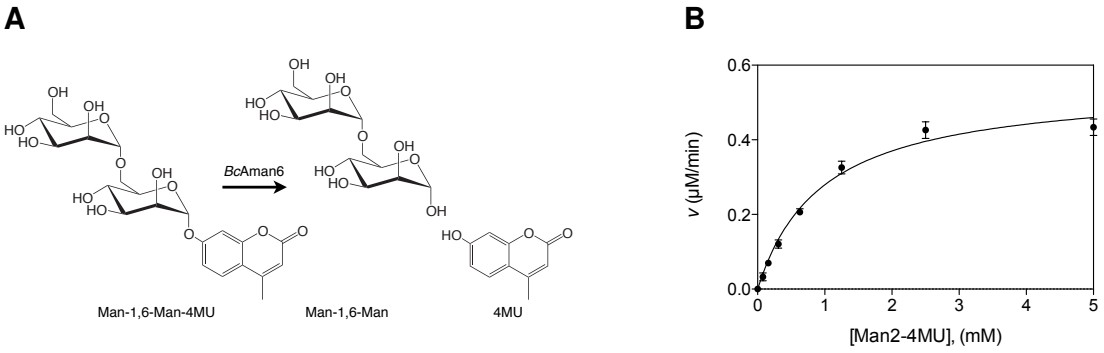

Figure 6.3: Fluorescent enzyme assay to determine *Bc*Aman6 activity. **A,** α-1,6-linked mannobiose-4MU is a substrate analogue of α-1,6-linked mannotriose and can be processed by *Bc*Aman6. The release of 4MU can be measured at an excitation wavelength of 360 nm and an emission wavelength of 460 nm. **B,** Steady state kinetics of *Bc*Aman6 WT. Error bars indicate standard error of the mean, n=3.

RaptorX (Källberg *et al.*, 2012). The model was refined to a final R_{work}/R_{free} of 0.16/0.22 (Table 6.1). *Bc*Aman6 consists of 12 helices that are tightly packed to form an α_6/α_6-barrel (Fig. 6.5A). The barrel is formed by six outer helices (α1, α3, α5, α7, α9, and α11) and six inner helices (α2, α4, α6, α8, α10, and α12). The helices are arranged along a plane with alternating directions. Two short β-strands (β1 and β2) form a small β-sheet that is located in a loop-rich part of *Bc*Aman6 (Fig. 6.5A). It is possible that the flexibility resulting from these loops is necessary for substrate recognition and binding.

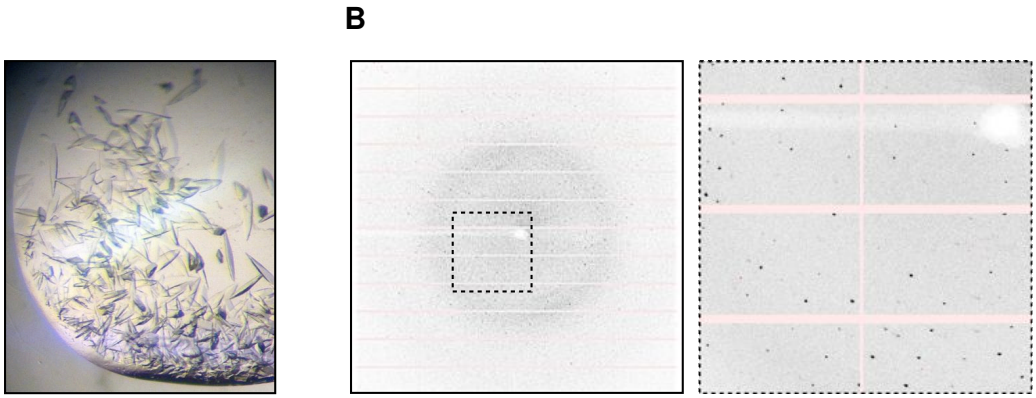

Figure 6.4: Crystallisation and diffraction of *Bc*Aman6. A, Crystals of *Bc*Aman6 grown in a solution containing PEG 6000 as precipitant. **B,** Diffraction of a crystal of *Bc*Aman6 collected at the Diamond Light Source (Didcot, UK). The right frame is a 100 % crop of the area indicated in the left frame.

Table 6.1: Details of data collection and structure refinement. Numbers in parenthesis represent the values in the highest resolution shell.

	*Bc*Aman6 apo
Space group	$P2_12_12_1$
Cell dimensions	
a, b, c (Å)	50.9, 65.1, 90.2
α, β, γ (°)	90, 90, 90
Resolution range (Å)	45.0–2.0 (2.1-2.0)
Number of observed reflections	238 674
Number of unique reflections	19 462 (1857)
Redundancy	12.2 (11.8)
$I/\sigma(I)$	18.8 (6.1)
Completeness (%)	99.7 (97.1)
R_{merge}	0.12 (0.45)
Number of protein residues	340
Number of water molecules	214
R_{work}, R_{free}	0.16/0.22
RMSD from ideal geometry	
bond lengths (Å)	0.007
bond angles (°)	0.96
B-factors (Å^2)	
protein	19.6
water	25.5

6.5 *Bc*Aman6 is structurally similar to GH-88 glycoside hydrolases

The α_6/α_6-helix barrel fold is common across GHs. It can be found in GHs of the families 8, 9, 15, 37, 48, 63, 65, 78, 88, 94, 95, and 125. The DALI server (Holm and Rosenström, 2010) was used to find structural homologs in a GH family other than GH-76. The prediction identified unsaturated glucuronyl hydrolase (UGL) from *Bacillus* spp. as a structural homolog (PDB: 2AHG, Z-score = 23.5, RMSD = 3.4 Å, 302 Cα atoms) (Itoh *et al.*, 2006) (Fig. 6.5B). This hydrolase cleaves oligosaccharides containing an α-linked unsaturated D-glucuronic acid (GlcA) (Hashimoto *et al.*, 1999). UGL belongs to the six-hairpin superfamily according to the SCOP database (number: 48208, Murzin *et al.* 1995) (Itoh *et al.*, 2004). Other members of this family are N-acetylglucosamine 2-epimerase (AGE) (Itoh *et al.*, 2000) and unsaturated rhamnogalacturonyl hydrolase (YteR) (Itoh *et al.*, 2006, Zhang *et al.*, 2005), both of which have been identified as structural homologs of *Bc*Aman6 by DALI too (AGE: Z-score = 24.2, RMSD = 3.2 Å, 309 Cα atoms; YteR: Z-score = 23.4, RMSD = 3.1 Å, 292 Cα atoms). Strikingly, despite the moderate similarity of the fold between *Bc*Aman6 and UGL, the active site groove is considerably different (Fig. 6.6). This may be the result of the UGL catalytic mechanism in which a vinyl ether group is hydrated to hydrolyse the glycosidic bond. This is a novel mechanism for GHs (Itoh *et al.*, 2006) and unlikely to be the reaction mechanism of *Bc*Aman6. The residues involved in this reaction are on helix α3 (N(D)88) and helix α4 (D149) in UGL, at a distance of 7.1 Å apart (Fig. 6.5B and 6.6B). In contrast, the proposed active site residues D124 and D125 of *Bc*Aman6 are both located on helix α4 (Fig. 6.5A and 6.6A). Extensive trials to soak and co-crystallise *Bc*Aman6 with the weak inhibitor α-1,6-mannobiose (Nakajima *et al.*, 1976) or the substrate analogue Man2-4MU did not lead to observable electron density in the active site. This may be the result of the tight packing of the protein crystals. The solvent content of *Bc*Aman6 crystals was as low as 30 %. Additionally, the active site of monomeric *Bc*Aman6 was partly blocked by R341 of a symmetry related molecule

(Fig. 6.6C). This could also explain why soaking experiments did not lead to complexes of *Bc*Aman6 with its substrate or product. No other crystals appeared in the conditions that were tested with *Bc*Aman6. Hence, it was not possible to explore an alternative crystal form with a more advantageous packing.

6.6 *Bc*Aman6 possesses a putative substrate binding groove

A channel is formed around residues D124 and D125 that point towards the solvent (Fig. 6.5A and 6.6A). Because both residues are conserved between *Bc*Aman6, *Sc*Dfg5, *Sc*Dcw1 and *Li*Lin0763 (Fig. 6.1) they are likely to act as the general acid/base and nucleophile that are necessary for the action of retaining GHs (Sinnott, 1990). Due to the lack of NMR data it is unknown if *Bc*Aman6 acts as a retaining or inverting hydrolase. However, the distance between D124 and D125 is 5 Å, which is a suitable distance for a retaining GH (average distance 5.5 Å) (McCarter and Withers, 1994). The active site groove spans the entire surface of *Bc*Aman6 (approx. 30 Å). This is in agreement with the length of a mannohexaose molecule. It has been shown that a longer substrate than α-1,6-mannotriose binds better and is hydrolysed faster by *Bc*Aman6 (Nakajima *et al.*, 1976). It is possible that a longer substrate chain changes the conformation of *Bc*Aman6 and has an allosteric effect on activity. This conformational change may be achieved through the flexible loops around the β-sheet (Fig. 6.5A). The high structural similarity between *Bc*Aman6 and *Li*Lin0763 (DALI Z-score = 41.5, RMSD = 2.1 Å over 321 backbone Cα atoms) (Holm and Rosenström, 2010) shows the conservation of this fold between the members of the GH-76 family. From sequence alignments between *Bc*Aman6, *Li*Lin0763, *Sc*Dfg5, and *Sc*Dcw1 it can be predicted that the yeast proteins also adopt this fold.

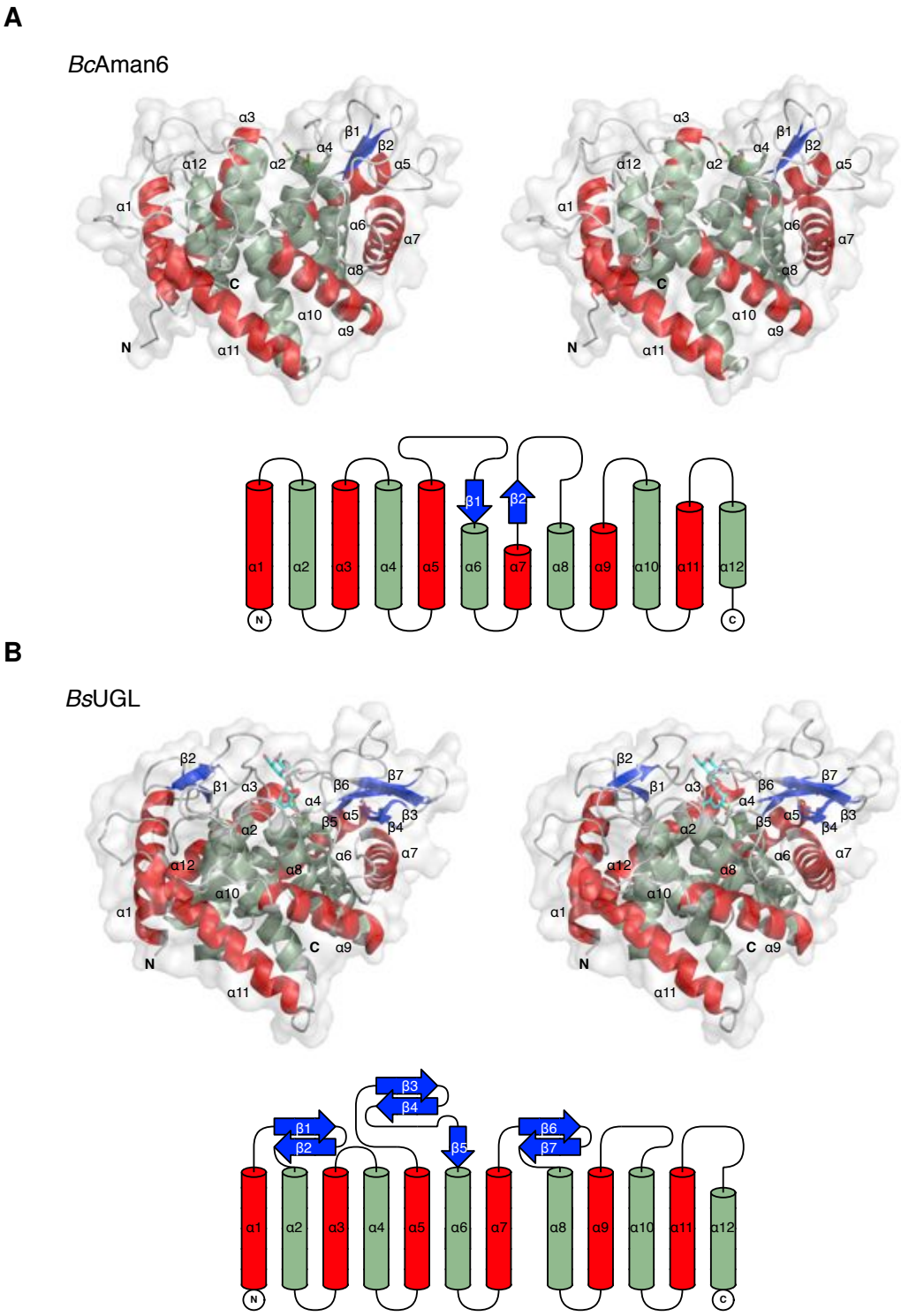

Figure 6.5: Stereoscopic images and topology of GH-76 *Bc*Aman6 and GH-88 *Bs*UGL. A, *Bc*Aman6 apo structure and topology. **B,** *Bs*UGL in complex with unsaturated chondroitin disaccharide (ΔGlcA-GalNAc) and its topology. Both GHs form an α_6/α_6 barrel with six inner and six outer α-helices. Structures are shown with the same viewing matrix applied.

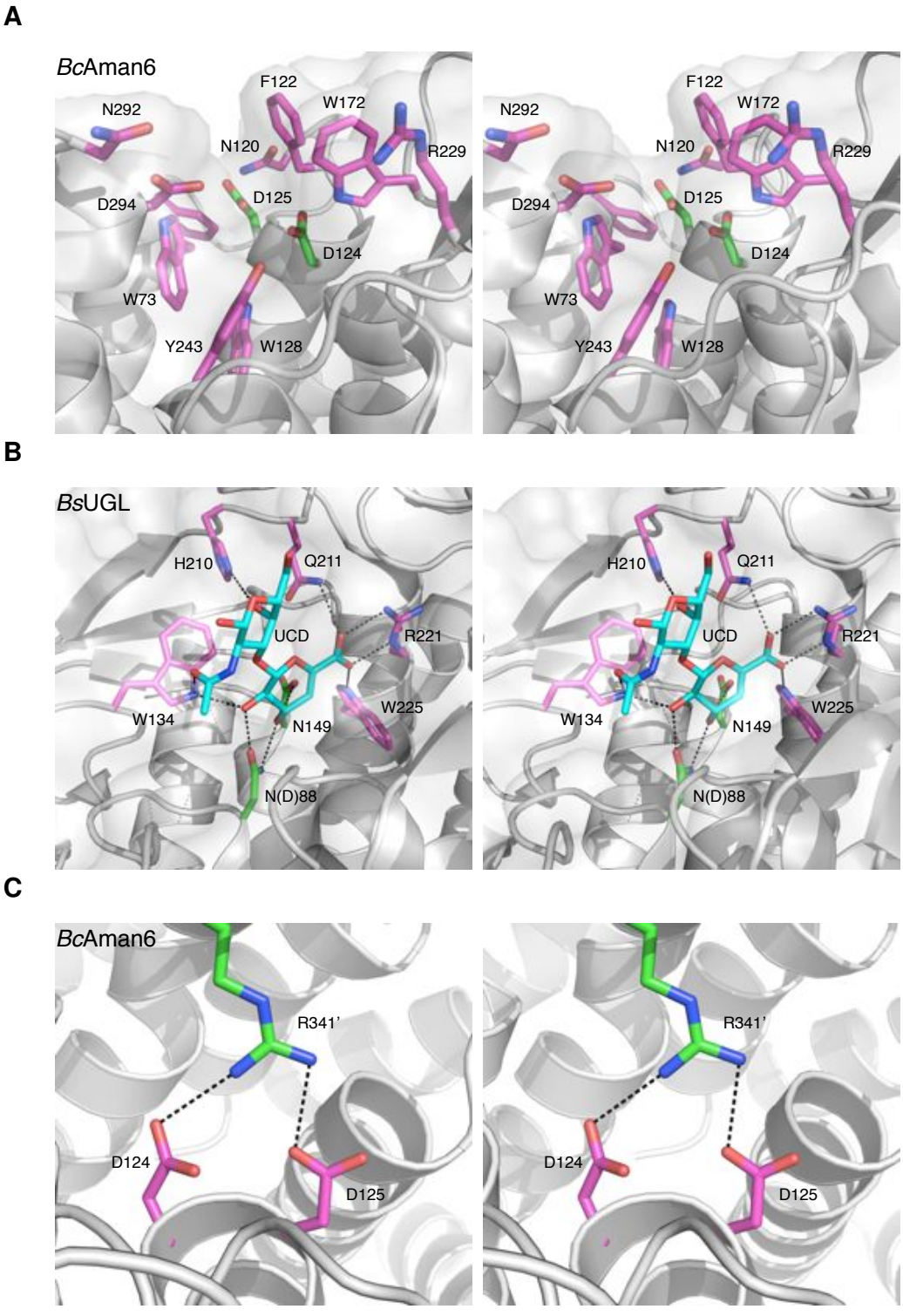

Figure 6.6: Stereoscopic images of the active site of *Bc*Aman6 and GH-88 *Bs*UGL A, Aspartic acid residues 124 and 125, which are likely involved in hydrolysis, are shown in green. Additional side chains that have been mutated in this thesis are shown in purple. **B,** *Bs*UGL in complex with ΔGlcA-GalNAc (UCD). Residues N(D)88 and N149, which are involved in hydrolysis, are shown in green. **C**, Arginine 341 (R314', green carbon atoms) of a symmetry related molecule of *Bc*Aman6 interacts with residues D124 and D125 (magenta carbon atoms) and blocks access to the active site of the enzyme.

6.7 The D124/D125 motif and interacting active site residues are required for catalytic activity

As noted above, complexes of *Bc*Aman6 with the substrate analogue Man2-4MU could not be obtained. However, the sequence alignment between *Bc*Aman6, *Sc*Dfg5, *Sc*Dcw1, and *Li*Lin0763 identified D124 and D125 as potential residues involved in the hydrolysis of the substrate since both residues are conserved across all four proteins. In order to test their involvement in activity, both aspartic acid residues were mutated to asparagine. Additionally, the structure was used to design mutants of other nearby residues (W73, W128, W172, and Y243) (Fig. 6.7A) that may be involved in hydrolysis or substrate binding. All mutants expressed equally well as compared to the *Bc*Aman6 WT protein (Fig. 6.7B), indicating that no mutation leads to unfolded protein that becomes degraded. The point mutants were used to determine steady state kinetics (Table 6.2 and Fig. 6.8). K_m and k_{cat} could not be determined for the W73A and W128A mutants, nor for the D124N and D125N single and double mutants even after 16 h assay time instead of 20 min. These mutants have to be considered as inactive, highlighting the importance of all four residues for activity of *Bc*Aman6. In particular, the abolishment of activity of *Bc*Aman6 in the D124N and D125N mutants supports the idea that these side chains act as the general base/acid and nucleophile in the hydrolytic reaction. The other residues are possibly not directly involved in the hydrolase activity. Instead, they are likely to be involved in binding and co-ordination of the substrate. Both residues W73 and W128 can provide a platform for the correct co-ordination of the substrate due to the hydrophobic nature of their aromatic side chains. Residues W172 and Y243 show a considerable decrease in activity (Table 6.2), however substrate binding does not seem to be affected as both K_m are comparable to *Bc*Aman6 WT.

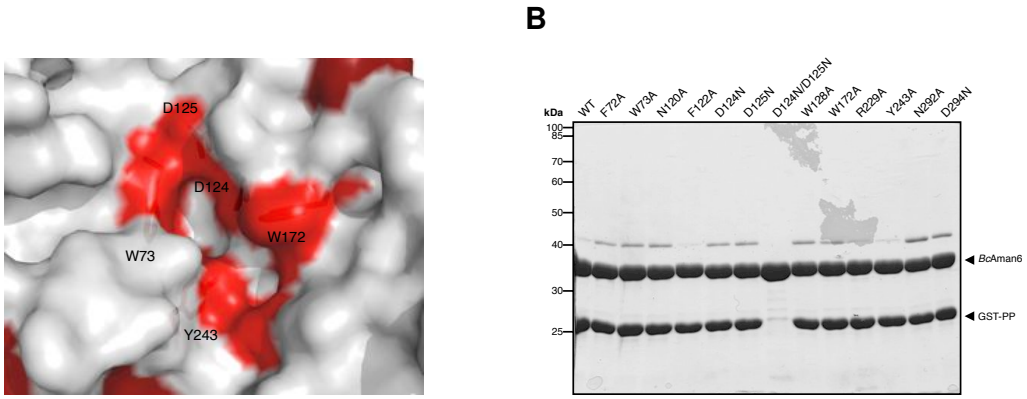

Figure 6.7: Conserved residues that form the active site of BcAman6 and expression of point mutations. A, Surface representation of *Bc*Aman6 with residues (red) around D124 and D125 that are conserved across the species compared in this thesis (Fig. 6.1). **B,** SDS-PAGE gel of *Bc*Aman6 WT and point mutants after enrichment on GSH resin and cleavage with PreScission protease. GST-PP, GST-PreScission protease cleavage site tag.

Table 6.2: Steady state kinetics of *Bc*Aman6 WT and point mutants. An asterisk indicates reactions that have been performed for 16 h instead of 20 min. N. D.=not detectable. Error is standard error of the mean, n = 3.

	K_m (mM)	k_{cat} (min^{-1})	k_{cat}/K_m (mM^{-1} min^{-1})	relative k_{cat}/K_m (%)
WT	1.0 ± 0.1	1.096 ± 0.0378	1.096	100.0
F72A	0.6 ± 0.2	0.002 ± 0.0002	0.003	0.3
W73A*	N. D.	N. D.	N. D.	N. D.
N120A	1.0 ± 0.2	0.005 ± 0.0003	0.005	0.5
F122A	1.1 ± 0.1	0.021 ± 0.0005	0.019	1.9
D124N*	N. D.	N. D.	N. D.	N. D.
D125N*	N. D.	N. D.	N. D.	N. D.
D124N/D125N*	N. D.	N. D.	N. D.	N. D.
W128A*	N. D.	N. D.	N. D.	N. D.
W172A*	1.4 ± 0.6	0.002 ± 0.0003	0.001	0.2
R229A*	1.1 ± 0.2	0.461 ± 0.0270	0.419	42.1
Y243A	1.0 ± 0.5	0.001 ± 0.0002	0.001	0.1
N292A	1.1 ± 0.2	0.331 ± 0.0198	0.301	30.2
D294N	0.5 ± 0.1	0.419 ± 0.0138	0.838	38.2

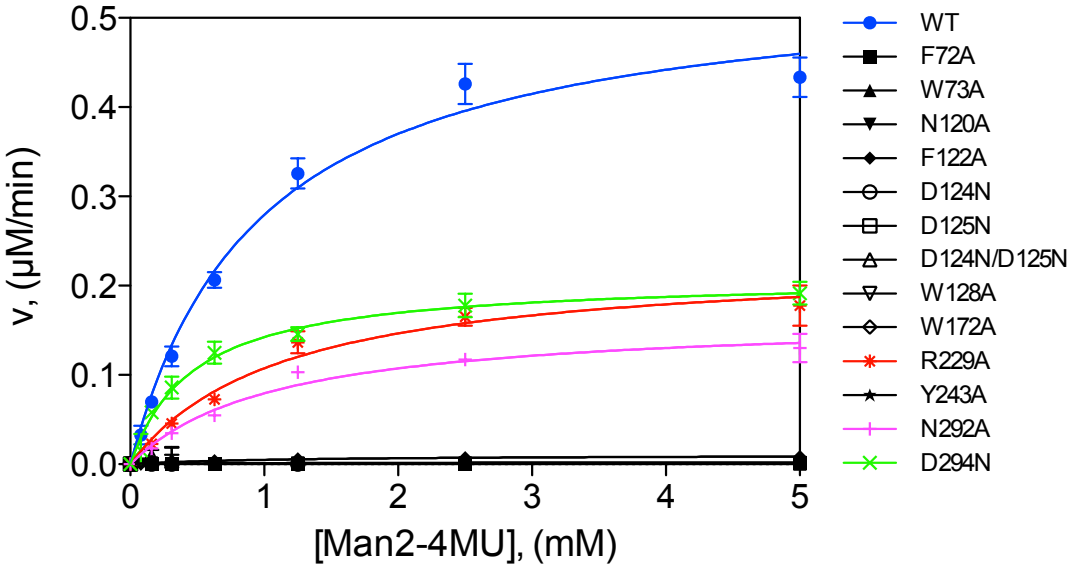

Figure 6.8: Steady state kinetics of *Bc*Aman6 WT and point mutants. *Bc*Aman6 WT or mutants were incubated with different concentrations of Man2-4MU to determine steady state kinetics.

6.8 Solvent exposed aromatic amino acids in the groove are indispensable for substrate binding

In addition to the residues that seemed to be directly involved in hydrolysis, residues important for substrate binding were identified. Using the structure of *Bc*Aman6 several mutations of side chains along the active site groove were made and steady state kinetics for these mutants were established (Table 6.2 and Fig. 6.8). The results can be grouped into two categories when compared with *Bc*Aman6 WT: 1) mutations with comparable binding constants but considerably reduced catalytic activity (F72A, N120A, F122A, W172A, and Y243), and 2) mutations with comparable binding constants and activity (R229A, N292A, D294N). Due to the lack of a substrate complex of *Bc*Aman6 it is difficult to explain the notable loss in activity of the mutations in group 1. The residues may be involved in the co-ordination of the substrate during the reaction as the binding is not affected by the mutations. This observation can also be the result of the synthetic substrate used in this assay. The group 2 mutations do not affect the steady state kinetics as substantially

as the mutations in group 1. The residues in group 2 may only provide weaker hydrogen-bond interactions that is not vital for binding. Additionally, they may provide non-essential interactions with the residues in their surrounding that, however, are beneficial for the rate of *Bc*Aman6 hydrolysis.

6.9 Identification of small fragment binders of *Bc*Aman6 as potential inhibitors

A bio-layer interferometry fragment screen approach (using an Octet RED384) was used to identify molecules that inhibit the activity of *Bc*Aman6 in order to obtain potential inhibitors for the two essential, extracellular yeast homologs *Sc*Dfg5p and *Sc*Dcw1p. This work was done in collaboration with Dr. David Robinson (Drug Discovery Unit, UoD). Six compounds were identified as reasonable binders with association and dissociation constants, and coefficients of determination (R^2) that result in fast binding and low dissociation (Fig. 6.9 and Table 6.3): 5-amino-2-methylindole, (1-methyl-1H-pyrrol-2-yl)methylamine, 2-(1H-imidazol-1-yl)aniline, 1-(4-chlorophenyl)-3-oxoisoindoline, and 2-(4-methylpiperazin-1-yl)aniline. These compounds were used for initial experiments to determine their inhibitory effect on *Bc*Aman6. Due to limitations in the supply of two of the six compounds, only four compounds were tested in an *Bc*Aman6 activity assay at concentrations of 0.1 mM and 1 mM (Table 6.4). None of the compounds resulted in a considerable inhibition of *Bc*Aman6 activity. This result shows one major drawback of the approach to identify inhibitors by bio-layer interferometry. This technique measures binding of a compound independent from its binding site and impact on activity, which is in contrast to classical high-throughput screens of large fragment libraries which are based on an activity assay. However, the advantage of the bio-layer interferometry is that a library of compounds can be rapidly decreased to only compounds that bind to the enzyme. This is very useful if components of an activity assay for the enzyme are limited. This is the case for Man2-4MU which is not commercially

available and can only be produced in moderate amounts in our group.

6.10 Concluding Remarks

The aim of the work on *Bc*Aman6 was to use the bacterial mannosidase as a model for the essential yeast proteins *Sc*Dfg5 and *Sc*Dcw1. The enzymatic activity of the fungal proteins is still unknown and even very recent research in the filamentous fungi *Neurospora crassa* does not reveal their mode of action (Maddi *et al.*, 2012). The structure of *Bc*Aman6 is the second in the GH-76 family, however it is the first with a known function. The α_6/α_6 barrel is a common fold across many different GH families, including GH-125 which also consists of mannosidases. Structure-guided mutagenesis identified D124 and D125 as the side chains that are potentially involved in the hydrolysis of the *Bc*Aman6 substrates. Both residues, and many other residues around both aspartic acids, are conserved between *Bc*Aman6, *Sc*Dfg5 and *Sc*Dcw1 (Fig. 6.1). These observations make *Bc*Aman6 a good model for the yeast proteins. However, the lack of a substrate or product complex or NMR data results in the inability to speculate about the mechanism of hydrolysis. Attempts to crystallise the mutants D124N, D125N and the double mutant did not result in crystals in the established condition. New screens for a different crystallisation condition will have to be carried out, since the mutations seem to result in a difference in packing of *Bc*Aman6. Attempts to obtain substrate complexes by others,

Table 6.3: Kinetics of compounds binding to *Bc*Aman6 during bio-layer interferometry.

	K_d (mM)	K_{on} (1/Ms)	K_{off} (1/s)	R^2
5-amino-2-methylindole	0.14	48.0	0.00676	0.94
(1-methyl-1H-pyrrol-2-yl)methylamine	0.19	47.9	0.00911	0.80
2-(1H-imidazol-1-yl)aniline	2.41	6.6	0.01590	0.93
2-(4-methylpiperazin-1-yl)aniline	0.14	1950.0	0.2790	0.76
1-(4-chlorophenyl)-3-oxoisoindoline	1.49	298.0	0.443	0.92
N-methyl-3,4-dihydro-2H-1,4-benzoxazine-2-carboxamide	57.90	0.3	0.0175	0.91

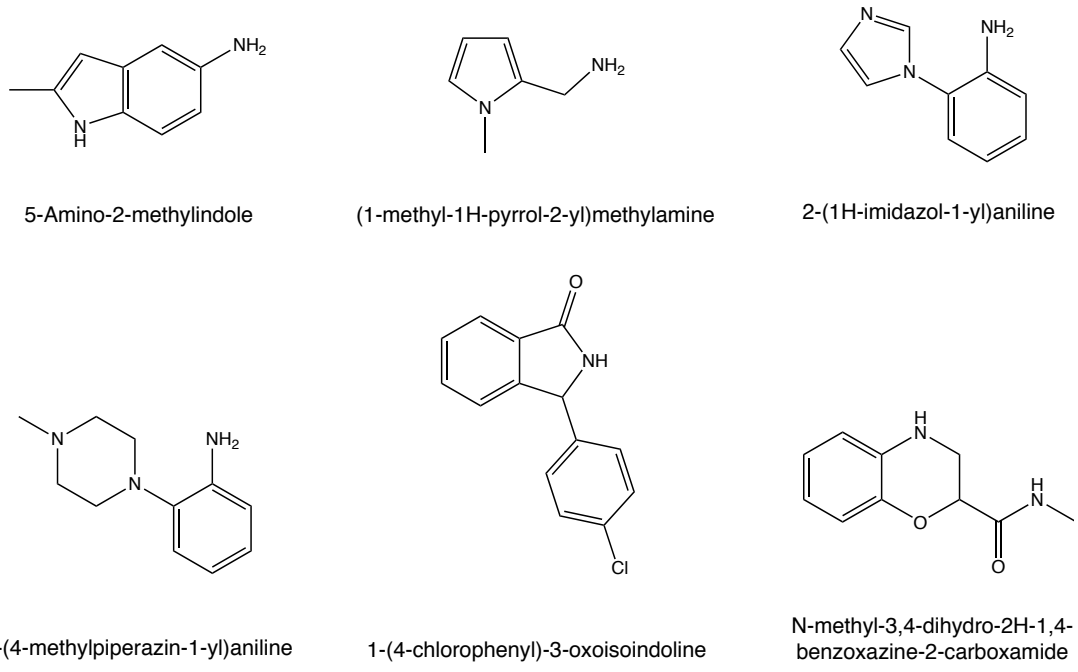

Figure 6.9: Chemical compounds identified to bind *Bc*Aman6. The compounds have been identified by bio-layer interferometry to be reasonable binders of *Bc*Aman6. Only compounds that showed a higher than 3σ above median response and where coefficients of determination (R^2) were above 0.75 were selected.

Table 6.4: Kinetics of *Bc*Aman6 with the compounds identified by bio-layer interferometry. Error indicates standard error of mean, n = 3.

Compound	Concentration (mM)	*V*, (nM/min)
–	–	102.8 ± 2.9
(1-methyl-1H-pyrrol-2-yl)methylamine	0.1	101.3 ± 2.5
	1.0	85.7 ± 0.5
2-(1H-imidazol-1-yl)aniline	0.1	84.4 ± 0.3
	1.0	76.5 ± 1.5
2-(4-methylpiperazin-1-yl)aniline	0.1	80.7 ± 2.0
	1.0	72.7 ± 1.5
1-(4-chlorophenyl)-3-oxoisoindoline	0.1	76.2 ± 1.3
	1.0	76.5 ± 2.2

such as replacing the oxygen in the glycosidic bond of mannobiose with a sulfur, have been proven useful (Gregg *et al.*, 2011).

The enzyme assay using Man2-4MU has been shown to give similar kinetic parameters for *Bc*Aman6 compared to previous work (Nakajima *et al.*, 1976). The limiting factor of the assay, however, is the availability of the substrate analogue, which is not commercially available. Nevertheless, the assay can still be considered as a strong tool to aid identification of inhibitors of the mannosidase. It is rapid (incubation times of approx. 10 min were enough to obtain an acceptable signal/background ratio) and does not involve any coupled enzymes that have to be screened independently after the identification of a good inhibitor of *Bc*Aman6. This work will be done in the future as the similarity of the active site between *Bc*Aman6, *Sc*Dfg5 and *Sc*Dcw1 is most likely the only exploitable target. The use of bio-layer interferometry is a useful technique if an activity assay for a target is not available and/or if costs for either a component of the assay or for a large screen are an issue. However, it should be noted that this approach is mainly useful if the protein tested is the target from the organism of interest. This is particularly important if a fragment binds to the protein in a region of low conservation.

The results presented here should be used for further investigations and screenings for inhibitors of the yeast proteins *Sc*Dfg5 and *Sc*Dcw1. Furthermore, more effort should be put into the expression and purification of both proteins as they still represent interesting drug targets without a known enzymatic function. With high yields of recombinant *Sc*Dfg5 and *Sc*Dcw1 it should be feasible to use micro array binding to identify potential substrates and elucidate the function the these two essential proteins.

7 Conclusions and Future Directions

In conclusion, the results in this thesis present the first structure of the GT-62 family, defining the fold of the entire GT family. *Sc*Mnn9Δ92 adapts the GT-A fold and carries an unusual loop formed by two β-strands in the C-terminus of the GT. The function is unknown but the loop could serve as a dimerisation domain for other GTs in the yeast Golgi (*e. g. Sc*Van1) or for the acceptor protein that will become mannosylated by *Sc*Mnn9. Through the development of a novel coupled enzyme assay, the steady-state kinetics for *Sc*Mnn9Δ92 could be determined. Compared with GTs that are structurally similar and use GDP-Man as the donor substrate, *Sc*Mnn9Δ92 shows comparatively weak binding to the substrate analogue 4MU-Man and the donor GDP-Man. However, the speed of the reaction of *Sc*Mnn9Δ92 is comparable to some the similar GTs explored in this thesis. Furthermore, *Sc*Mnn9Δ92 is not able to form α-1,2-glycosidic bonds *in vitro*. This is in contrast to previous data that suggests that *Sc*Mnn9 has the ability to form either an α-1,6- or α-1,2-glycosidic bond between two mannose residues (Rodionov *et al.*, 2009, Stolz and Munro, 2002). Additionally, *Sc*Van1Δ86 is only able to form oligomannose products in the presence of the product of *Sc*Mnn9Δ92, mannotriose, and *Sc*Mnn9Δ92. The activity of *Sc*Mnn9Δ92 for the formation of mannose oligomers is not necessary. This indicates, that the dimerisation between the two GTs transfers *Sc*Van1Δ86 into an activated state. However, activity is abolished in the absence of parts of the N-terminal linker region and the C-terminus of *Sc*Van1. These regions may be necessary for dimerisation of *Sc*Van1 with *Sc*Mnn9. The products formed by

*Sc*Van1Δ86 and *Sc*Mnn9Δ92 are solely linked via α-1,6-glycosidic bonds. This indicates that neither of the components of the M-Pol I complex appears to have α-1,2-transferase ability *in vitro*. Taken these results together, it is unlikely that M-Pol I is the complex that can differentiate between mannoproteins and core-type proteins where upon the GT complex changes its transferase activity accordingly. It is more likely that an unknown GT or a complex of GTs transfers the α-1,2-mannose onto core-type proteins.

The results in this thesis can be used for further attempts to crystallise M-Pol I in complex with a substrate analogue or the donor substrate and an acceptor protein. This could lead to the identification of the mechanism that results in the synergetic effect of *Sc*Mnn9 on *Sc*Van1 activity. The assay developed to measure steady-state kinetics of *Sc*Mnn9 could be used to screen for inhibitors of the mannosylation pathway in yeasts and other fungi. It has been shown that the absence of the highly decorated mannose structure abolishes virulence in a *C. albicans* mouse model completely (Hall *et al.*, 2013), making the mannosylation pathway a potential and interesting drug target.

Furthermore, this thesis reports the first crystal structure of a GH-76 GH with known enzymatic activity. Using a fluorescent enzyme assay important and conserved residues were identified that are involved in the hydrolysis of α-1,6-mannose. The combination of the structure and the assay can serve as a model for the identification of potent inhibitors for the essential fungal GH-76 members Dfg5 and Dcw1 that can be found in *S. cerevisiae* but also in the human pathogens *C. albicans* and *A. fumigatus*. This is in particular interesting, giving the fact that the active site residues are very well conserved across all species.

The assay developed in this thesis for the GH-76 *Bc*Aman6 is compatible with high-throughput inhibitor screens and should be used in such a screen to identify potent inhibitors. These inhibitors could also negatively affect the activity of the fungal proteins Dfg5 and Dcw1. Since both proteins are extracellular proteins, inhibitors that can effectively inhibit the activity of both enzymes could lead to the development of new anti-fungal drugs.

List of References

Absmanner, B.; Schmeiser, V.; Kaempf, M., and Lehle, L. Biochemical characterization, membrane association and identification of amino acids essential for the function of Alg11 from *Saccharomyces cerevisiae*, an alpha-1,2-mannosyltransferase catalysing two sequential glycosylation steps in the formation of the lipid-linked core oligosaccharide. *Biochem J*, 426:205–217, March 2010.

Adams, P. D.; Afonine, P. V.; Bunkóczi, G.; Chen, V. B.; Davis, I. W.; Echols, N.; Headd, J. J.; Hung, L.-W.; Kapral, G. J.; Grosse-Kunstleve, R. W.; McCoy, A. J.; Moriarty, N. W.; Oeffner, R.; Read, R. J.; Richardson, D. C.; Richardson, J. S.; Terwilliger, T. C., and Zwart, P. H. PHENIX: a comprehensive Python-based system for macromolecular structure solution. *Acta Crystallogr. D Biol. Crystallogr.*, 66(Pt 2):213–221, February 2010.

Aebi, M.; Gassenhuber, J.; Domdey, H., and Heesen, S.te . Cloning and characterization of the ALG3 gene of *Saccharomyces cerevisiae*. *Glycobiology*, 6(4): 439–444, June 1996.

Aebi, M.; Bernasconi, R.; Clerc, S., and Molinari, M. N-glycan structures: recognition and processing in the ER. *Trends Biochem Sci*, 35(2):74–82, February 2010.

Aguilar-Uscanga, B. and François, J. M. A study of the yeast cell wall composition and structure in response to growth conditions and mode of cultivation. *Lett Appl Microbiol*, 37(3):268–274, 2003.

Aimanianda, V.; Clavaud, C.; Simenel, C.; Fontaine, T.; Delepierre, M., and Latgé, J.-P. Cell wall beta-(1,6)-glucan of *Saccharomyces cerevisiae*: structural characterization and in situ synthesis. *J Biol Chem*, 284(20):13401–13412, May 2009.

Amaya, M. F.; Buschiazzo, A.; Nguyen, T., and Alzari, P. M. The high resolution structures of free and inhibitor-bound *Trypanosoma rangeli* sialidase and its comparison with *T. cruzi* trans-sialidase. *J Mol Biol*, 325(4):773–784, January 2003.

Amaya, M. F.; Watts, A. G.; Damager, I.; Wehenkel, A.; Nguyen, T.; Buschiazzo, A.; Paris, G.; Frasch, A. C.; Withers, S. G., and Alzari, P. M. Structural insights into the catalytic mechanism of *Trypanosoma cruzi* trans-sialidase. *Structure/Folding and Design*, 12(5):775–784, May 2004.

Andersen, O. A.; Nathubhai, A.; Dixon, M. J.; Eggleston, I. M., and Aalten, D. M. F.van . Structure-based dissection of the natural product cyclopentapeptide chitinase inhibitor argifin. *Chem Biol*, 15(3):295–301, March 2008.

Annaix, V.; Bouchara, J. P.; Larcher, G.; Chabasse, D., and Tronchin, G. Specific binding of human fibrinogen fragment D to *Aspergillus fumigatus* conidia. *Infection and Immunity*, 60(5):1747–1755, May 1992.

Ardèvol, A. and Rovira, C. The molecular mechanism of enzymatic glycosyl transfer with retention of configuration: evidence for a short-lived oxocarbenium-like species. *Angew Chem Int Ed Engl*, 50(46):10897–10901, November 2011.

Ashida, H.; Hong, Y. J.; Murakami, Y.; Shishioh, N.; Sugimoto, N.; Kim, Y. U.; Maeda, Y., and Kinoshita, T. Mammalian PIG-X and yeast Pbn1p are the essential components of glycosylphosphatidylinositol-mannosyltransferase I. *Molecular Biology of the Cell*, 16(3):1439–1448, March 2005.

Aufauvre-Brown, A.; Mellado, E.; Gow, N., and Holden, D. W. *Aspergillus fumigatus chsE*: A gene related to CHS3 of *Saccharomyces cerevisiae* and important for hyphal growth and conidiophore development but not pathogenicity. *Fungal Genet Biol*, 21(1):141–152, February 1997.

Azuma, I.; Kimura, H.; Hirao, F.; Tsubura, E.; Yamamura, Y., and Misaki, A. Biochemical and immunological studies on *Aspergillus* III. Chemical and immunological properties of glycopeptide obtained from *Aspergillus fumigatus*. *Jpn J Microbiol*, 15(3):237–&, 1971.

Bal, A. M. The echinocandins: three useful choices or three too many? *Int J Antimicrob Agents*, 35(1):13–18, January 2010.

Baladrón, V.; Ufano, S.; Dueñas, E.; Martín-Cuadrado, A. B.; Rey, F.del , and Aldana, C. R.Vázquez de . Eng1p, an endo-1,3-beta-glucanase localized at the daughter side of the septum, is involved in cell separation in *Saccharomyces cerevisiae*. *Eukaryotic Cell*, 1(5):774–786, October 2002.

Ballou, L.; Cohen, R. E., and Ballou, C. E. *Saccharomyces cerevisiae* mutants that make mannoproteins with a truncated carbohydrate outer chain. *J Biol Chem*, 255(12):5986–5991, June 1980.

Ballou, L.; Hernández, L. M.; Alvarado, E., and Ballou, C. E. Revision of the oligosaccharide structures of yeast carboxypeptidase Y. *Proc Natl Acad Sci USA*, 87(9):3368–3372, May 1990.

Ballou, L.; Hitzeman, R. A.; Lewis, M. S., and Ballou, C. E. Vanadate-resistant yeast mutants are defective in protein glycosylation. *Proc Natl Acad Sci USA*, 88 (8):3209–3212, April 1991.

Banno, Y.; Yamada, T., and Nozawa, Y. Secreted phospholipases of the dimorphic fungus, *Candida albicans*; separation of three enzymes and some biological properties. *Sabouraudia*, 23(1):47–54, February 1985.

Bardalaye, P. C. and Nordin, J. H. Chemical structure of galactomannan from cell wall of *Aspergillus niger*. *J Biol Chem*, 252(8):2584–2591, 1977.

Barnes, G.; Hansen, W. J.; Holcomb, C. L., and Rine, J. Asparagine-linked glycosylation in *Saccharomyces cerevisiae*: genetic analysis of an early step. *Mol Cell Biol*, 4(11):2381–2388, November 1984.

Baron, S. Introduction to mycology. In *Medical Microbiology*. University of Texas Medical Branch at Galveston, Galveston (TX), 1996.

Barretobergter, E. M. and Travassos, L. R. Chemical structure of the D-galacto-D-mannan component from hyphae of *Aspergillus niger* and other *Aspergillus* spp. *Carbohydr Res*, 86(2):273–285, 1980.

Barrett-Bee, K.; Hayes, Y.; Wilson, R. G., and Ryley, J. F. A comparison of phospholipase activity, cellular adherence and pathogenicity of yeasts. *J Gen Microbiol*, 131(5):1217–1221, May 1985.

Beauvais, A.; Monod, M.; Debeaupuis, J. P.; Diaquin, M.; Kobayashi, H., and Latgé, J. P. Biochemical and antigenic characterization of a new dipeptidyl-peptidase isolated from *Aspergillus fumigatus*. *J Biol Chem*, 272(10):6238–6244, March 1997.

Beauvais, A.; Maubon, D.; Park, S.; Morelle, W.; Tanguy, M.; Huerre, M.; Perlin, D. S., and Latgé, J. P. Two alpha-(1,3)-glucan synthases with different functions in *Aspergillus fumigatus*. *Applied and Environmental Microbiology*, 71(3):1531–1538, March 2005.

Beauvais, A.; Loussert, C.; Prevost, M. C.; Verstrepen, K., and Latgé, J.-P. Characterization of a biofilm-like extracellular matrix in FLO1-expressing *Saccharomyces cerevisiae* cells. *FEMS Yeast Research*, 9(3):411–419, May 2009.

Benachour, A.; Sipos, G.; Flury, I.; Reggiori, F.; Canivenc-Gansel, E.; Vionnet, C.; Conzelmann, A., and Benghezal, M. Deletion of GPI7, a yeast gene required for addition of a side chain to the glycosylphosphatidylinositol (GPI) core structure, affects GPI protein transport, remodeling, and cell wall integrity. *J Biol Chem*, 274(21):15251–15261, May 1999.

Benghezal, M.; Benachour, A.; Rusconi, S.; Aebi, M., and Conzelmann, A. Yeast Gpi8p is essential for GPI anchor attachment onto proteins. *EMBO J*, 15(23): 6575–6583, December 1996.

Bennett, J. E.; Bhattacharjee, A. K., and Glaudemans, C. P. J. Galactofuranosyl groups are immunodominant in *Aspergillus fumigatus* galactomannan. *Mol Immunol*, 22(3):251–254, 1985.

Bertani, G. Lysogeny at mid-twentieth century: P1, P2, and other experimental systems. *J Bacteriol*, 186(3):595–600, February 2004.

Bickel, T.; Lehle, L.; Schwarz, M.; Aebi, M., and Jakob, C. A. Biosynthesis of lipid-linked oligosaccharides in *Saccharomyces cerevisiae* - Alg13p and Alg14p form a complex required for the formation of GlcNAc(2)-PP-dolichol. *J Biol Chem*, 280 (41):34500–34506, October 2005.

Bodey, G. P. and Vartivarian, S. Aspergillosis. *Eur J Clin Microbiol Infect Dis*, 8(5): 413–437, May 1989.

Bojsen, R. K.; Andersen, K. S., and Regenberg, B. *Saccharomyces cerevisiae* – a model to uncover molecular mechanisms for yeast biofilm biology. *FEMS Immunol Med Microbiol*, 65(2):169–182, July 2012.

Bolard, J. How do the polyene macrolide antibiotics affect the cellular membrane properties. *Biochim Biophys Acta*, 864(3-4):257–304, December 1986.

Bond, C. S. and Schüttelkopf, A. W. ALINE: a WYSIWYG protein-sequence alignment editor for publication-quality alignments. *Acta Crystallogr. D Biol. Crystallogr.*, 65(Pt 5):510–512, May 2009.

Boone, C.; Sommer, S. S.; Hensel, A., and Bussey, H. Yeast KRE genes provide evidence for a pathway of cell wall beta-glucan assembly. *J Cell Biol*, 110(5): 1833–1843, May 1990.

Borges, N.; Marugg, J. D.; Empadinhas, N.; Costa, M. S.da , and Santos, H. Specialized roles of the two pathways for the synthesis of mannosylglycerate in osmoadaptation and thermoadaptation of *Rhodothermus marinus*. *J Biol Chem*, 279(11):9892–9898, March 2004.

Bosson, R.; Jaquenoud, M., and Conzelmann, A. GUP1 of *Saccharomyces cerevisiae* encodes an O-acyltransferase involved in remodeling of the GPI anchor. *Molecular Biology of the Cell*, 17(6):2636–2645, June 2006.

Bouchara, J. P.; Bouali, A.; Tronchin, G.; Robert, R.; Chabasse, D., and Senet, J. M. Binding of fibrinogen to the pathogenic *Aspergillus* species. *J Med Vet Mycol*, 26(6):327–334, 1988.

Bouchara, J. P.; Sanchez, M.; Chevailler, A.; MarotLeblond, A.; Lissitzky, J. C.; Tronchin, G., and Chabasse, D. Sialic acid-dependent recognition of laminin and fibrinogen by *Aspergillus fumigatus* conidia. *Infection and Immunity*, 65(7): 2717–2724, July 1997.

Bourne, Y. and Henrissat, B. Glycoside hydrolases and glycosyltransferases: families and functional modules. *Curr Opin Struct Biol*, 11(5):593–600, October 2001.

Brajtburg, J. and Bolard, J. Carrier effects on biological activity of amphotericin B. *Clin Microbiol Rev*, 9(4):512–&, October 1996.

Brajtburg, J.; Elberg, S.; Schwartz, D. R.; Vertutcroquin, A.; Schlessinger, D.; Kobayashi, G. S., and Medoff, G. Involvement of oxidative damage in erythrocyte lysis induced by amphotericin B. *Antimicrob Agents Chemother*, 27(2):172–176, 1985.

Breton, C. and Imberty, A. Structure/function studies of glycosyltransferases. *Curr Opin Struct Biol*, 9(5):563–571, October 1999.

Breton, C.; Bettler, E.; Joziasse, D. H.; Geremia, R. A., and Imberty, A. Sequence-function relationships of prokaryotic and eukaryotic galactosyltransferases. *J Biochem*, 123(6):1000–1009, June 1998.

Breton, C.; Fournel-Gigleux, S., and Palcic, M. M. Recent structures, evolution and mechanisms of glycosyltransferases. *Curr Opin Struct Biol*, pages 1–10, July 2012.

Brurberg, M. B.; Nes, I. F., and Eijsink, V. G. Comparative studies of chitinases A and B from *Serratia marcescens*. *Microbiology (Reading, Engl.)*, 142 (Pt 7): 1581–1589, July 1996.

Burda, P. and Aebi, M. The ALG10 locus of *Saccharomyces cerevisiae* encodes the alpha-1,2 glucosyltransferase of the endoplasmic reticulum: the terminal glucose of the lipid-linked oligosaccharide is required for efficient N-linked glycosylation. *Glycobiology*, 8(5):455–462, May 1998.

Burda, P.; Jakob, C. A.; Beinhauer, J.; Hegemann, J. H., and Aebi, M. Ordered assembly of the asymmetrically branched lipid-linked oligosaccharide in the endoplasmic reticulum is ensured by the substrate specificity of the individual glycosyltransferases. *Glycobiology*, 9(6):617–625, June 1999.

Burmeister, W. P.; Cottaz, S.; Rollin, P.; Vasella, A., and Henrissat, B. High resolution X-ray crystallography shows that ascorbate is a cofactor for myrosinase and substitutes for the function of the catalytic base. *J Biol Chem*, 275(50): 39385–39393, December 2000.

Buurman, E. T.; Westwater, C.; Hube, B.; Brown, A. J.; Odds, F. C., and Gow, N. A. Molecular analysis of CaMnt1p, a mannosyl transferase important for adhesion and virulence of *Candida albicans*. *Proc Natl Acad Sci USA*, 95(13):7670–7675, June 1998.

Cabib, E. Two novel techniques for determination of polysaccharide cross-links show that Crh1p and Crh2p attach chitin to both beta-(1-6)- and beta-(1-3)-glucan in the *Saccharomyces cerevisiae* cell wall. *Eukaryotic Cell*, 8(11):1626–1636, November 2009.

Cabib, E. and Durán, A. Synthase III-dependent chitin is bound to different acceptors depending on location on the cell wall of budding yeast. *J Biol Chem*, 280 (10):9170–9179, March 2005.

Cabib, E.; Blanco, N.; Grau, C.; Rodriguez-Peña, J. M., and Arroyo, J. Crh1p and Crh2p are required for the cross-linking of chitin to beta-(1-6)-glucan in the *Saccharomyces cerevisiae* cell wall. *Mol Microbiol*, 63(3):921–935, February 2007.

Cabib, E.; Farkaš, V.; Kosík, O.; Blanco, N.; Arroyo, J., and McPhie, P. Assembly of the yeast cell wall. Crh1p and Crh2p act as transglycosylases in vivo and in vitro. *J Biol Chem*, 283(44):29859–29872, October 2008.

Calderone, R. A. and Clancy, C. J. Candida and candidiasis. 2002.

Caldwell, S. A.; Jackson, S. R.; Shahriari, K. S.; Lynch, T. P.; Sethi, G.; Walker, S.; Vosseller, K., and Reginato, M. J. Nutrient sensor O-GlcNAc transferase regulates breast cancer tumorigenesis through targeting of the oncogenic transcription factor FoxM1. *Oncogene*, 29(19):2831–2842, May 2010.

Calera, J. A.; Paris, S.; Monod, M.; Hamilton, A. J.; Debeaupuis, J. P.; Diaquin, M.; Lopezmedrano, R.; Leal, F., and Latgé, J. P. Cloning and disruption of the antigenic catalase gene of *Aspergillus fumigatus*. *Infection and Immunity*, 65 (11):4718–4724, November 1997.

Cambi, A.; Netea, M. G.; Mora-Montes, H. M.; Gow, N. A. R.; Hato, S. V.; Lowman, D. W.; Kullberg, B. J.; Torensma, R.; Williams, D. L., and Figdor, C. G. Dendritic cell interaction with *Candida albicans* critically depends on N-linked mannan. *J Biol Chem*, 283(29):20590–20599, July 2008.

Campbell, J. A.; Davies, G. J.; Bulone, V., and Henrissat, B. A classification of nucleotide-diphospho-sugar glycosyltransferases based on amino acid sequence similarities. *Biochem J*, 326:929–939, September 1997.

Canivenc-Gansel, E.; Imhof, I.; Reggiori, F.; Burda, P.; Conzelmann, A., and Benachour, A. GPI anchor biosynthesis in yeast: phosphoethanolamine is attached to the alpha-(1),4-linked mannose of the complete precursor glycophospholipid. *Glycobiology*, 8(8):761–770, August 1998.

Cantarel, B. L.; Coutinho, P. M.; Rancurel, C.; Bernard, T.; Lombard, V., and Henrissat, B. The Carbohydrate-Active EnZymes database (CAZy): an expert resource for Glycogenomics. *Nucleic Acids Research*, 37(Database issue):D233–D238, January 2009.

Cappellaro, C.; Mrsa, V., and Tanner, W. New potential cell wall glucanases of *Saccharomyces cerevisiae* and their involvement in mating. *J Bacteriol*, 180 (19):5030–5037, October 1998.

Caro, L. H. P.; Tettelin, H.; Vossen, J. H.; Ram, A. F. J.; Ende, H.van den , and Klis, F. M. In silicio identification of glycosyl-phosphatidylinositol-anchored plasma-membrane and cell wall proteins of *Saccharomyces cerevisiae*. *Yeast*, 13(15): 1477–1489, December 1997.

Carotti, C.; Ragni, E.; Palomares, O.; Fontaine, T.; Tedeschi, G.; Rodríguez, R.; Latgé, J.-P.; Vai, M., and Popolo, L. Characterization of recombinant forms of the yeast Gas1 protein and identification of residues essential for glucanosyltransferase activity and folding. *Eur J Biochem*, 271(18):3635–3645, September 2004.

Castillo, L.; Martinez, A. I.; Garcera, A.; Elorza, M. V.; Valentin, E., and Sentandreu, R. Functional analysis of the cysteine residues and the repetitive sequence of *Saccharomyces cerevisiae* Pir4/Cis3: the repetitive sequence is needed for binding to the cell wall beta-1,3-glucan. *Yeast*, 20(11):973–983, August 2003.

Chantret, I.; Dancourt, J.; Barbat, A., and Moore, S. E. H. Two proteins homologous to the N- and C-terminal domains of the bacterial glycosyltransferase Murg are required for the second step of dolichyl-linked oligosaccharide synthesis in *Saccharomyces cerevisiae*. *J Biol Chem*, 280(18):18551–18552, May 2005.

Charnock, S. J. and Davies, G. J. Structure of the nucleotide-diphospho-sugar transferase, SpsA from *Bacillus subtilis*, in native and nucleotide-complexed forms. *Biochemistry*, 38(20):6380–6385, May 1999.

Chen, C.-I.; Keusch, J. J.; Klein, D.; Hess, D.; Hofsteenge, J., and Gut, H. Structure of human POFUT2: insights into thrombospondin type 1 repeat fold and O-fucosylation. *EMBO J*, 31(14):3183–3197, July 2012.

Chiu, C. P. C.; Watts, A. G.; Lairson, L. L.; Gilbert, M.; Lim, D.; Wakarchuk, W. W.; Withers, S. G., and Strynadka, N. C. J. Structural analysis of the sialyltransferase CstII from *Campylobacter jejuni* in complex with a substrate analog. *Nat Struct Mol Biol*, 11(2):163–170, February 2004.

Chryssanthou, E. In vitro susceptibility of respiratory isolates of *Aspergillus* species to itraconazole and amphotericin B. Acquired resistance to itraconazole. *Scand J Infect Dis*, 29(5):509–512, 1997.

Cipollo, J. F. and Trimble, R. B. The *Saccharomyces cerevisiae* alg12 Delta mutant reveals a role for the middle-arm alpha-1,2-Man- and upper-arm alpha-1,2-Man alpha-1,6-Man residues of Glc(3)Man(9)GlcNAc(2)-PP-Dol in regulating glycoprotein glycan processing in the endoplasmic reticulum and Golgi apparatus. *Glycobiology*, 12(11):749–762, November 2002.

Cipollo, J. F.; Trimble, R. B.; Chi, J. H.; Yan, Q., and Dean, N. The yeast ALG11 gene specifies addition of the terminal alpha-1,2-Man to the Man(5)GlcNAc(2)-PP-dolichol N-glycosylation intermediate formed on the cytosolic side of the endoplasmic reticulum. *J Biol Chem*, 276(24):21828–21840, June 2001.

Clements, J. S. and Peacock, J. E. Amphotericin B revisited - Reassessment of toxicity. *Am J Med*, 88(5N):N22–N27, May 1990.

Clerc, S.; Hirsch, C.; Oggier, D. M.; Deprez, P.; Jakob, C.; Sommer, T., and Aebi, M. Htm1 protein generates the N-glycan signal for glycoprotein degradation in the endoplasmic reticulum. *J Cell Biol*, 184(1):159–172, January 2009.

Cole, D. C.; Olland, A. M.; Jacob, J.; Brooks, J.; Bursavich, M. G.; Czerwinski, R.; DeClereq, C.; Johnson, M.; Joseph-McCarthy, D.; Ellingboe, J. W.; Lin, L.; Nowak, P.; Presman, E.; Strand, J.; Tam, A.; Williams, C. M. M.; Yao, S.; Tsao, D. H. H., and Fitz, L. J. Identification and characterization of acidic mammalian chitinase inhibitors. *J Med Chem*, 53(16):6122–6128, August 2010.

Cos, T.; Ford, R. A.; Trilla, J. A.; Duran, A.; Cabib, E., and Roncero, C. Molecular analysis of Chs3p participation in chitin synthase III activity. *Eur J Biochem*, 256 (2):419–426, September 1998.

Costello, L. C. and Orlean, P. Inositol acylation of a potential glycosyl phosphoinositol anchor precursor from yeast requires acyl coenzyme A. *J Biol Chem*, 267 (12):8599–8603, April 1992.

Coulot, P.; Bouchara, J. P.; Renier, G.; Annaix, V.; Planchenault, C.; Tronchin, G., and Chabasse, D. Specific interaction of *Aspergillus fumigatus* with fibrinogen and its role in cell adhesion. *Infection and Immunity*, 62(6):2169–2177, June 1994.

Coutinho, P. M.; Coutinho, P. M.; Deleury, E.; Deleury, E.; Davies, G. J.; Davies, G. J.; Henrissat, B., and Henrissat, B. An evolving hierarchical family classification for glycosyltransferases. *J Mol Biol*, 328(2):307–317, April 2003.

Couto, J. R.; Huffaker, T. C., and Robbins, P. W. Cloning and expression in *Escherichia coli* of a yeast mannosyltransferase from the asparagine-linked glycosylation pathway. *J Biol Chem*, 259(1):378–382, 1984.

Dallies, N.; François, J., and Paquet, V. A new method for quantitative determination of polysaccharides in the yeast cell wall. Application to the cell wall defective mutants of *Saccharomyces cerevisiae*. *Yeast*, 14(14):1297–1306, October 1998.

Davies, G. and Henrissat, B. Structures and mechanisms of glycosyl hydrolases. *Structure/Folding and Design*, 3(9):853–859, September 1995.

Groot, P. W. J.de ; Hellingwerf, K. J., and Klis, F. M. Genome-wide identification of fungal GPI proteins. *Yeast*, 20(9):781–796, July 2003.

Nobel, J. G.de and Barnett, J. A. Passage of molecules through yeast cell walls: a brief essay-review. *Yeast*, 7(4):313–323, May 1991.

Nobel, J. G.de ; Klis, F. M.; Priem, J.; Munnik, T., and Ende, H.van den . The glucanase-soluble mannoproteins limit cell wall porosity in *Saccharomyces cerevisiae*. *Yeast*, 6(6):491–499, November 1990.

De Sampaïo, G.; Bourdineaud, J. P., and Lauquin, G. J. M. A constitutive role for GPI anchors in *Saccharomyces cerevisiae*: cell wall targeting. *Mol Microbiol*, 34 (2):247–256, October 1999.

Dean, N. Yeast glycosylation mutants are sensitive to aminoglycosides. *Proc Natl Acad Sci USA*, 92(5):1287–1291, February 1995.

Denning, D. W. Invasive aspergillosis. *Clin Infect Dis*, 26(4):781–803, April 1998.

Denning, D. W.; Radford, S. A.; Oakley, K. L.; Hall, L.; Johnson, E. M., and Warnock, D. W. Correlation between in-vitro susceptibility testing to itraconazole and in-vivo outcome of *Aspergillus fumigatus* infection. *J Antimicrob Chemoth*, 40(3):401–414, September 1997a.

Denning, D. W.; Venkateswarlu, K.; Oakley, K. L.; Anderson, M. J.; Manning, N. J.; Stevens, D. A.; Warnock, D. W., and Kelly, S. L. Itraconazole resistance in *Aspergillus fumigatus*. *Antimicrob Agents Chemother*, 41(6):1364–1368, June 1997b.

Deresinski, S. C. and Stevens, D. A. Caspofungin. *Clin Infect Dis*, 36(11):1445–1457, June 2003.

Descroix, K.; Pesnot, T.; Yoshimura, Y.; Gehrke, S. S.; Wakarchuk, W.; Palcic, M. M., and Wagner, G. K. Inhibition of galactosyltransferases by a novel class of donor analogues. *J Med Chem*, 55(5):2015–2024, March 2012.

Dixon, D. M.; McNeil, M. M.; Cohen, M. L.; Gellin, B. G., and LaMontagne, J. R. Fungal infections – A growing threat. *Public Health Rep*, 111(3):226–235, May 1996.

Dobson, F. S. *Lichens: An illustrated guide to the British and Irish species*. Richmond Publishing Co Ltd, 2005.

Dong, D. L. and Hart, G. W. Purification and characterization of an O-GlcNAc selective N-acetyl-beta-D-glucosaminidase from rat spleen cytosol. *J Biol Chem*, 269(30):19321–19330, July 1994.

Dorfmueller, H. C. and Aalten, D. M. F.van . Screening-based discovery of drug-like O-GlcNAcase inhibitor scaffolds. *FEBS Lett*, 584(4):694–700, February 2010.

Dorfmueller, H. C.; Borodkin, V. S.; Schimpl, M.; Shepherd, S. M.; Shpiro, N. A., and Aalten, D. M. F.van . GlcNAcstatin: A picomolar, selective O-GlcNAcase inhibitor that modulates intracellular O-GlcNAcylation levels. *J Am Chem Soc*, 128(51):16484–16485, December 2006.

Dorfmueller, H. C.; Borodkin, V. S.; Schimpl, M.; Zheng, X.; Kime, R.; Read, K. D., and Aalten, D. M. F.van . Cell-Penetrant, nanomolar O-GlcNAcase Inhibitors selective against lysosomal hexosaminidases. *Chem Biol*, 17(11):1250–1255, November 2010.

Dranginis, A. M.; Rauceo, J. M.; Coronado, J. E., and Lipke, P. N. A biochemical guide to yeast adhesins: Glycoproteins for social and antisocial occasions. *Microbiology and Molecular Biology Reviews*, 71(2):282—-, June 2007.

Drgonová, J.; Drgon, T.; Tanaka, K.; Kollár, R.; Chen, G. C.; Ford, R. A.; Chan, C. S. M.; Takai, Y., and Cabib, E. Rho1p, a yeast protein at the interface between cell polarization and morphogenesis. *Science*, 272(5259):277–279, April 1996.

Dupres, V.; Dufrêne, Y. F., and Heinisch, J. J. Measuring cell wall thickness in living yeast cells using single molecular rulers. *ACS Nano*, 4(9):5498–5504, September 2010.

Ecker, M.; Mrsa, V.; Hagen, I.; Deutzmann, R.; Strahl, S., and Tanner, W. O-mannosylation precedes and potentially controls the N-glycosylation of a yeast cell wall glycoprotein. *EMBO Rep*, 4(6):628–632, June 2003.

Ecker, M.; Deutzmann, R.; Lehle, L.; Mrsa, V., and Tanner, W. Pir proteins of *Saccharomyces cerevisiae* are attached to beta-1,3-glucan by a new protein-carbohydrate linkage. *J Biol Chem*, 281(17):11523–11529, April 2006.

Emsley, P. and Cowtan, K. Coot: model-building tools for molecular graphics. *Acta Crystallogr. D Biol. Crystallogr.*, 60(Pt 12 Pt 1):2126–2132, December 2004.

Ernst, E. J.; Klepser, M. E.; Ernst, M. E.; Messer, S. A., and Pfaller, M. A. In vitro pharmacodynamic properties of MK-0991 determined by time-kill methods. *Diagn Microbiol Infect Dis*, 33(2):75–80, February 1999.

Errey, J. C.; Lee, S. S.; Gibson, R. P.; Martinez-Fleites, C.; Barry, C. S.; Jung, P. M. J.; O'Sullivan, A. C.; Davis, B. G., and Davies, G. J. Mechanistic insight into enzymatic glycosyl transfer with retention of configuration through analysis of glycomimetic inhibitors. *Angew Chem Int Ed Engl*, 49(7):1234–1237, February 2010.

Fabre, A. L.; Orlean, P., and Taron, C. H. *Saccharomyces cerevisiae* Ybr004c and its human homologue are required for addition of the second mannose during glycosylphosphatidylinositol precursor assembly. *FEBS J*, 272(5):1160–1168, March 2005.

Fankhauser, C.; Homans, S. W.; Thomasoates, J. E.; McConville, M. J.; Desponds, C.; Conzelmann, A., and Ferguson, M. A. J. Structures of glycosylphosphatidylinositol membrane anchors from S*accharomyces cerevisiae*. *J Biol Chem*, 268 (35):26365–26374, December 1993.

Finn, R. D.; Mistry, J.; Tate, J.; Coggill, P.; Heger, A.; Pollington, J. E.; Gavin, O. L.; Gunasekaran, P.; Ceric, G.; Forslund, K.; Holm, L.; Sonnhammer, E. L. L.; Eddy, S. R., and Bateman, A. The Pfam protein families database. *Nucleic Acids Research*, 38(Database issue):D211–22, January 2010.

Fleet, G. H. Cell Walls. *The Yeasts*, 4:199–277, 1991.

Fletterick, R. J. and Sprang, S. R. Glycogen-phosphorylase structures and function. *Acc Chem Res*, 15(11):361–369, 1982.

Flint, J.; Taylor, E.; Yang, M.; Bolam, D. N.; Tailford, L. E.; Martinez-Fleites, C.; Dodson, E. J.; Davis, B. G.; Gilbert, H. J., and Davies, G. J. Structural dissection and high-throughput screening of mannosylglycerate synthase. *Nat Struct Mol Biol*, 12(7):608–614, July 2005.

Fontaine, T.; Simenel, C.; Dubreucq, G.; Adam, O.; Delepierre, M.; Lemoine, J.; Vorgias, C. E.; Diaquin, M., and Latgé, J. P. Molecular organization of the alkali-insoluble fraction of *Aspergillus fumigatus* cell wall. *J Biol Chem*, 275(36):27594–27607, September 2000.

Fraering, P.; Imhof, I.; Meyer, U.; Strub, J. M.; Dorsselaer, A.van ; Vionnet, C., and Conzelmann, A. The GPI transamidase complex of *Saccharomyces cerevisiae* contains Gaa1p, Gpi8p, and Gpi16p. *Molecular Biology of the Cell*, 12(10):3295–3306, October 2001.

Frank, C. G. and Aebi, M. ALG9 mannosyltransferase is involved in two different steps of lipid-linked oligosaccharide biosynthesis. *Glycobiology*, 15(11):1156–1163, November 2005.

Frieman, M. B. and Cormack, B. P. The omega-site sequence of glycosylphosphatidylinositol-anchored proteins in *Saccharomyces cerevisiae* can determine distribution between the membrane and the cell wall. *Mol Microbiol*, 50(3):883–896, November 2003.

Frieman, M. B. and Cormack, B. P. Multiple sequence signals determine the distribution of glycosylphosphatidylinositol proteins between the plasma membrane and cell wall in *Saccharomyces cerevisiae*. *Microbiology*, 150(10):3105–3114, October 2004.

Fu, Y.; Rieg, G.; Fonzi, W. A.; Belanger, P. H.; Edwards, J. E., and Filler, S. G. Expression of the *Candida albicans* gene ALS1 in *Saccharomyces cerevisiae* induces adherence to endothelial and epithelial cells. *Infection and Immunity*, 66 (4):1783–1786, April 1998.

Fujita, M.; Yoko, T., and Jigami, Y. Inositol deacylation by Bst1p is required for the quality control of glycosylphosphatidylinositol-anchored proteins. *Molecular Biology of the Cell*, 17(2):834–850, February 2006.

Fujita, M. and Kinoshita, T. Structural remodeling of GPI anchors during biosynthesis and after attachment to proteins. *FEBS Lett*, 584(9):1670–1677, May 2010.

Gallis, H. A.; Drew, R. H., and Pickard, W. W. Amphotericin B – 30 years of clinical experience. *Rev Infect Dis*, 12(2):308–329, March 1990.

Galperin, M. Y. and Jedrzejas, M. J. Conserved core structure and active site residues in alkaline phosphatase superfamily enzymes. *Proteins*, 45(4):318–324, December 2001.

Gao, X. D.; Tachikawa, H.; Sato, T.; Jigami, Y., and Dean, N. Alg14 recruits alg13 to the cytoplasmic face of the endoplasmic reticulum to form a novel bipartite UDP-N-acetylglucosamine transferase required for the second step of N-linked glycosylation. *J Biol Chem*, 280(43):36254–36262, October 2005.

Gao, Y.; Wells, L.; Comer, F. I.; Parker, G. J., and Hart, G. W. Dynamic O-glycosylation of nuclear and cytosolic proteins: cloning and characterization of a neutral, cytosolic beta-N-acetylglucosaminidase from human brain. *J Biol Chem*, 276(13):9838–9845, March 2001.

Gastebois, A.; Clavaud, C.; Aimanianda, V., and Latgé, J.-P. *Aspergillus fumigatus*: cell wall polysaccharides, their biosynthesis and organization. *Future Microbiol*, 4(5):583–595, June 2009.

Gastinel, L. N.; Bignon, C.; Misra, A. K.; Hindsgaul, O.; Shaper, J. H., and Joziasse, D. H. Bovine alpha-1,3-galactosyltransferase catalytic domain structure and its relationship with ABO histo-blood group and glycosphingolipid glycosyltransferases. *EMBO J*, 20(4):638–649, February 2001.

Gaur, N. K. and Klotz, S. A. Expression, cloning, and characterization of a *Candida albicans* gene, ALA1, that confers adherence properties upon *Saccharomyces cerevisiae* for extracellular matrix proteins. *Infection and Immunity*, 65(12):5289–5294, December 1997.

Gaur, N. K.; Klotz, S. A., and Henderson, R. L. Overexpression of the *Candida albicans* ALA1 gene in *Saccharomyces cerevisiae* results in aggregation following attachment of yeast cells to extracellular matrix proteins, adherence properties similar to those of *Candida albicans*. *Infection and Immunity*, 67(11):6040–6047, November 1999.

Gaynor, E. C.; Mondesert, G.; Grimme, S. J.; Reed, S. I.; Orlean, P., and Emr, S. D. MCD4 encodes a conserved endoplasmic reticulum membrane protein essential for glycosylphosphatidylinositol anchor synthesis in yeast. *Molecular Biology of the Cell*, 10(3):627–648, March 1999.

Gerke, C.; Kraft, A.; Süssmuth, R.; Schweitzer, O., and Götz, F. Characterization of the N-acetylglucosaminyltransferase activity involved in the biosynthesis of the

Staphylococcus epidermidis polysaccharide intercellular adhesin. *J Biol Chem*, 273(29):18586–18593, July 1998.

Gibson, R. P.; Tarling, C. A.; Roberts, S.; Withers, S. G., and Davies, G. J. The donor subsite of trehalose-6-phosphate synthase - Binary complexes with UDP-glucose and UDP-2-deoxy-2-fluoro-glucose at 2 angstrom resolution. *J Biol Chem*, 279(3):1950–1955, January 2004.

Gietz, R. D. and Woods, R. A. Transformation of yeast by lithium acetate/single-stranded carrier DNA/polyethylene glycol method. *Meth Enzymol*, 350:87–96, 2002.

Gingras, A. R.; Girija, U. V.; Keeble, A. H.; Panchal, R.; Mitchell, D. A.; Moody, P. C. E., and Wallis, R. Structural basis of mannan-binding lectin recognition by its associated serine protease MASP-1: implications for complement activation. *Structure*, 19(11):1635–1643, November 2011.

Girrbach, V. and Strahl, S. Members of the evolutionarily conserved PMT family of protein O-mannosyltransferases form distinct protein complexes among themselves. *J Biol Chem*, 278(14):12554–12562, April 2003.

Girrbach, V.; Zeller, T.; Priesmeier, M., and Strahl-Bolsinger, S. Structure-function analysis of the dolichyl phosphate-mannose: Protein O-mannosyltransferase ScPmt1p. *J Biol Chem*, 275(25):19288–19296, June 2000.

Gloster, T. M. and Vocadlo, D. J. Developing inhibitors of glycan processing enzymes as tools for enabling glycobiology. *Nat. Chem. Biol.*, 8(8):683–694, August 2012.

Goldman, R. C.; Sullivan, P. A.; Zakula, D., and Capobianco, J. O. Kinetics of beta-1,3 glucan interaction at the donor and acceptor sites of the fungal glucosyltransferase encoded by the BGL2 gene. *Eur J Biochem*, 227(1-2):372–378, January 1995.

Gonzalez, M.; Lipke, P. N., and Ovalle, R. Chapter 15 GPI Proteins in Biogenesis and Structure of Yeast Cell Walls. pages 321–356. Elsevier, 2009.

Gonzalez Montoro, A.; Chumpen Ramirez, S.; Quiroga, R., and Valdez Taubas, J. Specificity of transmembrane protein palmitoylation in yeast. *PLoS ONE*, 6(2), February 2011.

Goossens, K. and Willaert, R. Flocculation protein structure and cell-cell adhesion mechanism in *Saccharomyces cerevisiae*. *Biotechnol Lett*, 32(11):1571–1585, November 2010.

Gosselin, S.; Alhussaini, M.; Streiff, M. B.; Takabayashi, K., and Palcic, M. M. A continuous spectrophotometric assay for glycosyltransferases. *Anal Biochem*, 220(1):92–97, July 1994.

Grabinska, K. A.; Magnelli, P., and Robbins, P. W. Prenylation of *Saccharomyces cerevisiae* Chs4p affects chitin synthase III activity and chitin chain length. *Eukaryotic Cell*, 6(2):328–336, February 2007.

Green, A. A. and Cori, G. T. Crystalline muscle phosphorylase I. Preparation, properties, and molecular weight. *J Biol Chem*, 1943.

Gregg, K. J.; Zandberg, W. F.; Hehemann, J.-H.; Whitworth, G. E.; Deng, L.; Vocadlo, D. J., and Boraston, A. B. Analysis of a new family of widely distributed metal-independent alpha-mannosidases provides unique insight into the processing of N-linked glycans. *J Biol Chem*, 286(17):15586–15596, April 2011.

Grimme, S. J.; Westfall, B. A.; Wiedman, J. M.; Taron, C. H., and Orlean, P. The essential Smp3 protein is required for addition of the side-branching fourth mannose during assembly of yeast glycosylphosphatidylinositols. *J Biol Chem*, 276 (29):27731–27739, July 2001.

Grimme, S. J.; Gao, X. D.; Martin, P. S.; Tu, K.; Tcheperegine, S. E.; Corrado, K.; Farewell, A. E.; Orlean, P., and Bi, E. F. Deficiencies in the endoplasmic reticulum (ER)-membrane protein Gab1p perturb transfer of glycosylphosphatidylinositol to proteins and cause perinuclear ER-associated actin bar formation. *Molecular Biology of the Cell*, 15(6):2758–2770, June 2004.

Haines, J. *Aspergillus* in compost: straw man or fatal flaw? *Biocycle*, 1995.

Hall, R. A.; Bates, S.; Lenardon, M. D.; MacCallum, D. M.; Wagener, J.; Lowman, D. W.; Kruppa, M. D.; Williams, D. L.; Odds, F. C.; Brown, A. J. P., and Gow, N. A. R. The Mnn2 Mannosyltransferase Family Modulates Mannoprotein Fibril Length, Immune Recognition and Virulence of *Candida albicans*. *PLoS Pathog*, 9(4):e1003276, April 2013.

Hamada, K.; Fukuchi, S.; Arisawa, M.; Baba, M., and Kitada, K. Screening for glycosylphosphatidylinositol (GPI)-dependent cell wall proteins in *Saccharomyces cerevisiae*. *Mol Gen Genet*, 258(1-2):53–59, April 1998a.

Hamada, K.; Terashima, H.; Arisawa, N., and Kitada, K. Amino acid sequence requirement for efficient incorporation of glycosylphosphatidylinositol-associated proteins into the cell wall of *Saccharomyces cerevisiae*. *J Biol Chem*, 273(41): 26946–26953, October 1998b.

Hamada, K.; Terashima, H.; Arisawa, M.; Yabuki, N., and Kitada, K. Amino acid residues in the omega-minus region participate in cellular localization of yeast glycosylphosphatidylinositol-attached proteins. *J Bacteriol*, 181(13):3886–3889, July 1999.

Hamburger, D.; Egerton, M., and Riezman, H. Yeast Gaa1p is required for attachment of a completed GPI anchor onto proteins. *J Cell Biol*, 129(3):629–639, May 1995.

Hartland, R. P.; Fontaine, T.; Debeaupuis, J. P.; Simenel, C.; Delepierre, M., and Latgé, J. P. A novel beta-(1-3)-glucanosyltransferase from the cell wall of *Aspergillus fumigatus*. *J Biol Chem*, 271(43):26843–26849, October 1996.

Harvey, C. and Longbottom, J. L. Characterization of a 2nd major antigen Ag-13 (Antigen-C) of *Aspergillus fumigatus* and investigation of its immunological reactivity. *Clin Exp Immunol*, 70(1):247–254, October 1987.

Hashimoto, H.; Sakakibara, A.; Yamasaki, M., and Yoda, K. *Saccharomyces cerevisiae* VIG9 encodes GDP-mannose pyrophosphorylase, which is essential for protein glycosylation. *J Biol Chem*, 272(26):16308–16314, June 1997.

Hashimoto, W.; Kobayashi, E.; Nankai, H.; Sato, N.; Miya, T.; Kawai, S., and Murata, K. Unsaturated glucuronyl hydrolase of *Bacillus sp*. GL1: novel enzyme prerequisite for metabolism of unsaturated oligosaccharides produced by polysaccharide lyases. *Arch Biochem Biophys*, 368(2):367–374, August 1999.

Häusler, A. and Robbins, P. W. Glycosylation in *Saccharomyces cerevisiae*: cloning and characterization of an alpha-1,2-mannosyltransferase structural gene. *Glycobiology*, 2(1):77–84, February 1992.

Häusler, A.; Ballou, L.; Ballou, C. E., and Robbins, P. W. Yeast glycoprotein biosynthesis: *MNT1* encodes an alpha-1,2-mannosyltransferase involved in O-glycosylation. *Proc Natl Acad Sci USA*, 89(15):6846–6850, August 1992.

Hearn, V. M.; Wilson, E. V., and Mackenzie, D. W. R. Analysis of *Aspergillus fumigatus* catalases possessing antigenic activity. *J Med Microbiol*, 36(1):61–67, January 1992.

Helenius, A. and Aebi, M. Roles of N-linked glycans in the endoplasmic reticulum. *Annu Rev Biochem*, 73:1019–1049, 2004.

Helenius, J.; Ng, D. T. W.; Marolda, C. L.; Walter, P.; Valvano, M. A., and Aebi, M. Translocation of lipid-linked oligosaccharides across the ER membrane requires Rft1 protein. *Nature*, 415(6870):447–450, January 2002.

Henrissat, B. A classification of glycosyl hydrolases based on amino acid sequence similarities. *Biochem J*, 280 (Pt 2):309–316, December 1991.

Henrissat, B. and Bairoch, A. New families in the classification of glycosyl hydrolases based on amino acid sequence similarities. *Biochem J*, 293 (Pt 3): 781–788, August 1993.

Henrissat, B. and Bairoch, A. Updating the sequence-based classification of glycosyl hydrolases. *Biochem J*, 316 (Pt 2):695–696, June 1996.

Henrissat, B.; Sulzenbacher, G., and Bourne, Y. Glycosyltransferases, glycoside hydrolases: surprise, surprise! *Curr Opin Struct Biol*, 18(5):527–533, October 2008.

Hernández, L. M.; Ballou, L.; Alvarado, E.; Gillece-Castro, B. L.; Burlingame, A. L., and Ballou, C. E. A new *Saccharomyces cerevisiae mnn* mutant N-linked oligosaccharide structure. *J Biol Chem*, 264(20):11849–11856, July 1989.

Herscovics, A. Processing glycosidases of *Saccharomyces cerevisiae*. *BBA - Gen Subjects*, 1426(2):275–285, January 1999.

Hese, K.; Otto, C.; Routier, F. H., and Lehle, L. The yeast oligosaccharyltransferase complex can be replaced by STT3 from *Leishmania major*. *Glycobiology*, 19(2): 160–171, February 2009.

Holm, L. and Rosenström, P. Dali server: conservation mapping in 3D. *Nucleic Acids Research*, 38(Web Server issue):W545–9, July 2010.

Holmes, A. R.; Wielen, P.van der ; Cannon, R. D.; Ruske, D., and Dawes, P. *Candida albicans* binds to saliva proteins selectively adsorbed to silicone. *Oral Surg Oral Med Oral Pathol Oral Radiol Endod*, 102(4):488–494, October 2006.

Holyoak, T.; Fenn, T. D.; Wilson, M. A.; Moulin, A. G.; Ringe, D., and Petsko, G. A. Malonate: a versatile cryoprotectant and stabilizing solution for salt-grown macromolecular crystals. *Acta Crystallogr. D Biol. Crystallogr.*, 59(Pt 12):2356–2358, December 2003.

Hong, Y. J.; Ohishi, K.; Kang, J. Y.; Tanaka, S.; Inoue, N.; Nishimura, J.; Maeda, Y., and Kinoshita, T. Human PIG-U and yeast Cdc91p are the fifth subunit of GPI transamidase that attaches GPI-anchors to proteins. *Molecular Biology of the Cell*, 14(5):1780–1789, May 2003.

Horsch, M.; Hoesch, L.; Vasella, A., and Rast, D. M. N-acetylglucosaminono-1,5-lactone oxime and the corresponding (phenylcarbamoyl)oxime. Novel and potent inhibitors of beta-N-acetylglucosaminidase. *Eur J Biochem*, 197(3):815–818, May 1991.

Hosoguchi, K.; Maeda, T.; Furukawa, J.-I.; Shinohara, Y.; Hinou, H.; Sekiguchi, M.; Togame, H.; Takemoto, H.; Kondo, H., and Nishimura, S.-I. An efficient approach to the discovery of potent inhibitors against glycosyltransferases. *J Med Chem*, 53(15):5607–5619, August 2010.

Hospenthal, D. R.; Kwon-Chung, K. J., and Bennett, J. E. Concentrations of airborne *Aspergillus* compared to the incidence of invasive aspergillosis: lack of correlation. *Med Mycol*, 36(3):165–168, June 1998.

Hu, Y. N. and Walker, S. Remarkable structural similarities between diverse glycosyltransferases. *Chem Biol*, 9(12):1287–1296, December 2002.

Hubbard, C.; McNamara, J. T.; Azumaya, C.; Patel, M. S., and Zimmer, J. The hyaluronan synthase catalyzes the synthesis and membrane translocation of hyaluronan. *J Mol Biol*, 418(1-2):21–31, April 2012.

Hube, B.; Turver, C. J.; Odds, F. C.; Eiffert, H.; Boulnois, G. J.; Köchel, H., and Ruchel, R. Sequence of the *Candida albicans* gene encoding the secretory aspartate proteinase. *J Med Vet Mycol*, 29(2):129–132, 1991.

Hughes, E. D.; Ingold, C. K., and Whitfield, I. C. The walden inversion in the replacement of hydroxyl by halogen. *Nature*, 1941.

Hurtado-Guerrero, R. and Aalten, D. M. F.van . Structure of *Saccharomyces cerevisiae* chitinase 1 and screening-based discovery of potent inhibitors. *Chem Biol*, 14(5):589–599, May 2007.

Hutzler, J.; Schmid, M.; Bernard, T.; Henrissat, B., and Strahl, S. Membrane association is a determinant for substrate recognition by PMT4 protein O-mannosyltransferases. *Proc Natl Acad Sci USA*, 104(19):7827–7832, May 2007.

Imai, T.; Watanabe, T.; Yui, T., and Sugiyama, J. The directionality of chitin biosynthesis: a revisit. *Biochem J*, 374:755–760, September 2003.

Inoue, S. B.; Takewaki, N.; Takasuka, T.; Mio, T.; Adachi, M.; Fujii, Y.; Miyamoto, C.; Arisawa, M.; Furuichi, Y., and Watanabe, T. Characterization and gene cloning of 1,3-beta-D-glucan synthase from *Saccharomyces cerevisiae*. *Eur J Biochem*, 231(3):845–854, August 1995.

Itoh, T.; Mikami, B.; Maru, I.; Ohta, Y.; Hashimoto, W., and Murata, K. Crystal structure of N-acyl-D-glucosamine 2-epimerase from porcine kidney at 2.0 A resolution. *J Mol Biol*, 303(5):733–744, November 2000.

Itoh, T.; Akao, S.; Hashimoto, W.; Mikami, B., and Murata, K. Crystal structure of unsaturated glucuronyl hydrolase, responsible for the degradation of glycosaminoglycan, from *Bacillus sp*. GL1 at 1.8 A resolution. *J Biol Chem*, 279 (30):31804–31812, July 2004.

Itoh, T.; Hashimoto, W.; Mikami, B., and Murata, K. Crystal structure of unsaturated glucuronyl hydrolase complexed with substrate: molecular insights into its catalytic reaction mechanism. *J Biol Chem*, 281(40):29807–29816, October 2006.

Itoh, Y.; Rice, J. D.; Goller, C.; Pannuri, A.; Taylor, J.; Meisner, J.; Beveridge, T. J.; Preston, J. F. I., and Romeo, T. Roles of pgaABCD genes in synthesis, modification, and export of the *Escherichia coli* biofilm adhesin poly-beta-1,6-N-acetyl-D-glucosamine. *J Bacteriol*, 190(10):3670–3680, May 2008.

Jackson, P. The use of polyacrylamide-gel electrophoresis for the high-resolution separation of reducing saccharides labelled with the fluorophore 8-aminonaphthalene-1,3,6-trisulphonic acid. Detection of picomolar quantities by an imaging system based on a cooled charge-coupled device. *Biochem J*, 270 (3):705–713, September 1990.

Jakob, C. A.; Burda, P.; Roth, J., and Aebi, M. Degradation of misfolded endoplasmic reticulum glycoproteins in *Saccharomyces cerevisiae* is determined by a specific oligosaccharide structure. *J Cell Biol*, 142(5):1223–1233, September 1998.

Jamaluddin, H.; Tumbale, P.; Withers, S. G.; Acharya, K. R., and Brew, K. Conformational changes induced by binding UDP-2F-galactose to alpha-1,3-galactosyltransferase - Implications for catalysis. *J Mol Biol*, 369(5):1270–1281, June 2007.

Jaques, A. K.; Fukamizo, T.; Hall, D.; Barton, R. C.; Escott, G. M.; Parkinson, T.; Hitchcock, C. A., and Adams, D. J. Disruption of the gene encoding the ChiB1 chitinase of *Aspergillus fumigatus* and characterization of a recombinant gene product. *Microbiology*, 149:2931–2939, October 2003.

Jigami, Y. and Odani, T. Mannosylphosphate transfer to yeast mannan. *BBA - Gen Subjects*, 1426(2):335–345, January 1999.

Jigami, Y. Yeast glycobiology and its application. *Biosci Biotechnol Biochem*, 72 (3):637–648, 2008.

Jimenez, C.; Sacristan, C.; Roncero, M. I. G., and Roncero, C. Amino acid divergence between the CHS domain contributes to the different intracellular behaviour of Family II fungal chitin synthases in *Saccharomyces cerevisiae*. *Fungal Genet Biol*, 47(12):1034–1043, December 2010.

Johnson, L. B. and Kauffman, C. A. Voriconazole: a new triazole antifungal agent. *Clin Infect Dis*, 36(5):630–637, March 2003.

Jungmann, J. and Munro, S. Multi-protein complexes in the cis Golgi of *Saccharomyces cerevisiae* with alpha-1,6-mannosyltransferase activity. *EMBO J*, 17(2): 423–434, January 1998.

Jungmann, J.; Rayner, J. C., and Munro, S. The *Saccharomyces cerevisiae* protein Mnn10p/Bed1p is a subunit of a Golgi mannosyltransferase complex. *J Biol Chem*, 274(10):6579–6585, March 1999.

Kaempf, M.; Absmanner, B.; Schwarz, M., and Lehle, L. Biochemical characterization and membrane topology of Alg2 from *Saccharomyces cerevisiae* as a bifunctional alpha-1,3- and 1,6-mannosyltransferase involved in lipid-linked oligosaccharide biosynthesis. *J Biol Chem*, 284(18):11900–11912, May 2009.

Kajiwara, K.; Watanabe, R.; Pichler, H.; Ihara, K.; Murakami, S.; Riezman, H., and Funato, K. Yeast ARV1 is required for efficient delivery of an early GPI intermediate to the first mannosyltransferase during GPI assembly and controls lipid flow from the endoplasmic reticulum. *Molecular Biology of the Cell*, 19(5): 2069–2082, May 2008.

Kakuda, S.; Shiba, T.; Ishiguro, M.; Tagawa, H.; Oka, S.; Kajihara, Y.; Kawasaki, T.; Wakatsuki, S., and Kato, R. Structural basis for acceptor substrate recognition of a human glucuronyltransferase, GlcAT-P, an enzyme critical in the biosynthesis of the carbohydrate epitope HNK-1. *J Biol Chem*, 279(21):22693–22703, May 2004.

Källberg, M.; Wang, H.; Wang, S.; Peng, J.; Wang, Z.; Lu, H., and Xu, J. Template-based protein structure modeling using the RaptorX web server. *Nat Protoc*, 7 (8):1511–1522, August 2012.

Kamst, E.; Bakkers, J.; Quaedvlieg, N. E. M.; Pilling, J.; Kijne, J. W.; Lugtenberg, B. J. J., and Spaink, H. P. Chitin oligosaccharide synthesis by rhizobia and zebrafish embryos starts by glycosyl transfer to O4 of the reducing-terminal residue. *Biochemistry*, 38(13):4045–4052, March 1999.

Kanbe, T. and Cutler, J. E. Minimum chemical requirements for adhesin activity of the acid-stable part of *Candida albicans* cell wall phosphomannoprotein complex. *Infection and Immunity*, 66(12):5812–5818, December 1998.

Kanbe, T.; Han, Y.; Redgrave, B.; Riesselman, M. H., and Cutler, J. E. Evidence that mannans of *Candida albicans* are responsible for adherence of yeast forms to spleen and lymph node tissue. *Infection and Immunity*, 61(6):2578–2584, June 1993.

Kang, J. Y.; Hong, Y. J.; Ashida, H.; Shishioh, N.; Murakami, Y.; Morita, Y. S.; Maeda, Y., and Kinoshita, T. PIG-V involved in transferring the second mannose in glycosylphosphatidylinositol. *J Biol Chem*, 280(10):9489–9497, March 2005.

Kang, M. S. and Cabib, E. Regulation of fungal cell wall growth: a guanine nucleotide-binding, proteinaceous component required for activity of (1-3)-beta-D-glucan synthase. *Proc Natl Acad Sci USA*, 83(16):5808–5812, August 1986.

Karaoglu, D.; Kelleher, D. J., and Gilmore, R. The highly conserved Stt3 protein is a subunit of the yeast oligosaccharyltransferase and forms a subcomplex with Ost3p and Ost4p. *J Biol Chem*, 272(51):32513–32520, December 1997.

Kelleher, D. J. and Gilmore, R. An evolving view of the eukaryotic oligosaccharyltransferase. *Glycobiology*, 16(4):47R–62R, April 2006.

Kelleher, D. J.; Banerjee, S.; Cura, A. J.; Samuelson, J., and Gilmore, R. Dolichol-linked oligosaccharide selection by the oligosaccharyltransferase in protist and fungal organisms. *J Cell Biol*, 177(1):29–37, April 2007.

Kim, H.; Yan, Q.; Heijne, G.von ; Caputo, G. A., and Lennarz, W. J. Determination of the membrane topology of Ost4p and its subunit interactions in the oligosaccharyl-transferase complex in *Saccharomyces cerevisiae*. *Proc Natl Acad Sci USA*, 100(13):7460–7464, June 2003.

Kitagaki, H.; Wu, H.; Shimoi, H., and Ito, K. Two homologous genes, DCW1 (YKL046c) and DFG5, are essential for cell growth and encode glycosylphosphatidylinositol (GPI)-anchored membrane proteins required for cell wall biogenesis in *Saccharomyces cerevisiae*. *Mol Microbiol*, 46(4):1011–1022, November 2002.

Kitagaki, H.; Ito, K., and Shimoi, H. A temperature-sensitive *dcw1* mutant of *Saccharomyces cerevisiae* is cell cycle arrested with small buds which have aberrant cell walls. *Eukaryotic Cell*, 3(5):1297–1306, October 2004.

Klebl, F. and Tanner, W. Molecular cloning of a cell wall exo-beta-1,3-glucanase from *Saccharomyces cerevisiae*. *J Bacteriol*, 171(11):6259–6264, November 1989.

Klinger, M. M.; Laine, R. A., and Steiner, S. M. Characterization of novel amino acid fucosides. *J Biol Chem*, 256(15):7932–7935, August 1981.

Klis, F. M.; Boorsma, A., and Groot, P. W. J.de . Cell wall construction in *Saccharomyces cerevisiae*. *Yeast*, 23(3):185–202, February 2006.

Klis, F. M.; Brul, S., and Groot, P. W. J.de . Covalently linked wall proteins in ascomycetous fungi. *Yeast*, 27(8):489–493, August 2010.

Knauer, R. and Lehle, L. The oligosaccharyltransferase complex from *Saccharomyces cerevisiae* - Isolation of the OST6 gene, its synthetic interaction with OST3, and analysis of the native complex. *J Biol Chem*, 274(24):17249–17256, June 1999.

Kobayashi, H.; Debeaupuis, J. P.; Bouchara, J. P., and Latgé, J. P. An 88 kilodalton antigen secreted by *Aspergillus fumigatus*. *Infection and Immunity*, 61(11):4767–4771, November 1993.

Kojima, H.; Hashimoto, H., and Yoda, K. Interaction among the subunits of Golgi membrane mannosyltransferase complexes of the yeast *Saccharomyces cerevisiae*. *Biosci Biotechnol Biochem*, 63(11):1970–1976, November 1999.

Kollár, R.; Reinhold, B. B.; Petráková, E.; Yeh, H. J. C.; Ashwell, G.; Drgonová, J.; Kapteyn, J. C.; Klis, F. M., and Cabib, E. Architecture of the yeast cell wall. Beta-(1-6)-glucan interconnects mannoprotein, beta-(1->)3-glucan, and chitin. *J Biol Chem*, 272(28):17762–17775, July 1997.

Kornberg, S. R.; Zimmerman, S. B., and Kornberg, A. Glucosylation of deoxyribonucleic acid by enzymes from bacteriophage-infected *Escherichia coli*. *J Biol Chem*, 236:1487–1493, May 1961.

Koshland, D. E. Stereochemistry and the mechanism of enzymatic reactions. *Biol Rev*, 1953.

Kreppel, L. K.; Blomberg, M. A., and Hart, G. W. Dynamic glycosylation of nuclear and cytosolic proteins. Cloning and characterization of a unique O-GlcNAc transferase with multiple tetratricopeptide repeats. *J Biol Chem*, 272(14):9308–9315, April 1997.

Krogh, A.; Larsson, B.; Heijne, G.von , and Sonnhammer, E. L. Predicting transmembrane protein topology with a hidden Markov model: application to complete genomes. *J Mol Biol*, 305(3):567–580, January 2001.

Krogh-Madsen, M.; Arendrup, M. C.; Heslet, L., and Knudsen, J. D. Amphotericin B and caspofungin resistance in *Candida glabrata* isolates recovered from a critically ill patient. *Clin Infect Dis*, 42(7):938–944, April 2006.

Kuranda, M. J. and Robbins, P. W. Chitinase is required for cell separation during growth of *Saccharomyces cerevisiae*. *J Biol Chem*, 266(29):19758–19767, October 1991.

Kurtz, M. B.; Heath, I. B.; Marrinan, J.; Dreikorn, S.; Onishi, J., and Douglas, C. Morphological effects of lipopeptides against *Aspergillus fumigatus* correlate with activities against (1,3)-beta-D-glucan synthase. *Antimicrob Agents Chemother*, 38(7):1480–1489, July 1994.

Laemmli, U. K. Cleavage of structural proteins during the assembly of the head of bacteriophage T4. *Nature*, 227(5259):680–685, August 1970.

Laine, R. A. A calculation of all possible oligosaccharide isomers both branched and linear yields 1.05 x 10(12) structures for a reducing hexasaccharide: the Isomer Barrier to development of single-method saccharide sequencing or synthesis systems. *Glycobiology*, 4(6):759–767, December 1994.

Lairson, L. L.; Henrissat, B.; Davies, G. J., and Withers, S. G. Glycosyltransferases: structures, functions, and mechanisms. *Annu Rev Biochem*, 77:521–555, 2008.

Lairson, L. L.; Chiu, C. P. C.; Ly, H. D.; He, S.; Wakarchuk, W. W.; Strynadka, N. C. J., and Withers, S. G. Intermediate trapping on a mutant retaining alpha-galactosyltransferase identifies an unexpected aspartate residue. *J Biol Chem*, 279(27):28339–28344, July 2004.

Lam, K. K. Y.; Davey, M.; Sun, B.; Roth, A. F.; Davis, N. G., and Conibear, E. Palmitoylation by the DHHC protein Pfa4 regulates the ER exit of Chs3. *J Cell Biol*, 174(1):19–25, July 2006.

Lamy, B. and Davies, J. Isolation and nucleotide sequence of the *Aspergillus restrictus* gene coding for the ribonucleolytic toxin restrictocin and its expression in *Aspergillus nidulans* – the leader sequence protects producing strains from suicide. *Nucleic Acids Research*, 19(5):1001–1006, March 1991.

Lamy, B.; Moutaouakil, M.; Latgé, J. P., and Davies, J. Secretion of a potential virulence factor, a fungal ribonucleotoxin, during human aspergillosis infections. *Mol Microbiol*, 5(7):1811–1815, July 1991.

Lariviere, L. and Morera, S. A base-flipping mechanism for the T4 phage beta-glucosyltransferase and identification of a transition-state analog. *J Mol Biol*, 324(3):483–490, November 2002.

Lariviere, L.; Gueguen-Chaignon, V., and Morera, S. Crystal structures of the T4 phage beta-glucosyltransferase and the D100A mutant in complex with UDP-glucose: Glucose binding and identification of the catalytic base for a direct displacement mechanism. *J Mol Biol*, 330(5):1077–1086, July 2003.

Larkin, A. and Imperiali, B. The expanding horizons of asparagine-linked glycosylation. *Biochemistry*, 50(21):4411–4426, May 2011.

Larriba, G.; Andaluz, E.; Cueva, R., and Basco, R. D. Molecular biology of yeast exoglucanases. *FEMS Microbiol Lett*, 125(2-3):121–126, January 1995.

Latgé, J. and Calderone, R. The fungal cell wall. *Growth*, 2006.

Latgé, J. P. *Aspergillus fumigatus* and aspergillosis. *Clin Microbiol Rev*, 12(2): 310–350, April 1999.

Latgé, J. P.; Moutaouakil, M.; Debeaupuis, J. P.; Bouchara, J. P.; Haynes, K., and Prévost, M. C. The 18 kilodalton antigen secreted by *Aspergillus fumigatus*. *Infection and Immunity*, 59(8):2586–2594, August 1991.

Latgé, J. P.; Kobayashi, H.; Debeaupuis, J. P.; Diaquin, M.; Sarfati, J.; Wieruszeski, J. M.; Parra, E.; Bouchara, J. P., and Fournet, B. Chemical and immunological characterization of the extracellular galactomannan of *Aspergillus fumigatus*. *Infection and Immunity*, 62(12):5424–5433, December 1994.

Lazarus, M. B.; Jiang, J.; Gloster, T. M.; Zandberg, W. F.; Whitworth, G. E.; Vocadlo, D. J., and Walker, S. Structural snapshots of the reaction coordinate for O-GlcNAc transferase. *Nat. Chem. Biol.*, 8(12):966–968, December 2012.

Lee, S. S.; Hong, S. Y.; Errey, J. C.; Izumi, A.; Davies, G. J., and Davis, B. G. Mechanistic evidence for a front-side, S(N)i-type reaction in a retaining glycosyltransferase. *Nat. Chem. Biol.*, 7(9):631–638, September 2011.

Leeson, P. D. and Springthorpe, B. The influence of drug-like concepts on decision-making in medicinal chemistry. *Nat Rev Drug Discov*, 6(11):881–890, November 2007.

Lefebvre, T.; Ferreira, S.; Dupont-Wallois, L.; Bussière, T.; Dupire, M.-J.; Delacourte, A.; Michalski, J.-C., and Caillet-Boudin, M.-L. Evidence of a balance between phosphorylation and O-GlcNAc glycosylation of Tau proteins–a role in nuclear localization. *Biochim Biophys Acta*, 1619(2):167–176, January 2003.

Lehle, L.; Strahl, S., and Tanner, W. Protein glycosylation, conserved from yeast to man: A model organism helps elucidate congenital human diseases. *Angew Chem Int Ed Engl*, 45(41):6802–6818, 2006.

Leidich, S. D. and Orlean, P. Gpi1, a *Saccharomyces cerevisiae* protein that participates in the first step in glycosylphosphatidylinositol anchor synthesis. *J Biol Chem*, 271(44):27829–27837, November 1996.

Leidich, S. D.; Kostova, Z.; Latek, R. R.; Costello, L. C.; Drapp, D. A.; Gray, W.; Fassler, J. S., and Orlean, P. Temperature-sensitive yeast GPI anchoring mutants *gpi2* and *gpi3* are defective in the synthesis of N-acetylglucosaminyl phosphatidylinositol – cloning of the *gp12* gene. *J Biol Chem*, 270(22):13029–13035, June 1995.

Lennarz, W. J. Studies on oligosaccharyl transferase in yeast. *Acta Biochim Pol*, 54(4):673–677, 2007.

Lesage, G. and Bussey, H. Cell wall assembly in *Saccharomyces cerevisiae*. *Microbiology and Molecular Biology Reviews*, 70(2):317–343, June 2006.

Levin, D. E. Regulation of cell wall biogenesis in *Saccharomyces cerevisiae*: the cell wall integrity signaling pathway. *Genetics*, 189(4):1145–1175, December 2011.

Lewis, E. S. and Boozer, C. E. The kinetics and stereochemistry of the decomposition of secondary alkyl chlorosulfites. *J Am Chem Soc*, 1952.

Lewis, M. S. and Ballou, C. E. Separation and characterization of 2 alpha-1,2-mannosyltransferase activities from *Saccharomyces cerevisiae*. *J Biol Chem*, 266(13):8255–8261, May 1991.

Li, G. T.; Yan, Q.; Oen, H. O., and Lennarz, W. J. A specific segment of the transmembrane domain of Wbp1p is essential for its incorporation into the oligosaccharyl transferase complex. *Biochemistry*, 42(37):11032–11039, September 2003.

Li, G.; Yan, Q.; Nita-Lazar, A.; Haltiwanger, R. S., and Lennarz, W. J. Studies on the N-glycosylation of the subunits of oligosaccharyl transferase in *Saccharomyces cerevisiae*. *J Biol Chem*, 280(3):1864–1871, January 2005.

Lira-Navarrete, E.; Valero-González, J.; Villanueva, R.; Martínez-Júlvez, M.; Tejero, T.; Merino, P.; Panjikar, S., and Hurtado-Guerrero, R. Structural insights into the mechanism of protein O-fucosylation. *PLoS ONE*, 6(9):e25365, 2011.

Liu, J. and Mushegian, A. Three monophyletic superfamilies account for the majority of the known glycosyltransferases. *Protein Sci*, 12(7):1418–1431, July 2003.

Liu, K.; Paterson, A. J.; Zhang, F.; McAndrew, J.; Fukuchi, K.-I.; Wyss, J. M.; Peng, L.; Hu, Y., and Kudlow, J. E. Accumulation of protein O-GlcNAc modification inhibits proteasomes in the brain and coincides with neuronal apoptosis in brain areas with high O-GlcNAc metabolism. *J Neurochem*, 89(4):1044–1055, May 2004.

Liu, Q. P.; Sulzenbacher, G.; Yuan, H.; Bennett, E. P.; Pietz, G.; Saunders, K.; Spence, J.; Nudelman, E.; Levery, S. B.; White, T.; Neveu, J. M.; Lane, W. S.; Bourne, Y.; Olsson, M. L.; Henrissat, B., and Clausen, H. Bacterial glycosidases for the production of universal red blood cells. *Nat Biotechnol*, 25(4):454–464, April 2007.

Livanova, N. B.; Chebotareva, N. A.; Eronina, T. B., and Kurganov, B. I. Pyridoxal 5'-phosphate as a catalytic and conformational cofactor of muscle glycogen phosphorylase B. *Biochemistry Mosc*, 67(10):1089–1098, October 2002.

Lizak, C.; Gerber, S.; Numao, S.; Aebi, M., and Locher, K. P. X-ray structure of a bacterial oligosaccharyltransferase. *Nature*, 474(7351):350–355, June 2011.

Lobsanov, Y. D.; Romero, P. A.; Sleno, B.; Yu, B.; Yip, P.; Herscovics, A., and Howell, P. L. Structure of Kre2p/Mnt1p - A yeast alpha-1,2-mannosyltransferase involved in mannoprotein biosynthesis. *J Biol Chem*, 279(17):17921–17931, April 2004.

Lommel, M. and Strahl, S. Protein O-mannosylation: Conserved from bacteria to humans. *Glycobiology*, 19(8):816–828, August 2009.

Lommel, M.; Schott, A.; Jank, T.; Hofmann, V., and Strahl, S. A conserved acidic motif is crucial for enzymatic activity of protein O-mannosyltransferases. *J Biol Chem*, 286(46):39768–39775, November 2011.

Lopezmedrano, R.; Ovejero, M. C.; Calera, J. A.; Puente, P., and Leal, F. An immunodominant 90 kilodalton *Aspergillus fumigatus* antigen is the subunit of a catalase. *Infection and Immunity*, 63(12):4774–4780, December 1995.

Lussier, M.; Sdicu, A. M.; Camirand, A., and Bussey, H. Functional characterization of the *YUR1*, *KTR1*, and *KTR2* genes as members of the yeast *KRE2*/*MNT1* mannosyltransferase gene family. *J Biol Chem*, 271(18):11001–11008, May 1996.

Lussier, M.; Sdicu, A. M.; Bussereau, F.; Jacquet, M., and Bussey, H. The Ktr1p, Ktr3p, and Kre2p/Mnt1p mannosyltransferases participate in the elaboration of yeast O- and N-linked carbohydrate chains. *J Biol Chem*, 272(24):15527–15531, June 1997.

Lussier, M.; Sdicu, A. M., and Bussey, H. The *KTR* and *MNN1* mannosyltransferase families of *Saccharomyces cerevisiae*. *Biochim Biophys Acta*, 1426(2): 323–334, January 1999.

Macauley, M. S.; Whitworth, G. E.; Debowski, A. W.; Chin, D., and Vocadlo, D. J. O-GlcNAcase uses substrate-assisted catalysis - Kinetic analysis and development of highly selective mechanism-inspired inhibitors. *J Biol Chem*, 280(27):25313–25322, July 2005.

Madan, T.; Eggleton, P.; Kishore, U.; Strong, P.; Aggrawal, S. S.; Sarma, P. U., and Reid, K. B. M. Binding of pulmonary surfactant proteins A and D to *Aspergillus fumigatus* conidia enhances phagocytosis and killing by human neutrophils and alveolar macrophages. *Infection and Immunity*, 65(8):3171–3179, August 1997.

Maddi, A.; Fu, C., and Free, S. J. The *Neurospora crassa* dfg5 and dcw1 genes encode alpha-1,6-mannanases that function in the incorporation of glycoproteins into the cell wall. *PLoS ONE*, 7(6):e38872, June 2012.

Mader, M. M. and Bartlett, P. A. Binding energy and catalysis: The implications for transition-state analogs and catalytic antibodies. *Chem Rev*, 97(5):1281–1302, August 1997.

Maeda, Y.; Watanabe, R.; Harris, C. L.; Hong, J. J.; Ohishi, K.; Kinoshita, K., and Kinoshita, T. PIG-M transfers the first mannose to glycosylphosphatidylinositol on the lumenal side of the ER. *EMBO J*, 20(1-2):250–261, January 2001.

Magnelli, P.; Cipollo, J. F., and Abeijon, C. A refined method for the determination of *Saccharomyces cerevisiae* cell wall composition and beta-1,6-glucan fine structure. *Anal Biochem*, 301(1):136–150, February 2002.

Mark, B. L. and James, M. N. G. Anchimeric assistance in hexosaminidases. *Can J Chem*, 80(8):1064–1074, August 2002.

Martins, L. O.; Empadinhas, N.; Marugg, J. D.; Miguel, C.; Ferreira, C.; Costa, M. S.da , and Santos, H. Biosynthesis of mannosylglycerate in the thermophilic bacterium *Rhodothermus marinus*. Biochemical and genetic characterization of a mannosylglycerate synthase. *J Biol Chem*, 274(50):35407–35414, December 1999.

Maruyama, Y. and Nakajima, T. The aman6 gene encoding a yeast mannan backbone degrading 1,6-alpha-D-mannanase in *Bacillus circulans*: cloning, sequence analysis, and expression. *Biosci Biotechnol Biochem*, 64(9):2018–2020, September 2000.

Matuo, R.; Sousa, F. G.; Soares, D. G.; Bonatto, D.; Saffi, J.; Escargueil, A. E.; Larsen, A. K., and Henriques, J. A. P. *Saccharomyces cerevisiae* as a model system to study the response to anticancer agents. *Cancer Chemother. Pharmacol.*, 70(4):491–502, October 2012.

Mazáň, M.; Ragni, E.; Popolo, L., and Farkaš, V. Catalytic properties of the Gas family beta-(1,3)-glucanosyltransferases active in fungal cell-wall biogenesis as

determined by a novel fluorescent assay. *Biochem J*, 438(2):275–282, September 2011.

Mazur, P. and Baginsky, W. In vitro activity of 1,3-beta-D-glucan synthase requires the GTP-binding protein Rho1. *J Biol Chem*, 271(24):14604–14609, June 1996.

Mazur, P.; Morin, N.; Baginsky, W.; Sherbeini, M.el ; Clemas, J. A.; Nielsen, J. B., and Foor, F. Differential expression and function of two homologous subunits of yeast 1,3-beta-D-glucan synthase. *Mol Cell Biol*, 15(10):5671–5681, October 1995.

McCarter, J. D. and Withers, S. G. Mechanisms of enzymatic glycoside hydrolysis. *Curr Opin Struct Biol*, 4(6):885–892, December 1994.

McCoy, A. J.; Grosse-Kunstleve, R. W.; Adams, P. D.; Winn, M. D.; Storoni, L. C., and Read, R. J. Phaser crystallographic software. *J Appl Crystallogr*, 40(Pt 4): 658–674, August 2007.

McNeil, M. M.; Nash, S. L.; Hajjeh, R. A.; Phelan, M. A.; Conn, L. A.; Plikaytis, B. D., and Warnock, D. W. Trends in mortality due to invasive mycotic diseases in the United States, 1980-1997. *Clin Infect Dis*, 33(5):641–647, September 2001.

Mehrotra, R. S. and Aneja, K. R. *An introduction to mycology*. New Age International Publishers, 1990.

Mellado, E.; Aufauvre-Brown, A.; Gow, N., and Holden, D. W. The *Aspergillus fumigatus* chsC and chsG genes encode class III chitin synthases with different functions. *Mol Microbiol*, 20(3):667–679, May 1996a.

Mellado, E.; Specht, C. A.; Robbins, P. W., and Holden, D. W. Cloning and characterization of chsD, a chitin synthase-like gene of *Aspergillus fumigatus*. *FEMS Microbiol Lett*, 143(1):69–76, September 1996b.

Mellado, E.; Dubreucq, G.; Mol, P.; Sarfati, J.; Paris, S.; Diaquin, M.; Holden, D. W.; Rodriguez-Tudela, J. L., and Latgé, J. P. Cell wall biogenesis in a double chitin synthase mutant (chsG(-)/chsE(-)) of *Aspergillus fumigatus*. *Fungal Genet Biol*, 38(1):98–109, February 2003.

Merzendorfer, H. The cellular basis of chitin synthesis in fungi and insects: Common principles and differences. *European Journal of Cell Biology*, 90(9):759–769, September 2011.

Mischnick, P. and Deruiter, G. A. Application of reductive cleavage in the structural investigation of the antigenic polysaccharides of *Aspergillus fumigatus* and *Penicillium digitatum* with respect to the determination of the ring size of the galactose moieties. *Carbohydr Polymers*, 23(1):5–12, 1994.

Mitchell, E. P.; Withers, S. G.; Ermert, P.; Vasella, A. T.; Garman, E. F.; Oikonomakos, N. G., and Johnson, L. N. Ternary complex crystal structures of glycogen phosphorylase with the transition state analogue nojirimycin tetrazole and phosphate in the T and R states. *Biochemistry*, 35(23):7341–7355, June 1996.

Miyakawa, Y.; Kuribayashi, T.; Kagaya, K.; Suzuki, M.; Nakase, T., and Fukazawa, Y. Role of specific determinants in mannan of *Candida albicans* serotype A in adherence to human buccal epithelial cells. *Infection and Immunity*, 60(6):2493–2499, June 1992.

Monegal, A. and Planas, A. Chemical rescue of alpha 3-galactosyltransferase. Implications in the mechanism of retaining glycosyltransferases. *J Am Chem Soc*, 128(50):16030–16031, December 2006.

Monteiro, M. A.; Slavic, D.; St Michael, F.; Brisson, J. R.; MacInnes, J. I., and Perry, M. B. The first description of a (1-6)-beta-D-glucan in prokaryotes: (1-6)-beta-D-glucan is a common component of *Actinobacillus suis* and is the basis for a serotyping system. *Carbohydr Res*, 329(1):121–130, October 2000.

Moore, R. T. Taxonomic proposals for the classification of marine yeasts and other yeast-like fungi including the smuts. *Bot Mar*, 23:361–373, 1980.

Morgan, J. L. W.; Strumillo, J., and Zimmer, J. Crystallographic snapshot of cellulose synthesis and membrane translocation. *Nature*, 493(7431):181–186, January 2013.

Moukadiri, I.; Jaafar, L., and Zueco, J. Identification of two mannoproteins released from cell walls of a *Saccharomyces cerevisiae mnn1 mnn9* double mutant by reducing agents. *J Bacteriol*, 181(16):4741–4745, August 1999.

Moukadiri, I. and Zueco, J. Evidence for the attachment of Hsp150/Pir2 to the cell wall of *Saccharomyces cerevisiae* through disulfide bridges. *FEMS Yeast Research*, 1(3):241–245, December 2001.

Mouyna, I.; Fontaine, T.; Vai, M.; Monod, M.; Fonzi, W. A.; Diaquin, M.; Popolo, L.; Hartland, R. P., and Latgé, J. P. Glycosylphosphatidylinositol-anchored glucanosyltransferases play an active role in the biosynthesis of the fungal cell wall. *J Biol Chem*, 275(20):14882–14889, May 2000a.

Mouyna, I.; Monod, M.; Fontaine, T.; Henrissat, B.; Léchenne, B., and Latgé, J. P. Identification of the catalytic residues of the first family of beta(1-3)glucanosyltransferases identified in fungi. *Biochem J*, 347 Pt 3:741–747, May 2000b.

Mouyna, I.; Sarfati, J.; Recco, P.; Fontaine, T.; Henrissatz, B., and Latgé, J. P. Molecular characterization of a cell wall-associated beta(1-3)endoglucanase of *Aspergillus fumigatus*. *Med Mycol*, 40(5):455–464, October 2002.

Mouyna, I.; Morelle, W.; Vai, M.; Monod, M.; Léchenne, B.; Fontaine, T.; Beauvais, A.; Sarfati, J.; Prevost, M. C.; Henry, C., and Latgé, J.-P. Deletion of GEL2 encoding for a beta(1-3)glucanosyltransferase affects morphogenesis and virulence in *Aspergillus fumigatus*. *Mol Microbiol*, 56(6):1675–1688, June 2005.

Mrsa, V.; Klebl, F., and Tanner, W. Purification and characterization of the *Saccharomyces cerevisiae* BGL2 gene product, a cell wall endo-beta-1,3-glucanase. *J Bacteriol*, 175(7):2102–2106, April 1993.

Mrsa, V.; Seidl, T.; Gentzsch, M., and Tanner, W. Specific labelling of cell wall proteins by biotinylation. Identification of four covalently linked O-mannosylated proteins of *Saccharomyces cerevisiae*. *Yeast*, 13(12):1145–1154, September 1997.

Mulichak, A. M.; Losey, H. C.; Walsh, C. T., and Garavito, R. M. Structure of the UDP-Glucosyltransferase GtfB that modifies the heptapeptide aglycone in the biosynthesis of vancomycin group antibiotics. *Structure/Folding and Design*, 9 (7):547–557, July 2001.

Mulichak, A. M.; Losey, H. C.; Lu, W.; Wawrzak, Z.; Walsh, C. T., and Garavito, R. M. Structure of the TDP-epi-vancosaminyltransferase GtfA from the chloroeremomycin biosynthetic pathway. *Proc Natl Acad Sci USA*, 100(16):9238–9243, August 2003.

Mulichak, A. M.; Lu, W.; Losey, H. C.; Walsh, C. T., and Garavito, R. M. Crystal structure of vancosaminyltransferase GtfD from the vancomycin biosynthetic pathway: Interactions with acceptor and nucleotide ligands. *Biochemistry*, 43 (18):5170–5180, May 2004.

Munro, C. A. and Gow, N. Chitin synthesis in human pathogenic fungi. *Med Mycol*, 39:41–53, 2001.

Murshudov, G. N.; Vagin, A. A., and Dodson, E. J. Refinement of macromolecular structures by the maximum-likelihood method. *Acta Crystallogr. D Biol. Crystallogr.*, 53(Pt 3):240–255, May 1997.

Murzin, A. G.; Brenner, S. E.; Hubbard, T., and Chothia, C. SCOP: a structural classification of proteins database for the investigation of sequences and structures. *J Mol Biol*, 247(4):536–540, April 1995.

Nagahashi, S.; Sudoh, M.; Ono, N.; Sawada, R.; Yamaguchi, E.; Uchida, Y.; Mio, T.; Takagi, M.; Arisawa, M., and Yamadaokabe, H. Characterization of chitin synthase-2 of *Saccharomyces cerevisiae* - implication of 2 highly conserved domains as possible catalytic sites. *J Biol Chem*, 270(23):13961–13967, June 1995.

Nakajima, T.; Maitra, S. K., and Ballou, C. E. An endo-alpha-1-6-D-mannanase from a soil bacterium. Purification, properties, and mode of action. *J Biol Chem*, 251(1):174–181, January 1976.

Nakayama, K.; NakanishiShindo, Y.; Tanaka, A.; HagaToda, Y., and Jigami, Y. Substrate specificity of alpha-1,6-mannosyltransferase that initiates N-linked mannose outer chain elongation in *Saccharomyces cerevisiae*. *FEBS Lett*, 412(3): 547–550, August 1997.

Newman, H. A.; Romeo, M. J.; Lewis, S. E.; Yan, B. C.; Orlean, P., and Levin, D. E. Gpi19, the *Saccharomyces cerevisiae* homologue of mammalian PIG-P, is a subunit of the initial enzyme for glycosylphosphatidylinositol anchor biosynthesis. *Eukaryotic Cell*, 4(11):1801–1807, November 2005.

Nielsen, M. M.; Suits, M. D. L.; Yang, M.; Barry, C. S.; Martinez-Fleites, C.; Tailford, L. E.; Flint, J. E.; Dumon, C.; Davis, B. G.; Gilbert, H. J., and Davies, G. J. Substrate and metal ion promiscuity in mannosylglycerate synthase. *J Biol Chem*, 286(17):15155–15164, April 2011.

Nuoffer, C.; Jeno, P.; Conzelmann, A., and Riezman, H. Determinants for glycophospholipid anchoring of the *Saccharomyces cerevisiae* Gas1 protein to the plasma-membrane. *Mol Cell Biol*, 11(1):27–37, January 1991.

Nuoffer, C.; Horvath, A., and Riezman, H. Analysis of the sequence requirements for glycosylphosphatidylinositol anchoring of *Saccharomyces cerevisiae* Gas1 protein. *J Biol Chem*, 268(14):10558–10563, May 1993.

Odds, F. C. Candida and candidosis. 1988.

Ohishi, K.; Inoue, N.; Maeda, Y.; Takeda, J.; Riezman, H., and Kinoshita, T. Gaa1p and Gpi8p are components of a glycosylphosphatidylinositol (GPI) transamidase that mediates attachment of GPI to proteins. *Molecular Biology of the Cell*, 11 (5):1523–1533, May 2000.

Ohishi, K.; Inoue, N., and Kinoshita, T. PIG-S and PIG-T, essential for GPI anchor attachment to proteins, form a complex with GAA1 and GPI8. *EMBO J*, 20(15): 4088–4098, August 2001.

Ohtsubo, K.; Imajo, S.; Ishiguro, M.; Nakatani, T.; Oka, S., and Kawasaki, T. Studies on the structure-function relationship of the HNK-1 associated glucuronyltransferase, GlcAT-P, by computer modeling and site-directed mutagenesis. *J Biochem*, 128(2):283–291, August 2000.

O'Reilly, M. K.; Zhang, G., and Imperiali, B. In vitro evidence for the dual function of Alg2 and Alg11: Essential mannosyltransferases in N-linked glycoprotein biosynthesis. *Biochemistry*, 45(31):9593–9603, August 2006.

Orlean, P. 2 Chitin Synthases In *Saccharomyces cerevisiae*. *J Biol Chem*, 262(12): 5732–5739, April 1987.

Orlean, P. Dolichol phosphate mannose synthase is required in vivo for glycosyl phosphatidylinositol membrane anchoring, O-mannosylation, and N-glycosylation of protein in *Saccharomyces cerevisiae*. *Mol Cell Biol*, 10(11): 5796–5805, November 1990.

Orlean, P. Phosphoethanolamine addition to glycosylphosphatidylinositols. *The Enzymes*, 2009.

Orlean, P.; Arnold, E., and Tanner, W. Apparent inhibition of glycoprotein synthesis by *S. cerevisiae* mating pheromones. *FEBS Lett*, 184(2):313–317, May 1985.

Orlean, P.; Ammer, H.; Watzele, M., and Tanner, W. Synthesis of an O-glycosylated cell-surface protein induced in yeast by alpha-factor. *Proc Natl Acad Sci USA*, 83(17):6263–6266, September 1986.

Orlean, P. Architecture and biosynthesis of the *Saccharomyces cerevisiae* cell wall. *Genetics*, 192(3):775–818, January 2013.

Orlean, P. and Menon, A. K. GPI anchoring of protein in yeast and mammalian cells, or: how we learned to stop worrying and love glycophospholipids. *J Lipid Res*, 48(5):993–1011, May 2007.

Pak, J. E.; Arnoux, P.; Zhou, S.; Sivarajah, P.; Satkunarajah, M.; Xing, X., and Rini, J. M. X-ray crystal structure of leukocyte type core 2 beta 1,6-N-acetylglucosaminyltransferase - Evidence for a convergence of metal ion-independent glycosyltransferase mechanism. *J Biol Chem*, 281(36):26693–26701, September 2006.

Pang, K.-A. P.; Godet, C.; Fekkar, A.; Scholler, J.; Nivoix, Y.; Letscher-Bru, V.; Massias, L.; Kauffmann-Lacroix, C.; Elsendoorn, A.; Uzunov, M.; Datry, A., and Herbrecht, R. Breakthrough invasive mould infections in patients treated with caspofungin. *J Infect*, 64(4):424–429, April 2012.

Parta, M.; Chang, Y.; Rulong, S.; Pintodasilva, P., and Kwonchung, K. J. Hyp1, a hydrophobin gene from *Aspergillus fumigatus*, complements the rodletless phenotype in *Aspergillus nidulans*. *Infection and Immunity*, 62(10):4389–4395, October 1994.

Patenaude, S. I.; Seto, N. O. L.; Borisova, S. N.; Szpacenko, A.; Marcus, S. L.; Palcic, M. M., and Evans, S. V. The structural basis for specificity in human ABO(H) blood group biosynthesis. *Nat Struct Biol*, 9(9):685–690, September 2002.

Pathak, R.; Hendrickson, T. L., and Imperiali, B. Sulfhydryl modification of the yeast Wbp1p inhibits oligosaccharyl transferase-activity. *Biochemistry*, 34(13): 4179–4185, April 1995.

Pedersen, L. C.; Tsuchida, K.; Kitagawa, H.; Sugahara, K.; Darden, T. A., and Negishi, M. Heparan/chondroitin sulfate biosynthesis. Structure and mechanism of human glucuronyltransferase I. *J Biol Chem*, 275(44):34580–34585, November 2000.

Pedersen, L. C.; Darden, T. A., and Negishi, M. Crystal structure of beta 1,3-glucuronyltransferase I in complex with active donor substrate UDP-GlcUA. *J Biol Chem*, 277(24):21869–21873, June 2002.

Perfect, J. R.; Marr, K. A.; Walsh, T. J.; Greenberg, R. N.; DuPont, B.; Torre-Cisneros, J.de la ; Just-Nübling, G.; Schlamm, H. T.; Lutsar, I.; Espinel-Ingroff, A., and Johnson, E. Voriconazole treatment for less-common, emerging, or refractory fungal infections. *Clin Infect Dis*, 36(9):1122–1131, May 2003.

Perrakis, A.; Morris, R., and Lamzin, V. S. Automated protein model building combined with iterative structure refinement. *Nat Struct Biol*, 6(5):458–463, May 1999.

Persson, K.; Ly, H. D.; Dieckelmann, M.; Wakarchuk, W. W.; Withers, S. G., and Strynadka, N. C. J. Crystal structure of the retaining galactosyltransferase LgtC from *Neisseria meningitidis* in complex with donor and acceptor sugar analogs. *Nat Struct Biol*, 8(2):166–175, February 2001.

Pesnot, T.; Palcic, M. M., and Wagner, G. K. A novel fluorescent probe for retaining galactosyltransferases. *Chem Eur J of Chem Bio*, 11(10):1392–1398, July 2010.

Petersen, T. N.; Brunak, S.; Von Heijne, G., and Nielsen, H. SignalP 4.0: discriminating signal peptides from transmembrane regions. *Nat Methods*, 8(10): 785–786, 2011.

Pfeiffer, C. D.; Fine, J. P., and Safdar, N. Diagnosis of invasive aspergillosis using a galactomannan assay: a meta-analysis. *Clin Infect Dis*, 42(10):1417–1427, May 2006.

Pitt, J. I. The current role of *Aspergillus* and *Penicillium* in human and animal health. *J Med Vet Mycol*, 32 Suppl 1:17–32, 1994.

Pittet, M. and Conzelmann, A. Biosynthesis and function of GPI proteins in the yeast *Saccharomyces cerevisiae*. *Biochim Biophys Acta*, 1771(3):405–420, March 2007.

Pollastri, G. and McLysaght, A. Porter: a new, accurate server for protein secondary structure prediction. *Bioinformatics*, 21(8):1719–1720, April 2005.

Popolo, L. and Vai, M. The Gas1 glycoprotein, a putative wall polymer cross-linker. *Biochim Biophys Acta*, 1426(2):385–400, January 1999.

Popolo, L.; Gilardelli, D.; Bonfante, P., and Vai, M. Increase in chitin as an essential response to defects in assembly of cell wall polymers in the ggp1delta mutant of *Saccharomyces cerevisiae*. *J Bacteriol*, 179(2):463–469, January 1997.

Qadota, H.; Python, C. P.; Inoue, S. B.; Arisawa, M.; Anraku, Y.; Zheng, Y.; Watanabe, T.; Levin, D. E., and Ohya, Y. Identification of yeast Rho1p GTPase as a regulatory subunit of 1,3-beta-glucan synthase. *Science*, 272(5259):279–281, April 1996.

Qasba, P. K.; Ramakrishnan, B., and Boeggeman, E. Substrate-induced conformational changes in glycosyltransferases. *Trends Biochem Sci*, 30(1):53–62, January 2005.

Qian, X.; Palcic, M. M.; Ernst, B.; Hart, G. W., and Sinaý, P. Carbohydrates in chemistry and biology. In *Glycosyltransferase Inhibitors*, pages 293–312. Wiley-VCH Verlag GmbH, January 2008.

Quinn, R. P.; Mahoney, S. J.; Wilkinson, B. M.; Thornton, D. J., and Stirling, C. J. A novel role for Gtb1p in glucose trimming of N-linked glycans. *Glycobiology*, 19 (12):1408–1416, December 2009.

Ragni, E.; Coluccio, A.; Rolli, E.; Rodriguez-Peña, J. M.; Colasante, G.; Arroyo, J.; Neiman, A. M., and Popolo, L. GAS2 and GAS4, a pair of developmentally regulated genes required for spore wall assembly in *Saccharomyces cerevisiae*. *Eukaryotic Cell*, 6(2):302–316, February 2007a.

Ragni, E.; Fontaine, T.; Gissi, C.; Latgé, J.-P., and Popolo, L. The Gas family of proteins of *Saccharomyces cerevisiae*: characterization and evolutionary analysis. *Yeast*, 24(4):297–308, April 2007b.

Raibaud, O. and Schwartz, M. Positive control of transcription initiation In bacteria. *Annu Rev Genet*, 18:173–206, 1984.

Rajan, S. S.; Yang, X.; Collart, F.; Yip, V. L. Y.; Withers, S. G.; Varrot, A.; Thompson, J.; Davies, G. J., and Anderson, W. F. Novel catalytic mechanism of glycoside hydrolysis based on the structure of an NAD+/Mn2+ -dependent phospho-alpha-glucosidase from *Bacillus subtilis*. *Structure/Folding and Design*, 12(9):1619–1629, September 2004.

Ram, A. F.; Brekelmans, S. S.; Oehlen, L. J., and Klis, F. M. Identification of two cell cycle regulated genes affecting the beta-1,3-glucan content of cell walls in *Saccharomyces cerevisiae*. *FEBS Lett*, 358(2):165–170, January 1995.

Ram, A. F.; Kapteyn, J. C.; Montijn, R. C.; Caro, L. H.; Douwes, J. E.; Baginsky, W.; Mazur, P.; Ende, H.van den , and Klis, F. M. Loss of the plasma membrane-bound protein Gas1p in *Saccharomyces cerevisiae* results in the release of beta-1,3-glucan into the medium and induces a compensation mechanism to ensure cell wall integrity. *J Bacteriol*, 180(6):1418–1424, March 1998.

Ram, A. F. J.; Ram, A. F.; Wolters, A.; Wolters, A.; Tenhoopen, R.; Ten Hoopen, R.; Klis, F. M., and Klis, F. M. A new approach for isolating cell-wall mutants in *Saccharomyces cerevisiae* by screening for hypersensitivity to calcofluor white. *Yeast*, 10(8):1019–1030, August 1994.

Ramakrishnan, B. and Qasba, P. K. Crystal structure of lactose synthase reveals a large conformational change in its catalytic component, the beta 1,4-galactosyltransferase-1. *J Mol Biol*, 310(1):205–218, June 2001.

Ramakrishnan, B.; Balaji, P. V., and Qasba, P. K. Crystal structure of beta 1,4-galactosyltransferase complex with UDP-Gal reveals an oligosaccharide acceptor binding site. *J Mol Biol*, 318(2):491–502, April 2002.

Ramasamy, V.; Ramakrishnan, B.; Boeggeman, E.; Ratner, D. M.; Seeberger, P. H., and Qasba, P. K. Oligosaccharide preferences of beta 1,4-galactosyltransferase-I: Crystal structures of Met340His mutant of human beta 1,4-galactosyltransferase-I with a pentasaccharide and trisaccharides of the N-glycan moiety. *J Mol Biol*, 353(1):53–67, October 2005.

Ramos, H.; Demurciano, A. A.; Cohen, B. E., and Bolard, J. The polyene antibiotic amphotericin B acts as a Ca-2+ ionophore in sterol-containing liposomes. *Biochim Biophys Acta*, 982(2):303–306, July 1989.

Rao, F. V.; Dorfmueller, H. C.; Villa, F.; Allwood, M.; Eggleston, I. M., and Aalten, D. M. F.van . Structural insights into the mechanism and inhibition of eukaryotic O-GlcNAc hydrolysis. *EMBO J*, 25(7):1569–1578, April 2006.

Raper, K. B. and Fennell, D. I. The genus *Aspergillus*. *The Genus Aspergillus*, 1965.

Raschke, W. C.; Kern, K. A.; Antalis, C., and Ballou, C. E. Genetic control of yeast mannan structure. Isolation and characterization of mannan mutants. *J Biol Chem*, 248(13):4660–4666, July 1973.

Rayner, J. C. and Munro, S. Identification of the *MNN2* and *MNN5* mannosyltransferases required for forming and extending the mannose branches of the outer chain mannans of *Saccharomyces cerevisiae*. *J Biol Chem*, 273(41):26836–26843, October 1998.

Reiss, G.; Heesen, S.te ; Zimmerman, J.; Robbins, P. W., and Aebi, M. Isolation of the ALG6 locus of *Saccharomyces cerevisiae* required for glucosylation in the N-linked glycosylation pathway. *Glycobiology*, 6(5):493–498, July 1996.

Reiss, G.; teHeesen, S.; Gilmore, R.; Zufferey, R., and Aebi, M. A specific screen for oligosaccharyltransferase mutations identifies the 9 kDa OST5 protein required for optimal activity *in vivo* and *in vitro*. *EMBO J*, 16(6):1164–1172, March 1997.

Reynolds, T. B. and Fink, G. R. Bakers' yeast, a model for fungal biofilm formation. *Science*, 291(5505):878–881, February 2001.

Rodicio, R. and Heinisch, J. J. Together we are strong - cell wall integrity sensors in yeasts. *Yeast*, 27(8):531–540, August 2010.

Rodionov, D.; Romero, P. A.; Berghuis, A., and Herscovics, A. Expression and purification of recombinant M-Pol I from *Saccharomyces cerevisiae* with alpha-1, 6 mannosylpolymerase activity. *Protein Expres Purif*, 66(1):1–6, 2009.

Rodriguez-Pena, J. M.; Cid, V. J.; Arroyo, J., and Nombela, C. A novel family of cell wall-related proteins regulated differently during the yeast life cycle. *Mol Cell Biol*, 20(9):3245–3255, May 2000.

Romero, P. A.; Dijkgraaf, G. J. P.; Shahinian, S.; Herscovics, A., and Bussey, H. The yeast *CWH41* gene encodes glucosidase I. *Glycobiology*, 7(7):997–1004, October 1997.

Romero, P. A.; Lussier, M.; Veronneau, S.; Sdicu, A. M.; Herscovics, A., and Bussey, H. Mnt2p and Mnt3p of *Saccharomyces cerevisiae* are members of the Mnn1p family of alpha-1,3-mannosyltransferases responsible for adding the terminal mannose residues of O-linked oligosaccharides. *Glycobiology*, 9(10): 1045–1051, October 1999.

Rosa Insenser, M.; Luisa Hernaez, M.; Nombela, C.; Molina, M.; Molero, G., and Gil, C. Gel and gel-free proteomics to identify *Saccharomyces cerevisiae* cell surface proteins. *J Proteomics*, 73(6):1183–1195, April 2010.

Rouvinen, J.; Bergfors, T.; Teeri, T.; Knowles, J. K., and Jones, T. A. Three-dimensional structure of cellobiohydrolase II from *Trichoderma reesei*. *Science*, 249(4967):380–386, July 1990.

Ruiz-Herrera, J. and Sentandreu, R. Site of initial glycosylation of mannoproteins from *Saccharomyces cerevisiae*. *J Bacteriol*, 124(1):127–133, October 1975.

Ruiz-Herrera, J.; Manuel Gonzalez-Prieto, J., and Ruiz-Medrano, R. Evolution and phylogenetic relationships of chitin synthases from yeasts and fungi. *FEMS Yeast Research*, 1(4):247–256, January 2002.

Salamon, S. A.; Fuursted, K.; Egeblad, H.; Petersen, E., and Ott, P. *Candida albicans* tricuspid and pulmonic valve endocarditis: challenge of relapsing risk and role of combined medical treatment and surgery. *Scand J Infect Dis*, 39 (6-7):641–644, 2007.

Santos, B. and Snyder, M. Targeting of chitin synthase 3 to polarized growth sites in yeast requires Chs5p and Myo2p. *J Cell Biol*, 136(1):95–110, January 1997.

Santos, B.; Duran, A., and Valdivieso, M. H. CHS5, a gene involved in chitin synthesis and mating in *Saccharomyces cerevisiae*. *Mol Cell Biol*, 17(5):2485–2496, May 1997.

Sato, K.; Noda, Y., and Yoda, K. Pga1 is an essential component of glycosylphosphatidylinositol-mannosyltransferase II of *Saccharomyces cerevisiae*. *Molecular Biology of the Cell*, 18(9):3472–3485, September 2007.

Saxena, I. M.; Brown, R. M.; Fevre, M.; Geremia, R. A., and Henrissat, B. Multidomain architecture of beta-glycosyl transferases - implications for mechanism of action. *J Bacteriol*, 177(6):1419–1424, March 1995.

Schaefer, K.; Albers, J.; Sindhuwinata, N.; Peters, T., and Meyer, B. A new concept for glycosyltransferase inhibitors: nonionic mimics of the nucleotide donor of the human blood group B galactosyltransferase. *Chem Eur J of Chem Bio*, 13(3): 443–450, February 2012.

Schimpl, M.; Zheng, X.; Borodkin, V. S.; Blair, D. E.; Ferenbach, A. T.; Schüttelkopf, A. W.; Navratilova, I.; Aristotelous, T.; Albarbarawi, O.; Robinson, D. A.; Macnaughtan, M. A., and Aalten, D. M. F.van . O-GlcNAc transferase invokes nucleotide sugar pyrophosphate participation in catalysis. *Nat. Chem. Biol.*, 8 (12):969–974, December 2012.

Schulz, B. L. and Aebi, M. Analysis of glycosylation site occupancy reveals a role for Ost3p and Ost6p in site-specific N-glycosylation efficiency. *Mol Cell Proteomics*, 8(2):357–364, February 2009.

Schüttelkopf, A. W.; Andersen, O. A.; Rao, F. V.; Allwood, M.; Rush, C. L.; Eggleston, I. M., and Aalten, D. M. F.van . Bisdionin C – a rationally designed, submicromolar inhibitor of family 18 chitinases. *ACS Med Chem Lett*, 2(6):428–432, 2011.

Schwarz, M.; Knauer, R., and Lehle, L. Yeast oligosaccharyltransferase consists of two functionally distinct sub-complexes, specified by either the Ost3p or Ost6p subunit. *FEBS Lett*, 579(29):6564–6568, December 2005.

Seelig, M. S. Mechanisms by which antibiotics increase the incidence and severity of candidiasis and alter the immunological defenses. *Bacteriol Rev*, 30(2):442–459, June 1966.

Sestak, S.; Hagen, I.; Tanner, W., and Strahl, S. Scw10p, a cell-wall glucanase/transglucosidase important for cell-wall stability in *Saccharomyces cerevisiae*. *Microbiology*, 150(Pt 10):3197–3208, October 2004.

Sharma, C. B.; Knauer, R., and Lehle, L. Biosynthesis of lipid-linked oligosaccharides in yeast: the ALG3 gene encodes the Dol-P-Man : Man(5)GlcNAc(2)-PP-Dol mannosyltransferase. *Biol Chem*, 382(2):321–328, February 2001.

Sheldrick, G. M. Experimental phasing with SHELXC/D/E: combining chain tracing with density modification. *Acta Crystallogr. D Biol. Crystallogr.*, 66(Pt 4):479–485, April 2010.

Shematek, E. M.; Braatz, J. A., and Cabib, E. Biosynthesis of the yeast cell wall. I Preparation and properties of beta-(1-3)-glucan synthetase. *J Biol Chem*, 255 (3):888–894, February 1980.

Shi, Y.; Tomic, J.; Wen, F.; Shaha, S.; Bahlo, A.; Harrison, R.; Dennis, J. W.; Williams, R.; Gross, B. J.; Walker, S.; Zuccolo, J.; Deans, J. P.; Hart, G. W., and Spaner, D. E. Aberrant O-GlcNAcylation characterizes chronic lymphocytic leukemia. *Leukemia*, 24(9):1588–1598, September 2010.

Shibata, N.; Kobayashi, H., and Suzuki, S. Immunochemistry of pathogenic yeast, *Candida* species, focusing on mannan. *Proc Jpn Acad, Ser B, Phys Biol Sci*, 88 (6):250–265, 2012.

Shoji, J.-Y.; Arioka, M., and Kitamoto, K. Possible involvement of pleiomorphic vacuolar networks in nutrient recycling in filamentous fungi. *Autophagy*, 2(3): 226–227, July 2006.

Sikorski, R. S. and Hieter, P. A system of shuttle vectors and yeast host strains designed for efficient manipulation of DNA in *Saccharomyces cerevisiae*. *Genetics*, 122(1):19–27, May 1989.

Sinnott, M. L. Catalytic mechanism of enzymic glycosyl transfer. *Chem Rev*, 90(7): 1171–1202, November 1990.

Sobering, A. K.; Watanabe, R.; Romeo, M. J.; Yan, B. C.; Specht, C. A.; Orlean, P.; Riezman, H., and Levin, D. E. Yeast Ras regulates the complex that catalyzes the first step in GPI-anchor biosynthesis at the ER. *Cell*, 117(5):637–648, May 2004.

Southard, S. B.; Specht, C. A.; Mishra, C.; Chen-Weiner, J., and Robbins, P. W. Molecular analysis of the *Candida albicans* homolog of *Saccharomyces cerevisiae MNN9*, required for glycosylation of cell wall mannoproteins. *J Bacteriol*, 181(24):7439–7448, December 1999.

Soya, N.; Fang, Y.; Palcic, M. M., and Klassen, J. S. Trapping and characterization of covalent intermediates of mutant retaining glycosyltransferases. *Glycobiology*, 21(5):547–552, April 2011.

Spirig, U.; Glavas, M.; Bodmer, D.; Reiss, G.; Burda, P.; Lippuner, V.; teHeesen, S., and Aebi, M. The STT3 protein is a component of the yeast oligosaccharyltransferase complex. *Mol Gen Genet*, 256(6):628–637, November 1997.

Spirig, U.; Bodmer, D.; Wacker, M.; Burda, P., and Aebi, M. The 3.4 kDa Ost4 protein is required for the assembly of two distinct oligosaccharyltransferase complexes in yeast. *Glycobiology*, 15(12):1396–1406, December 2005.

Spreghini, E.; Davis, D. A.; Subaran, R.; Kim, M., and Mitchell, A. P. Roles of *Candida albicans* Dfg5p and Dcw1p cell surface proteins in growth and hypha formation. *Eukaryotic Cell*, 2(4):746–755, August 2003.

Staab, J. F.; Ferrer, C. A., and Sundstrom, P. Developmental expression of a tandemly repeated, proline-and glutamine-rich amino acid motif on hyphal surfaces on *Candida albicans*. *J Biol Chem*, 271(11):6298–6305, March 1996.

Staab, J. F.; Bradway, S. D.; Fidel, P. L., and Sundstrom, P. Adhesive and mammalian transglutaminase substrate properties of *Candida albicans* Hwp1. *Science*, 283(5407):1535–1538, March 1999.

Stagljar, I.; Heesen, S.te , and Aebi, M. New phenotype of mutations deficient in glucosylation of the lipid-linked oligosaccharide - cloning of the alg8 locus. *Proc Natl Acad Sci USA*, 91(13):5977–5981, June 1994.

Stolz, J. and Munro, S. The components of the *Saccharomyces cerevisiae* mannosyltransferase complex M-Pol I have distinct functions in mannan synthesis. *J Biol Chem*, 277(47):44801–44808, November 2002.

Strahl-Bolsinger, S. and Scheinost, A. Transmembrane topology of Pmt1p, a member of an evolutionarily conserved family of protein O-mannosyltransferases. *J Biol Chem*, 274(13):9068–9075, March 1999.

Strahl-Bolsinger, S.; Gentzsch, M., and Tanner, W. Protein O-mannosylation. *BBA - Gen Subjects*, 1426(2):297–307, January 1999.

Strahlbolsinger, S.; Immervoll, T.; Deutzmann, R., and Tanner, W. Pmt1, the gene for a key enzyme of protein P-glycosylation in *Saccharomyces cerevisiae*. *Proc Natl Acad Sci USA*, 90(17):8164–8168, September 1993.

Studier, F. W. Protein production by auto-induction in high density shaking cultures. *Protein Expres Purif*, 41(1):207–234, May 2005.

Sturtevant, J. E. and Latgé, J. P. Interactions between conidia of *Aspergillus fumigatus* and human-complement component C3. *Infection and Immunity*, 60(5): 1913–1918, May 1992.

Sumita, T.; Yoko-o, T.; Shimma, Y., and Jigami, Y. Comparison of cell wall localization among pir family proteins and functional dissection of the region required for cell wall binding and bud scar recruitment of Pir1p. *Eukaryotic Cell*, 4(11): 1872–1881, November 2005.

Surarit, R. and Shepherd, M. G. The effects of azole and polyene antifungals on the plasma-membrane enzymes of *Candida albicans*. *J Med Vet Mycol*, 25(6): 403–413, December 1987.

Sutterlin, C.; Escribano, M. V.; Gerold, P.; Maeda, Y.; Mazon, M. J.; Kinoshita, T.; Schwarz, R. T., and Riezman, H. *Saccharomyces cerevisiae* GPI10, the functional homologue of human PIG-B, is required for glycosylphosphatidylinositol-anchor synthesis. *Biochem J*, 332:153–159, May 1998.

Takahashi, M.; Inoue, N.; Ohishi, K.; Maeda, Y.; Nakamura, N.; Endo, Y.; Fujita, T.; Takeda, J., and Kinoshita, T. PIG-B, a membrane protein of the endoplasmic reticulum with a large lumenal domain, is involved in transferring the third mannose of the GPI anchor. *EMBO J*, 15(16):4254–4261, August 1996.

Tan, S. A modular polycistronic expression system for overexpressing protein complexes in Escherichia coli. *Protein Expres Purif*, 21(1):224–234, February 2001.

Tanaka, S.; Maeda, Y.; Tashima, Y., and Kinoshita, T. Inositol deacylation of glycosylphosphatidylinositol-anchored proteins is mediated by mammalian PGAP1 and yeast Bst1p. *J Biol Chem*, 279(14):14256–14263, April 2004.

Terashima, H.; Hamada, K., and Kitada, K. The localization change of Ybr078w/Ecm33, a yeast GPI-associated protein, from the plasma membrane to the cell wall, affecting the cellular function. *FEMS Microbiol Lett*, 218(1):175–180, January 2003.

Scheltinga, A. C.Terwisscha van ; Armand, S.; Kalk, K. H.; Isogai, A.; Henrissat, B., and Dijkstra, B. W. Stereochemistry of chitin hydrolysis by a plant chitinase/lysozyme and X-ray structure of a complex with allosamidin: evidence for substrate assisted catalysis. *Biochemistry*, 34(48):15619–15623, December 1995.

Thau, N.; Monod, M.; Crestani, B.; Rolland, C.; Tronchin, G.; Latgé, J. P., and Paris, S. Rodletless mutants of *Aspergillus fumigatus*. *Infection and Immunity*, 62(10): 4380–4388, October 1994.

Thompson, G. R.; Wiederhold, N. P.; Vallor, A. C.; Villareal, N. C.; Lewis, J. S., and Patterson, T. F. Development of caspofungin resistance following prolonged therapy for invasive candidiasis secondary to *Candida glabrata* infection. *Antimicrob Agents Chemother*, 52(10):3783–3785, October 2008.

Tiede, A.; Nischan, C.; Schubert, J., and Schmidt, R. E. Characterisation of the enzymatic complex for the first step in glycosylphosphatidylinositol biosynthesis. *Int J Biochem Cell B*, 32(3):339–350, March 2000.

Tiels, P.; Baranova, E.; Piens, K.; De Visscher, C.; Pynaert, G.; Nerinckx, W.; Stout, J.; Fudalej, F.; Hulpiau, P.; Tännler, S.; Geysens, S.; Van Hecke, A.; Valevska, A.; Vervecken, W.; Remaut, H., and Callewaert, N. A bacterial glycosidase enables mannose-6-phosphate modification and improved cellular uptake of yeast-produced recombinant human lysosomal enzymes. *Nat Biotechnol*, 30 (12):1225–1231, December 2012.

Tillmann, U.; Günther, R.; Schweden, J., and Bause, E. Subcellular location of enzymes involved in the N-glycosylation and processing of asparagine-linked oligosaccharides in *Saccharomyces cerevisiae*. *Eur J Biochem*, 162(3):635–642, February 1987.

Tobin, M. B.; Peery, R. B., and Skatrud, P. L. An electrophoretic molecular karyotype of a clinical isolate of *Aspergillus fumigatus* and localization of the MDR-like genes AfuMDR1 and AfuMDR2. *Diagn Microbiol Infect Dis*, 29(2):67–71, October 1997.

Tohe, A.; Yasunaga, S.; Nisogi, H.; Tanaka, K.; Oguchi, T., and Matsui, Y. 3 yeast genes, *PIR1*, *PIR2* And *PIR3*, containing internal tandem repeats, are related to each other, and *PIR1* and *PIR2* are required for tolerance to heat-shock. *Yeast*, 9(5):481–494, May 1993.

Trilla, J. A.; Duran, A., and Roncero, C. Chs7p, a new protein involved in the control of protein export from the endoplasmic reticulum that is specifically engaged in the regulation of chitin synthesis in *Saccharomyces cerevisiae*. *J Cell Biol*, 145 (6):1153–1163, June 1999.

Trombetta, E. S.; Simons, J. F., and Helenius, A. Endoplasmic reticulum glucosidase II is composed of a catalytic subunit, conserved from yeast to mammals, and a tightly bound noncatalytic HDEL-containing subunit. *J Biol Chem*, 271(44): 27509–27516, November 1996.

Tronchin, G.; Esnault, K.; Renier, G.; Filmon, R.; Chabasse, D., and Bouchara, J. P. Expression and identification of a laminin-binding protein in *Aspergillus fumigatus* conidia. *Infection and Immunity*, 65(1):9–15, January 1997.

Trow, J. and Cormack, B. *Saccharomyces cerevisiae DCW1 DFG5* mutants exhibit decreased viability and aberrant GPI-CWP incorporation into the cell wall. In *9TH ASM CONFERENCE ON CANDIDA AND CANDIDIASIS*, pages 1–1, Jersey City, October 2009. John Hopkins University School of Medicine, Baltimore, MD.

Tsai, P. K.; Frevert, J., and Ballou, C. E. Carbohydrate structure of *Saccharomyces cerevisiae mnn9* mannoprotein. *J Biol Chem*, 259(6):3805–3811, March 1984.

Unligil, U. M. and Rini, J. M. Glycosyltransferase structure and mechanism. *Curr Opin Struct Biol*, 10(5):510–517, October 2000.

Valdivieso, M. H.; Ferrario, L.; Vai, M.; Duran, A., and Popolo, L. Chitin synthesis in a gas1 mutant of *Saccharomyces cerevisiae*. *J Bacteriol*, 182(17):4752–4757, September 2000.

Van Bruggen-Van Der Lugt, A. W.; Kamphuis, H. J.; Deruiter, G. A.; Mischnick, P.; Vanboom, J. H., and Rombouts, F. M. New structural features of the antigenic extracellular polysaccharides of *Penicillium* and *Aspergillus* species revealed with exo-beta-D-galactofuranosidase. *J Bacteriol*, 174(19):6096–6102, October 1992.

Bossche, H.van den ; Willemsens, G., and Marichal, P. Anti-*Candida* drugs–the biochemical basis for their activity. *Crit Rev Microbiol*, 15(1):57–72, 1987.

Vidugiriene, J. and Menon, A. K. Early lipid intermediates in glycosylphosphatidylinositol anchor assembly are synthesized in the er and located in the cytoplasmic leaflet of the er membrane bilayer. *J Cell Biol*, 121(5):987–996, June 1993.

Vishwakarma, R. A. and Menon, A. K. Flip-flop of glycosylphosphatidylinositols (GPIs) across the ER. *Chem Commun*, (4):453–455, January 2005.

Vocadlo, D. J.; Davies, G. J.; Laine, R., and Withers, S. G. Catalysis by hen egg-white lysozyme proceeds via a covalent intermediate. *Nature*, 412(6849):835–838, August 2001.

Vocadlo, D. J. and Withers, S. G. Detailed comparative analysis of the catalytic mechanisms of beta-N-acetylglucosaminidases from families 3 and 20 of glycoside hydrolases. *Biochemistry*, 44(38):12809–12818, September 2005.

Vrielink, A.; Ruger, W.; Driessen, H. P., and Freemont, P. S. Crystal-structure of the DNA modifying enzyme beta-glucosyltransferase in the presence and absence of the substrate uridine diphosphoglucose. *EMBO J*, 13(15):3413–3422, August 1994.

Wacker, M.; Linton, D.; Hitchen, P. G.; Nita-Lazar, M.; Haslam, S. M.; North, S. J.; Panico, M.; Morris, H. R.; Dell, A.; Wren, B. W., and Aebi, M. N-linked glycosylation in *Campylobacter jejuni* and its functional transfer into *E. coli*. *Science*, 298 (5599):1790–1793, November 2002.

Wang, X. H.; Nakayama, K.; Shimma, Y.; Tanaka, A., and Jigami, Y. *MNN6*, a member of the *KRE2*/*MNT1* family, is the gene for mannosylphosphate transfer in *Saccharomyces cerevisiae*. *J Biol Chem*, 272(29):18117–18124, July 1997.

Watanabe, R.; Kinoshita, T.; Masaki, R.; Yamamoto, A.; Takeda, J., and Inoue, N. PIG-A and PIG-H, which participate in glycosylphosphatidylinositol anchor biosynthesis, from a protein complex in the endoplasmic reticulum. *J Biol Chem*, 271(43):26868–26875, October 1996.

Watanabe, R.; Ohishi, K.; Maeda, Y.; Nakamura, N., and Kinoshita, T. Mammalian PIG-L and its yeast homologue Gpi12p are N-acetylglucosaminylphosphatidylinositol de-N-acetylases essential in glycosylphosphatidylinositol biosynthesis. *Biochem J*, 339:185–192, April 1999.

Watson, K. A.; Mitchell, E. P.; Johnson, L. N.; Son, J. C.; Bichard, C. J. F.; Orchard, M. G.; Fleet, G. W. J.; Oikonomakos, N. G.; Leonidas, D. D.; Kontou, M., and Papageorgiou, A. C. Design of inhibitors of glycogen-phosphorylase – a study of alpha-C-glucosides and beta-C-glucosides and 1-thio-beta-D-glucose compounds. *Biochemistry*, 33(19):5745–5758, May 1994.

Watts, A. G.; Damager, I.; Amaya, M. L.; Buschiazzo, A.; Alzari, P.; Frasch, A. C., and Withers, S. G. *Trypanosoma cruzi* trans-sialidase operates through a covalent sialyl-enzyme intermediate: tyrosine is the catalytic nucleophile. *J Am Chem Soc*, 125(25):7532–7533, June 2003.

Wei, M.; Madia, F., and Longo, V. D. Studying age-dependent genomic instability using the *S. cerevisiae* chronological lifespan model. *J Vis Exp*, (55), 2011.

Welten-Verstegen, G. W.; Boer, P., and Steyn-Parvé, E. P. Lipid-mediated glycosylation of endogenous proteins in isolated plasma membrane of *Saccharomyces cerevisiae*. *J Bacteriol*, 141(1):342–349, January 1980.

Wiggins, C. A. R. and Munro, S. Activity of the yeast *MNN1* alpha-1,3-mannosyltransferase requires a motif conserved in many other families of glycosyltransferases. *Proc Natl Acad Sci USA*, 95(14):7945–7950, July 1998.

Wilkins, M. R.; Gasteiger, E.; Bairoch, A.; Sanchez, J. C.; Williams, K. L.; Appel, R. D., and Hochstrasser, D. F. Protein identification and analysis tools in the ExPASy server. *Methods Mol Biol*, 112:531–552, 1999.

Wisplinghoff, H.; Bischoff, T.; Tallent, S. M.; Seifert, H.; Wenzel, R. P., and Edmond, M. B. Nosocomial bloodstream infections in US hospitals: analysis of 24,179 cases from a prospective nationwide surveillance study. *Clin Infect Dis*, 39(3): 309–317, August 2004.

Woods, J. W.; Manning, I. H., and Patterson, C. N. Monilial infections complicating the therapeutic use of antibiotics. *J Am Med Assoc*, 145(4):207–211, January 1951.

Wright, R. J.; Carne, A.; Hieber, A. D.; Lamont, I. L.; Emerson, G. W., and Sullivan, P. A. A second gene for a secreted aspartate proteinase in *Candida albicans*. *J Bacteriol*, 174(23):7848–7853, December 1992.

Yabe, T.; Yamada-Okabe, T.; Nakajima, T.; Sudoh, M.; Arisawa, M., and Yamada-Okabe, H. Mutational analysis of chitin synthase 2 of *Saccharomyces cerevisiae* - Identification of additional amino acid residues involved in its catalytic activity. *Eur J Biochem*, 258(3):941–947, December 1998.

Yamaguchi, M.; Namiki, Y.; Okada, H.; Mori, Y.; Furukawa, H.; Wang, J.; Ohkusu, M., and Kawamoto, S. Structome of *Saccharomyces cerevisiae* determined by freeze-substitution and serial ultrathin-sectioning electron microscopy. *J Electron Microsc (Tokyo)*, 60(5):321–335, 2011.

Yamamoto, F.; Clausen, H.; White, T.; Marken, J., and Hakomori, S. I. Molecular genetic-basis of the histo-blood group AB0 system. *Nature*, 345(6272):229–233, May 1990.

Yan, A. X. and Lennarz, W. J. Two oligosaccharyl transferase complexes exist in yeast and associate with two different translocons. *Glycobiology*, 15(12):1407–1415, December 2005.

Yan, B. C.; Westfall, B. A., and Orlean, P. Ynl038wp (Gpi I 5p) is the *Saccharomyces cerevisiae* homologue of human Pig-Hp and participates in the first step in glycosylphosphatidylinositol assembly. *Yeast*, 18(15):1383–1389, November 2001.

Yan, Q. and Lennarz, W. J. Studies on the function of oligosaccharyl transferase subunits. Stt3p is directly involved in the glycosylation process. *J Biol Chem*, 277 (49):47692–47700, December 2002.

Yang, Z. R.; Thomson, R.; McNeil, P., and Esnouf, R. M. RONN: the bio-basis function neural network technique applied to the detection of natively disordered regions in proteins. *Bioinformatics*, 21(16):3369–3376, August 2005.

Yin, Q. Y.; Groot, P. W. J.de ; Dekker, H. L.; Jong, L.de ; Klis, F. M., and Koster, C. G.de . Comprehensive proteomic analysis of *Saccharomyces cerevisiae* cell walls: identification of proteins covalently attached via glycosylphosphatidylinositol remnants or mild alkali-sensitive linkages. *J Biol Chem*, 280(21):20894–20901, May 2005.

Yin, Q. Y.; Groot, P. W. J.de ; Jong, L.de ; Klis, F. M., and Koster, C. G.de . Mass spectrometric quantitation of covalently bound cell wall proteins in *Saccharomyces cerevisiae*. *FEMS Yeast Research*, 7(6):887–896, September 2007.

Yip, C. L.; Welch, S. K.; Klebl, F.; Gilbert, T.; Seidel, P.; Grant, F. J.; O'Hara, P. J., and MacKay, V. L. Cloning and analysis of the *Saccharomyces cerevisiae MNN9* and *MNN1* genes required for complex glycosylation of secreted proteins. *Proc Natl Acad Sci USA*, 91(7):2723–2727, March 1994.

Yip, V. L. Y.; Varrot, A.; Davies, G. J.; Rajan, S. S.; Yang, X.; Thompson, J.; Anderson, W. F., and Withers, S. G. An unusual mechanism of glycoside hydrolysis involving redox and elimination steps by a family 4 beta-glycosidase from Thermotoga maritima. *J Am Chem Soc*, 126(27):8354–8355, July 2004.

Yuzwa, S. A.; Macauley, M. S.; Heinonen, J. E.; Shan, X.; Dennis, R. J.; He, Y.; Whitworth, G. E.; Stubbs, K. A.; McEachern, E. J.; Davies, G. J., and Vocadlo, D. J. A potent mechanism-inspired O-GlcNAcase inhibitor that blocks phosphorylation of tau in vivo. *Nat. Chem. Biol.*, 4(8):483–490, August 2008.

Yuzwa, S. A.; Shan, X.; Macauley, M. S.; Clark, T.; Skorobogatko, Y.; Vosseller, K., and Vocadlo, D. J. Increasing O-GlcNAc slows neurodegeneration and stabilizes tau against aggregation. *Nat. Chem. Biol.*, 8(4):393–399, April 2012.

Zadrag, R.; Bartosz, G., and Bilinski, T. Is the yeast a relevant model for aging of multicellular organisms? An insight from the total lifespan of Saccharomyces cerevisiae. *Curr Aging Sci*, 1(3):159–165, December 2008.

Zhang, R.; Minh, T.; Lezondra, L.; Korolev, S.; Moy, S. F.; Collart, F., and Joachimiak, A. 1.6 A crystal structure of YteR protein from *Bacillus subtilis*, a predicted lyase. *Proteins*, 60(3):561–565, August 2005.

Zhang, Y.; Swaminathan, G. J.; Deshpande, A.; Boix, E.; Natesh, R.; Xie, Z.; Acharya, K. R., and Brew, K. Roles of individual enzyme-substrate interactions by alpha-1,3-galactosyltransferase in catalysis and specificity. *Biochemistry*, 42 (46):13512–13521, November 2003.

Zhu, P.; Boykins, R. A., and Tsai, C.-M. Genetic and functional analyses of the lgtH gene, a member of the beta-1,4-galactosyltransferase gene family in the genus *Neisseria*. *Microbiology*, 152(Pt 1):123–134, January 2006.

Zhu, Z.; Zheng, T.; Homer, R. J.; Kim, Y. K.; Chen, N. Y.; Cohn, L.; Hamid, Q., and Elias, J. A. Acidic mammalian chitinase in asthmatic Th2 inflammation and IL-13 pathway activation. *Science*, 304(5677):1678–1682, June 2004.

Ziman, M.; Chuang, J. S.; Tsung, M.; Hamamoto, S., and Schekman, R. Chs6p-dependent anterograde transport of Chs3p from the chitosome to the plasma membrane in *Saccharomyces cerevisiae*. *Molecular Biology of the Cell*, 9(6): 1565–1576, June 1998.

Zlotnik, H.; Fernandez, M. P.; Bowers, B., and Cabib, E. *Saccharomyces cerevisiae* mannoproteins form an external cell-wall layer that determines wall porosity. *J Bacteriol*, 159(3):1018–1026, 1984.